

Indoor Localisation of Scooters from Ubiquitous Cost-Effective Sensors: Combining Wi-Fi, Smartphone and Wheel Encoders

Ivy Ijeoma Okike

Principal supervisor [Dr. Salvatore Livatino](#)

Secondary supervisor [Dr. Sara Chaychian](#)

Second secondary supervisor [Mr Johann Siau](#)

A thesis submitted to the University of Hertfordshire in partial fulfilment of the
requirements for a degree of Doctor of Philosophy

March 2019

ABSTRACT

Indoor localisation of people and objects has been a focus of research studies for several decades because of its great advantage to several applications. Accuracy has always been a challenge because of the uncertainty of the employed sensors. Several technologies have been proposed and researched, however, accuracy still represents an issue.

Today, several sensor technologies can be found in indoor environments, some of which are economical and powerful, such as Wi-Fi. Meanwhile, Smartphones are typically present indoors because of the people that carry them along, while moving about within rooms and buildings. Furthermore, vehicles such as mobility scooters can also be present indoor to support people with mobility impairments, which may be equipped with low-cost sensors, such as wheel encoders.

This thesis investigates the localisation of mobility scooters operating indoor. This represents a specific topic as most of today's indoor localisation systems are for pedestrians. Furthermore, accurate indoor localisation of those scooters is challenging because of the type of motion and specific behaviour.

The thesis focuses on improving localisation accuracy for mobility scooters and on the use of already available indoor sensors. It proposes a combined use of Wi-Fi, Smartphone IMU and wheel encoders, which represents a cost-effective energy-efficient solution.

A method has been devised and a system has been developed, which has been experimented on different environment settings. The outcome of the experiments are presented and carefully analysed in the thesis. The outcome of several trials demonstrates the potential of the proposed solutions in reducing positional errors significantly when compared to the state-of-the-art in the same area. The proposed combination demonstrated an error range of 0.35m - 1.35m, which can be acceptable in several applications, such as some related to assisted living.

As the proposed system capitalizes on the use of ubiquitous technologies, it opens up to a potential quick take up from the market, therefore being of great benefit for the target audience.

DEDICATED

To, my fiancé, parents, siblings, supervisors, friends and colleagues.

ACKNOWLEDGEMENTS

Firstly, I must thank God for blessing me with the opportunity to attain a PhD.

I like to express my deepest gratitude to my supervisors for their consistent support, patience and guidance. They not only instilled the fire I needed to complete this research, their positive 'can-do' attitude thought me to persevere in times of uncertainty. Dr Salvatore Livatinos, I sincerely appreciate the drive you instilled in me. Thank you for your attention to details, and your support that guaranteed my writing and presentation were of high standards. Dr Sara Chaychian, I appreciate the gentle encouragements you always rendered. Johann Siau, you encouraged me to embark on this journey, I appreciate your unwavering faith in me. Thank you for the technical support and resources.

I must extend sincere thanks to my colleagues and friends at the smart systems research group, Al Lalani, Angus Hutton-McKenzie, Anthony Onuorah, Chengqi Yang, Emilio Mistretta and Rahi. You all made my time of study special by being wonderful and exceptional people. I have learned so much from you all. This appreciation will be incomplete without my mentioning our diverse discussions that spanned across various levels of relevance and intelligence.

I would also like to thank Solomon for supporting me with knowledge outside my field of study, which played an integral part of this research.

To my friends, thank you for the prayers, encouragements and continuous support.

To my family; you cheered me on throughout this journey. This will not be possible without your support and encouragement. Thank you.

Finally, and most importantly, I must thank my fiancé, I am grateful for the prayers, reassurances and support. You are the MVP.

From the bottom of my heart, thank you.

Table of Contents

ABSTRACT.....	2
DEDICATED.....	4
List of Figures.....	10
List of Tables.....	15
List of Equations.....	17
List of Abbreviations.....	19
Chapter 1 Introduction.....	23
1.1 Indoor Localisation.....	23
1.2 Business Motivations.....	26
1.3 Technology Focus.....	28
1.4 Proposed Investigation.....	32
1.4.1 Aim and Objectives.....	32
1.5 Motivation and Challenges.....	33
1.6 Contribution to Knowledge.....	35
1.7 Thesis Outline.....	36
Chapter 2 Background Knowledge.....	38
2.1 Physical Localisation Based Category.....	39
2.1.1 Network Localisation Systems.....	39
2.1.2 Conclusion and Analysis of Physical Localisation Based Systems.....	51
2.2 Topographical Positioning Systems.....	52
2.2.1 Outdoor Localisation Systems and Methods.....	52
2.2.2 Indoor Localisation Systems.....	55
2.3 Conclusion and Analysis.....	63
2.4 Mathematical Models, Methods and Algorithms.....	66
2.4.1 Inertial Sensor Fusion Using Complementary Fusion.....	66
2.4.2 Moving Average Filter.....	68
2.4.3 Full Width at Half Maximum (FWHM).....	68

2.4.4	RSSI – SDRS Log Normal Shadowing Model	70
2.4.5	Trilateration and Multi-trilateration	73
2.4.6	Average Localisation Error Model (ALE) for Performance Evaluation	75
2.4.7	Euclidean Distance Error.....	76
2.4.8	Locating Coordinates of Centroid of a Shaded Area	77
2.5	Mobility Scooter	77
2.6	Overall Summary	79
Chapter 3 State of the Art.....		81
3.1.	Overview.....	81
3.2.	Passive Indoor Localisation.....	85
3.2.1.	Differential Air Pressure.....	86
3.2.2.	Differential Barometer.....	87
3.2.3.	Physical Contact Based System	90
3.2.4.	Light.....	93
3.2.5.	Ultra Wideband (UWB).....	93
3.2.6.	Computer Vision.....	94
3.2.7.	Device-Free Passive (DfP).....	95
3.2.8.	Smart Wiring and Socket.....	96
3.2.9.	Camera.....	97
3.3.	Active Indoor Localisation.....	97
3.3.1.	Radio Frequency Identification (RFID)	98
3.3.2.	Ultra Wide Band (UWB)	100
3.3.3.	Cellular Networks.....	102
3.3.4.	Ultra Sonic Localisation	103
3.3.5.	AM, FM and TV Signals.....	104
3.3.6.	Bluetooth.....	106
3.3.7.	Field Strength Systems- IMU.....	106
3.3.8.	WLAN – Wi-Fi.....	107
3.4.	Hybrid System.....	113
3.4.1.	Propagation Based Hybrid System.....	114
3.4.2.	Technology and Technique (TT) Based Hybrid System	115
3.5.	Summary and Analysis	116

Chapter 4 Proposed Investigation	122
4.1. Research Question	122
4.2. Core Idea and Motivation	122
4.3. WTP-HAMS System Elements Functionality	136
4.4. Analysis of Proposed Technology Solution	146
4.5. Research Development Plan.....	151
Chapter 5 System Implementation	156
5.1. WTP-HAMS System overview	156
5.2. WTP-HAMS System requirements	157
5.3. System Architecture.....	163
5.3.1. WTP-HAMS system phase implementation	166
5.4. Summary and Analysis	182
Chapter 6 Experimentation.....	186
6.1. Design.....	188
6.2. Experimental Strategy.....	189
6.2.1. Focused study.....	189
6.2.2. Comprehensive study	192
6.3. Wi-Fi.....	192
6.3.1. First Study: LOS versus NLOS.....	193
6.3.2. Second Study: Position Accuracy Based On Multi-Trilateration	194
6.4. Smartphone IMU Modalities.....	195
6.4.1. Third Study: Navigation Heading.....	196
6.4.2. Fourth Study: Smartphone Pose.....	197
6.5. Wheel Encoders	198
6.5.1. Fifth Study: Relative Pose Accuracy	198
6.6. Comprehensive Study.....	200
6.7. Experiment Implementation and Results Analysis.....	203
6.7.1. Pilot Test Phase	203
6.7.2. Main test phase	209
6.7.3. Summary of Comprehensive Study Findings.....	235
6.7.4. Overall Results and Analysis.....	236

Chapter 7 Conclusion and Future Work	238
7.1. Thesis Summary	238
7.2. Outcomes	241
7.3. Lessons Learned	248
7.3.1. Technical Lessons.....	248
7.3.2. Personal Lessons.....	252
7.4. Future Directions	253
References	255
Appendices	269
Appendix A: Additional Figures	269
Appendix B – Development Code Snippet	269

List of Figures

Figure 2-1 Triangulation method.....	41
Figure 2-2 E-OTD positioning solution [30].....	42
Figure 2-3 Graphical illustration of positioning techniques [28].....	43
Figure 2-4 Device-to-device cellular communication [34].....	45
Figure 2-5 Odometry showing pose uncertainty growth in straight line movement [54]	56
Figure 2-6 a) Time of arrival approach with trilateration calculation; B) angle of arrival approach [58].....	59
Figure 2-7 Received signal strength [58].....	59
Figure 2-8 Converting smartphone coordinate to earth coordinate [68].....	62
Figure 2-9 Proposed investigation (WTP-HAMS system) based on background knowledge	64
Figure 2-10 Magnetometer and gyroscope filtration combination.....	67
Figure 2-11 Complementary fusion of filtered IMU sensor output.....	67
Figure 2-12 Shows the relationship between the variance σ and FWHM [73].....	68
Figure 2-13 Shaded areas of importance contained within the limits $\mu \pm 1\sigma$, $\mu \pm 2\sigma$ and $\mu \pm 3\sigma$ in a Gaussian distribution [73].....	69
Figure 2-14 Proposed investigation (WTP-HAMS system).....	79
Figure 3-1 Indoor walking measurement [113].....	88
Figure 3-2 Astrium Satellites GmbH InLite technology [114].....	89

Figure 3-3 InLite Architecture illustrating 8 base stations, control unit and user reception station [114].....	90
Figure 3-4 Framework of developed RFID tracking approach [135].....	100
Figure 3-5 Simple threshold method application on a smoothed vertical acceleration pattern for step identification	110
Figure 4-1 WTP-HAMS working scheme	124
Figure 4-2 triangular error from AMO1 is within circular error shape from W2	133
Figure 4-3 Test comparing the distance between triangle error from AMO1 and circular error from W2 to determine true error overlap or intersection occurrence.....	133
Figure 4-4 Check for vertices of error triangle AMO1 intersecting/overlapping error circle W2.....	134
Figure 4-5 Check to verify error circle intersects error triangle along vertices LF.....	135
Figure 4-6 improved position accuracy from error shape intersection with the new position estimation	136
Figure 4-7 Flow chart displaying the WTP-HAMS system combining estimated relative positions and pose to improve position accuracy.....	139
Figure 4-8 Associated formula or models for relative position based on the flow chart in Figure 4-8.....	140
Figure 4-9 Associated formula or models for pose estimation based on the flow chart in Figure 4 8.....	141
Figure 4-10 Associated formula or models for estimated absolute position based on the flow chart in Figure 4 8.....	142
Figure 4-11 Heading error reduction in WTP-HAMS odometry showing triangular error shapes experienced in AMO1.....	145

Figure 4-12 Research development plan with timelines	155
Figure 5-1 WTP-HAM API on SP displaying data extracted from internal and external technologies.....	158
Figure 5-2 Developed wheel encoder components necessary for distance estimation	159
Figure 5-3 Wheel encoder system communication flow to SP.....	160
Figure 5-4 Wheel encoder circuit schematic.....	161
Figure 5-5 wheel encoder mounted onto the wheels of the mobility scooter	161
Figure 5-6 Bluetooth communication protocol between wheel encoder and SP	162
Figure 5-7 Proposed WTP-HAMS system Architecture.....	163
Figure 5-8 SP to the online database communication flow.....	165
Figure 5-9 Wi-Fi state in loop from the beginning to the size of each scanned result ...	169
Figure 5-10 High-frequency rates for SensorManager governing data retrieval from the accelerometer, magnetometer and gyroscope sensor	170
Figure 5-11 display organisation of pitch (x), azimuth (y) and roll (z) of accelerometer, magnetometer and gyroscope post matrix implementation	171
Figure 5-12 gyroOrientation matrix calculating SP behaviour	172
Figure 5-13 orientation calculation from accelerometer/magnetometer fusion.....	172
Figure 5-14 Fusing all IMU sensors.....	173
Figure 5-15 travel distance of each wheel over time	173
Figure 5-16 WiFiManager JSON array transfer to the database.....	174
Figure 5-17 SensorManager JSON array transfer to the database.....	175
Figure 5-18 Calculating for absolute time.....	176

Figure 5-19 Mac addresses identifying unique APs for RSSI propagation	177
Figure 5-20 SDRS log-normal shadowing model to get relative RSSI distance.....	178
Figure 5-21 multi-trilateration computation for four APs/router	178
Figure 5-22 distance travelled computation based on SOTA.....	179
Figure 5-23 identifying AM2 with respect to the globe.....	180
Figure 5-24 Odometry model for position estimation with error.....	181
Figure 6-1 Purpose for experimenting on Wi-Fi, smartphone modalities including IMU sensors - accelerometer, magnetometer and wheel encoder based on evaluations by the State-of-The-Art (SOTA)	188
Figure 6-2 To scale representation of the test environment (room 1) for testing LOS and NLoS.....	204
Figure 6-3 graphical analysis of dataset showing deviation of the estimated distance from the ground truth.....	207
Figure 6-4 schematic map of the experimental site (room 2) and reference point distribution	210
Figure 6-5 Graphical illustration showing deviation of estimated position from the true position in the test room with three routers/APs	213
Figure 6-6 Graphical illustration showing deviation of estimated position from the true position in the test room with four routers/APs.....	215
Figure 6-7 Accelerometer measurements indicating inactivity when SP is stationary.	219
Figure 6-8 gyroscope (G) and drift eliminated gyroscope (GD) output frequency spectrum with high amplitude and noise.....	220
Figure 6-9 Accelerometer output frequency spectrum with high amplitude and noise	221

Figure 6-10 Frequency spectrum of fused accelerometer and magnetometer sensors demonstrating travel over time	222
Figure 6-11 Sensor fusion outcome on x and y-axis of the smartphone (SP).....	223
Figure 6-12 Accelerometer and magnetometer combination (AMY) is best for deriving heading direction in our system	223
Figure 6-13 FWHM applied to AMY frequency spectrum identifying acceleration, change and deceleration	229
Figure 6-14 Relative pose accuracy using our proposed novel odometry model.....	230
Figure 6-15 Proposed WTP-HAMS system showing improved localisation for the mobility scooter with a mounted smartphone in horizontal orientation with LOS in room 2.....	232

List of Tables

Table 1-1 Document organisation	37
Table 2-1 Pattern matching method collecting multipath characteristics as the “fingerprinting” of mobile phones [23]	46
Table 2-2 A triangulation of Wi-Fi routers using AoA of smart antennas [34].....	47
Table 2-3 Indoor Wi-Fi Localisation System Utilizing 3 Smart Antennas [34]	48
Table 2-4 Literature works adopted in our proposed WTP-HAMS system	52
Table 2-5 IndoorNav using inertial sensors and dead-reckoning approach [56]	61
Table 2-6 Path loss exponent based on environmental dynamics [64][77]	72
Table 3-1 Indoor localisation system and their classifications.....	83
Table 3-2 Survey Paper accumulation table.....	85
Table 3-3 Performance results of our manually-labelled experiments with the HVAC in operation [112].....	87
Table 3-4 The assumptions for RSS WPL algorithm as proposed by [146]	108
Table 3-5 Analysis of state-of-the-art.....	119
Table 4-1 Overview of the research development plan	152
Table 6-1 Critical elements of the evaluation methods and setup.....	200
Table 6-2 Critical elements for Comprehensive study.....	202
Table 6-3 Distance accuracy deviation between true distance and relative RSSI distance estimates.....	206
Table 6-4 LOS and NLoS influences based on RSSI and its LQI.....	208

Table 6-5 representation table of the schematic map in Figure 6.2-3.....	210
Table 6-6 Comparison table comparing true position to estimated relative position using three routers at RP1	213
Table 6-7 Comparison table for RSSI min, average and max outcomes	214
Table 6-8 Comparison table comparing true position to estimated relative position using four routers at RP1.....	215
Table 6-9 minimum and maximum travelled distance from the start point to endpoint	225
Table 6-10 Comparing percentage error of drift for travelled distance considering the minimum, maximum and average values.....	226
Table 6-11 Results showing improved travelled distance using our drift mitigation model for minimum, maximum and average travelled distance estimates	227
Table 6-12 Descriptive table for Figure 6-15.....	232
Table 6-13 Results of all proposed studies to achieve improved position accuracy using our proposed WTP-HAMS system.....	233
Table 6-14 WTP-HAMS system improvement on RSSI and odometry	235
Table 6-15 Comparing WTP-HAMS to literature works.....	236
Table 7-1 Indepth comparison of the SOTA to our proposed WTP-HAMS system	243

List of Equations

Equation 1.....	57
Equation 2.....	57
Equation 3.....	57
Equation 4.....	69
Equation 5.....	71
Equation 6.....	73
Equation 7.....	74
Equation 8.....	74
Equation 9.....	75
Equation 10.....	76
Equation 11.....	76
Equation 12.....	109
Equation 13.....	109
Equation 14.....	110
Equation 15.....	111
Equation 16.....	127
Equation 17.....	127
Equation 18.....	127
Equation 19.....	128

Equation 20.....	129
Equation 21.....	131
Equation 22.....	131
Equation 23.....	132
Equation 24.....	133
Equation 25.....	134
Equation 26.....	134
Equation 27.....	135
Equation 28.....	135
Equation 29.....	173

List of Abbreviations

Abbreviation	Description
ADC	Analog-Digital converter
AM	Accelerometer and magnetometer fusion
AM	Amplitude Modulation
AoA	Angle of arrival
AP	Access point
APs	Access points (also referred to routers in this thesis)
Avg	Average
BEAM01	Best position Estimate of fused Accelerometer and Magnetometer output combined with Odometry
BERW2	Best position error of Wi-Fi
BrAMO 1	Best relative position of fused accelerometer and magnetometer output combined with odometry
BrW2	Best relative position of Wi-Fi
CDF	Cumulative distribution function
CDMA	Code Division Multiple Access
Cell ID	Cellular Identification
DC	Direct Current
DFP	Device-free Passive
EERAM01	Estimated Error of fused Accelerometer and Magnetometer output combined with Odometry
EERW2	Estimated Error of Wi-Fi
EKF	Extended Kalman Filter
E-OTA	Enhanced Observed Time of Arrival
E-OTD	Enhanced Observed Time Difference
FM	Frequency Modulation

GD	Gyroscope output without Drift
GPS	Global Positioning System
GRF	Ground Reaction Force
GSM	Global System for Mobile Communication
HB	Hutton hub
HVAC	Heating, Ventilation, and Air Conditioning
ICP-based	Iterative Closest Point-based
IEEE802.11g	Institute of Electrical and Electronics Engineers (IEEE) LAN/MAN Standards amendment to IEEE 802.11
IMU	Inertial Measuring Units
IoT	Internet of Things
IPS	Indoor Positioning System
IR	Infrared sensor
KCF	Kalman-Consensus Filter
K-NN	K-Nearest Neighbour
LDPL	Log-Normal Distance Path Loss model
LNG	Liquefied Natural Gas
LOS	Line-Of-Sight
Max	Maximum value
MCU	Micro Controller Unit
MIMO	Multiple Input Multiple Output
Min	Minimum Values
MILPS	Magnetic signal Indoor Local Positioning System
MSVR	Multidimensional Support Vector Regression
NLOS	None Line of Sight
OFCOM	Office of Communications

PHY	Physical Layer
PMV-SET	Predicted Mean Vote Set
RANSAC	Recognition and random sample consensus
RFID	Radio Frequency Identification
RIOT-OS	Real-Time Operating System
RMSE	Root Mean Square Error
ROS	Robotic Operating System
RSS	Received Signal Strength
RSSI	Received Signal Strength Indicator
RTCs	Real-Time Clocks
SDL	Speed and Direction Learning
SDRS	Steepest Descent Random Start Algorithm
SF	Sensor Fusion
SLAM	Simultaneous Localisation and Mapping
SOTA	State Of The Art
SP	Smart Phone
SURF	Speeded Up Robust Feature
SVM	Support vector machine
TDMA	Time Division Multiple Access
TDOA	Time Difference of Arrival
ToA	Time of Arrival
TT	Technology and technique based hybrid localisation
TV	Television
UBIROU	UBIquitousRObot
UWB	Ultra Wide Band
VSN	Visual Sensor Network

Wi-Fi

Wireless Fidelity

WTP-HAMS

Wi-Fi Timed inertial combined with odometry Pulse in a Hybrid Active Mobility Scooter

Chapter 1 Introduction

This chapter introduces the thesis starting with an introduction to indoor localisation including advantages and related challenges. It states the purpose of the research including its aim, main objectives and reasons behind the research, objectives of this research and its achievements. It also describes the business and technical motivations of this research, especially the target audience. Furthermore, it highlights the challenges concerning indoor localisation, including the limitations experienced during indoor localisation system development. Finally, it briefly summarises all chapters of this thesis in a tabular form.

1.1 Indoor Localisation

According to D. Zhang et al [1] in 2010, Dempsey defined indoor localisation as “a system that can determine the position of something or someone in a physical space such as in a hospital, a gymnasium, a school, etc. continuously and in real time”.

The interest in providing accurate indoor localisation has steadily grown over the years because there is potential for indoor localisation to revolutionise the way users navigate indoors, similar to how GPS revolutionised how users navigate outdoors. With knowledge of this ever-growing interest, researchers and scientist within academia and industry have committed over a decade worth of their efforts and resources into resolving this indoor localisation challenge. Especially because there is a recognition of the significance of indoor localisation as a crucial component of future location-based systems. This research area is discussed consistently in comprehensive investigations from W. D. Rencken [2] in 1994 to R. McConville et al [3] in 2018.

With reference to papers [2][3], it is our prediction that interest in indoor localisation would continue to increase as human needs continue to be more technology dependent. In particular, the exploitation of the steadily growing wireless communication systems such as indoor location detection and tracking systems. These systems have entered the world of consumers in several forms, like, health care, assisted-living, industrial,

transport, logistics and public safety systems to mention a few. This proliferation has encouraged ubiquitous systems.

The term “ubiquitous” in computing refers to the presence of technology everywhere and anywhere. Ubiquitous technology is a hybrid computing concept which involves seamlessly high integration of technology and with communication capacity in existing environments such that they recede into the background of our everyday lives. Our world has become ubiquitous because, technology has become smart enough to automatically and proactively predict an address or location of each user, especially in outdoor environments.

The GPS technology has satisfied the outdoor location positioning and navigation with the help of the satellite [10]. Software companies such as Google have used such technologies to their benefit. There is a wide range of applications dependent on this technology such as vehicular navigation, personal navigation/map reading and fleet management; to mention a few. As wonderful as GPS technology is, it is only limited to outdoor activities and applications. Its inability to be seen indoors is a challenge to technologists everywhere.

Therefore, to mitigate the limitations of GPS, wireless network sensor systems are used in many buildings and rooms because they realise the ubiquitous goal for users, internet and the environment to be connected constantly to a network. Specifically, it allows the development of systems such as smart devices, with real-time location messaging and management of seamless location detection experience for users within buildings.

The advancement of technology in the world today has led to the high proliferation of smart devices and the birth of next-generation systems, algorithms, services and applications with sensor support focused on improving the quality of life of its users, in terms of, health care, security efficiency, home automation, social interaction within communities and social platforms. Continued research in indoor positioning using smart devices within smart environments has not only activated a shift in the paradigm of

location-based technologies but has also contributed to the expansion of services including logistics and navigation.

So far, scientists have been able to achieve indoor accuracy of about 2 - 3 meters using Wi-Fi technology [4] on pedestrians and 3m – 5m using wheel encoders [5] on mobile robots but it is undeniable that such precision within a care homes or hospitals will be inadequate in scenarios where the subject of interest is the location of a mobility scooter user in an emergency or in a crowd.

Indoor localisation is an area of particular interest due to its social-economic relevance and implementation in several applications. It is particularly relevant to individuals such as the elderly, people with physical impairment, carers and corporate bodies like service providers as it enhances services and users' quality of life. This, therefore, calls for an intelligent system that can better estimate its user's true location within buildings to provide services such as tracing and tracking, security and pattern recognition amongst others.

Some of the challenges indoor localisation technologies pose for our target audience are the legality and ethical acceptability. These challenges include unwanted monitoring and tracking of mobility scooter users who are vulnerable individuals suffering from either physical impairment or old age related sicknesses such as Alzheimer. These challenges are mitigated by providing users with

- Sense of independence and individuality
- Option to turn off and turn on the system at will.

Life expectancy since the 1980s till now has steadily increased due to accessibility to innovative medical science and technology, unprecedented wealth, better nutrition and healthier lifestyles.

Presently, there are 125 million accounted for people aged 80 years and beyond in the world. World Health Organisation (WHO) [22], reveals that the population aged 60 and over will total 2 billion by 2020, which is a huge jump from 900 million in 2015. It is

predicted that this ageing population will approximately double according to the World Health Organisation (WHO) [22], from its current 12% to 22% between 2015 and 2050. More than half of the annual population increase will be from India, Pakistan, China, Bangladesh, Nigeria and the United States [6]. Their findings also predict that by 2020, the populace of over 60's will outnumber children aged 5 years and younger.

Improved indoor localisation would be relevant to the ageing population, 60 years and older in areas of health care and security. In the united kingdom, the National Health Service (NHS) constitution has created special health provisions for persons who fall under the Old Age Dependency Ratio (OADR) category, in particular, people with mobility impairment [7]. It is estimated that the NHS sees over 1 million patients every 36 hours, therefore, it is virtually unfeasible to monitor and assure each patient's wellbeing [3]. Therefore, health care institutions such as care homes, hospitals and assisted living environments would benefit from an improved indoor localisation system that provides immediate trustworthy positioning of their guests (mobility scooter users), especially in instances of emergencies.

Unfortunately, a solution to accurately track a mobility scooter user in rooms is not in existence, to the best of our knowledge. Therefore, a system is proposed to provide more accurate indoor positions with an error range of 0.35m – 1.35m for indoor mobility scooter users. The system is highly cost-effective because it exploits already existing ubiquitous technologies such as Wi-Fi routers, wheel encoders and smartphone with its IMU modalities including accelerometer and magnetometer.

1.2 Business Motivations

Having discussed the target audience [in section 1], the proposed investigation would provide the following benefits for mobility scooter users:

- High sense of independence for users and peace of mind for caregivers
- Transmission of the improved estimated true location of users to relevant authorities for security and rescue purposes.

- Point of interest detection. These include elevators within shopping malls, finding specific stores or person of interest etc.
- Enhancement of user's efficiency and convenience in accomplishing daily tasks that require physical movement.

It should be pointed out that the exploration not only focuses on the ageing population (especially those who fall under the OADR) but particularly individuals who use mobility scooters. A very small population of this target audience can afford health care luxuries and necessities because a larger majority are either pensioners or health patients aged under 65 and over with limited financial resources. However, the smartphone is now a ubiquitous technology and in the UK about 64% of senior people own one according to statista [8].

The ubiquitous smartphone is appreciated for its familiarity, ease of use, supporting sensors and applications. It offers an excellent platform for localisation, which can potentially influence existing localisation methods beyond the popular GPS and ZigBee. Smartphones in comparison to platforms such as ZigBee [15] boast of easy user understanding thanks to its ubiquitous nature, higher efficiency, accessibility, usability and flexibility [8][15]. In particular, statista [8] which, demonstrate the high demand for precise indoor localisation Location Based Services (LBS) running on smartphones with Android operation systems (OS). This is considerable true because a very large percentage of the target users use smartphones with Android OS.

Typically, indoor positioning systems tend to be quite expensive [9] with costs comprising of numerous constituents such as the costs of infrastructure, the technology that transmits and receives position information for each test, system set-up and maintenance. To ensure cost is inexpensive, it would be beneficial to investigate a system that exploits already available and accessible technologies for mobility scooter users which include, mobility scooter, a smartphone with IMU modalities and Wi-Fi routers which both have no extra incurred costs (such as sensor installation charges), thus providing economic advantage.

A realisation that not all mobility scooters come with wheel encoders, it would be advisable that the proposed system develops its custom inexpensive wheel encoders. This is the only incurred cost. This cost can be avoided by purchasing mobility scooters with inbuilt wheel encoders.

It should make great use of available technologies, therefore, challenges like cost, inaccessibility and foreignness would not be a source of concern to users and developers.

With awareness of the need for a cost-effective improved indoor localisation system, and the ubiquitous nature of technologies like Wi-Fi routers, smartphone, wheel encoders and even mobility scooters, it is safe to predict a high likelihood of users would have a long term dependency on our proposed system in the near future because of its several advantages to users.

1.3 Technology Focus

Indoor localisation gap begs our research to exploit environmental sensors (Wi-Fi technology), mobility scooter technology (wheel encoders) and smartphone sensors (IMU sensors), as much as possible. It also encourages the combination of the above technologies, in a proposed investigation (WTP-HAMS system) to get better indoor positions.

Why Wi-Fi?

Of all environmental sensors, Wi-Fi is the most ubiquitous because it is present in most commercial environments and homes. This ubiquitous technology is beneficial for designing wireless systems capable of calculating position estimation in rooms.

Thriving commercial environments like care homes, hospitals and offices have a minimum of seven access points in their buildings at floor level as recommended by CICSO bestpractice [10]. Each access point signal is accessible by any smartphone within range. Exploring the opportunity to use the barest minimum number of routers/Access

points (APs) to improve accuracy utilizing the widely used smartphone is still an area of keen interest.

RSSI is a technology propagated from the ubiquitous Wi-Fi technology. Typically exploited for tracking and localising indoor target objects. It is, however, unreliable in providing accurate positioning of target objects.

Prevailing relevant representative research by Alex Maria kakis et al [11], tested with one router in a commercial environment, where they calculated an error mean of 2.3m using adopted dead-reckoning techniques and geometric methods. Other studies, by [4][12][13][14][15][16][17], proposed that an increment in the number of propagated routers would better the position accuracy. Therefore, K. Chintalapudi [4], proposed to use two routers in their own indoor localisation solution, where they implemented EZ localisation model and resulted in a median error of 2m and 7m in small and large buildings respectively. Then, D. Omkar and P. S. S. Koul [12], proposed to test for position accuracy improvement with three routers. They adapted the trilateration method that combines RSSI distance measurements from three routers, to result in an error of approximately 9m. Since three routers underperformed, J. Yang and Y. Chen [13], proposed to experiment with four routers for improved position accuracy. Their study reported a result of 29% median error, using regression-based and correlation-based approaches. To further investigations in using four routers for indoor localisation, S. Boonsriwai and A. Apavatjirut [14], explored multi-trilateration which resulted in a promising approximate error of 2.816m. Then, researchers, A. S. Paul and E. a. Wan [15], proposed to combine five routers/access points (APs). They adapting sigma point Kalman filtering and resulted in an average error of 3.45m. Following the poor performance from five routers [15], S. Boonsriwai and A. Apavatjirut [14], proposed to test for position accuracy using multi-trilateration of six routers. The result was an approximate average error of 6.641m, which is unsatisfactory compared to the 2.816m error from combined four routers. S. Mazuelas et al [16], explored the combination of eight routers/access points (APs) which resulted in a mean error of 3.987m. This system will be quite expensive because it would require commercial environments to install additional hardware more than the recommended minimum of seven. Later, J. Cheng et

al [17], explored the combination of 10 routers, using a decentralised scheme based on matrix completion. Their system result was a median absolute error of 1.1m. Unfortunately, investigations such as that from J. Cheng et al [17] are simulated and expensive. Therefore, its feasibility and implementation in real-world scenarios are unclear.

It is our deduction that more is not always better. Therefore, in the real world environment, we would be testing 3 and 4 routers because they show best position estimates in realistic settings wherein a commercial environment, the smartphone can get RSSI signal from at least three routers/APs. It is expected that our proposed WTP-HAMS (Wi-Fi Timed inertial combined with odometry Pulse in a Hybrid Active Mobility Scooter) system would best adopt 4-router combination.

Why wheel encoders?

Wheel encoder technology is ubiquitously used by vehicles to compute travelled distances. Therefore, we suspect it would be beneficial for calculating travelled distances and pose of an indoor vehicle mobility scooter.

We noticed most indoor localisation practices are predominantly tailored to pedestrians [18][19][20][21]. However, this proposed investigation is for users moving in translational motion on a mobility scooter.

To the best of our knowledge, there are no studies for localising mobility scooters, however, because of its translational motion similarities with robots, an understanding of the principles surrounding robotics kinematics, odometry and motion like in the paper by A. Jha and M. Kumar [19] are recommended.

A. Jha and M. Kumar [19], discussed how the position accuracy of robots is an issue, especially when considering the odometry of a robot to find an accurate pose estimation. This is because odometry inevitably suffers from drift, which is an accumulation of errors over a period. It is predominantly due to wheel slippage and unequal wheels diameter,

amongst other factors. Proposing odometry models, their results showed an accuracy error of 3m – 5m when using the robots in-built wheel encoders only and an error of 33cm - 51cm when combining robots in-built wheel encoders with IMU.

We propose to adopt odometry models of the robot [19] when calculating relative pose estimates of our mobility scooter. This is important because it produces good pose result, especially when combined with our proposed IMU combination.

Why smartphone IMU modalities?

The smartphone is one technology that is not only ubiquitous but has fast become a vital device for users, especially because of its efficiency in the daily lives of users (such as communication and outdoor navigation) and its easy accessibility.

This technology has 512 inbuilt modalities and amongst them is the IMU sensors, which is responsible for measuring the direction, rotation and orientation of the smartphone. Therefore, the proposed investigation considers using smartphone IMU modalities to measure navigation heading of the mobility scooter.

Representative research by O. Woodman and R. Harle [22] tackled a pedestrian localisation problem using IMU (otherwise referred to as inertial measuring units), which includes a combination of accelerometer, magnetometer and gyroscope. Their investigations resulted in heading estimation accuracy of 75% - 95%. This is an impressive result, however, it is for the pedestrian who move in pedestrian motion with the mobile device in a vertical orientation. While for robotics [19] combined inbuilt IMU with odometry from its wheel encoders will result in the improvement of accuracy error from 3m – 5m to 33cm -51cm.

1.4 Proposed Investigation

This study addresses the problem of improving indoor accuracy, in particular with the use of cost-effective and energy efficient methods. It specifically includes combining ubiquitous technologies such as smartphone IMU modalities accelerometer and magnetometer, with inexpensive complementary technologies usually found in indoor environments like Wi-Fi routers, and, technologies generally found in automobiles such as wheel encoders, to improve indoor localisation for mobility scooter users.

1.4.1 Aim and Objectives

This research is aimed at improving indoor positioning accuracy for mobility scooter users (such as the elderly and people with mobility impairment) through effective combination of sensor data from ubiquitous technologies, within an ecosystem of integrated outputs from environmental sensors (Wi-Fi technology), smartphone devices (IMU sensors) and vehicle systems (wheel encoders).

In particular, a server-based smart system combining the results from all mentioned technologies for indoor positioning improvement is proposed. This includes the objectives of the research, highlighted below –

- Learn about the environment, smartphone and indoor vehicle sensors and how these can be used to localize environment static and dynamic objects.
- Understand the state of the art of indoor localisation and the different used methods.
- Learn appropriate software tools and hardware specifications to allow me to implement and experiment with the relevant sensors and to devise and engineer new solutions.
- Design a new approach that combines environment, smartphone and indoor vehicle sensors. Produce development and experimentation plan.
- Carry out pilot and formal evaluations to assess the potential and advantages of the proposed new approach.

- Present and analyse evaluation outcomes. This includes learning about related statistics.
- Produce scientific publications based on the developed experimentations and results analysis.
- Write the thesis manuscript.

These above-mentioned objectives will lead to the conceptual design and development of a new system, called: WTP-HAMS (Wi-Fi Timed inertial combined with odometry Pulse in a Hybrid Active Mobility Scooter) system which is a unique combination of mathematical concepts, techniques and models. It combines position estimates from RSSI (Wi-Fi) with relative pose estimates from a proposed novel odometry model (combined wheel encoders and IMU sensors) to result in new absolute position with reduced errors.

1.5 Motivation and Challenges

Why propose WTP-HAMS system?

WTP-HAMS system would combine the advantages of the following –

- Wi-Fi – position estimation with room reference
- Wheel encoders – distance travelled and pose with reference to the mobility scooter
- Smartphone IMU modalities – In particular accelerometer and magnetometer for navigation heading

Unlike robots, conventional mobility scooters are not designed with inbuilt wheel encoders and IMU sensors. Therefore, inexpensive wheel encoders were built and a smartphone with IMU modalities was employed. Also, the smartphone consolidates all data from Wi-Fi, Wheel encoders, and combined accelerometer and magnetometer sensors.

The proposed system WTP-HAMS offers a complementary combination of RSSI, odometry and inertial measurements to reduce position error to an average range of 0.35m to 1.35m.

Challenges

It is not unusual for positioning performance to degenerate when –

- In the case of the smartphone, its hardware constraint reduces dataset resolution by approximately 10%. The age of the Samsung galaxy note 1 and the discontinuity of its operating system (OS), support encourages system crash or freeze. This ends up influencing timestamp results.
- In the case of Wi-Fi, the Line of Sight (LOS) between transmitter and receiver is affected, and None-Line-of-Sight (NLoS) is present. This factor involves the ability of the positioning system to comfortably detect target objects like mobility scooter when the positioning scope gets wider. Also, obstructions such as human presence or large furniture influence the system's positioning accuracy.
- In the case of wheel encoders, the drift in the relative travelled distance is high. This significantly negatively influences pose accuracy.
- In the case for smartphone IMU modalities,
 - Smartphone orientation including vertical orientation and horizontal orientation can influence heading navigation results of a translational moving mobility scooter. This is important because predominant trials by literature have been for pedestrians with a smartphone in a horizontal orientation in their pockets.
 - The right IMU combination is a challenge because to better get heading navigation, the following combinations should be considered – accelerometer and magnetometer versus gyroscope, accelerometer and magnetometer

Location systems usually scale on two axes: density and geographic scales. Geographic scale refers to the area or volume covered (this information is usually provided by a map)

while density refers to the number of units detected per unit geographic space per time period. Current indoor location systems locate target objects in 2-D space.

Depending on the number of units gathered in space or expanse of space covered, indoor localisation, especially wireless systems can become congested, thus resulting in errors. This is true in particular for wireless systems including RSSI (Wi-Fi) and odometry (wheel encoders).

The thesis investigates the proposed WTP-HAMS system which would combine the results and errors of RSSI (Wi-Fi) and a proposed novel odometry model (consisting of a combination of wheel encoders, accelerometer and magnetometer). The idea is to design a more robust system because it takes advantage of the errors the technologies demonstrate.

Our research investigates how WI-FI, IMU sensors and wheel encoders will be beneficial for our proposed WTP-HAMS system. Although each of the aforementioned technologies has their limitations, they are necessary for accomplishing the aim of this research which is indoor position accuracy improvement. It is expected that noisy environments such as care homes with a smooth wooden tiled floor will benefit from our proposed WTP-HAMS system.

1.6 Contribution to Knowledge

Thesis novel contributions to the current state of knowledge are summarised as follows:

Novelty in application

- **WTP-HAMS system** – the unique combination of technologies, techniques and models to achieve indoor localisation. This includes the following –
 - **Wi-Fi technology** – SDRS log-normal shadowing model for distance estimation + multi-trilateration for position estimation.

- **Smartphone technology (including IMU)** – a combination of Magnetic angular rate update (MARU) and acceleration gradient update (AGU) of MAGYQ filter.
- **Wheel encoder technology on wheels of a mobility scooter** – odometry model.

The novelty in mathematical models

- **New drift mitigation model** which improves travelled distance by adding a deviation error percentage to initial calculated travelled distance.
- **Novel odometry model** which provides combines heading navigation (from accelerometer and magnetometer) with new travelled distance estimates of the new drift mitigation model.

New unique classification of Hybrid indoor localisation

- Proposed two categorisation
 - Technology and Technique Hybrid (TTH).
 - Propagation based hybrid system.

1.7 Thesis Outline

This thesis consists of seven chapters detailing four years of investigation into the improvement of indoor localisation accuracy and the proposal of WTP-HAMS system.

A document organisation of this thesis is summarised in Table 1-1 on page 37.

Chapter	Description
1	Presents an overview of the research area. This chapter embodies the justification of the research direction by outlining aims, motivations, challenges and contribution to knowledge.
2	Reviews background knowledge on related technologies, methods and protocols associated with our research.
3	Elucidates on the in-depth comprehension of state-of-the-art related to the research area.
4	Describes the research methodology with an emphasis on our proposed WTP-HAMS system. This includes system development strategy and design and novel conceptual methods.
5	Discusses the implementation of our proposed methodology, including the software architecture and technique used in our proposed WTP-HAMS system.
6	Examines and analyses the assessment and results of all studies necessary for our proposed WTP-HAMS system to achieve improved indoor localisation. It discusses WTP-HAMS system tests and lessons learned.
7	Concludes the thesis with a summary, outcomes from the research and future works

Table 1-1 Document organisation

Chapter 2 Background Knowledge

This chapter provides basic knowledge of relevant technologies, methods and techniques adopted based on the two categories of location positioning systems, including physical localisation and topographical based categories. It discusses examples in detail with the results, advantages and limitations of the two aforementioned categories. Furthermore, it introduces and describes key mathematical techniques, models and methods our proposed WTP-HAMS system will employ. Then, it lightly reviews state of the art of mobility scooter with regards to indoor localisation. Finally, it presents a summary of this chapter stating technology, methods, models and algorithms the proposed WTP-HAMS system will be employing.

Overview

Location localisation is very crucial as it plays a significant role in numerous applications such as vehicle navigation, location identification, emergency services, fleet management, automated billing, network optimisation, resource management and travel aids which are usual location-based service (LBS) applications in this area [23]. Continuous research into location localisation, have developed several plausible approaches, methods, algorithms and techniques, which aim at finding a target object's true location/ground truth.

When developing a system that aims at improving indoor position accuracy for both stationary and moving target objects, a complete investigation into the background of existing localisation technologies, algorithms and techniques applied for outdoor and indoor environment must be conducted.

Location positioning systems can be grouped into several categories, but, prevailing understanding provides two best categories, including –

- *Physical localisation-based category*, which groups localisation systems in terms of techniques and technologies.
- *Topographical based category*, which groups positioning systems in reference to their environment, i.e. indoor and outdoor.

2.1 Physical Localisation Based Category

The physical localisation category refers to a target object's current location in environments such as homes, virtual environments, offices, shopping malls or hospitals. This category can be subdivided into three [24], namely,

- Illustrative localisation
- Spatial localisation
- Network localisation systems

Illustrative localisation utilises data such as name, number or identity to describe geographical object locations of structures, cities, countries or mountains. In professional applications where illustrative localisation is insufficient, **spatial localisation** is applied as it is the point denoted by two-three dimensional coordinates within Euclidean space. **Network localisation systems** fall under the physical location class of localisation that is reliant on the topography of a communications network. Network localisation system is typical for tracking and locating target objects. It is generally based on address protocol.

Our proposed system is based on network communication, therefore further discussions on network localisation systems are examined.

2.1.1 Network Localisation Systems

In recent times, network localisation systems are fast becoming the preferred localisation technique due to their capability to provide more refined data in terms of object accuracy. Networking systems are evident in many indoor and outdoor localisation solutions. To

attain localisation ubiquitous goal, every user and surrounding objects will be connected to a network constantly through easily accessible technologies. It should detect and manage the position of target objects in real time.

Investigations display the two categories of network localisation systems, namely,

- Cellular network systems
- Sensor network systems

2.1.1.1 Cellular Network

Over time, cellular networks have evolved rapidly into a comprehensive wireless communication infrastructure with almost worldwide coverage [25]. By 2012, a record of more than two million base stations (BS) was deployed due to the development of new generation cellular networks [26]. It is observed that these new generation cellular networks experienced limitations due to a significantly high amount of energy consumed when signals are transmitted over wireless channels. Consequently, cellular networks experienced unprecedented data overload as it continues to struggle keeping up with other technologies [27]. Major investment in the radio access network and core infrastructures is to be provided to accommodate growth.

Position accuracy in cellular networks is limited by interference exacerbating methods and non-line-of-sight propagation (NLoS), thus resulting in the transmission of inconsistent data [28]. Traditionally, cellular service areas are divided into cells and each cell possesses its infrastructure base station or cellular tower. Several techniques have been adopted to track mobile client within the network. A successfully deployed technique is the establishment of two-way communication between the mobile client and the network. This technique of utilising cellular networks to predict client location involves the usage of the mobile network and the network-based positioning determinant equipment to locate the location of the mobile device. Cell identification is the most basic method of location determination using cellular networks. Cell ID is determined from base stations with known locations when the allocation of the connected mobile device

to a base station that transmits the strongest field strength is realised. Evidently, studies have shown that cell sizes alone are not adequate enough for location localisation but the provision of supporting technologies will potentially enhance the mobile location accuracy due to its low air interference requirement, its decency on sector size and its propensity for hybridization with other techniques. G. Deak et al[29], classifies cellular network techniques under either *standard* or *non-standard communication* categories.

- **Standard Communication**

Standard communication techniques include triangulation, Time of Arrival (ToA), Time Difference of Arrival (TDOA), Enhanced Observed Time Difference (E-OTD) and Angle of Arrival (AoA).

Triangulation [5] technique can be established when the two necessary reference nodes are determined. With this method, the location of the target node can be determined by the intersection of direction lines. The illustration in Figure 2-1 shows how triangulation works in 3D. A and B symbolize reference nodes, after obtaining the angles θ_1 and θ_2 , the physical target position T can be estimated based on the set coordinates of the reference nodes.

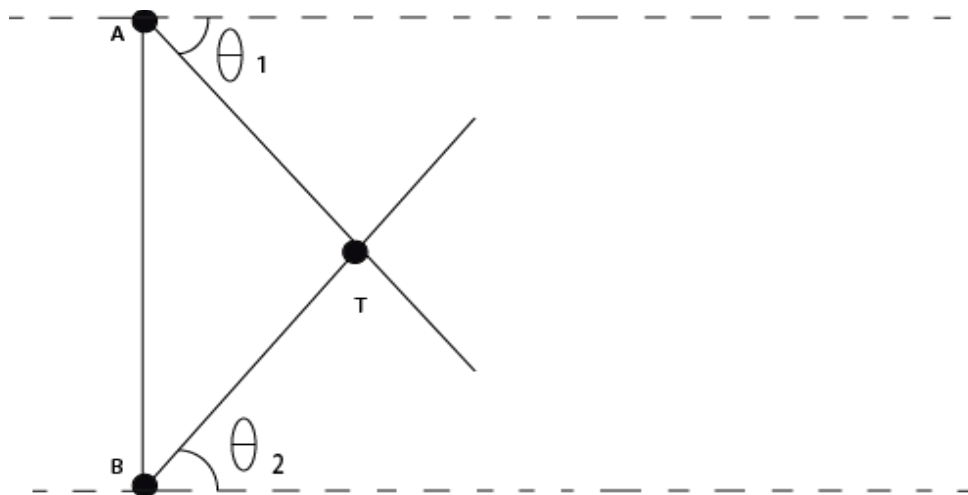


Figure 2-1 Triangulation method

Time of Arrival (ToA) [30], requires the synchronisation between base stations and mobile stations for distance. This standard works by calculating the conversion of time taken between bursts sent by the mobile and the base stations, to derive distance. It is therefore adopted by triangulation for target object localisation estimate.

Time Difference of Arrival (TDOA) [30] (see Figure 2-2) technique is very much like the ToA. Compared to ToA that only measures the time it takes for one signal to travel from emitter to receiver, TDoA method requires each the base stations to simultaneously transmit two signals having different frequencies at different times.

TDoA, like ToA, requires the conversion of the time difference to distance and the trilateration of three distances from a base station for target object position estimation.

Enhanced Observed Time Difference (E-OTD) [30] (see Figure 2-2), is a modification of the ToA method and it measures the difference of arrival time of a transmitted signal from the synchronization between at least three base stations and a mobile device within a network. This particular technique is best suited for outdoor environments as it possesses a lag of about 5secs and an accuracy estimation within 50 m – 125m.

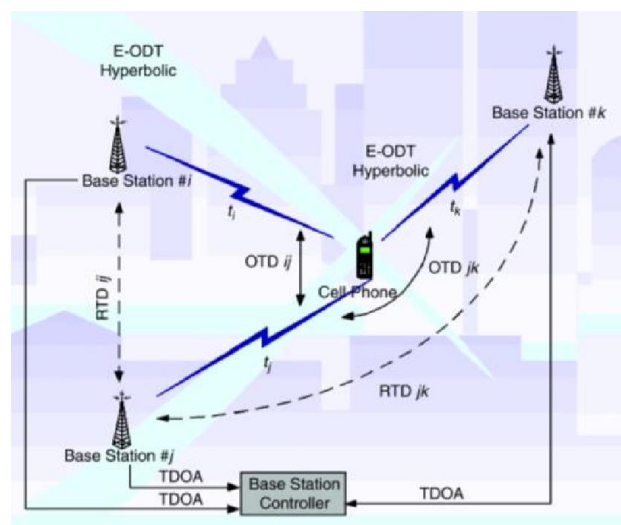


Figure 2-2 E-OTD positioning solution [30].

A developed technique which is not widely adopted because of low accuracy estimation is **Angle of Arrival (AoA)** [31]. AoA requires the use of directive antennae or an array of antennas. To reduce the accuracy error of this technique, researchers have hybridized the technique by combining it with TDOA distance estimation techniques in its application as illustrated in Figure 2-3. Triangulation is a technique applied to complement AoA measurements. This calculation can be used to determine the position of the target node as it is based on the measurement of angles. Furthermore, observations show that triangulation can be translated to trilateration as the distance between nodes can be derived from the bearings between them. All afore-described standards depend on various means of triangulation and trilateration of signals from cell sites servicing mobile devices/phones within a network [28].

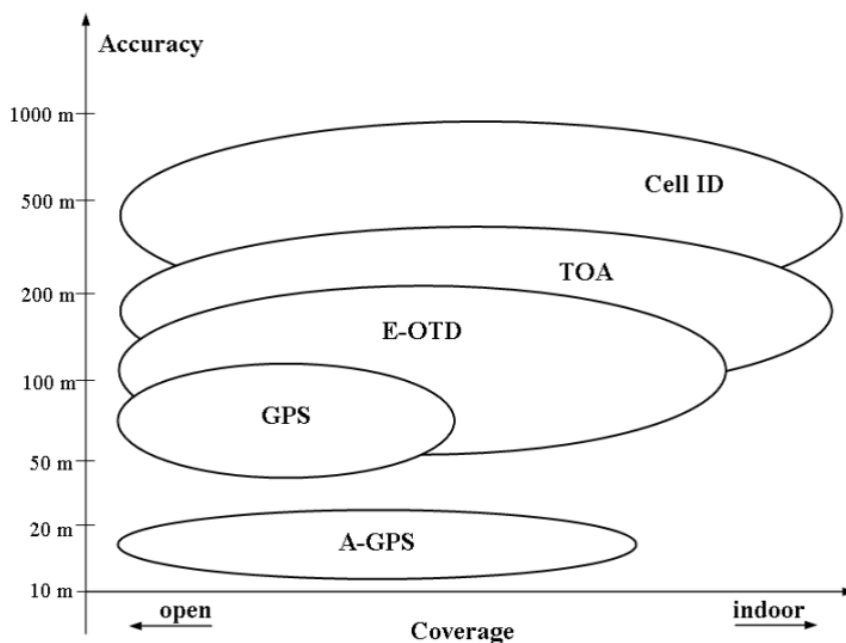


Figure 2-3 Graphical illustration of positioning techniques [28]

In Figure 2-3, M. Yassin and E. Rachid [28] summaries localisation prowess of each technique within standard communication mentioned above against the common GPS standard. The performance criteria adopted for positioning comparison are accuracy and coverage. Observation in the literature [28] supports the already accepted truth that localisation methods are best acceptable when the accuracy error (which is the distance between real physical geographical location and estimated location) is lower while its coverage is great.

○ **Non-standard D2D**

Localisation solutions have progressed from the standard methods mentioned above by embracing non-standard methods to improve the localisation accuracy of target objects in cellular networks. This non-standard is categorised into three, namely,

- D2D communication
- Location detection using pattern matching,
- Localisation utilising smart antennas

D2D communication

D2D communication [32][33] in cellular networks, allows a direct communication link between two devices without requiring radio signal to travel through the base station (BS) or core network. Traditionally, communications are required to travel through the BS regardless of devices short proximity. To accomplish D2D communication, a quick transfer of large data set is possible between mobile devices over a short range. This provides shorter traversal paths and there are advantages in its ultra-low latency in communication.

Short range technology like LTE and Wi-Fi can be employed in the enabling of D2D communication [32]. Parameters such as data rates, applications, signal strength, range between 1-hop devices and device discovery mechanisms greatly influence calculation

outcome. For example, LTE direct provides a range of 500m at rates up to 13.5Mbs while Bluetooth provides a range of 240m at a maximum data rate of 50Mbps.

D2D communication is beneficial in supporting information sharing, coverage extension, machine to machine communication, data computation offloading and local data services via three data transportation modes, namely unicast, broadcast and multicast. Unicast also regarded as one-to-one, is the transmission of information from one source to destination. Broadcast referred to one-to-all, is the transportation or offloading of data information from one source to all possible destinations. Finally, multicast, which can be called one-to-many is the transmission of sent and received data sets or signals from one source to multiple destinations.

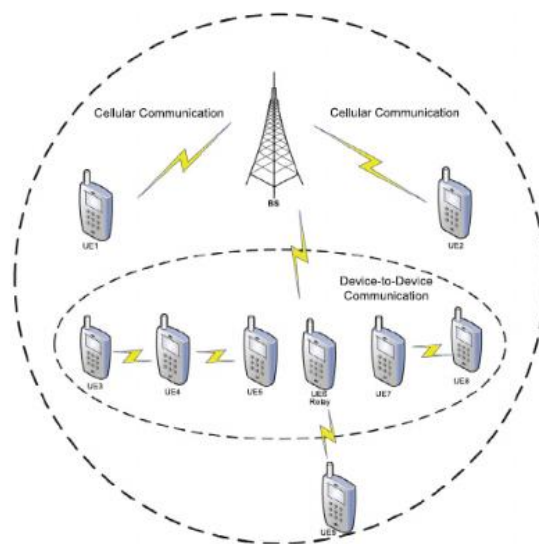


Figure 2-4 Device-to-device cellular communication [34]

Asides from Wi-Fi being ubiquitous, it can work in unicast, broadcast or multicast transportation mode. This is especially advantageous for our proposed WTP-HAMS system because our system works in a unicast environment where power requirement is minimised and data rate to the smartphone is maximised.

Pattern matching

Location detection using pattern matching acknowledges the multipath attributes of a mobile phone as fingerprints. This non-standard technique tackles problems some standard techniques such as AoA and ToA/TDoA might encounter in metropolitan areas where multipath is intense. This involves location servers and databases that contain actual and estimated location measurements of signals. The client location is estimated by comparing the received signals to the signal values saved within the database. This method does not rely only on the signal values, it allows other characteristics of the signal to be utilized.

Pattern matching allows for device detection by utilising and applying multipath delay. This is illustrated in Table 2-1.

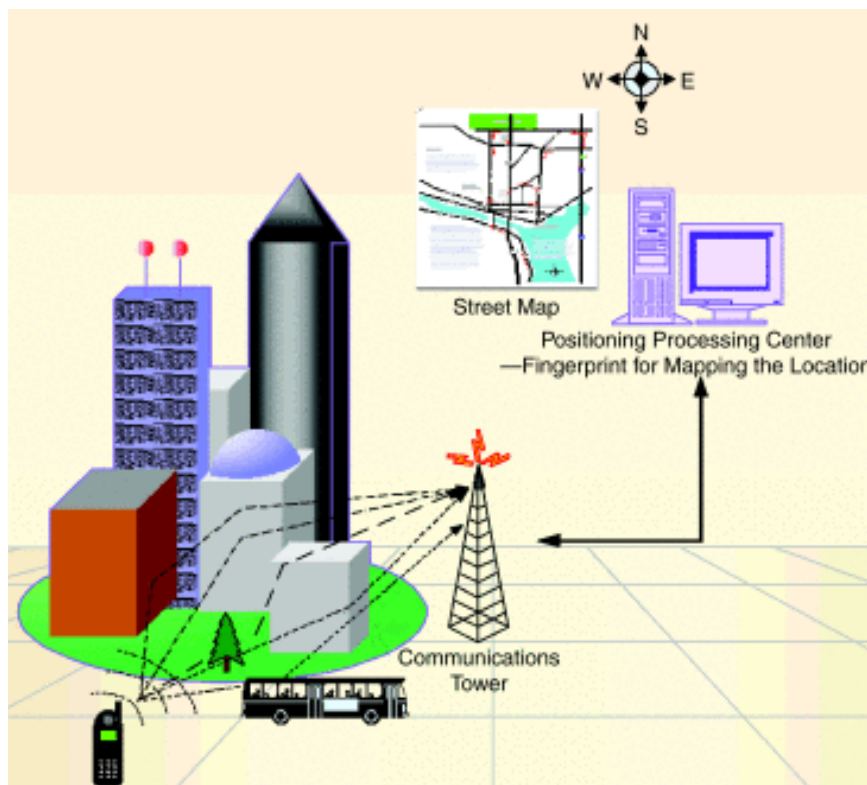


Table 2-1 Pattern matching method collecting multipath characteristics as the “fingerprinting” of mobile phones [23]

Localisation utilising smart antennas

This non-standard technique relies on angle-of-arrival (AOA) and direction of arrival (DOA) standard communication techniques as the measurement factor. The technique offers diverse means to improve the performance of wireless systems. This improvement includes higher coverage provision, improved system capacity and sensitivity to non-ideal activities reduction [34].

Smart antennas like the adaptive antenna system is a combined network that utilises an array of low gain sensor elements and real-time adaptive signal processors [34][35]. The antennas are initially calibrated and programmed for automatic adjustment of performance parameters such as beamforming weights and RSSI to enhance positioning. An on-line capturing system which consists of three readers and a target is developed by C. H. Lim et al[34]. Their system required a PC with a parallel port to control the beam former of a 4-element uniform linear array smart antenna. The PC which acts as a server within the processing network estimates the client's location through triangulation calculation of consolidated angle and RSS data only (see **Table 2-2**). Using room dimension 8m x 9m (shown in **Table 2-3**), they conducted simulated experiments with their proposed system to result in a 1m range accuracy.

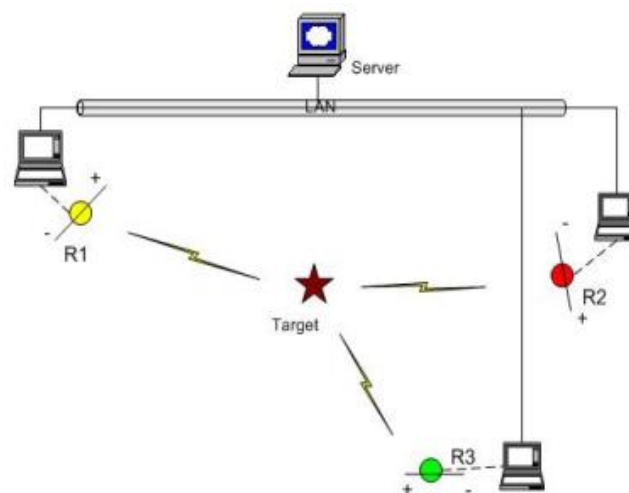


Table 2-2 A triangulation of Wi-Fi routers using AoA of smart antennas [34]

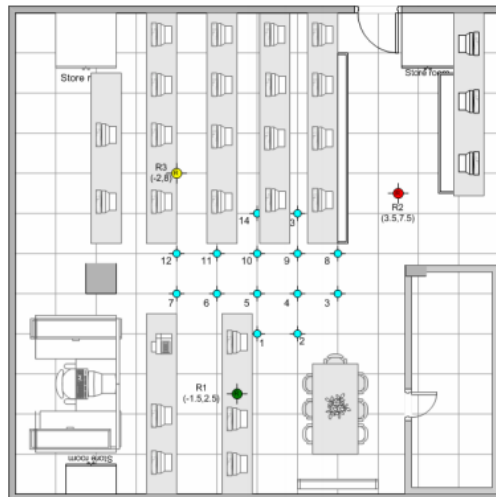


Table 2-3 Indoor Wi-Fi Localisation System Utilizing 3 Smart Antennas [34]

Although this approach displayed a resolution accuracy better than some established solutions such as RADAR and RF fingerprinting [34], it is limited due to unavailability of the database to store new data and access previously saved data. This implies the system will be required to spend more power and time re-calculating previously calculated areas. The system is very dependent on cell sizes and is disadvantaged because each reference point must be deployed in a permanent direction thus rendering the system impractical in dynamic environments.

In summary, non-standard communication-based systems use combined methods from standard communication to achieve its improved indoor localisation. This, therefore, produces robust systems that result in better indoor position estimates.

2.1.1.2 Sensor Network

Sensor networks are popularly employed by indoor localisation researchers because they are beneficial in solving “localisation problem” especially within smart environments [35][36][37]. In particular, wireless technologies used for indoor location estimation. It is important because, it is an ad hoc network which has relatively small, standardised, cooperative, and inexpensive sensors with inexpensive low power processors and

wireless networking [35]. Sensor networks have autonomous nodes that are empowered with capabilities for calculating, sensing and wireless communication.

Sensor dependability is becoming a preference by scientists due to the considerable amount of location-aware protocols being proposed for networking and 'ad-hoc' tracking.

Although there exist several algorithms and techniques for indoor positioning improvement, our document will be focusing on Node localisation methods. This is important because it is relevant to the proposed investigation method.

• **Node Localisation Methods**

Sensor networks rely on deployed nodes with known location to transmit to other nodes with unknown coordinates at known as reference points) to promote localisation of the unknown nodes. This includes nodes that possess unique location aware devices such as beacons.

This method can be analysed in the following categories –

- Localisation with static beacons
- Localisation with moving beacon
- Beacon-free localisation methods

Localisation with static beacons

Nodes, like Wi-Fi routers, within a sensor network work with localisation devices like smartphones which have Wi-Fi receivers because it calculates and presents location information based on data from Wi-Fi.

Wi-Fi routers can be referred to as a beacon because its location is known. Otherwise, nodes like smartphones that are unaware of their location are referred to as unknown location. When a localisation system is built using methods like proximity and ranging in

the literature [73][74], it is run with the purpose of calculating the unknown's location relative to the coordinate system of the beacons.

This is further explained in journals [35][36], where it was discussed that an unknown node can approximate its location if three or more beacons (also referred to as known nodes) are present in a 2D space. The unknown node becomes a beacon after its location is known. This new beacon becomes the node through which, new unknowns can estimate their location within an indoor environment.

Although static beacon is advantageous in determining positions, it is however challenged with its need for more beacons to compensate the blind spots where signals might get lost. Therefore, it begs the need to improve localisation robustness using a lesser number of beacons (like Wi-Fi routers).

Localisation using moving-beacons

To address the challenge stated in 'localisation with static beacons', relevant literature work [35] offers a solution to provide a robust localisation system using moving-beacons.

This system is described to involve the calculating of location estimations via mobile observers (also known as moving beacons) moving in an organised form within a global coordinate system. The location of each node is estimated by applying a transformation method to the range measurements. The expected result is a more robust system that effectively localises a moving target object using a smaller amount of reference nodes. This is because the practicability and cost-effectiveness of the system are of importance.

Beacon-free localisation methods

This is typically implemented in larger networks. In this scheme, the location of every node is established through native node-to-node communication. It is recommended that this positioning scheme be a fully decentralized solution with all nodes beginning with a random initial coordinate task. The nodes then collaborate by means of only local

distance estimations to work out a coordinated task. The resultant coordinate task possesses both translation and orientation which must be measured appropriately. Using reference data from sources such as wheel encoders and smartphone IMU modalities, a post-process is required to convert the orientation and translation coordinate task to absolute location data.

2.1.2 Conclusion and Analysis of Physical Localisation Based Systems

Indoor localisation is achievable through different physical localisation-based systems that provide position measurements. The dependencies of users to physical localisation-based systems vary with regards to accessibility, complexity, cost-effectiveness and accuracy.

The physical localisation-based system is categorised into illustrative, spatial and network localisation systems. Of all three categories, the network localisation systems show more promise, due to its ability to use easily accessible technologies in building cost-effective and accurate positioning system.

Within the network localisation system, it is observed that the sensor network system uses communication standards of cellular network systems to operate. This typically applies non-standard communication, (such as D2D communication, localisation utilising smart antennas and adaptive hybrid systems using data fusion methods) to node localisation methods like static beacons, moving beacons and beacon free based sensor network systems. This is important because it calculates for the position of moving objects in stationary and moving instances within real environments.

The proposed WTP- HAMS system is a sensor network which aims to design a less complicated, effective and inexpensive localisation system that would provide improved position accuracy to its users. In particular, it combines the benefits of the methods to achieve the described aim. This is shown in Table 2-4.

Adopted methods and communication standards for the proposed WTP-HAMS system		
Methods	Features	Benefits
Non-standard communication for cellular network systems	D2D communication	Wi-Fi and wheel encoder communication with smartphone
	Adaptive hybrid systems utilising data fusion methods	Combination of techniques such as RSSI position estimation and odometry based relative position estimation
Node localisation methods for sensor networks	Static beacons	Proposed to use less than 5 Wi-Fi routers for location estimation
	Moving beacon	Proposes to combine the odometry of wheel encoders with heading from accelerometer and magnetometer sensors
		Proposed to track moving objects like a mobile phone and mobility scooter
	Beacon free localization methods	Promotes node to node and D2D communication
Proposes a decentralised solution		
Promotes the calculation orientation and translations coordinate task		

Table 2-4 Literature works adopted in our proposed WTP-HAMS system

2.2 Topographical Positioning Systems

Based on literature works [28][40]–[42], it is typical to categorise localisation system into that groups based on topography. This includes –

- Outdoor localisation systems
- Indoor localisation systems

2.2.1 Outdoor Localisation Systems and Methods

Early position localisation systems were originally designed to cater for outdoor navigation systems such as aircraft, military and commercial navigation [43]–[45]. This is discussed to be important in the paper by H. Balakrishnan, et al [43] because location information was very instrumental to early navigators. These navigators used tools such as the sextant and quadrant, to calculate angle measurements of different solar bodies to the earth’s horizon. Then, these angle measurements were then used as location references. This was beneficial because solar bodies are known to travel in predictive paths relative to the earth, thus behaving like a group of likely reference points [43].

The twentieth century ushered in a drastic advancement in the quality and accuracy of outdoor positioning systems. This includes the Global positioning system (GPS)[46], Aircraft Radar [47] and mobile phone localisation [48].

Global Positioning System (GPS)

GPS is a popular technology adopted for outdoor tracking such as pedestrian and automobile navigation [49]–[51].

According to the literature work [46], today, a GPS satellite constellation comprises of twenty-four satellites that orbit the earth. The constellations follow familiar orbit, thus making GPS based location estimation predictable.

Each satellite uses atomic clocks to synchronise encrypted distinctive bit patterns of the transmitted radio signals with time. This is because the atomic clock is a highly reliable, low weight and stable technology, which guarantees 1m geo -location accuracy using very precise time when measuring radio signals path from the satellite to earth, as well as, the distance between the satellite and GPS receiver. The GPS receiver measures the time shift between each received signal stream from the different satellites.

The GPS positioning systems have been greatly developed on, to satisfy outdoor environments and today, it is currently used in many smart mobile devices [44]. However, GPS performs poorly in an indoor environment because it requires a clear line-of-sight (LOS) to perform effectively. In particular, the presence of walls and metallic objects, reflect, refract and attenuate GPS signals, thus making it unsuitable for indoor environments. This is a severe limitation because GPS will produce significantly large errors in an indoor environment.

Aircraft RADAR

This technology uses radio frequency (RF) signal to measure vehicle speed, weather prediction or aircraft recognition.

Proposed by E. B. Quist and R. W. Beard [47], the architecture of aircraft RADAR technology comprises of a rotating antenna with connected radio receiver and transmitter. The radio receives short bursts of radio signals transmitted from radio transmitters in vehicles or aircraft. It then considers radio frequency (RF) signal speed as it calculates the time difference of each received pulse at different distances with respect to the earth.

Mobile Phone Location Systems for 199 Or 112

This system was developed by the United Kingdom's office of communications (OFCOM) and regulatory body for telecommunications to enforce mobile phone operators successfully provide location information of users dialling 999 or 112.

In the past, emergency calls tracking were possible using landlines registered to addresses but as technology ushered in the era of wireless mobile phones, people evolved and position accuracy of users reduced significantly [52].

In the quest for a more reliable and accurate location detection service, OFCOM has encouraged collaboration with communication providers to provide accurate and reliable caller location information at no charge to emergency organisations using cell identification and zone codes which provides an accuracy of 20 meters [52], which is a significantly large estimation area.

This system will be insufficient in situations where the emergency call is from indoors, and time is of the essence. This could potentially endanger the lives of users, therefore systems for indoor localisation is essential.

2.2.2 Indoor Localisation Systems

Wireless systems have witnessed an overwhelming steady growth rate over the recent years and indoor localisation systems are not exempt as they are a critical need. This is because, these technologies have entered the world of the consumer in several forms including industrial, medical, transport system, logistics and public safety, to mention a few.

Generally, indoor localisation is categorised under the following three –

- Passive indoor localisation
- Active indoor localisation
- Hybrid indoor localisation

The above-mentioned categories above are expatiated on in chapter 3.

It is the goal of our research to design a system that improves indoor position accuracy, therefore, this thesis discusses a proposed WTP-HAMS system which considers wheel encoders, Wi-Fi and smartphone IMU modalities including accelerometers, magnetometers, and gyroscope (where most relevant IMU sensors in this system are accelerometers and magnetometers).

A background into the considered technologies is discussed below.

Wheel Encoders

Wheel encoders are part of the core sensors used in localising wheeled mobile robots. It is used to calculate travelled distances for each wheel in the robot.

The wheeled robot typically has inbuilt wheel encoders for performing localisation tasks. It combines outputs from each wheel to deliver direct measurements of the robot poses. However, these poses contain position errors because of drift over calculated travelled distance.

Relevant studies [5][19][53][54][55], discussed an odometry calibration system that potentially improves navigation accuracy. The researchers explored the conventional odometry model on wheeled mobile robots.

In the conventional odometry model, the centre if the robot is tracked using calculated parameters including left wheel travelled distance, right wheel radius travelled distance and wheel separation between the wheels. This performs good pose estimates over short distances. However, when longer distances are travelled, the system begins to suffer offset or drift as illustrated in Figure 2-5. Seongwoo Jang et al [54], describes drift as the cumulative error generated during long-distance travel.

The paper [5], tackled odometry error by creating an error matrix convenience model to achieve an error of 3-5m for a 720m travel path. Still, odometry [5] is observed to suffer drift over distances. This makes odometer from wheel encoder data unreliable and therefore inefficient in accurately localising robots over prolonged periods of time. Further study on odometry using wheel encoders can be found in reference paper by Y. Pei and L. Kleeman [55].

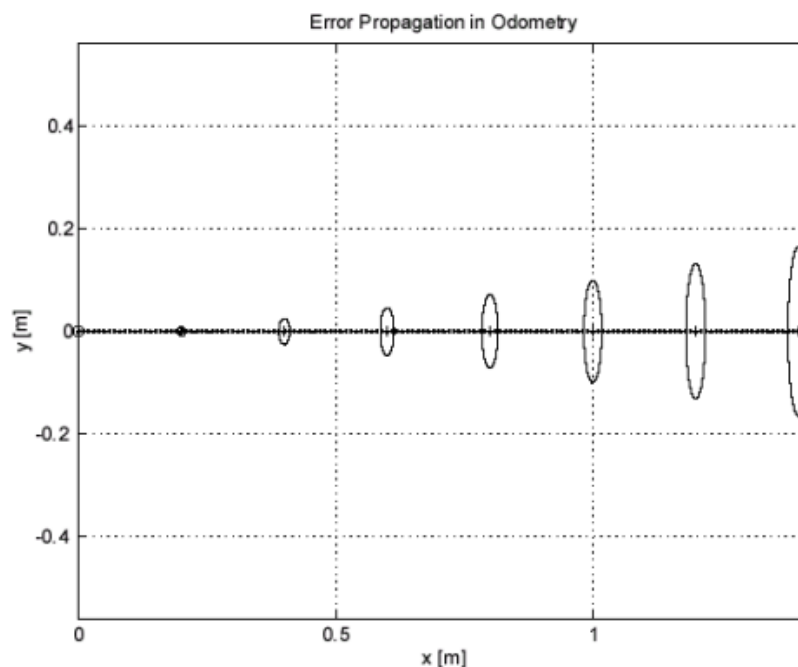


Figure 2-5 Odometry showing pose uncertainty growth in straight line movement [54]

Another research by A. Jha and M. Kumar [19], investigated the improvement of robot poses by combining the wheel encoders with IR range sensors. An odometry mathematical model was proposed using the conventional odometry model to uniquely combine kinematic model and Taylor's series as shown in Equation 1, Equation 2 and Equation 3.

$$x_{k+1} = x_k + D_c \cos(\phi)$$

Equation 1

$$y_{k+1} = y_k + D_c \sin(\phi)$$

Equation 2

$$\phi_{k+1} = \phi_k + \frac{D_r - D_l}{L}$$

Equation 3

Where,

x_{k+1} , is the current position from the previous position x_k ,

y_{k+1} , is the current position from the previous position y_k ,

ϕ_{k+1} , is the current direction from the previous orientation ϕ_k ,

D_c , is the distance travelled from the robot's centre,

D_r , is the distance travelled by the right wheel,

D_l , is the distance travelled by the left wheel,

L , is the length between the two wheels of the robot.

Their simulated system was designed to identify the behaviour of the robot as it obeys its program and travels to the next position while sensing landmarks around it. Results from their simulated experiments showed an error of 33cm. This result is good; however, drift is still experienced by the system.

Our proposed WTP-HAMS system intends to adopt and evolve elements of the proposed odometry model [19] for a user-controlled mobility scooter with three wheels. Our system proposes to design a cost-effective system that will produce results with errors lower than 33cm.

Wi-Fi

Wi-Fi-based indoor localisation has fast become an attractive approach of high importance due to its ubiquitous nature. It is used to calculate indoor position estimation using various measurement techniques such as ToA, AOA and RSS (discussed in 2.1 above, and illustrated below in Figure 2-6 and Figure 2-7).

○ **ToA vs AOA**

Based on a survey conducted by J. Xiao et al [56], it was highlighted that Yamasaki achieved 2.4m positioning accuracy at the 67th percentile using ToA from 10 Wi-Fi routers. It was their observation that the performance of their system significantly degraded under non-line of sight (NLOS) conditions.

Xiong et al ToA [57], exploited the multiple antennas present within Wi-Fi routers because it enables fine-grained AoA-based heuristics. It leveraged MIMO techniques with 16 antennas based on WARP platform to achieve 23cm median accuracy. The MIMO technique included intra-router triangulation for differentiating between line-of-sight (LOS) and non-line-of-sight (NLOS) path and pseudo spectrum correspondence to eliminate multipath reflections.

This system proved to be expensive and impractical as they are constrained to the hardware which demands complicated organisation of 16 antennas within each router.

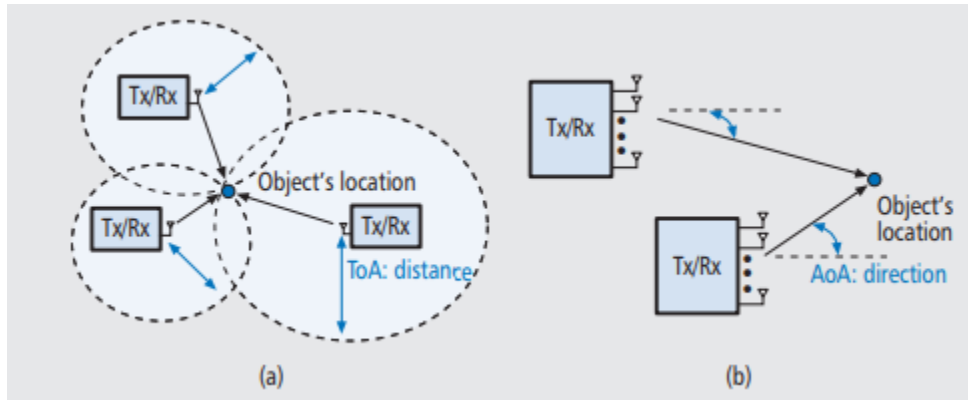


Figure 2-6 a) Time of arrival approach with trilateration calculation; B) angle of arrival approach [58]

○ RSS

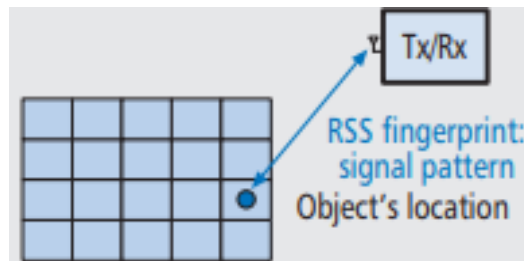


Figure 2-7 Received signal strength [58]

Received signal strength (RSS) is one of the most used signal feature for Wi-Fi-based indoor localisation [57][59][60]. It is described by C. Yang and H. R. Shao [58] to be a site survey approach to determining indoor position.

The RSS between transmitter and receiver is used to calculate distance estimation. Distance estimation of a beacon and a node is derived through the calibration of transmitting power with matching free-space channel model established when measuring distance and power at each reference point.

Typically, indoor spaces are challenged with path loss shadowing effects in two propagation conditions – Line-of-sight (LOS) and None-Line-of-Sight (NLOS).

In the LOS condition, there is clear unobstructed signal visibility between the beacon and the tracked node in an uncongested room. While in None-Line-of-Sight (NLOS), there are obstructions between the beacon and tracked node. (Read reference papers [58][61] for further information)

Poor RSS propagation in both LOS and NLOS environment conditions produces inaccurate distance measurements. This challenge is tackled by representative research [38][39][62][63][64], where log shadowing models are used to predict propagation loss for an extensive range of environments. This includes Friis free space model. This is explained further in 2.4.2.

Position based on Wi-Fi is calculated from a combination of RSS measured distances from 3 or more routers. According to studies [14][65], this combination is achievable with either trilateration or multi-trilateration models. Trilateration is for three routers and multi-trilateration is for more than three routers, as the name implies. Further explanation Wi-Fi position is in 2.4.5

It should be known that commercially, RSS indication (RSSI) is employed in the estimation of positions [14][38][39][62][63][64][65]. This is because it is used in active tracking when the distance is estimated between beacon nodes and tracked nodes. Then, combine in either trilateration or multi-trilateration for position calculations. It is the general deduction that the system experiences challenges, especially performance degradation when in dynamic environments or in instances where there is a large distance between transmitting beacon and tracked node.

IMU sensors

Considering the fast growth of technology, modern commercial smartphones now have a variety of embedded sensors, including accelerometers, gyroscopes and magnetometers. Several indoor localisation systems [56][66][67][68] have exploited these sensors because of their low-cost and low power advantages.

A survey in 2016 by J. Xiao et al [56] discusses a proposed IndoorNav system that uses an accelerometer to calculate step detection and, uses gyroscope and magnetometers to calculate direction estimation of a tracked user (see Table 2-5). IndoorNav system used stride length of the use in its personalised step detection algorithms. Their experiments demonstrated a meter level mean accuracy of 1.5m in a testbed of 31m x 5m. The advantage of this system by J. Xiao et al [56] is that it does not need additional infrastructure. However, it is limited to pedestrian tracking. This similar to other representative papers [66][67].

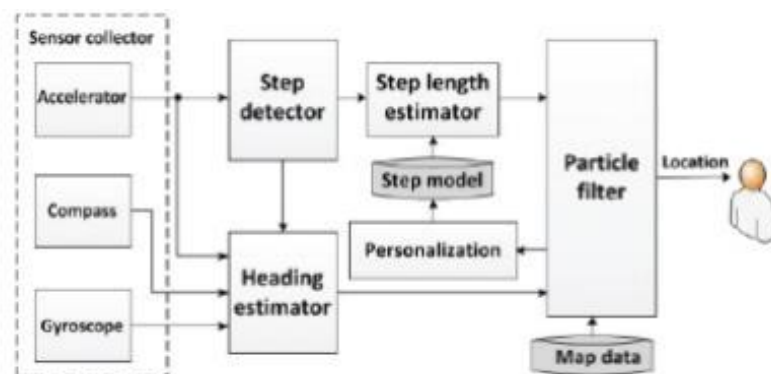


Table 2-5 IndoorNav using inertial sensors and dead-reckoning approach [56]

How smartphone IMU works?

Most smartphones measure their values with regards to the device coordinate system demonstrated in Figure 2-8a. It should be noted that the coordinate of smartphones is not the same as the earth coordinate system [68]. An instance by R. Henken and M. A. Wiering [68], discusses how an increase in gyroscope values when the phone is in a particular direction shows an angular velocity of the smartphone but not its absolute orientation in the physical world. To make sensory output useful for indoor localisation, there is a necessity to create a mapping translation from smartphone to earth's coordinate Figure 2-8b.

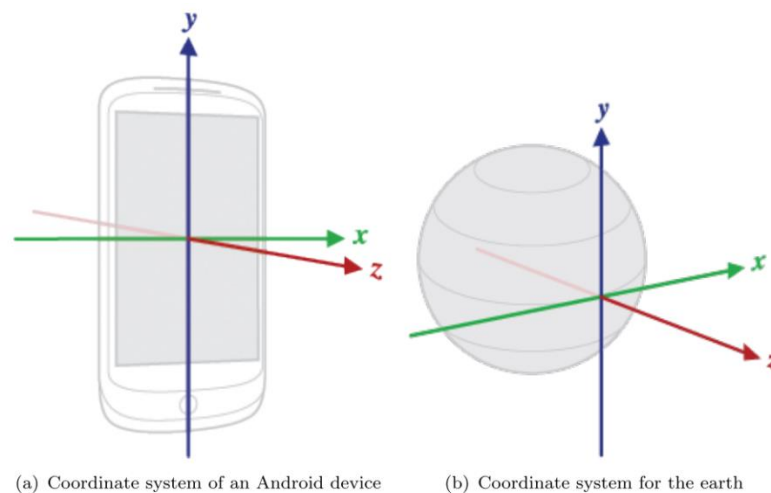


Figure 2-8 Converting smartphone coordinate to earth coordinate [68]

The smartphone coordinate system has x, y and z defined axes relative to its screen. Supposed the smartphone is held with its screen facing the user, then its x axis will be identified as horizontal with positive values towards its right. The y axis points vertically with positive values identified at the top of the smartphone. Finally, the z axis out of the smartphone's screen with positive values when pointing towards the user. For the earth coordinate system, x axis always points towards the east with its tangent to the ground at the present location of the smartphone. The y axis, like the x axis, is also tangential to ground at present location of the smartphone but it points to the geomagnetic North Pole.

Finally, the z axis is perpendicular to the plane defined by x and y axes as it points towards the sky.

Our proposed WTP-HAMS system opts to represent device orientation with quaternions, which is similar to methods by R. Henken and M. A. Wiering [68]. The advantage of using quaternions has over other methods like matrices and Euler angles are its compactness and relatively simple object rotation identification. Furthermore, quaternions are much easier to work with as they manage complex numbers effectively.

Indoor localisation is further discussed in chapter three, state of the Art.

2.3 Conclusion and Analysis

Indoor localisation systems are typically designed using wireless technologies such as Wi-Fi, cameras, IMU sensors and cellular networks. These systems are discussed in sections 2.1 and 2.2 to be categorised into physical localisation or topographical based systems. These categories are analysed in conclusion sections 2.1.2 and 2.3, where we propose an investigation to design an easy to deploy effective inexpensive localisation system that uses everyday ubiquitous technologies that are familiar to the mobility user users. These include a smartphone, Wi-Fi and wheel encoders.

What is the proposed investigation?

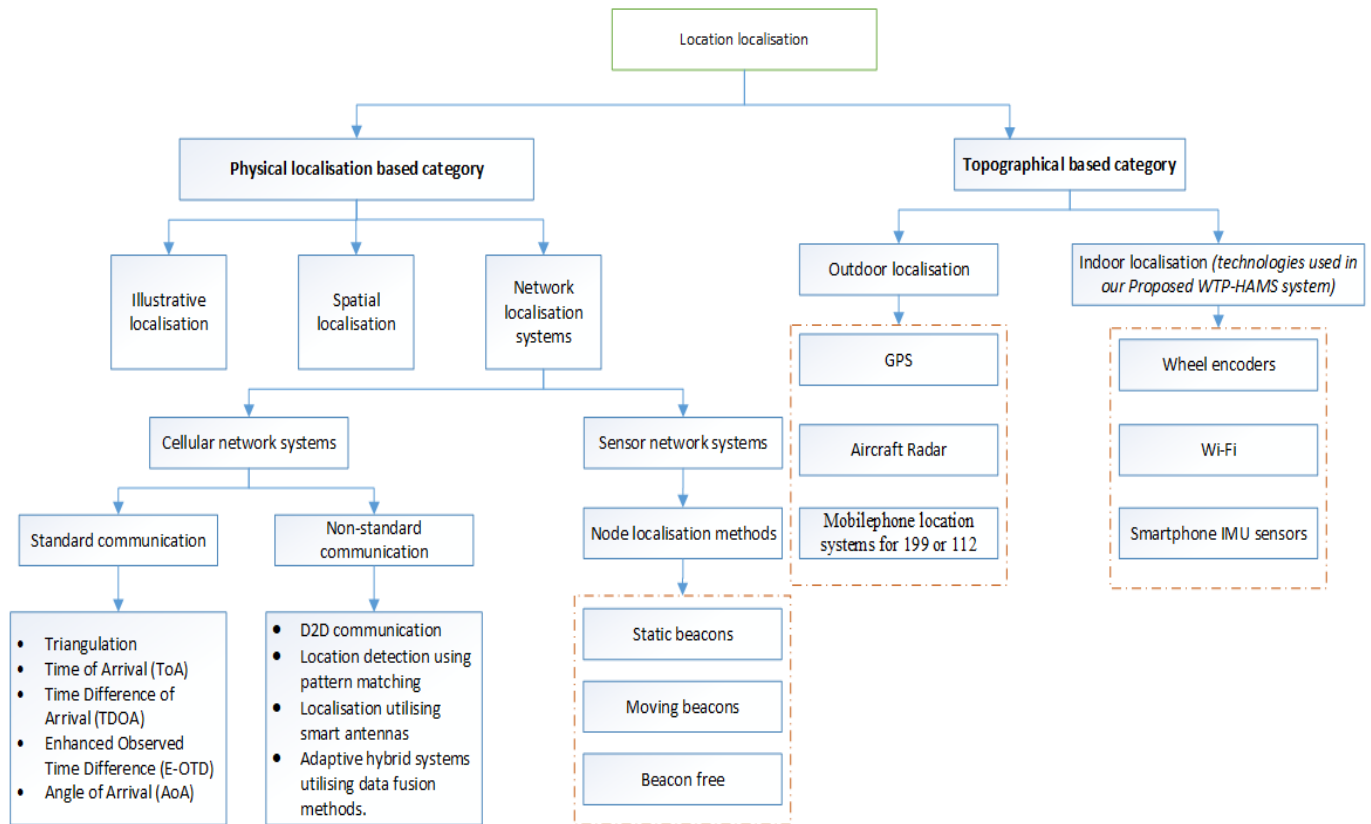


Figure 2-9 Proposed investigation (WTP-HAMS system) based on background knowledge

Our investigation will explore cellular and sensor network systems, in particular, node localisation methods that will use non-standard communication methods including D2D communication and adaptive hybrid systems data fusion methods (displayed in Figure 2-9). This is important because it will benefit from localisation methods including

- Static beacons for Wi-Fi.
- Moving beacons for wheel encoders and IMU sensors.
- Beacon-free for decentralised solutions, node to node and D2D communication, and orientation and translations tasks.

The proposed investigation will plan to combine all the above elements in network localisation systems when designing the indoor localisation system with exploited

technologies (such as Wi-Fi, smartphone IMU modalities and wheel encoders), to improve position accuracy. In particular, the proposed investigation will combine these exploited technologies using mathematical models, methods and algorithms (discussed in 2.4) including –

- Inertial sensor fuses **complementary fusion** of output from smartphone IMU sensors. This uses adaptive hybrid system data fusion methods on beacon free localisation, which is the IMU sensors within the smartphone. This is discussed in 2.4.1 below
- **Moving average filter** reduces noise and high amplitudes of IMU output. This is discussed in 2.4.2 below.
- **Full- width half maximum** is used to measure the acceleration distribution of a tracked node (mobility scooter). This is important for synchronising outputs from wheel encoders with IMU sensors in data fusion methods. This is discussed in 2.4.3 below.
- **RSSI – SDRS log-normal shadowing model** employs D2D communication methods to facilitate distance calculation between a static beacon (Wi-Fi) and moving tracked node (smartphone). This is discussed in 2.4.4 below.
- **Trilateration and Multi-trilateration** for calculating position estimates of the tracked node using calculated distances from the static beacons (Wi-Fi routers). This is discussed in 2.4.5 below.
- **Average localisation error model performance evaluation** measures the performance of trilateration and multi-trilateration algorithm by its average localisation error. This is discussed in 2.4.6 below.
- **Euclidean distance error** is used to measure the shortest distance between two coordinates in a straight line. This is employed to calculate the localisation error between ground truth and the estimated position. In particular, for the deviation of estimation based on odometry model and combined overall system deviation computation from the ground truth. This is discussed in 2.4.7 below.
- **Locating coordinates of the centroid of a shaded area** calculates the centre point where the error shapes from odometry Euclidean distance error overlap the trilateration/multi-trilateration average localisation error. The coordinates of this

centre overlap are the new and improved position estimate. This is discussed in 2.4.8 below.

2.4 Mathematical Models, Methods and Algorithms

2.4.1 Inertial Sensor Fusion Using Complementary Fusion

The heading navigation is calculated using complementary fusion process suggested by W. Zijlstra [69]. In particular the behaviour of the smartphone including orientation and rotation. This is important because it calculates if the smartphone is in a horizontal or vertical orientation while identifying the directional impact.

The complementary fusion includes a triple integral of gyroscope, accelerometer and magnetometer. The developer [69], originally designed this system to measure head rotations of users with improved sensitivity to motion.

The process in the recommendation by W. Zijlstra [69] uses an accelerometer to calculate gravity vector and magnetometer as a compass. This is because the output combination of both accelerometer and magnetometer is sufficient for orientation computation of the smartphone. To avoid errors from the combination, low pass noise filtering is implemented to its sensor data that is provided at regular time intervals (see Figure 2-10). This is important because it measures the orientation angle averaged over time within a consistent timeframe. A major advantage of combining magnetometer with accelerometer outputs is the data support over longer period computation.

The gyroscope in the explanation by W. Zijlstra [69] system calculates angular rotation. This was important in their research because the rotation of the user's head was to be considered. However, it is limited by its short response time and its high drift susceptibility. This drift is gotten from small amounts of errors that are injected into the system process at each iteration. Mitigation of the drift is proposed by W. Zijlstra [69], where high pass filtering is applied to the gyroscope sensor data (see Figure 2-10). Still, it is observed that an error build-up resulted in a constant slow rotation of calculated orientation.

A recommendation by W. Zijlstra [69] to combine filtered outputs of all three IMU sensors by replacing the filtered high frequency of combined accelerometer and magnetometer outputs with its corresponding gyroscope outputs (see Figure 2-11). The purpose to increase head motion sensitivity. However, this is not expected to perform well in translational motion.

The overall requirement for the proposed WTP-HAMS system is to calculate the precise orientation of the smartphone and the navigation heading of a mobility scooter moving in translational motion. Therefore, an adaptation of the sensor fusion method [69] to only integrate values from accelerometer and magnetometers is sufficient.

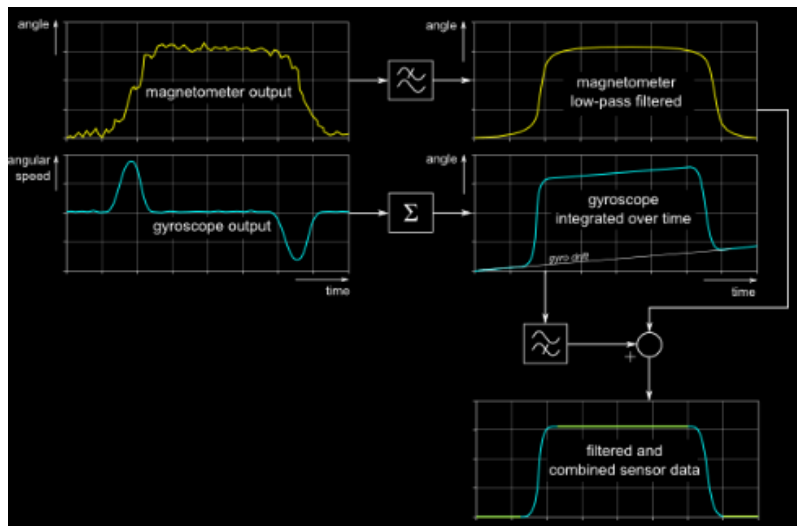


Figure 2-10 Magnetometer and gyroscope filtration combination

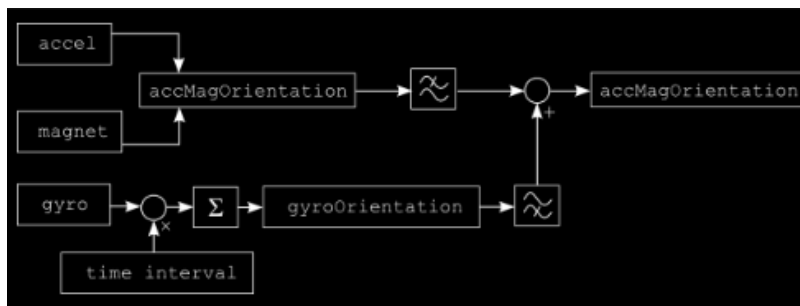


Figure 2-11 Complementary fusion of filtered IMU sensor output

2.4.2 Moving Average Filter

A moving average filter is a form of finite impulse response (FIR) filter frequently employed in analysing time series within a time domain. Its filtration procedure includes temporal statistics used for calculating a few samples of a signal along its time axis. These samples are stored and displayed in a temporal moving window for averaging. This is important because it produces output at various points of time [70]. More information on moving average filter is further discussed in reference papers [70][71].

For our proposed WTP-HAMS system, moving average filter is important to reduce the noise in the IMU signal, as well as the high amplitude. In particular, the signal smoothing from the beacon free, data fused IMU.

2.4.3 Full Width at Half Maximum (FWHM)

FWHM is used in several fields such as image processing, to identify the boundaries of objects.

FWHM is instrumental in probability distributions because it provides the best-case approximation to the true governing distribution. In particular, it analytically calculates a distribution curve. According to statistic articles [72][73], the analysis of a distribution curve of acceleration levels is calculated using FWHM with relation to amplitude like that shown in Figure 2-12. Refer to statics papers [72][73] for supporting information.

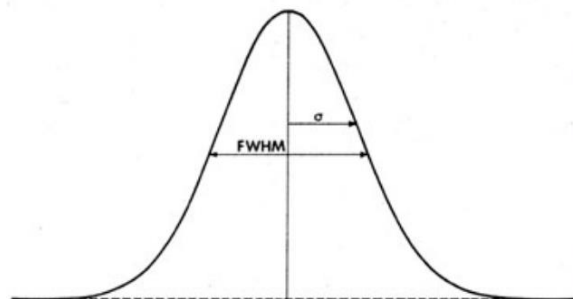


Figure 2-12 Shows the relationship between the variance σ and FWHM [73]

The FWHM shown in Figure 2-13 below is adapted from a paper by M. Galotto and P. Ulloa [73], where discussions reveal how Gaussian density is calculated by numerical integration. This is because Gaussian density cannot be analytically calculated. Therefore, the variable is transformed into a reduced form shown in Equation 4.

$$z = \frac{x - \mu}{\sigma}$$

Equation 4

Where,

z , distributed reduced Gaussian;

x , original distribution;

μ , the mean deviation;

σ , standard deviation;

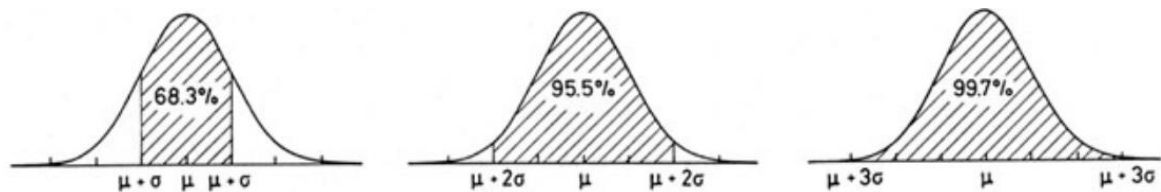


Figure 2-13 Shaded areas of importance contained within the limits $\mu \pm 1\sigma$, $\mu \pm 2\sigma$ and $\mu \pm 3\sigma$ in a Gaussian distribution [73]

In practical situations, the area of importance is under the shaded Gaussian between the integral intervals of σ . This is shown in Figure 2-13 where results of $x \pm \sigma$, means that true values have $\approx 68\%$ probability of being within the limits of $x - \sigma$ and $x + \sigma$, $\approx 96\%$ probability of bring within the limits of $x - 2\sigma$ and $x + 2\sigma$, and $\approx 100\%$ probability of being within the limits of $x - 3\sigma$ and $x + 3\sigma$.

Examples of researches that implemented FWHM include studies by N. I. C. R. P. H. F. M. S. M. Inagaki [74] and Elizabeth G. Armstrong et al [75].

Research by N. I. C. R. P. H. F. M. S. M. Inagaki [74], used FWHM to calculate reliable values of lattice constraints and crystallite sizes of carbon materials. Their system recommended 66.7% probability area of the sensors diffraction profile.

Elizabeth G. Armstrong et al [75], designed an intelligent tire testing system where it used FWHM to analyse the rotation signal width to measure the difference between patch and stress distribution within the patch. It is our observation that the research used $\approx 65\%$ probability area of signal distribution in the data analysis of their system.

Our proposed investigation considers using FWHM on combined IMU signals (with moving average filtered IMU amplitudes) to identify the different acceleration levels, including initiation, acceleration and deceleration over a travelled distance of the mobility scooter with relation to time.

2.4.4 RSSI – SDRS Log Normal Shadowing Model

Received signal strength (RSS) is one of the most prevalent power features in the MAC layer signatures which is easily propagated from ZigBee, ultra-wideband (UWB), cellular networks and Wi-Fi. The major limitation of RSSI technology is its temporal fluctuations when propagated in complex indoor environments which produce unreliable coarse-grained features. RSSI-based ranging is misled by propagated multipath signals within multipath-rich indoor environments. To achieve better accuracy, the research by A. Wu and Z. Zeng [76] buttresses the necessity for characterizing and modelling of the small-scale multipath effects.

RSSI signal can be propagated in three models namely, Log Normal Shadowing Model (LNSM), Free Space propagation model and Two-ray ground Model. Unlike the last two propagation models, the Log Normal Shadowing Model propagation is a popular signal propagation model for Wi-Fi that does not require special requirements for its

application environment [38][39]. However, it has no linear function between RSSI values collected from Wi-Fi and distance values between the beacon and tracked node.

Researchers W. W. L et al [64], studied the popular Log Normal Shadowing Model for Wi-Fi and evolved it into an adaptable lightweight steepest descent random start (SDRS) positioning algorithm, that better calculated for the distance between all beacons and tracked node in a stationary instance. In particular, SDRS is important because it creates a linear functional relationship between RSSI and distance values (see Equation 5), i.e. especially the path-loss log-normal shadowing model and Gaussian random noise variables.

$$f(\mathbf{K}(n)) = \sum_{j \in N_a} \left(iRssi_j(n) - s_j^a + 10\eta_j \log_{10} \frac{\|\mathbf{K}(n) - \mathbf{K}_j^a\|}{d_0} \right)^2$$

Equation 5

Where,

$\mathbf{K}(n)$, represents the position of the smartphone;

$iRssi(n)$, represents signal measurement values at location i ;

s_j^a , is the transmitting power of the **AP** in **dBm**;

η_j , signifies path loss exponent;

\mathbf{K}_j^a , is the position of the access points (APs);

d_0 , represents reference distance between transmitter and receiver.

The SDRS log-normal shadowing model in the paper by W. W. L et al [64] assumes that measurement error indicated as $x_o(n)$, is estimated Gaussian noise. This is important so

that the maximum-probable position approximation will correspond to the objective function $f(\mathbf{K}(n))$ minimum.

W. W. L et al [64], aimed to solve phase-retrieval limitation and the single particle $\hat{\mathbf{R}}$, by considering a light weight SDRS log-normal shadowing algorithm with multiple initiated initial starting points $\mathbf{K}^{L,0}$ in a scenario region where $L = 1, \dots, N_{\text{start}}$ is uniformly distributed. N_{start} , is the reference point calculated in parallel to N_L iterations. (see the document by R. A. Iltis and S. Barbara [77] for further discussions on SDRS algorithm).

Similar to the general Log Normal Shadowing Model, the lightweight SDRS log-normal shadowing model [64] uses the global environmental standards in Table 2-6 to calculate its path loss exponent. The path loss exponent η_j of the SDRS algorithm is calculated to gauge the accuracy of the system. For the indoor environment, the free space dynamic shown in Table 2-6 is typically adopted. This is because it allows for indoor localisation systems to consider the two major free space variances, including $\{\text{LOS} : \eta_j = 2\}$.

It should be known that the variance of shadowing can vary depending on the complexity of the environment. That is the reason Table 2-6 below shows the value of path loss exponent of different environments and building type.

Environment	Path Loss Exponent (η)
Free space	2.0
Urban area cellular radio	2.7~3.5
In-building LOS	1.6~1.8
Obstructed in-building	4~6
Shadowed urban area cellular radio	3~5

Table 2-6 Path loss exponent based on environmental dynamics [64][77]

The proposed investigation will use lightweight SDRS log-normal shadowing model [64] to calculate the distance between the beacon and the tracked node based on the relationship between the beacon's RSSI and distance values. This is because it can be

interpreted as a lightweight particle filter where difference start positions correspond with an initial selection of particles and the single particle remaining at the completion of the algorithm.

2.4.5 Trilateration and Multi-trilateration

Trilateration is used by researchers [65] to find the relative location of users through the geometric combination measured distances from three Wi-Fi routers. This method finds a position from the convergence point of localisation area circles formed by the distances between each Wi-Fi router (beacon) and the tracked node. When a similar method is used for combining four Wi-Fi routers, it is called multi-trilateration, as described in the literature [14].

The popular measurement propagation for trilateration and multi-trilateration is RSSI. This is important because calculated distances between beacon and tracked node based on RSSI signals, can be easily combined in the easily adopted algorithms, trilateration and multi-trilateration. These algorithms use little computational time and therefore is used in live environments.

Both trilateration and multi-trilateration is expressed Equation 6 as:

$$(x_i - x_r)^2 + (y_i - y_r)^2 = r_i^2$$

Equation 6

Here,

x_i, y_i , represent coordinate of *reference point i*;

x_r, y_r , represents *unknown location*;

r_i^2 , is position estimate.

Equation 6 is rewritten in the journal [14] as the matrices in Equation 7 and Equation 8

$$AX = b$$

Where

$$A = 2 \cdot \begin{bmatrix} x_n - x_1 & y_n - y_1 \\ \vdots & \\ x_n - x_{n-1} & y_n - y_{n-1} \end{bmatrix}$$

Equation 7

And

$$b = \begin{bmatrix} (r_1^2 - r_n^2) - (x_1^2 - x_n^2) - (y_1^2 - y_n^2) \\ \vdots \\ (r_{n-1}^2 - r_n^2) - (x_{n-1}^2 - x_n^2) - (y_{n-1}^2 - y_n^2) \end{bmatrix}$$

Equation 8

The solution in Equation 7 and Equation 8 according to S. Boonsriwai et al [14], is resolved through the use of minimum mean square error techniques and the square of the Euclidean norm. (refer to study by S. Boonsriwai et al [14] for more information). Researches [14][65], that have adopted this technique got results ranging from 2m – 10m depending on the propagated area.

The proposed investigation will consider combining three and four router using trilateration and multi-trilateration algorithms respectively. This is important because it would get position estimates from the Wi-Fi routers.

2.4.6 Average Localisation Error Model (ALE) for Performance Evaluation

It is ideal to measure the localisation error of a system after calculating its position using algorithms like trilateration and multi-trilateration. An assumption by L. Cheng et al [78] proposed to test the performance of their 2D localisation system with an average localisation error model performance evaluator. In simulated experiments, the researchers [78] tested the performance of 7 beacons and one tracked mobile node in their proposed system which is a no-filter (NF) method. Each of their simulations used N number of beacon nodes in the Monte Carlo runs, which is important in calculating the performance of their system.

$$error = \frac{1}{N \cdot t_n} \sum_{i=1}^K \sum_{k=1}^{t_n} \sqrt{(\hat{x}_k - x_k^i)^2 + (\hat{y}_k - y_k^i)^2}$$

Equation 9

Where,

N, is the number of beacon nodes;

i , is beacon node;

(\hat{x}_k, \hat{y}_k) , is estimated location at time k ;

$k = 1, \dots, t_n$.

(x_k^i, y_k^i) , is the true location of the mobile node.

Unlike the simulated experiments in the solution by L. Cheng et al [78], our proposed WTP-HAMS system would be measuring the performance of its Wi-Fi component based on real values from experiments live environments. In particular, our proposed

investigation will benefit from this ALE performance evaluator, when it would have to measure the localisation deviation of the results from trilateration and multi-trilateration from true position (also referred to as the ground truth).

2.4.7 Euclidean Distance Error

This is the most adopted distance metric which is described to be the shortest distance between two coordinates, in the length of a straight line. According to H. Aksu et al [79], Euclidean distance between two topologies can be calculated using the following expressions –

$$d_{Euclidian}(P_i, P'_i) = \sqrt{(x_i - x'_i)^2 + (y_i - y'_i)^2}$$

Equation 10

$$\mu_{Euclidian}(T, T') = \frac{1}{N} \sum_{i=1}^N d_{Euclidian}(P_i, P'_i)$$

Equation 11

Here,

P_i is (x_i, y_i) the coordinate of the tracked node i

P'_i is (x'_i, y'_i) estimated position of the tracked node i

x_i, y_i are true coordinates of tracked node i ;

x'_i, y'_i are estimated coordinates of the tracked node;

N , represents the number of tracked objects within the network;

$\mu_{Euclidian}(T, T')$, represents error caused by the localisation algorithm when accounting for the position of the tracked object and its estimate.

The proposed investigation will use Euclidean distance error to measure the position accuracy error between the true position of the mobility scooter and the estimated position. This is important to get a distance measurement between the positions.

2.4.8 Locating Coordinates of Centroid of a Shaded Area

The centroid of a shaded area is the point where all medians of a shape intersect. For triangles, it is the intersection of three medians and for circle, it is the intersection of two diameters. The solutions from U. S. River [80], discusses formulas used in the computations of centroids and their coordinates. Refer to U. S. River [80] for details.

The proposed investigation would need the formulas in the calculations by U. S. River [80] when calculating the centroid of the error shapes when it overlaps. This is important because the coordinates of the centroid will be the new and improved position estimate based on the combination of Wi-Fi, wheel encoders and smartphone IMU modalities.

2.5 Mobility Scooter

Why Mobility Scooter?

It is observed that a wealth of indoor and outdoor localisation investigations conducted by scientists focus on pedestrian users. Although indoor localisation is continually being developed, it is safe to mention that most investigated systems do not cater to users who use mobility scooters. This research, therefore, aims to bridge the aforementioned gap as it is an overlooked and neglected market.

There has not been adequate research accommodating mobility scooters for indoor localisation purposes to the best of our knowledge, however, research has been done on power wheelchairs such as the SOTA [81][82].

J. S. Ju et al [81], proposed an intelligent wheelchair that uses head tilt and mouth shape recognition to drive it. In their system, a head tilt of the user calculated navigation direction, while the mouth shape of the user stopped the motion of the intelligent wheelchair. Although this system by J. S. Ju et al [81] focuses on controlling the motion of the intelligent wheelchair, it is our plan that systems similar to it will benefit from our proposed investigation.

Another relevant research was conducted by T. Carlson and Y. Demiris [82], where computer-vision based approach was proposed to measure the location of a powered wheelchair. Their system used ceiling fixed cameras with adaptive Gaussian threshold to result in a position accuracy of 5cm and 2degrees orientation. The limitation of the localisation solution by T. Carlson and Y. Demiris [82] faces is in the necessity for additional expensive infrastructure such as fixed cameras.

Unlike the power wheelchairs that are specialist technologies, mobility scooter is a popular three or four-wheeled powered mobility technology typically used by the elderly and people with mobility challenges. In particular, for indoor and outdoor environments. Mobility scooter technology is different from power wheelchairs because it comes with driving controls with speed adjustments, height adjustable comfortable seating, tiller and handler bars.

Our investigation proposal will be to exploit mobility scooter wheel encoders in terms of its capability to provide indoor position. It is important in population dense environments like public and private health care institutions and residential buildings that need indoor localisation technologies to not only detect user's absolute location within a room but to also guide and track users at meter level accuracy. The proposed investigation would provide centimetre/meter level indoor localisation for mobility scooter users in healthcare, private and public sectors. In particular, a sophisticated level of real-time monitoring and security to improve the quality of life. This would invariably boost the user's sense of independence and would reassure trust between medical service providers, patients, carers and families.

2.6 Overall Summary

Indoor localisation systems are typically designed using wireless technologies such as Wi-Fi, cameras, IMU sensors and cellular networks. These systems are discussed in sections 2.1 and 2.2 to be categorised into physical localisation or topographical based systems. These categories are analysed in conclusion sections 2.1.2 and 2.3, where we propose an investigation to design an easy to deploy effective inexpensive localisation system that uses everyday ubiquitous technologies that are familiar to the mobility user users. These include a smartphone, Wi-Fi and wheel encoders.

How will the proposed investigation work?

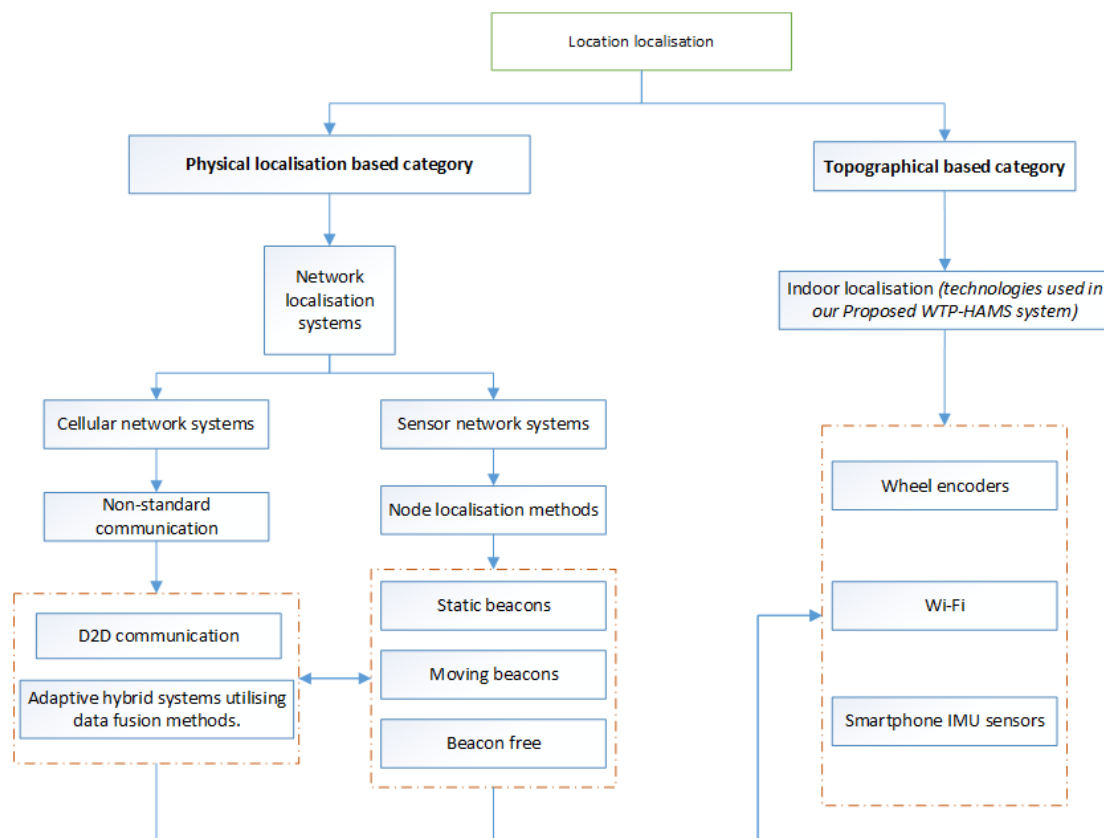


Figure 2-14 Proposed investigation (WTP-HAMS system)

Our investigation will explore cellular and sensor network systems, in particular, node localisation methods that will use non-standard communication methods including D2D communication and adaptive hybrid systems data fusion methods (shown in Figure 2-14). This is important because it will benefit from localisation methods including -

- Static beacons for Wi-Fi.
- Moving beacons for wheel encoders and IMU sensors.
- Beacon-free for decentralised solutions, node to node and D2D communication, and orientation and translations tasks.

The proposed investigation will plan to combine all the above elements in network localisation systems when designing the indoor localisation system with exploited technologies (such as Wi-Fi, smartphone IMU modalities and wheel encoders), to improve position accuracy. In particular, the proposed investigation will combine these exploited technologies using mathematical models, methods and algorithms (discussed in 2.4) including –

- Moving average filter for smoothing IMU signals.
- FWHM for synchronising smoothed IMU signals with distance travelled from wheel encoders.
- RSSI-SDRS log-normal shadowing model for distance estimated for Wi-Fi.
- Trilateration and multi-trilateration for position estimation based on Wi-Fi.
- ALE for performance evaluation of trilateration and multi-trilateration.
- Euclidean distance error for calculating position deviation between the estimated position and ground truth.
- Locating coordinates of the centroid of a shaded area used for calculating the centre of the errors from combined results of Wi-Fi, smartphone IMU modalities and wheel encoders. This is the new improved position.

We will investigate further the state of the art for localisation system in chapter 3, with the inclusion of literate works that employed the technologies, mathematical techniques, models and methods mentioned in chapter 2. This will be juxtaposed with other existing indoor localisation systems.

Chapter 3 State of the Art

This chapter discusses in in-depth the state of the art of indoor localisation with focus on the three main categories, namely passive, active and hybrid localisation methods. We present an up to date review and evaluation of most relevant 38 state-of-the-art indoor localisation systems in terms of technology, algorithm, key features, experiments, methods, robustness, complexity, accuracy, precision, limitations, costs and results. Also, we propose a new standardisation for hybrid localisation systems.

3.1. Overview

GPS signal has satisfied the outdoor location positioning with a navigation system that uses satellite according to the literature [49][83][84]. Software companies such as Google have used GPS technologies to their benefit, especially because they have a wide range of applications which are GPS dependent. These include vehicular navigation, personal navigation/map reading and fleet management to mention a few [85][50]. As wonderful as the GPS technology is, it is not sufficient for indoor localisation and therefore is limited to outdoor activities and applications [86][87]. Its insufficiency for indoor positioning has proven to be a challenge to technologists everywhere [88][89].

The demand for acute indoor localisation is on a steady rise as access to wireless information has become readily available. In particular, the internet of things (IoT) including location sensing and radiolocation technologies [49][90][91][92][93][94][95][96].

Over the last few years, the internet of things (IoT), has gained huge popularity within research communities. IoT, which is a continuous wireless internet-based communication of interconnected things, has been predicted in the survey by B. Alsinglawi [97], that its interconnectivity will extend beyond interactions between applications and humans to an exciting realm. Today, IoT has birthed smart technologies and smart environments which are now becoming a pervasive necessity in today's world

and is evident in applications in several fields such as e-health, smart homes, assisted living, and smart cities among many other services that were once deemed unachievable.

With the rapid growth of IoT, smart technologies are such as smart sensor nodes are now embedded in devices or appliances including Wi-Fi, light switches, refrigerators, smartphones, and heating control. This is important in designing technologies such as intelligent self-regulator of temperature, smart self-organisation of a timer, surveillance in secure environments and especially, indoor localisation in navigation systems.

Indoor localisation explored by experts are categorised into three, including –

- Passive localisation
- Active localisation
- Hybrid localisation

Passive localisation [24][98]–[102], are systems that do not require the user to actively participate in the localisation process. In particular, the user is not required to physically carry an electronic device to achieve localisation. It achieves localisation through which the detection, monitoring and analysis of changes of a smart static beacon within a measured environment. These include RFID, Wi-Fi, Light, camera, Device-free Passive (DfP) technology, Physical Contact, Ultra-wideband (UWB), Computer Vision, and Differential Air Pressure. (See Table 3-1 for highlights on the passive localisation systems and section 3.2 for further information on passive localisation).

Active localisation [24][92][100][101][103]–[105], unlike passive localisation, needs the tracked user to physically participate with the system. Specifically, active localisation systems, demand that the tracked user physically carry a trackable electronic device in the localisation process. This is important because the tracked electronic device will collect and transfer the necessary data to a server for positioning calculation and analysis. Systems that fall under active localisation include Wi-Fi, RFID, GSM, ultrasound, field strength system (IMU), Am, FM and TV signals and UWB. (See Table 3-1 for highlights on the active localisation systems and section 3.3 for further information on active localisation).

Finally, hybrid localisation [106][107][108][109], are localisation systems that combine technologies or techniques from both passive and active localisation system. There is no standard to this approach therefore, we propose a new unique classification system, including

- Propagation based hybrid localisation
- Technology and technique (TT) based hybrid localisation.

The new classifications of hybrid localisation are further discussed in section 3.4.

Table showing technologies that fall under passive, active or hybrid localisation

Technology	Active	Passive
RFID [112]	✓	✓
Wi-Fi [18], [105]	✓	✓
GSM [113]	✓	
Ultra Sound [114]	✓	
Light [111]		✓
Accelerometer [115]	✓	
Am and Fm signal [108]	✓	
Tv signals [116]	✓	
Physical contact systems based on proximity [24]		✓
DFP [45]		✓
Computer vision [117]		✓
Camera [9]		✓
Ultra-Wide Band (UWB) [118], [119]	✓	✓
Infrared	✓	
Differential air pressure [120]		✓
Differential barometer [121]		✓
WLAN [28]	✓	
Bluetooth	✓	
Smartphone sensors	✓	
Hybrid systems	✓	✓

Table 3-1 Indoor localisation system and their classifications

With knowledge of the rapid growth in this indoor localisation research area, R. Mautz [110] stresses that the quantifications of some indoor localisation technologies provided 10 years ago may no longer be valid today. Therefore, R. Mautz buttressed the necessity for an up to date comprehensive literature reviews be developed at least every 3-5 years as an accurate state of the art guide.

In 2009, Gu et al [40] conducted a survey of indoor positioning systems (IPS) for wireless personal networks. They focused on evaluating the security, privacy, cost, robustness, complexity and limitations of IPS. Then, Deak et al [24] in 2012, presented an assessment of active and passive indoor localisation systems based on wireless technology used, accuracy, scalability, algorithm and costs. Two years later, in 2014, Mainetti et al [111] published a survey that reviewed state-of-the-art indoor positing systems employed in real-world scenarios. In 2015, Yang et al [67] published a paper examining wireless indoor localisation using inertial sensors. Their study focused on human mobility measurements and mobility enhancement with respect to the accuracy, decreasing deployment cost and enriching location context. Finally, a more recent investigation was carried out in 2016 by Xiao et al. [56], where they reviewed wireless indoor localisation from the perspective of the device with an emphasis on the recent trends such as leveraging integrated wireless technology for specific feature extraction to trigger novel human-centric localisation.

Although the survey representatives above have analysed indoor localisation systems and techniques, it should, however, be noted that it is challenging to achieve a complete objective holistic performance benchmark for indoor localisation systems. Therefore, this chapter analyses each indoor localisation state-of-the-art, with key focus on accuracy, cost, scalability and energy efficiency. This is because it is a similar structure to papers in the resources shown in Table 3-2.

Resources	2009	2011	2012	2013	2014	2015	2016	2017	2018
IEEE	1	2	1	2	4	2	4	1	
Springer Link		1	1	1		1			
Science direct		1		1		2	1		
MDPI							1	1	
ELSEVIER		1	1	1		1		2	
ACM		1			1	2	1		
Sage journals			1						
IOPSCIENCE						1			
IET		1		1			2		
IJAET			1						
Research gate				1				1	
INDERSCIENCE				2		1	1		

Table 3-2 Survey Paper accumulation table

^a This table is to the best of our knowledge. *(Table footnote)*

3.2. Passive Indoor Localisation

Passive indoor localisation is the achievement of target user identification, recognition and tracking without active user participation. This mode of localisation does not require its users to carry any localisation device. This is because passive localisation applications commonly achieve their goals through the exploitation of wireless data networks and environmental anomalies.

There exists a significant amount of research in this area [7][9][18]–[21]. Examples of areas beneficial of this category of localisation include security for intruder detection, emergency response to alarms and health care, amongst others. Typically, this approach appeals to users uninterested in carrying devices.

As highlighted in section 3.1 above, passive localisation techniques include Differential Air Pressure, Computer Vision, Physical Contact based systems, ultra-wideband (UWB), Differential barometer, and Device-free Passive (DfP) technologies.

3.2.1. Differential Air Pressure

This technique involves the employment of relative measurement of atmospheric pressure, such as the research conducted by S. N. Patel et al [112]. Their research [112] proposed a sensing system that perceives human movement through the deployment of affordable sensors such as instrument filter and motion sensor. The system depended on existing ductwork infrastructure of heating, ventilation, and air conditioning (HVAC) systems, which is a single sensing unit with an instrument air filter that performs classification functions from one point of the home through its connection to an embedded computer.

S. N. Patel et al [112] carried out experiments in four different homes over a period of 3 to 4 weeks. *Home 1* was a large property with three separate central HVAC units. *Home 2* was a larger property than Home 1, with two separate HVAC units, while *Homes 3* and *4* were smaller apartments with single central HVAC systems. The HVAC provided a convenient single monitoring point for airflow circuit due to its centralised airflow source from closed circuits of air circulation within the experimented homes. Using instances of clocked thresholds and doorways, human movements influenced the static pressure and displayed results when the HVAC air handler unit was in operation. The researchers concluded that their system outperformed other existing systems using similar techniques because their system senses and records the pressure changes from differential sensors attached to the air filter, which then, classifies exact locations of certain movements within the investigated building. Their research resulted in an accuracy of 75-80% in particular door movement alteration and 65% in user movement. Comparing results between the homes, it was deduced that their system performed best in the smaller homes without doorways (see results in Table 3-3).

This system is an expensive solution with low user position accuracy. It is observed to be an impractical solution because all homes have doors and not all own HVAC units.

Home/ Floor	No. of Doorways Tested	No. of Door Instances/People Instances	Door Majority Classif. (%)	Door Classif. Accuracy (%)	People Majority Classif. (%)	People Classif. Accuracy (%)
1/1	5	375/375	21	84	23	72
1/2	4	300/300	18	61	18	42
1/3	11	825/600	9	77	12	61
2	10	750/400	8	73	10	63
3	5	375/375	20	74	20	70
4	4	300/300	26	81	25	76

Table 3-3 Performance results of our manually-labelled experiments with the HVAC in operation [112]

3.2.2. Differential Barometer

Altitude information accuracy is necessary for some localisation and navigation systems such as the examination by J. Parviainen et al [113]. J. Parviainen et al acknowledge that satellite navigational systems provide altitude information but are insufficient in identifying correct floors or estimating positions within buildings. Therefore, the researchers proposed to use barometer sensors to get an indoor position using altitude information. The primary purpose of their investigation was to determine relevant error sources of referenced barometer-based altitude in indoor navigation. In particular, various scenarios where varied disturbances influence pressure reading, the MEMS barometer was used to collect data. Then, an analysis containing the influences of ventilation, change of speed, car fan and distance to the referenced barometer, estimated road profile in terms of the direction of movement and user navigation within tall buildings.

In their experiments, which involved carrying a barometer sensor in hand and travelling from floor to floor via an elevator, it was observed that experimental results in differential mode demonstrate high accurate altitudes. However, the high sensitivity of the

barometer to temperature produced significant altitude measurement errors ranging from tens of centimetres to meters, as shown in Table 3-1. The error was more evident in cases where the barometer was moved from inside to outside a house or from room to room of a five-floor building with different ventilation conditions. Hence, the research recommends that reference barometer reading taken during temperature change must be considered when taking the next reading. This system does not translate to position estimation in indoor environments. This is because, J. Parviainen et al, have revealed that accurate pressure sensing does not directly translate to position estimation.

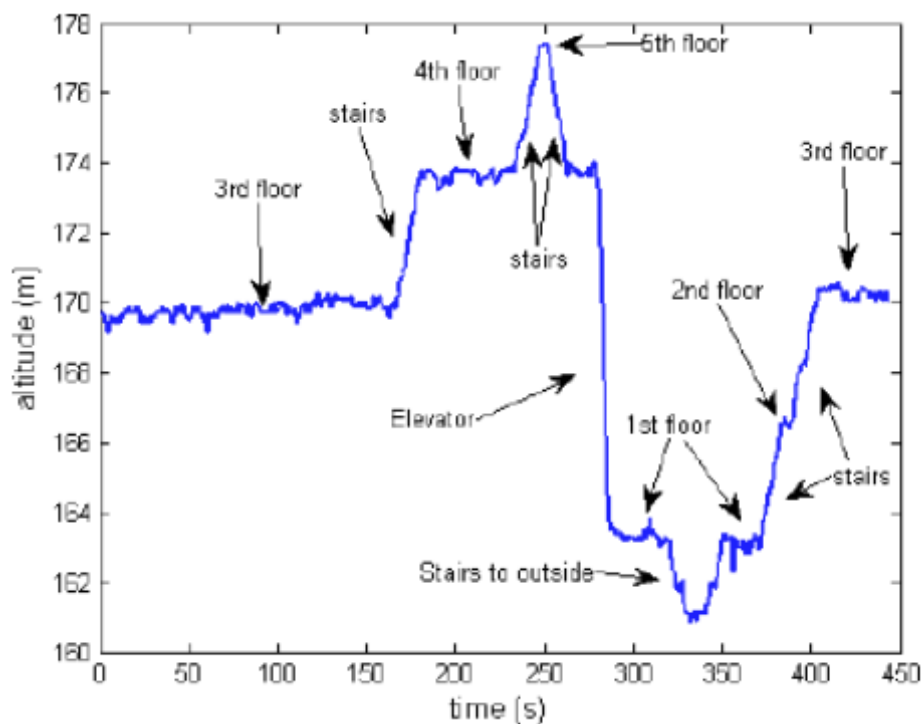


Figure 3-1 Indoor walking measurement [113]

Another research that adopted barometer in its positioning system is an indoor navigation system (InLite) by Astrium Satellites GmbH [114]. Astrium Satellites GmbH recommended InLite to allow positioning of users within large multi-level buildings with 2 meters accuracy and 5 m degradation depending on multipath effects in certain areas of the building. InLite, illustrated in Figure 3-2, is a preinstalled navigation system with

major components being a barometer connected to a WLAN datalink modem and embedded PC.

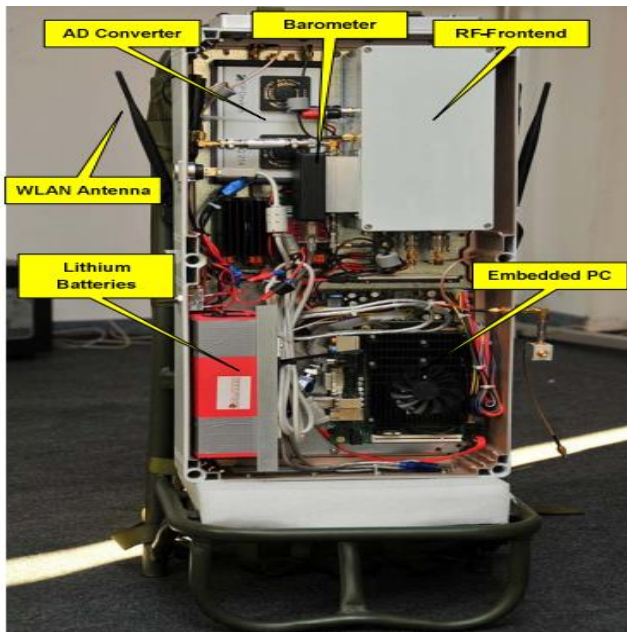


Figure 3-2 Astrium Satellites GmbH InLite technology [114]

Testing of the InLite system occurred at an isolated 11m x 66m area of the Ottobrunn building in Germany and an unoccupied hotel in Newport Wales. The experiment included, 6 to 8 stationed transmitting stations around a building, user terminals, and a control unit to monitor transmitting stations and broadcast information to user receiver that includes a barometer (see Figure 3-3). This is because the transmitting stations broadcast 420 to 460 MHz range of multi-carrier navigation signals and the new location is estimated on receipt of the transmitted signals. The study by A. Schmitz-Peiffer et al [114] compares their proposed technology to similar technologies as it attains 2 meters accuracy and effectively reduces multipath effects suffered in gigantic multi-level houses built with concrete, metal-shielded windows and steel.

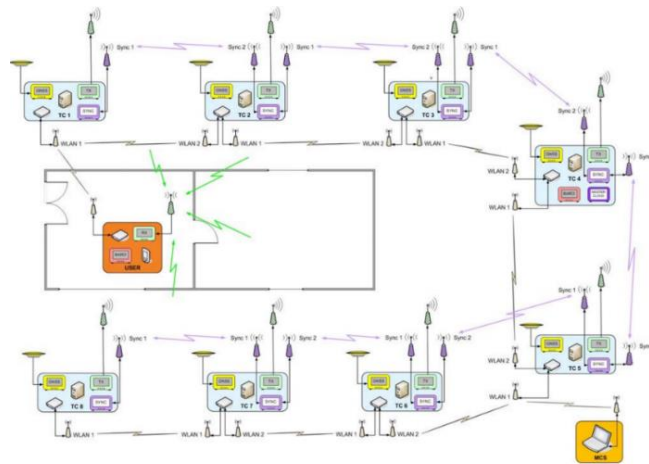


Figure 3-3 InLite Architecture illustrating 8 base stations, control unit and user reception station [114]

A. Schmitz-Peiffer [114], recognised the limitations of their system estimating more accurate positioning information. It is expressed that its limitation can be mitigated when different error sources are processed for positioning performance such as analysis of the near-far effect, analysis of operative distance, extensive investigations and experiments to understand error sources and finally, redesign the user receiver system into a more portable system.

Further observed is the bulkiness of the system [114] (shown in Figure 3-2), which we speculate might be uncomfortable for some users, especially our target mobility scooter users with mobility impairment. Also, it is our opinion that this system is expensive to design as the developers have indicated that additional infrastructure is required in its design and development. Therefore, making this system unsuitable for our audience.

3.2.3. Physical Contact Based System

Technologies based on physical contact rely on proximity sensing for target object localisation within buildings. Proximity sensing technologies comprise of capacitive field sensors, pressure sensors and touch sensors [41][115].

3.1.1.1 Capacitive Field Sensor

This is a dated technology focused on achieving localisation via exploitation of influences created by target node on a generated electric field [21][116][117]. This technology is commonly implemented in industrial applications for material detection and finger-controlled touch-screen devices. Unlike pressure sensing that relies on the weight distribution and step of a user, capacitive field sensor technology relies on smart materials with integrated electronic components such as sensing mats [116] that wirelessly communicate node state with its central system.

In 2011, due to the high cost of implementing capacitive field sensor for localisation, Braun et al. [116] proposed a flexible integrated solution relying on affordable open-source hardware that actualises indoor localisation and fall detection through wireless data transmission from sensing mats strategically placed under floor covering via a central platform to connected ambient assisted living (AAL) platform. The open-source hardware is a firmware which provides a control unit that supports capacitive sensing of up to eight sensor elements. This system was limited by its inability to recognise objects by their capacitive profile and its difficult scalability [118][116].

Unlike the expensive, cumbersome to deploy and limited system proposed by Braun et al [116] in 2011, more recently, in 2017, Fu et al. [98] proposed an easier to install, low maintenance and low power consuming architecture that relies on the deployment of manually laid passive wires grid of 20cm spacing underneath any non-conductive floor surface to track users that move about the surface. Data analysis of this study included the application of low pass filter on sensors and individual weighted average respectively. Results from a relatively restricted experimental setup included 12 mobile participants walking along predefined reference paths to achieve positioning mean errors of 12.7cm (with shoes) and 18cm without shoes. This system was dependent on the flooring technology, therefore, localisation using this technology may not be achievable in all environments. Furthermore, this system is limited to localising a user at a time as it is yet to be tested on multiple users neither has it been implemented in real uncontrolled dynamic environments.

3.1.1.2 Pressure Sensor

In comparison to other localisation technologies, pressure sensors are most conventional. This technology mandates a laborious task of setting up pressure-sensitive sensors on or beneath the floor surface. Usually, the flooring is required to be flexible and also have installation space beneath the floor. Localisation is achieved when the pressure generated by a user corresponds with the user's unique weight and gait [99]. Instances of researches that adopted the not computationally heavy approach and provided high accuracy are the studies by S. Pirttikangas et al. [119] and Robert J. et al. [120]. Robert J. et al. invented a smart floor to identify and track users. Experiments conducted by R. J. Orr and G. D. Abowd [120] included the use of steel plate, data acquisition hardware and cells for the measurement of user's feet ground reaction force (GRF) during walks on a programmed measuring tile. An accumulation of 1680 training footstep GRF profiles in a ten-dimensional feature space was archived for match identification to nearest-neighbour in instances of unidentified footsteps. This technology achieved an accuracy of 93% through the use of smaller tiles. This technology is limited to one user at a time. R. J. Orr and G. D. Abowd [120] compared their result of 93% to that of Addelse et al. [121] who adopted the use of Markov models (HMM) and achieved an accuracy of 91%. S. Pirttikangas et al [119] conducted an experiment in a 100 square meters Electro-Mechanical Film covered research area at the University of Oulu. The stripes of the Electro-Mechanical Film made up a matrix of 30 x 34 with a cell size of 30 cm x 30 cm. Each of the 64 stripes emitting a continuous signal of 100Hz sampling rate is streamed to a PC for analysis. Although S. Pirttikangas et al. [119] demonstrated the difficulty in identifying several users walking within the same environment at the same time by footstep identification from pressure signals using hidden Markov models, it is evident from the investigations by Addelse et al [121] that its accuracy is quite high for single users.

3.1.1.3 Touch Sensor

Sunhong et al. [122] proposed an algorithm that autonomously approximates the positioning of a mobile robot identified as UBIquitousRObot – UBIRO. The localisation was achievable based on UBIRO's dependencies to – A, passive trigonometric functions aimed at orientation determination; B, radio-frequency identification (RFID); C, Cartesian coordinates of distributed IC tags in a distinctive grid-like pattern on the test area floor; D, UBIRO's external sensors such as odometer and touch sensors. Experiments on UBIRO were conducted in a 420cm x 620cm obstacle-free environment with 198 passive IC tags distributed across the floor. Each tile is spaced in a 34cm x 34cm grid. Compared to conventional methods, UBIRO showed high location accuracy and it demonstrated a localisation error of 13.3cm at x-axis and 5.7 cm at Y-axis.

3.2.4. Light

Jinyuan Zhao et al. [123] described the advantages of employing light technology in indoor localisation. Wang et al. Jinyuan Zhao et al developed light reflections model and proposed a system utilising 12 ceiling mounted intensity controlled LED light sensors and 12 light fixtures. A LASSO and localised ridge regression algorithms were developed to assist in single object position estimation. Experiments conducted in a simulated environment of 7 ft. x 12 ft. adequately located different sized objects. It resulted in localisation error range of 0.24 *in* to 1.39 *in* when localised ridge regression algorithm was applied. Real-world controlled experiment in localizing two participants and a chair proved system reliability due system high localisation capability.

3.2.5. Ultra Wideband (UWB)

The Ultra-wideband (UWB) has demonstrated to be effective in indoor positioning [125]. Abdurrahman Alarifi et al. [125] published a comprehensive survey paper analysing the recent advances of UWB. UWB is applied in three application areas namely, radar; communications and sensors; and positioning and tracking. Relevant research conducted by Stefania Bartoletti et al. [126], proposed a mathematical framework to analyse UWB

monostatic WSRs. UWB monostatic WSRs is reliant on passive navigation design based on estimated time-of-arrival (ToA). This is categorised by network experiments and environment propagation. An analysis of Bayesian navigation algorithm based on particle filter application and the task of inferring the target node location of the mobility model is demonstrated. The researchers developed two models in their case study, speed known and direction unknown (SKDU) and speed and direction learning (SDL). The results revealed a root mean square error (RMSE) of 1.2 m for SKDU and 1.35 m for SDL.

3.2.6. Computer Vision

Mihai Andries et al. [118] recommended a floor pressure-imagery segmenting method to track and recognize multiple objects using low-resolution sensors and weight ambiguity detection. The method includes floor pressure image processing through the separation of blobs comprising objects, content recognition and tracking via inference and combinatorial fusion. The research's objective was to provide an object recognition approach which localises and recognises multiple objects simultaneously through analysis of load exertion on the floor surface. The researchers [118] employed dynamic programming to solve the prevalent computational complexity experienced in the state of the art due to the volume of possibilities in correlating a known object to observations made by the researchers. Conducted experiments included participants with reflectors attached to their waists as they carrying out daily life activities in a controlled prototype apartment. The system demonstrated a result of 20 cm human localisation error.

Another example is research accomplished by Yamin Li et al. [127]. Their study proposed the building of real environment scenarios in 3D panoramic environments and the localisation of a micro aerial vehicle (MAV) without external navigation assistance. A quick 3-D model of the experimental test area of 4m x 3.5m x 3m environment is built utilizing speeded up robust feature (SURF) extraction algorithm and iterative closest point-based (ICP-based) reconstruction algorithm applied to the multiple RGB-Depth (RGD-D) sensors of the visual sensor network (VSN). With the employment of a distributive data fusion algorithm, Kalman-consensus filter (KCF), a mean error of 9.3869 cm and the trajectory of mini MAV were estimated. The system is observed to be limited

due to its poor image quality of objects and reduced range identification. Investigation showed that objects made of glass or mirror were incapable of reflecting infrared light, thus, depth values were illustrated as black outliers. This is due to the unsuccessful attempt of retrieving depth values by depth sensors. Further observation showed that increased distance from the depth sensors resulted in decreased depth accuracy.

3.2.7. Device-Free Passive (DfP)

Kosba et al. [128] addressed the ubiquitous constraint in developing an accurate, robust and low-overhead DfP motion recognition solution. The scientists [128] introduced RASID system; a robust WLAN DfP motion detection system that enables a wide set of applications such as intrusion detection and border protection through the provision of software-only solution using already installed wireless networks. System evaluations in two experimental testbeds sized 2000ft² and 1500ft² both displayed accuracy capability of at least 0.93ft. RASID employs a non-parametric statistical anomaly detection technique for detection capability. Although this system needs further investigations to reduce data collection and training time from about an hour and 15 minutes, it proved to outperform some DfP state-of-the-art in terms of robustness and accuracy in 2012.

In 2015, IEEE published PLAS; a signal eigenvector-based device free passive localisation system using array sensor by Jihnoon.H et al. [61]. This system relies on RSS fingerprinting technique using multiclass support vector machines (SVMs) with dependency on a combination of array signal characteristics with spatial and temporal averaging. The significance of the array sensor is to utilise modifications caused by an event in the propagation environment. In a 7m x 7m single room test environment, the researchers conducted 4 different experiments using a continuously transmitting single band of 2.4 GHz (IEEE802.11g) labelled transmitter (Tx), a four-element antenna array labelled receiver (Rx) and three human subjects standing at data collection location for 10s-30s during training and testing phases. The research explored localisation performances of the proposed system in both Line-of-sight (LOS) and non-line-of-sight (NLOS) propagation environments measuring signal paths between Tx and Rx and further analysed two methods of placing receiver antenna, i.e. in centralised and

distributed antenna format. The methods and algorithms employed by the researchers included root-mean-square error (RMSE), MDE, and the cumulative distribution function (CDF) versus distance error. The centralised antenna proved to demonstrate improved localisation accuracy deviation RMSE of 1.32m and MDE of 0.67m when compared to K-NN, and RMSE of 0.2m and MDE of 0.17m when compared to Nuzzer. This system, unfortunately, performed poorly in two rooms with dense environments.

3.2.8. Smart Wiring and Socket

Tian Zhou et al. [129] introduced E-locas their socket level localisation system that achieves indoor human localisation through the usage of existing indoor electric wiring. This system estimates human position through injected signal into protected earth line of the existing residential power network. It is observed that electromagnetic features modified by human within a room can be used to deduce a resident's location because the system treats the human body as an electrical conductor that is affected by EM waves. Through the characterisation of 'change degree' measurements, the resident's position can be adequately guesstimated. Their system consisted of an injected signal into building wiring, a collection of power spectrum surrounding injected signal frequency at different sockets, noise filtered RSS peak energy and support vector machine (SVM) classifier necessary for location classification.

Experiments were conducted in an artificially divided space of 1.2m x1.2m grids where 5 power spectrum analysers which act as receivers are placed in 5 sockets, injectors are stationed in corners of the grid room totally 46 cells at the top floor of Tsinghua Rohm building, Tsinghua-Berkeley Shenzhen Institute China. Results illustrated an average accuracy of 90.76% with RSS peak value of 70MHz. It is also observed that the misclassification rate of cells close to injector or receiver is relatively higher in comparison to other cells. This is due to the distance of a participant to the near-field region of the transmitter.

3.2.9. Camera

In a paper written by Shou Liu et al. [130], a tracking cooling fan using geo-fence and camera is proposed to be combined for achieving indoor localisation. The researchers presented a personal cooling service that detects an occupant through vision analysis within virtual geo-fence bound areas of 5 office cubicles. The tracking fan utilising calibrated mapping algorithm to provide a required airspeed based on PMV-SET thermal comfort model. The system uses a three-phase brushless direct current (DC) fan that delivers a 32-level speed setting at a power range of 3.8w to 19.3w, especially, within speed levels 1-20.

Shou Liu et al conducted experiments that were heavily dependent on images collected by a ceiling mounted Model Exmor RS, Sony cell phone camera with a frame rate of 30 frames per second and attached IMX135 CMOS sensor possessing a maximum resolution of 4224 x 3176 pixels. They employed algorithms considering air flow direction, calibrated mapping curves, mean radiant temperature, natural logarithm model of average airspeed to calculate occupant-fan distance. A total of 16200 samples at 2s sampling interval were collected for the experiment measuring point of airspeeds 26 C, 27.5 C and 29 C at different distances 0.55 m/s, 0.64 m/s and 0.78 m/s respectively from the fan. For all temperature cases at respective distances, the corresponding thermal sensation was observed to be within a comfort zone of ($0.5 < PMV < 0.5$).

3.3. Active Indoor Localisation

Active indoor localisation, unlike passive, predominantly requires the active participation of its target object in the localisation process. Technologies adopting this method require its users to actively carry trackable electronic devices for transmission and data receipt [18][21][24]–[26].

This field is of high interest to researchers as it enables user identification in dynamic multi-user environments. Solutions adapting this method sometimes exploit ubiquitous technologies for management of development cost and infrastructure requirements.

Wide-ranging coverage and simple calibration are additional benefits this method encourages [131]. Metrics implemented in active indoor localisation include Received Signal Strength Indicator (RSSI) [16], Time of Arrival (TOA) [100], Direction of Arrival (DoA) [132], Angle of Arrival (AOA) [133], or Time Difference of Arrival (TDOA) [31]. The techniques for positioning include Radio Frequency identification (RFID) [134][135], Ultra Wide Band (UWB) [136], [137], Global System for Mobile (GSM) [138][139], Ultra sonic localisation techniques [140][141], AM, FM and TV signals [142][143][144], Bluetooth [104], Field strength systems [145], and WLAN [106][146].

3.3.1. Radio Frequency Identification (RFID)

RFID is a low-cost positioning technique that can be employed in both active and passive localisation solutions. It is predominantly utilized by supply chain enterprises for inventory tracking and management efficiency. Compared to passive RFID solutions where tracked object need not carry devices, RFID for active localisation presents solutions involving the system's active interaction with the target object through a wearable or carried RFID device or tracking tag.

In 2011, House et al. [134] proposed wearable prototype consisting of a small RFID tag reader with drift-sensitive IMU to combat the significant sensor drift limitation exhibited by unaided PDR for localisation. All tri-axial measurements from accelerometer, gyroscope and magnetometer sensors that make up the 8cm x 4cm single axis system IMU are oriented on a board in a co-axial manner. The MCU then samples IMU and RFID tags (85mm x 54mm x 1mm) data at 50Hz post initialisation and calibration. Samples gotten from IMU are filtered through the examination of the largest singular value of the accelerometer variance for footfall detection and samples from RFID are necessary for RFID fiducial transformations. Kalman data filter is applied to the footfalls for updating estimates of position, velocity and orientation. Real environment testing was conducted in a four RFID fiducial markers equipped Kelley Engineering centre located on the second floor of Oregon State University where a volunteer walked a simple rectangular set path. Experimental results captured in a 55m x 20m two-dimensional floor area showed 1200% improvement in average error rate using the proposed RFID-fused system. This

result was non-comparable to previous pedestrian dead reckoning state-of-the-art with high vulnerabilities to sensor drift inaccuracies.

Chai et al. [135] in 2017 designed an RFID tracking method that integrates Kalman filter and Multidimensional Support Vector Regression (MSVR). The focus of their study was to improve RFID tracking performance within industrial sites through active RFID technology. Experiments were conducted in a very dense Liquefied Natural Gas (LNG) facility training site. Four intrinsically-safe protected RFID readers alongside a grid of 165 reference tags are set up and allocated across the test environment with known locations. All tags are tested through the measurement of their RSS at different distances; only tags with consistent measurements are retained to avoid draining of batteries. In the static state where tags are situated at the same position, using the framework in Figure 3-4, The study [135] achieved an RMSE of 0.88 m and in real time dynamic state where RFID tags are fixed onto a moving trolley, it achieved an RMSE of 1.40m, 0.66m and 0.71m in three trajectory testing.

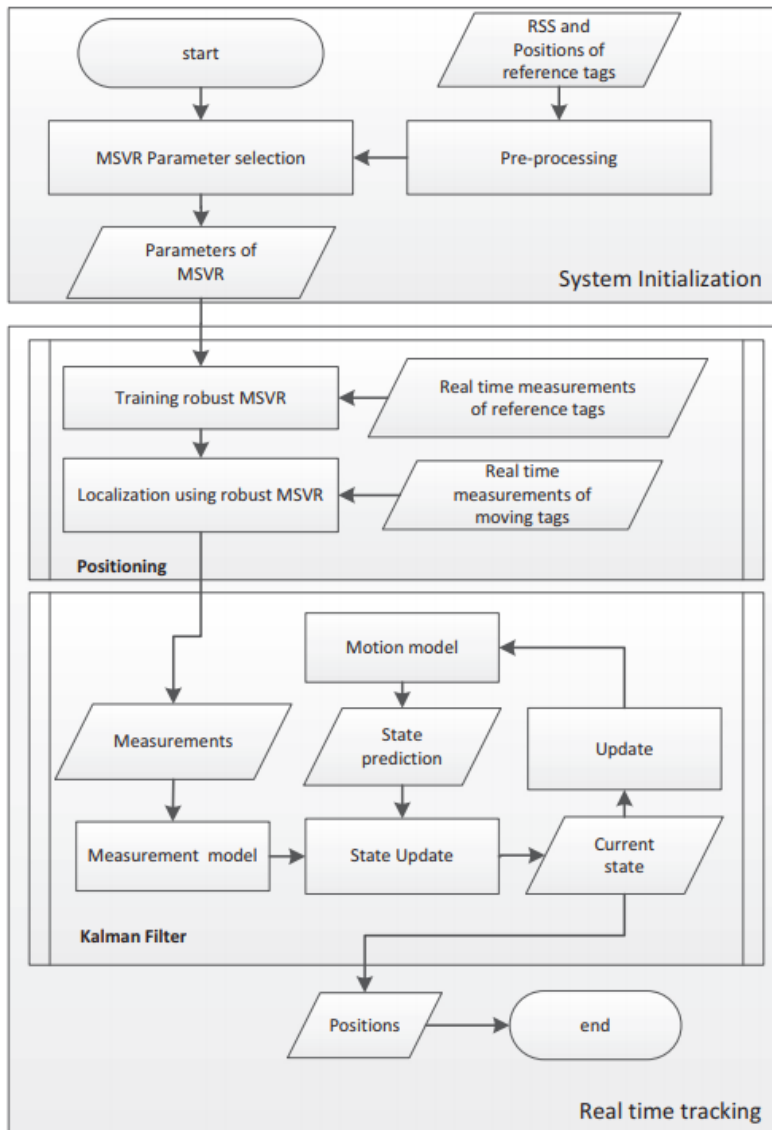


Figure 3-4 Framework of developed RFID tracking approach [135]

3.3.2. Ultra Wide Band (UWB)

Kempke et al. [136] proposed a system called SurePoint, which builds on existing commercial UWB hardware through constructive interference and phenomenon implementation of different modulation schemes that includes frequency and spatial diversity. The system also used a smartphone and a mounted tripoint microcontroller module to achieve a 53% decrease in median ranging error. This is because it relied on

the capturing of high-fidelity range estimates between nodes through UWB radios and a TriPoint module, to provide embedded devices with immediate access to their locations.

Since UWB radios are assumed to spread RF power across wider bandwidth when compared to other narrowband radio such as Wi-Fi 802.15.4 or RFID, the system adopts a ranging protocol to exploit frequency and spatial diversity with minimal impact on update rate and trilateration flood synchronisation methods.

Quality evaluation of SurePoint localisation system was done with the inclusion of two experiments using nine deployed anchors in two evaluation environments.

Their first experiment focused on stationary tracking, where 50 positions of a cross within the evaluation area were recorded after approximately 15s of standing at each position. Each point followed the spacing of the measured floor tiles of the evaluation area which is 1 foot apart. At stationary tracking, SurePoint achieved a median accuracy of 0.29m, a median precision of 0.12m and a sub-meter 99th percentile accuracy and precision in 3D Euclidian.

The second experiment focuses on tracking motion where SurePoint proves to track an object moving at up to 2.4m/s without quality degradation. In motion, SurePoint could find a median error of 0.06m in the x -axis and Median error of 0.07m in y -axis but defaulted to finding a large multiplication in z -axis which therefore resulted in a triple value of 0.15m of median error in the z -axis.

Another research from Kempke et al. [137] proposed Harmonium tag, which is an asymmetric localisation system which utilises low-cost, ultra-wideband tags and slightly-altered narrowband anchors that initiate frequency-stepped band-stitching architecture to achieve UWB-based localisation. This approach achieves decimetre level accuracy through the usage of small, inexpensive, lightweight and FCC-compliant UWB transmitter or tag, fixed infrastructure with pre-set locations and a centralised processor for tag location calculation.

The Harmonium tag system hardware consists of UWB RF radios, quadrotors, Natural Point OptiTrack motion capture system and fixed location infrastructure (otherwise referred to as anchors), and free space UWB signal broadcast of a mobile tag. The anchor hardware monitors and observes tag transmission of UWB pulses. This system adopted the following techniques and methods –

- TDoA of UWB pulses to estimate tag location and impulse response of the channel
- ToA for anchor estimation through an examination of the first observable edge.
- Line-of-sight (LOS) differentiation from subsequent reflecting paths.

The researchers [137] conducted an experiment in a rectangular room measured 4.6 x 7.2 x 2.7 m of a commercial building with dense multipath characteristics. It demonstrated a Median 14 cm error with a 90th-percentile error of 31 cm and median precision of 9 cm through the sub-mm accuracy calibrated Natural Point OptiTrack motion capture system [147].

3.3.3. Cellular Networks

Otsason et al. [138] proposed an approach involving wide fingerprinting of RSSI readings from the strongest 6 GSM cells. They designed a system which included a laptop, Sony/Ericsson GM28 GSM modem (cell phone), and Orinoco Gold wireless card. Then, they implemented a K-nearest neighbour algorithm to the following comparative studies in the structure as follows –

- Readings from 802.11 access point only;
- One cell - utilises reading of the single strongest GSM cell;
- Six-cell - utilises readings of the 6-strongest GSM cells;
- Chann utilises readings from up to 35 GSM channels.

The comparative studies in the structure above were conducted in two multi-floor office buildings and one private detached house. One of the office buildings is home to Intel Research Seattle Lab and the other is part of the department of computer science at the University of Toronto. Intel Research Seattle Lab is situated at a busy downtown while

the University of Toronto and the private house are situated in Seattle's commercial mid-town and quiet residential neighbourhood respectively. Results from this research showed Median accuracy range of 3.4m to 11m with 6 strongest GSM cells and 2.5m to 5.4m with wide fingerprints. It is observed that three out of seven experiments proved GSM accuracy with wide fingerprint to underperform when compared to Wi-Fi localisation.

Another research for localisation using GSM was proposed by Varshavsky et al. [139]. The research utilises wide signal strength fingerprints from 6 strongest cells and additional cells that are strong enough to be detected but are considered too weak to be used for efficient communication. This research used Bluetooth, ultrasound, technologies, Sony Ericsson GM28 modem, Audiovox SMT 5600 phone, 802.11 technology and infrared technologies for the realisation of their localisation system. Fingerprinting technique and K-nearest neighbour algorithm are adopted and applied to data collected from the GSM cells. Similar experiments were conducted within the same environment and parameters as those implemented by Otsason et al [138]. Results from research conducted by Varshavsky et al [139] presented an assumed first accurate localisation system that accomplished 4m floor median accuracy in large buildings and up-to 60% floor identification accuracy with 98% accuracy within 2 floors of tall multi-floor buildings.

3.3.4. Ultra Sonic Localisation

In 2015, UgurYayan et al. [140] presented ICKON, a low cost ultrasonic based positioning system for indoor navigation of mobile robots with centimetre level accuracy. ICKON employs ultrasonic signals for position calculation of the mobile robot within a large indoor environment. It consists of ultrasonic transmitters, tracked mobile units, P3-DX mobile robots and LAN for the signal channel. The system utilises ultrasonic transmitters that periodically send signals from a known fixed location. The mobile robots act as receivers as they calculate their own location through the adoption of TDoA method and multi-trilateration algorithm. Least squares method is then applied to the mobile ultrasound receiver possessing maximal velocity of 0.2 m/s to achieve centimetre level accuracy. The intervals and the sender positions are assumed to be known prior to

evaluation. Furthermore, the receiver is assumed to receive signals from all senders whilst remaining in the same position. It is observed that this method of position estimation would lead to high positioning errors in instances where the receiver moves at a velocity higher than 0.2m/s. Unlike the study by UgurYayan et al.[140], other ultrasonic systems [148][149][150][151] are recognised to not be suitable in medical accommodations or similar environments due to the adverse influence to human health caused by systems' dependency on continuous RF and ultrasonic signal transmission.

Naoki F. et al. [141] proposed an error correction technique centred on an attenuation model using signals in detection circuit and multiple frequencies with directivity models from ultrasonic waves in air. Arduino Uno, transmitter units, comparator, ultrasonic receivers and a microcontroller are all technologies used in this study. In an experimental test area of 80cm x 80cm x 117cm, each transmitter was attached to the top corners of the ceilings, pointing towards the centre of the floor and the receivers were stationed at each 9x9 grid points at 10cm intervals with a height of 21.5cm pointing towards the ceiling. Within the test area, Time of Flight (ToF) algorithm was applied to the comparator for ultrasonic wave detection, and, Low Pass Filter was applied to the output of the compared signal of the attenuation model. This was important to get an average error reduction of 2.52cm. This results in 18% less than Linear which exhibited significant errors due to miscalculated 25.0 kHz or 32.7 kHz receiver detection time during far ranges from the transmitter.

3.3.5. AM, FM and TV Signals

Sungro. Y et al. [142] presented ACMI, an FM-dependent localisation system which does not need proactive site profiling. This system builds fingerprint database from the true estimation of RSS distribution of commercial FM radio stations only. The investigations in investigations by Sungro. Y et al. [142] repurposed Wi-Fi signal propagation model to control FM radio features and read FM information from transmission towers as well as building the floor plan. Evaluation of the research was from eight different FM stations in seven campus locations of dimensions 35m x 85m and 55m x 85m and three downtown buildings including two public museums and a shopping mall (through Wi-Fi signalling

and Bluetooth of mobile phones – Samsung Galaxy Note 2, LG and Sony smartphones). For position estimation, a two-step process; parameter calibration and path matching are implemented in the positioning refinement of stored FM RSS fingerprint information in the database. The result showed an error of 6 m and 10 m in the seven campus locations and downtown buildings respectively. Limitations encountered by S. Yoon et al [142] include poor signal attenuation of FM signal in the presence of obstacles; potential model implementation difficulty in the 3D environment; the system will potentially fail to estimate the true location of target audience if the floor of all measured environment have similar structures and insignificant height differences because ACMI [142] identifies location through the identification of structural unit indigenous to a particular floor's floor plan and the single RSS DB created from it.

In their indoor localisation study, Rahman et al. [143] combined probabilistic and deterministic fingerprinting technologies. The study mentions that an advantage AM/FM had over Wi-Fi, which was its dedicated bands that prevent interferences from other signals in other bands. In two test areas, with dimensions 28m x 12m, Rahman et al. [143] implemented Nearest Neighbour, K-Nearest Neighbour and K-Weighted Nearest Neighbour to calculate mean distance error of less than 3m. *Test area 1*, was a ground floor with 29 Reference points and 13 Transmission Points, while, *test area 2*, was the first-floor with 22 Reference points and 7 Transmission points. In particular, used for both experiments are the strongest reception of 8 Sydney-focussed AM radio broadcasting channels at a frequency band of 526.5kHz - 1606.5kHz.

Due to research [144] that analysed TV-based localisation systems and their limited success at leveraging the high bandwidth of TV signals through time-based approaches, Eggert [152] adopted the time difference of arrival (TDOA) method on analogue TV signals and resulted in indoor positioning errors of up to 300 m. The outcomes were bettered by the Rosum system, which employed digital TV (DTV) synchronization signals to achieve 23m mean accuracy. It is acknowledged by the researchers [144][153] that only fingerprinting investigation relating to DTV signals is implementable in outdoor environments only with a median accuracy of 130m.

3.3.6. Bluetooth

Teran et al. [104] used low energy Bluetooth technology in designing an IoT based system for indoor localisation. Their solution consisted of two major systems: an acquisition system, and a central server regulated by a Client-Server paradigm and IoT philosophy. The investigation included the adoption of a simple location algorithm derived from LBS and Received Signal Strength (RSS) fingerprinting method and K-Nearest Neighbour (K-NN) classifier to measure Bluetooth beacons.

The researchers assessed their system in a 25 m² sized room partitioned into 1m x 1m grid cells at Pontificia Universidad Javeriana, Bogota, Colombia. They deployed four fixed Bluetooth beacons fixed at a height of 30cm and positioned at square corners (0m, 0m), (0m, 5 m), (5 m, 0 m), and (5 m, 5 m) of the test area. The results included a correct classification of 70.2% and 29.85% incorrect classification thereby resulting in a precision of 2m².

3.3.7. Field Strength Systems- IMU

Research conducted by Hellmers et al. [145], introduced MILPS, which is an indoor localisation system based on a combination of artificially generated magnetic fields and Inertial Measurement Units (IMU). They further combined the artificially generated magnetic fields and Inertial Measurement Units (IMU) with pressure sensors and adaptive filtering methods to estimate altitudes, position and direction of a mobile platform.

MILPS is an infrastructure based system consisting of multiple coils that generate artificial magnetic signals which act as reference points. Then, these reference points are positioned at strategic locations of the test area for better coverage attainment. This is important because it will enable the system to better measure position estimates through the implementation of basic sensor fusion principles and Kalman filter based kinematic motion model. The MILPS is designed to use a decentralisation synchronisation process that applies serial control to the implemented coil and mobile station. This

synchronisation process is particularly done through the implementation of Time Division Multiple Access (TDMA) scheme. This is because it is reliant on Real-Time Clocks (RTCs) and Real-Time Operating System (RIOT-OS).

The literature conducted two experiments in a 440m² surface area of Technical University of Darmstadt Institute building with 2 installed ramps. This was to identify altitude change in 2 thick walled closed rooms. The experimental results demonstrated that moving objects can be localised with accuracies of less than 1.5m in the horizontal plane and 0.5m in z- direction.

3.3.8. WLAN – Wi-Fi

Wi-Fi is a ubiquitous technology generally exploited by developers for indoor localisation. This is discussed in a review by Suining He [106]. Suining investigated the latest developments in Wi-Fi-based indoor localisation with importance to efficient system deployment and localisation techniques.

There are various localisation techniques for Wi-Fi, these include a model by Chen et al. [146] created to optimise the fusion of Wi-Fi WPL and PDR landmark (shown in Table 3-4). Chen et al. [146], designed a smartphone based indoor localisation system that used Kalman filter to combine Pedestrian Dead Reckoning (PDR) with log-distance path loss model. This was important because PDR measured the motion process of the user from IMU sensors in the smartphone, and, path loss shadowing model provided relative distance estimates between the tracked node (user with a smartphone) and the Wi-Fi routers based on RSSI.

Similar to popular realisation, the researchers [146] observed that RSSI signals of the used routers fluctuated due to Wi-Fi signal variations. Traditionally, to tackle RSSI fluctuations, RSSI fingerprinting technique is popularly implemented. Although fingerprinting is popular, it requires the manual collection and training of huge datasets. Also, in cases where the environment is modified, the system would require retraining to learn the new environment. Therefore, to overcome the shortcomings of fingerprinting,

the researchers adopted and repurposed the successful RFID weighted path loss algorithm in a three steps process.

- First step - distance calculation between the Wi-Fi router and smartphone using log-distance path loss model.
- Second step - weight determination using distance reciprocal.
- Third step - determination of smartphone location through the summation of weighted router locations.

Steps	Equations	Description
First step	Distance calculation between the router and smartphone using log-distance path loss model. Based on signal propagation model, it is assumed S_t^i is RSS of router i at time step t $s_t^i = PL_0 + 10\alpha \log (d_t^i)$	Where PL_0 is the reference path loss coefficient, α is the path loss exponent, d_t^i is the distance between the routers i and the device at time step t
		(see Equation (5) in chapter 2 for extended formula)
Second step	Weight determination using distance reciprocal. Weight of each router can be calculated as: $w_t^i = \frac{1}{\sum_{i=1}^N \frac{1}{d_t^i}}$	Where, N is the number of routers and distance between device and routers can be expressed as vector $\{ d_t^1, d_t^2, \dots, d_t^N \}$ at time step
Third step	Determining location (x, y) of the smart phone through summation of weighted router locations. $w_t^i = \frac{1}{\sum_{i=1}^N \frac{1}{d_t^i}}$	Where, (X , y) is the location of the router

Table 3-4 The assumptions for RSS WPL algorithm as proposed by [146]

WPL algorithm was observed by Chen et al. [146] to be a suitable realistic lightweight algorithm because it sits on a resource-limited smartphone as opposed to a server. Specific parameters such as **initial point, step length** and **walking direction**, make a huge significance because the adopted PDR technique is reliant on relative information from IMU. This, therefore, makes it only suitable for pedestrians walking short ranges as it will

drift if employed for long distances. Some calculations conducted for some PDR parameters are highlighted below in Equation12-Equation 14.

Determining the target object's initial point

$$\mathbf{X}_t = \mathbf{X}_{t-1} + L_t \begin{bmatrix} \sin(\theta_t) \\ \cos(\theta_t) \end{bmatrix}$$

Where,

\mathbf{X}_t , refers to the position at time step t ,

L_t , refer to step length,

θ_t , refers to walking direction at time step t .

Equation12

The initial point, being one of the most vital parameters necessary for the success of Chen et al.s' [146] proposed indoor localisation is obtainable through the leveraging of landmarks as the system holds no prior location information.

Step detection with step length

Step detection is obtained from smoothened accelerometer data from periodic vertical acceleration pattern of walking users. This can be expressed as, a_t^m and calculated as;

$$a_t^m = \frac{\sum_{i=t}^{t+m-1} a_i}{m}$$

Where,

$\{a_t, t \in 1, \dots, K\}$, refers to vertical acceleration time series. m , refers to ordered smooth function output at time step.

Equation 13

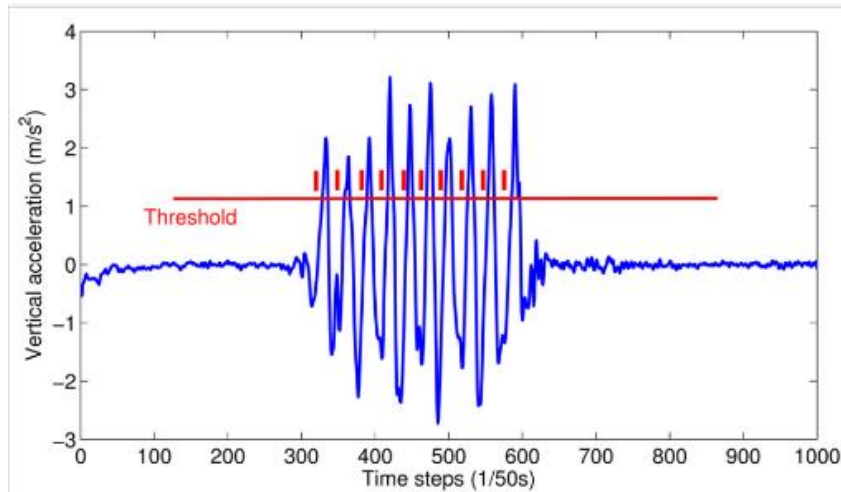


Figure 3-5 Simple threshold method application on a smoothed vertical acceleration pattern for step identification

Researchers Chen et al. [146] adopted step length estimation illustrated in Figure 3-5 to determine the linear relationship between step length and pedestrian's height.

This adopted approach considers the dynamics of step length when a pedestrian is walking as calculated in equation 13.

$$L = height * k$$

Where,

L, refers to step length

k, refers to the coefficient. This is usually determined by the pedestrian's gender.

Equation 14

To accommodate variance in step strides, the adopted solution observed by Chen et al. [146] provides a relationship between acceleration magnitude and step length. This considers the dynamics of step length when a pedestrian is walking in Equation 15.

Walking direction

$$L = \beta(a_{max} - a_{min})^{1/4}$$

Where,

L , refers to step length,

β , refers to adjustable coefficients. This is subject dependent.

a_{min} , refers to the minimum acceleration magnitude

a_{max} , refers to the maximum acceleration magnitude.

Equation 15

To estimate walking direction, scientist Chen et al. [146] adopted Equation 15, combining angle and orientation sensor outputs from a gyroscope, magnetometer and accelerometer using Kalman filter. This angular acceleration from the gyroscope manages the sensitivity and drift of magnetometer and accelerometer respectively.

Landmarking is introduced to mitigate PDR drift over long ranges and Wi-Fi RSS fluctuation. Landmarks provide new starting points for PDR when the user approaches them. Therefore, S. He and S. H. G. Chan [106] proposed the incorporation of Wi-Fi,

gyroscope, accelerometer, magnetometer and barometer to determine investigated landmarks such as doors, stairs, elevators, turns and escalators.

Wi-Fi WPL and PDR approaches were combined to compensate for each other's weaknesses. Due to Wi-Fi signal variation, Wi-Fi WPL is not vigorous enough and PDR is highly dependent on relative information from IMU. Therefore, its short-range position estimation is accurate and its longer range estimations are inaccurate because of drift. Their idea was for Wi-Fi WPL to assist in correcting PDR drift while PDR smoothens Wi-Fi variations in the Wi-Fi WPL.

Three experiments were conducted in a standard 19.0m x 16.3m research lab and a 27.5m x 16.4m test bed at the Nanyang Technological University of Hertfordshire campus using a handheld Google Nexus 4 smartphone running Android 4.4 operating system. The first experiment being Wi-Fi WPL and PDR with landmarks resulted in mean localisation errors of 2.877m and 1.7547m respectively. The experimental results showcase an average accuracy of 1m.

Considerations from Active Localisation

Aside from providing meter level accuracy, investigations by S. He and S. H. G. Chan [106] also diagnoses inadequacies of the solution in detecting pedestrians within a multi-floor environment. Multi-floor localisation is perceived to be attainable through Wi-Fi WPL and PDR landmark combinations.

Although the solution by S. He and S. H. G. Chan [106] presents an improvement of about 1m compared to the lightweight multi-trilateration result of 1.5m – 3.1m in representative literature [14][65]. Our proposed investigations would adopt the combination of Wi-Fi and IMU sensors of a smartphone to estimate the position of our tracked mobility scooter. In particular,

- For Wi-Fi, RSSI- SDRS log-normal shadowing model [64], which is a proposed update of the log-normal distance path loss model used in research by S. He and S. H. G. Chan [106].
- For IMU, we would propose to investigate further how the combination of accelerometer, gyroscope and magnetometers will work for mobility scooters.

We expect the following -

- Multi-trilateration on the results from the RSSI- SDRS log-normal shadowing model [64] will outperform results from log-normal distance path loss model used by S. He and S. H. G. Chan [106].
- PDR is best for pedestrian motion and therefore will be inadequate for translational motion.

3.4. Hybrid System

Hybrid systems are a combination of techniques, technologies or propagation adapted in both passive and active systems for localisation attainment. A huge variety of localisation systems are of the hybrid variety as they involved the combination of technologies for position estimation.

According to A. Correa et al [107], there exist no definite standards for hybrid positioning systems. This is due to a large number of viable IPS combinations need for the development of a hybrid system. After careful analysis of over 150 literature works, section 3.4, proposes classifications for hybrid localisation systems. These include –

- Propagation based hybrid system only
- Technology and Technique (TT) based hybrid system.

See below for relevant literature examples representing the above classifications.

3.4.1. Propagation Based Hybrid System

Propagation based hybrid system is a localisation system that combines different technologies that have similar propagation techniques. For example, RSSI can be propagated from two different technologies such as Wi-Fi and Zigbee. This is important for systems that adopt this approach because it provides data compensation in weakness or NLoS instances.

Representative state-of-the-art demonstrating this standard is the research conducted by Daniel et al. in 2017 [108]. The researchers [108] exploited ZigBee and Wi-Fi technologies and combined their propagated RSSI using a simple token ring network. These technologies were selected because, both technologies propagate RSSI, and, Wi-Fi is a ubiquitous IEEE 802.11 standardised technology while ZigBee is a cost-effective low power wireless communication technology, standardised under the IEEE 802.15.4.

This combination is important because the node RSSI pair communication of both Wi-Fi and ZigBee would not depend on LOS for estimation, it will, however, measure a response directly relational to entity breaking its link path. It, therefore, removes interferences from contesting Wi-Fi signals in urban areas. In particular, through the deployment of top Zigbee 802.15.4 standard channel and new frame control measures in the Wi-Fi's white space.

Daniel et al. configured a token ring DFL node consisting of MRF24J40 radio and PIC32MX440F256H paired microcontrollers running in a Mesh with slaves. They conducted evaluations in a static environment using nominal post-processing of RSSI results, utilizing K-Nearest Neighbour, and Euclidian Distance for variance mean computation. It was revealed by Daniel et al. that their system provided an accuracy of 80% for DFL in a 3m x 3m quadrant, 95% for Active tracking in a 2m x 2m area, and 98% in coupled Active tracking utilizing DFL measurements.

It was their observation their system performed poorly in NLoS conditions. In particular, large RSSI variations were noticed in a histogram plot of 15 00 RSSI sample values.

3.4.2. Technology and Technique (TT) Based Hybrid System

TT based hybrid systems are localisation systems that estimate position through the combination of different technologies and techniques. This is important because limitations of one individual technology are mitigated with another complementary technology. For example the proposal by Alatise et al. [109] to combine IMU and camera vision. This is because of the advantages of IMU sensors (discussed in 3.3.7 3.2.9) and camera vision (discussed in 3.2.9).

Alatise et al. [109] proposed to estimate the pose of a four-wheeled mobile robot using a fusion of the inbuilt IMU sensors (6-DoF) and single mounted LS-Y201-2MP LinkSprite's new generation high-resolution serial port camera module for the vision. This is because the researchers determined that improved pose estimation of a robot required more than one sensor and a blend of object recognition and feature matching methods.

The assessments of their system, included, object recognition of camera captured images and random sample consensus (RANSAC) algorithms. This is because RANSAC differs from traditional methods in that it approximately calculates the constraints of a mathematical model from a set of obtained data employing an iterative technique.

The literature showed experiments in a test area of 4m x 5.2m, where, IMU and camera recorded maximum error values of 0.145m in position and 0.95° in the orientation.

Our proposed investigation would fall under TT based hybrid systems. This is because it would combine different technologies including Wi-Fi, IMU and wheel encoders to improve indoor position accuracy. Although each technology is different, it is expected that these technologies would complement each other.

3.5. Summary and Analysis

The scope of this review is limited to indoor localisation. This chapter examined different indoor localisation systems, algorithms and techniques designed by researchers with emphasis on trade-offs observed amongst them.

State-of-the-art indoor localisation systems offered in the literature is categorised into passive, active and hybrid localisation systems.

Passive indoor localisation appeal to users as it does not require users to carry a device. This, therefore, enhances convenience for users as they are not required to carry additional devices on their person. It is observed that the majority of indoor localisation solutions within this category provide accuracies of tens of centimetres to meters. In most cases they are predominantly cost-effective for users, however, a good majority are non-scalable, bulky, expensive, and, complex to set up and implement. Thus, becoming a less appealing approach to solving indoor localisation problem. This is emphasized in Table 3-5.

Active indoor localisation is more popularly employed by scientists in attaining the improved position. This has demonstrated an accuracy achievement from centimetre level accuracy [141] to 5.4 m [139] accuracy. Unlike passive indoor localisation, active indoor localisation requires users to carry traceable trans-receiving devices to determine location. This requirement formally posed as an inconvenience to users, especially in cases where carried devices were bulky. Most solutions under active localisation were observed to be popularly expensive. Today, active indoor localisation has become more appealing to researchers and users because of the opportunity to exploit user dependent everyday technology such as a smartphone. Thus, significantly reducing the cost. These are highlighted in Table 3-5.

The examination of hybrid indoor localisation uncovered the ambiguity of its characterisations. There were no standards or categorisation for this type of indoor localisation. This research uncovered and presented two identifiable hybrid localisation

classifications, which include *Propagation based hybrid system only* and *Technology and Technique (TT) based hybrid system*. Both classifications can be a permutation of passive and active positioning technology and localisation combinations. The former, *Propagation based hybrid system only*, is observed as different technologies with similar propagation techniques exploited to attain an improved position. The representative paper [109] demonstrated high accuracy of 95%. However, the representative of this classification is neither robust nor scalable as both Wi-Fi and ZigBee need to be at most 5 meters apart for adequate communication. ZigBee is unlike Wi-Fi, is not ubiquitous, so, commercial development will become expensive in mass production situations. *Technology and Technique (TT) based hybrid system*, combines different positioning technologies and techniques to get an improved position. Representative literature [110] of *Technology and Technique (TT) based hybrid system* demonstrated a high accuracy of 0.145 m. Although it showed high accuracy, it is identified that this solution is intended for localising robots with inbuilt IMU sensors. The solution required the addition of a high-resolution camera. Due to the non-ubiquity of camera technology, the solution is considered to be expensive. These are highlighted in Table 3-5.

As a majority of the indoor localisation systems are limited in one or more key areas such as accuracy, scalability, energy efficiency and cost, the research encourages the development of WTP-HAMS system which favours mentioned key areas.

Our proposed investigation would employ *Technology and Technique (TT) based hybrid system* in the designing of a novel WTP-HAMS system, which includes Wi-Fi, smartphone IMU modalities and wheel encoders. This is important because the exploited technologies are ubiquitous, thus significantly reducing the cost of the system development. The proposed system would be scalable and easy to use by the users because of the familiar technologies exploited.

Furthermore, it is our observation that a majority of the SOTA is designed for pedestrian users moving in pedestrian motion, and, it is our suspicion that SOTA solution would not be suitable for mobility scooter users moving in translational motion. This is an

overlooked and neglected gap, thus the proposal to design the novel WTP-HAMS system that would reduce position errors and provide better accuracy for mobility scooter users.

Table 3-5 Analysis of state-of-the-art

	Technique	Technologies	Scalability	Accuracy	Cost	Energy efficiency	Experiment area	Additional details
Passive indoor localisation	Differential Air Pressure	Heating, ventilation, and air conditioning (HVAC) systems [113]	Yes	75-80% in particular door movement alteration and 65% in user movement	Moderate	No	<p>Home 1 was a large property with three separate central HVAC units.</p> <p>Home 2 larger than <i>Home 1</i>, with two separate HVAC units</p> <p>Homes 3 and 4 are smaller apartments with single central HVAC systems</p>	Performs best in small homes 3 and 4 with no doors
	Differential barometer	MEMS barometer [114]	No	Tens of centimetres to meters accuracy in estimating altitudes	Moderate	Yes	Floor levels via elevators and stairs	Insufficient for estimating position
		InLite by Atrium Satellites GmbH [115]	No	2 meters accuracy	Expensive	N/A	11m x 66m area	Bulky High errors
	Physical contact based system	Capacitive field sensor - sensing mats [117]	No	50cm accuracy	Expensive	No	6msq	Cumbersome Difficult to deploy
		Capacitive field sensor - passive wires grid [99]	No	12.7cm mean errors with shoes 18cm mean errors without shoes	Expensive	No	20cm spacing of passive wire grids	simulated and untested in real environments Pedestrian users limited to one user at a time
		Pressure sensor - smart floor [121]	Average	93%	Expensive	No	N/A	used smaller tiles Pedestrian users
		Pressure sensor - Electro-Mechanical Film smart floor [120]	Average	91%	Expensive	No	100 square meters	Pedestrian users limited to one user at a time
		Touch sensor - UbiquitousRobot – UBIRO [123]	Average	Error of 13.3cm at x axis and 5.7 cm at Y axis	Expensive	Yes	420cm x 620cm	Deployed 198 IC tags Deployed in obstacle free environment
		Light	LED light sensors [125]	Average	0.24 in to 1.39 in	Expensive	Moderate	7 ft. x 12 ft
	Ultra-wideband (UWB)	UWB monostatic WSRs [127]	No	Root mean square error 2 m for SKDU and 1.35 m for SDL	Expensive	Yes	N/A	Reliable LOS dependent
	Computer Vision	Floor pressure-imagery [119]	Yes	20 cm human localisation error	Expensive	Yes	30cm x 30cm floor tiles	Pedestrian users
		Micro aerial vehicle (MAV) [128]	Yes	Mean error of 9.3869 cm	Inexpensive		4m x 3.5m x 3m	Poor range identification
	Device-free passive (DFP)	RASID system [129]	Yes	0.93ft	Inexpensive	No	2000ft ² and 1500ft ²	Best for motion detection
		PLAS [61]	Yes	RMSE of 1.32m and MDE of 0.67m	Inexpensive	Yes	7m x 7m	Pedestrian users Unsuitable in dense environments
	Smart wiring and socket	E-locas - socket level localisation system [130]	Moderate	90.76%	Expensive	N/A	1.2m x 1.2m grids	Not robust
Camera	Tracking fan [131]	Yes	0.5 < PMV < 0.5	Moderate	Yes	N/A	Simulated and untested in real environments	

Active indoor localisation	Radio Frequency identification (RFID)	Wearable RFID [135]	Yes	1200% improvement	Moderate	Yes	55m x 20m	Supported with IMU Pedestrian users Commercial office environment
		RFID tracking method [136]	No	In static instance RMSE is 0.88m In real time dynamic state RMSE of 1.40m, 0.66m and 0.71m	Expensive	Yes	N/A	Industrial site Trolley tracking
	Ultra-wideband (UWB)	SurePoint [138]	Yes	In stationary median accuracy of 0.29m In motion, median error of 0.06m in x axis 0.07m in y axis	Moderate	No	N/A	Pedestrian users For industrial environment
		Asymmetric localisation system - Harmonium tag [137]	Moderate	Error of 31 cm	Expensive	Yes	4.6 x 7.2 x 2.7 m	commercial building with dense multipath characteristics Limited to Line of Sight
	Cellular Networks	GSM wide fingerprinting system [139]	Moderate	Accuracy of 2.5m to 5.4m	Moderate	Yes	N/A	Office building Commercial office environment Requires 6 strong GSM cells
		GSM wide fingerprinting system [140]	No	4m floor median accuracy	Expensive	No	N/A	Floor level accuracy Requires 6 strong GSM cells, plus additional strong cells Multi-floor buildings
	Ultra sonic localisation	ICKON [141]	No	Centimetre level accuracy	Expensive	N/A	N/A	High errors when robot moves faster than 0.2m/s
		Error correction technique using ultrasound [142]	No	Average error reduction of 2.52cm	Expensive	N/A	80cm x 80cm x 117cm	No suitable for medical and health environments including care homes
	AM, FM and TV signals	AM signals [144]	No	Error of less than 3m	Moderate	N/A	28m x 12m	Needs atleast 8 AM broadcasting channels
		FM signals - ACMI [143]	Moderate	Error of 6 m and 10 m	Moderate	N/A	35m x 85m and 55m x 85m	8 different FM stations used Error caused by poor signal attenuation Environment have similar structures will result in system failure
		TV signals - digital TV (DTV) based localisation [153]	Yes	23m mean accuracy	Inexpensive	Yes	N/A	High inaccuracy
	Bluetooth	IoT based indoor localisation using bluetooth [105]	No	Accuracy of 2msq	Expensive	Yes	25 msq sized room	Low range
	Field strength systems	MILPS [146]	Yes	Accuracy of less than 1.5m	No	N/A	440msq sized room	Uses IMU sensors
	WLAN- Wi-Fi	Wi-Fi WPL and PDR landmark combinations [147]	Yes	Mean error of 2.877m	No	Yes	19.0m x 16.3m	Wifi, IMU sensors, barometer Pedestrian users

Hybrid localisation systems	Propagation based hybrid localisation	Wi-fi + Zigbee [109]	No	95%	Moderate	Yes	2m x 2m	RSSI exploitation
								Used coupled Active tracking utilizing DFL
								Static environment
	Technology and technique (TT) based hybrid system	IMU + camera [110]	Yes	0.145 m	Moderate	N/A	4m x 5.2m	Inbuilt IMU + additional camera infrastructure
								Robot pose estimation
								High accuracy
								Expensive

Chapter 4 Proposed Investigation

This chapter introduces the proposed investigation, which is the design and development of a novel WTP-HAMS system. This includes the aims and objectives of the study, the working scheme and conceptual flow of the proposed investigation. It also describes the research development plan, including the milestones that will be undertaken in the realisation of the developing the proposed WTP-HAMS system. This chapter also includes a summary and analysis. Finally, it clearly describes our contribution to knowledge.

4.1. Research Question

It would be very beneficial to the use of different available cost-effective sensors for mobility scooter indoor localisation if they could lead to sufficiently accurate pose estimation. It is believed there is potential to achieve this. Therefore the thesis research question is:

Is it possible to improve indoor vehicle position and orientation estimates by combining Wi-Fi, smartphone IMU and wheel encoders, so that this can be effectively exploited for scooter navigation?

4.2. Core Idea and Motivation

For a more accurate inexpensive indoor positioning system to be accomplished, ubiquitous technologies need to be exploited. A positioning accuracy improvement system using a combination of Wi-Fi, wheel encoders, accelerometer and magnetometer is proposed and discussed in this chapter as it applies to the techniques, mathematical models and system description of WTP-HAMS.

The main idea is to exploit the errors experienced by two ubiquitous technologies used in indoor localisation to attain improved positioning. Wi-Fi provides positioning information, but its imprecision is high and therefore insufficient in determining precise location detection. To improve this imprecision, complementary position estimation

technology is introduced. This introduced technology is the wheel encoders. Though the wheel encoders provide better position accuracy, it is susceptible to drift. To mitigate drift in the distance and angular updates, a unique drift mitigation model is designed to manage errors experienced in distance and combined with fused accelerometer and magnetometer sensors to provide more accurate heading estimates. This combination provides better results because the fused accelerometer & magnetometer sensors produce accurate world direction with reference to the global system. This contributes to qualitatively improve the position of the already estimated wheel encoder. However, the position is with reference to the mobility scooter reference system and therefore needs to be positioned with a reference system of the room. The Wi-Fi, therefore, is advantageous as it provides a position with the room as the reference system. Therefore, combining Wi-Fi RSSI estimates with the novel odometry model provides improved position accuracy according to the measured room reference system.

The tracked object in this study is a mobility scooter with a smartphone (**SP**) mounted on its arm. **SP** collects data from all exploited technologies.

This research aims at designing the WTP-HAMS system which is an innovative positioning system using a complementary combination of Wi-Fi, wheel encoders, accelerometer and magnetometer, to improve location accuracy of mobility scooter users within rooms. WTP-HAMS contains a unique combination of techniques that aim at significantly reducing resultant position errors. The combined techniques are grouped under RSSI derived position estimates and odometry pose position outcomes. WTP-HAMS uniquely leverages error shapes experienced by RSSI and Odometry to determine improved new position as demonstrated in the working scheme of Figure 4-1. Compared to SOTA that shows an error of 1.5m – 3.1m from Wi-Fi and 33cm error from odometry, WTP-HAMS system demonstrates better accuracy with an error range of 0.35m – 1.35m. Our system adopts a similar assumption [19][14], to track an object travelling in a straight line with 50 experiments. A working scheme of WTP-HAMS system is illustrated below.

Relative position derivation using RSSI

Pose estimation with relative position using Odometry

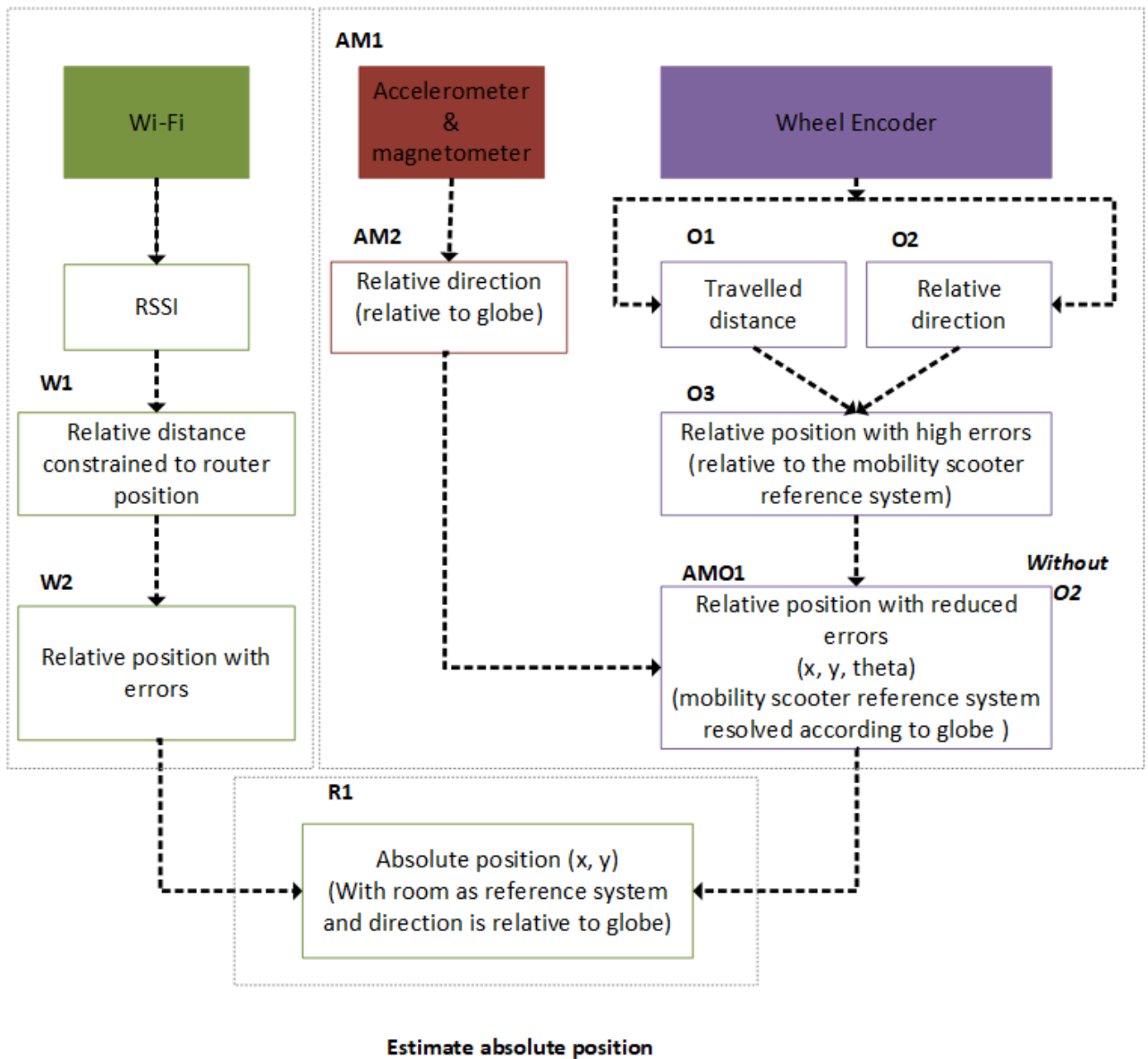


Figure 4-1 WTP-HAMS working scheme

Position Estimation using RSSI

Wi-Fi is a ubiquitous technology which emits received signal strength indicator (RSSI) for propagation for use in indoor localisation systems. The exploitation of RSSI for indoor localisation is a continuously developing area of intense study [16][154]–[157]. Employed indoor localisation methods are reliant on the propagation environment, as it influences positioning results thereby causing significant localisation errors.

It is proposed that the WTP-HAMS system employs Wi-Fi to estimate the position between the APs and the Mobility Scooter relative to the room. As shown in Figure 4-1, this is proposed to be achieved by first estimating **W1** and then **W2**.

W1 is estimated using the SDRS path-loss shadowing propagation model [64][77] represented by Equation 5 on page 68. This model is chosen because it takes environmental dynamics into account as it causes noise reduction to propagated RSSI and converts its values into relative distances constrained to the routers' positions within a room.

Although **W1** provides relative distances between routers and reference points, it fails to provide position estimates of the mobility scooter. Therefore, WTP-HAMS system adopts multi-trilateration algorithm [14] (Equation 6 on page 73) to combine the estimated distances (**W1**) and the known APs positions (relative to the room's reference frame) resulting in one position for the mobile scooter relative to the room's reference frame. This is referenced as **W2**.

The error associated with **W2** can be estimated using Equation 9 on page 75 which performs the distance of the position error between true position and estimated position. This measures the performance of **W2** by average localisation error as proposed in the paper by L. Cheng et al [78]. The distance of the error from ground truth acts as the radius of the circle encompassing estimated position from the ground truth.

Though the outcome of **W2** is relative position estimate, its positioning accuracy is low due to relative distance **W1** inaccuracies the SDRS path-loss shadowing propagation model experiences when interferences such as shadowing, and path-loss are present.

The outcome display limitation of RSSI as it provides inaccurate Mobility Scooter position with large average error ranging between 2 and 3 meters. Furthermore, there is no navigational information.

Pose Estimation using Proposed Novel Odometry Model

WTP-HAMS system then introduces wheel encoder technology by using complementary odometry modelling to better ascertain position. In particular, odometry is capable of providing pose estimates based on navigation trajectory as it refers to the mobility scooter which can be very precise provided its covered travelled distance is accurate.

Traditionally, odometry models are used in localising mobile robots in an indoor environment [19]. Odometry is performed using travelled distance output from inbuilt wheel encoders of the mobile robots to derive pose estimates x, y and θ . These derivatives are expressed in Equation 1, Equation 2 and Equation 3 (from page 57) to ensure Equation 16, Equation 17 and Equation 18 to be true.

$$x_{k+1} = x_k + D_c \cos(\theta)$$

Equation 1

$$y_{k+1} = y_k + D_c \sin(\theta)$$

Equation 2

$$\theta_{k+1} = \theta_k + \frac{D_r - D_l}{L}$$

Equation 3

Equation 1, Equation 2 and Equation 3 are translated working components **O1**, **O2** and **O3** of the working scheme illustrated in Figure 4-1. This is expressed in Equation 16, Equation 17 and Equation 18 on page 127.

$$\mathbf{O1} = D_c = (D_r + D_l) / 2$$

Equation 16

$$\mathbf{O2} = \text{Equation 3}$$

Equation 17

$$\mathbf{O3} = \text{Equation 1 and Equation 2}$$

Equation 18

Unfortunately, odometry suffers from drift when the robot travels over a period of time. This, therefore, encouraged researchers [158] to propose the integration of standard odometry with IMU sensors and camera. The results from this study lead to an error of 51cm when the odometer is used alone, 33 cm when the odometer is combined with IMU; and a position error between 1cm and 10cm when camera vision is added.

Although the method is promising, it is evident that without cameras there is poor accuracy. Nonetheless, the author is interested in experimenting without a camera because the aim is to experiment in a natural not prepared environment while the camera would bring an extra environment setup cost.

Therefore, WTP-HAMS employs wheel encoders to get the distance travelled **O1** and relative direction **O2** both are relative to the mobile scooter reference frame.

Proposing New Drift Mitigation Model

The relative position **03** is expected to include a positional error due to drift in distance and heading accumulated while the scooter is in motion. To improve the drift issue would then be relevant to determine better odometry based position. Suffered drift is the accumulation of errors in the travelled distance over time, thus a drift mitigation technique is proposed in this study. In particular, it is recommended to use Equation 19 and to run a set of trials to estimate $Err_x\%$.

The proposed drift mitigation model adds calculated percentage deviation of estimated travelled distance.

$$Dist_R = D_c^m + Err_x\%$$

Equation 19

$Dist_R$ is new improved distance with reduced error, D_c^m represents the maximum estimated travelled distance and $Err_x\%$ is the estimated drift (which is a percentage error of the travelled distance). $Err_x\%$ is derived from the percentage of the difference between actual distance value and the estimated distance value of the maximum value with the highest reoccurrence. The maximum value is the best fit in the study due to outcomes derived by experimentation described in chapter 6.

This is a simple but effective way to provide a more robust and reliable system for deriving better travel distance estimate, which is uncommon in literature works.

Proposing To Estimate Better Navigation Heading

The neo 4 mobility scooter used in this research has aligned wheels with anti-slippage and anti-tip puncture-proof solid tyres. Its solid tyres are advantageous particularly because they do not require pressure monitoring or inflation. Nevertheless, slippage is expected to occur if the depth of the tyre tread is below 0.5mm. However, our employed

mobility scooter has a tyre tread above 0.5mm and will be tested in a representative environment with smooth wooden floors and none slippage events.

The neo 4 is a tricycle drive employs a single driven front wheel and two passive rear wheels. It is a fairly common AGV application because of their inherent simplicity. In most cases, the rear wheels are used for heading determination. However, it is inclined to causing loss of traction and high error in heading estimates because of the tracked vehicle's centre of gravity is shifted from the front wheels. Based on our comprehension from the report written by L.Feng et al [159], it is our conclusion that the error associated with this vehicle is systematic error caused by encoder resolution error and the average of the actual wheel difference from nominal wheel diameter. This systematic error in heading estimates are prevalent and will derail the mobility scooter over distance and time. Therefore, to mitigate this heading error and correct bias, WTP-HAMS system then proposes a combination of accelerometer and magnetometer sensors using an adopted combination of Magnetic angular rate update (MARU) and acceleration gradient update (AGU) of MAGYQ filter in the study by V. Renaudin and C. Combettes [160]. Accelerometer and magnetometer sensor fusion produces the orientation and heading of the mobility scooter through the monitoring of smartphone's behaviour. This behaviour is derived from the influences on the orientation angles. These orientation angles are based on the accelerometer and magnetometer output. The accelerometer and magnetometer technologies are represented as **AM1**. Outcomes from the technologies within **AM1** are fused together to provide true heading estimation of the mobility scooter with respect to the globe. This fusion outcome is represented as **AM2**, which identifies variations of smartphone behaviour and heading. Variations between two successive epochs in the smartphone body frame with regards to navigation frame are determined and expressed as:

$$(field^b(t))_q = q_\omega(t) \otimes (field^b(t+T))_q \otimes \bar{q}_\omega(t)$$

Equation 20

Where, $(field^b(t))_q$ are acceleration and magnetic field with respect to navigation and rotation to frame b where q refers to the unit quaternion which can be rewritten as $q = \begin{pmatrix} \cos \phi \\ \sin \phi u \end{pmatrix}$; u is unit vector and $\phi \in [-\pi, \pi]$.

$$q_\omega = f(\omega_{nb}^b) = \begin{bmatrix} \cos\left(\frac{|\omega_{nb}^b|}{2} T_s\right) \\ \sin\left(\frac{|\omega_{nb}^b|}{2} T_s\right) \frac{\omega_{nb}^b}{|\omega_{nb}^b|} \end{bmatrix}, \text{ and } \omega_{nb}^b \text{ is the angular rate of the body frame}$$

with respect to navigation frame and assumption is that the latter is constant over period t to $t + T_s$.

In the dynamic state when the field senses consistency in navigation frame, WTP-HAMS system proposes a novel odometry model which updates its directional information with adopted MARU and AGU [160] to mitigate drift and provide improved positioning information as it analyses the navigational frame of the SP. This model substitutes **O2** with **AM2** to present an improved position. To achieve this, a distinctive filter-Sync processing stage is required, to smoothen signal and synchronise it to acceleration, change and deceleration of the mobility scooter. This consists of the following below:

- a) Frequency spectrum smoothing of **AM2** waveform using moving average filtration (described in 2.4.3). This will be referred to as **SS1**. The moving average filtration also categorised as a low pass filter produces smoothed curves representing processed signals. It mitigates noise experienced by the waveforms as it uses average signal range which in turn reduces high magnitudes of the signal.
- b) The synchronisation of frequency to **O1** using FWHM. This will be referred to as **SS2**. **FWHM** analytically calculates for precise distribution of acceleration levels level within the distribution curve of **SS1**. This must be taken into account in the identification of acceleration, change and deceleration of the mobility scooter over time.

Proposing a Novel Odometry Model for Improved Pose Estimation

WTP-HAMS system then proposes the combination of **SS2** with improved travelled distance estimates Dist_R using odometry model from Equation 1, Equation 2 and Equation 3 to introduce unique odometry model identified as **AM01**. This provides significantly improved pose estimates of the mobility scooter. The combination is expressed in Equation 21, Equation 22, as:

$$x_{t+1} = x_t + \text{Dist}_R \cos((field^b(t))_{qz})$$

Equation 21

$$y_{t+1} = y_t + \text{Dist}_R \sin((field^b(t))_{qz})$$

Equation 22

Where, x_{t+1} and y_{t+1} represents position estimate on x and y axis; x_t is the previous position; $(field^b(t))_{qz}$ represents heading estimates with respect to time; t is time. **AM01** provides improved pose estimates with a relative position which elevates tracking of the mobility scooter from its frame to the global frame as it travels within the room.

WTP-HAMS assumes the current state of the mobility scooter to be represented as $M_{(x_{t+1}, y_{t+1}, (field^b(t))_q)}$ with $(field^b(t))_q$ casting a triangular shaped error

$$\begin{vmatrix} L_x & L_y & (field^b(t))_q \\ J_x & J_y & (field^b(t))_{q_{t+1}} \\ F_x & F_y & (field^b(t))_{q_{t+1}} \end{vmatrix} \text{ from current position estimate } L_{(x,y,(field^b(t))_q)}. \text{ Estimated}$$

heading error at positions $J_{(x,y,(field^b(t))_{q_{t+1}})}$ and $F_{(x,y,(field^b(t))_{q_{t+1}})}$ are approximated at distances \overline{LJ} , \overline{LF} and \overline{JF} . The expansion of this error is mitigated using high sampling frequency T'_s . This expressed in Equation 23 as:

$$\Delta_{err} = M_{(x_{t+1}, y_{t+1}, (field^b(t))_q)} \cdot T'_S$$

Equation 23

Where, Δ_{err} represents triangular error shape from the current state, T'_S is high sampling frequency of 1.0f / 1000000000.0f.

Proposal to Combine Errors from RSSI and Novel Odometry Model for Better Position Estimation

Although **AM01** provides improved pose estimates of the mobility scooter frame with heading reference to the globe, it ignores the measured environment. To improve indoor localisation accuracy, the environment needs to be accounted for in the process. WTP-HAMS system, therefore, employs the room reference advantage provided by Wi-Fi in **W2** for combination with global reference advantage of **AM01**. WTP-HAMS system proposes to combine circular error shape in **W2** and triangular error shape in **AM01** to get improved position area estimate with room reference system and direction relative to the global system.

To find the area of improved position estimate, a verification of error shapes intersection or overlap occurrence need be established. Adopting the check recommendation solution [161], WTP-HAMS assumes that the error triangle of **AM01** is non-degenerate and therefore, lets $cx + sy = a$ be the normal form of equation for a line consisting of two edges LF of error triangle $\Delta L J F$. Here, $f(x, y) = cx + sy - a$ is the signed distance of the point (x, y) to line \overline{LF} . Third vertex J of $\Delta L J F$ is represented as (s, k) outside line \overline{LF} . Also anticipated by WTP-HAMS system is the centre O of **W2** circle error represented as (c, u) with radius r . First check is for edges LF of $\Delta L J F$ where circle centre $O = (c, u)$ is on opposing side of vertex $J = (s, k)$. This is expressed in Equation 24

$$f(c, u) \cdot f(s, k) < 0$$

Equation 24

The check is successful if edges LF does not exist. This indicates that the centre of the circle is within or on the triangle as indicated in Figure 4-2

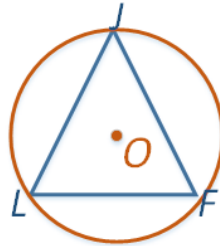


Figure 4-2 triangular error from AMO1 is within circular error shape from W2

Supposing error triangle edge is discovered, then a comparison of the perpendicular distance $p = |f(c, u)|$ from the centre of the error circle O to line LF to radius r is conducted. If $p > r$, then the check fails as it indicates that the error circle and error triangles do not intersect. This is shown in Figure 4-3

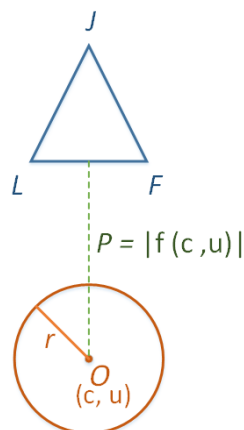


Figure 4-3 Test comparing the distance between triangle error from AMO1 and circular error from W2 to determine true error overlap or intersection occurrence

Next check is for distances from the error circle centre $O = (c, u)$ to error triangle vertices L, F , using Equation 25 and Equation 26.

$$d_L = \text{dist} (O, L)$$

Equation 25

$$d_F = \text{dist} (O, F)$$

Equation 26

If $d_L, d_F \leq r$ then the test is a success as it shows a vertex of the error triangle is within the circle. See Figure 4-4.

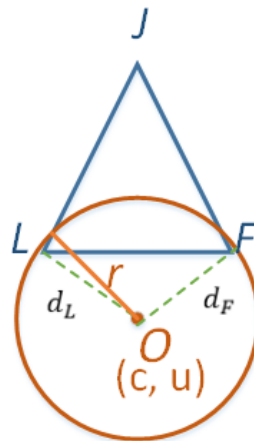


Figure 4-4 Check for vertices of error triangle AMO1 intersecting/overlapping error circle W2

Last of the check is an evaluation comparing two projected distances along the line \overline{LF} with the length of edge LF using Equation 27 and Equation 28.

$$k_L = \sqrt{d_L^2 - p^2} < \text{dist}(L, F)$$

Equation 27

$$k_F = \sqrt{d_F^2 - p^2} < \text{dist}(L, F)$$

Equation 28

If inequalities in Equation 27 and Equation 28 are true, then the check is a success as it verifies that circle and triangle intersect along edge LF . This is demonstrated in **Figure 4-5**

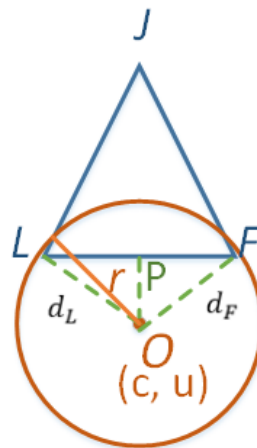


Figure 4-5 Check to verify error circle intersects error triangle along vertices LF

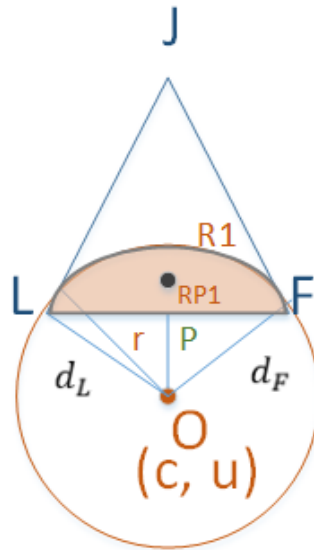


Figure 4-6 improved position accuracy from error shape intersection with the new position estimation

The checks show how error shapes experienced in **W2** and **AM01** intersect or overlap within the room to provide new position area. The convergence area of triangle error shape in **AM01** and circle error shape in **W2** is the new position area **R1**.

Centroid coordinate of shaded **R1** the assumed new position **RP1** when equations from the physics article [80][162] are used. **RP1** is an improved position estimate with significantly reduced errors. New position **RP1** from combined **W2** and **AM01** show significant accuracy improvements when compared to independent results in **W2**, **AM01** and **SOTA**. This improvement is the core aim of this research as it produces our WTP-HAMS system which secures better position estimates **RP1** through the exploitation of error shapes formed by **W2** and **AM01** respectively.

4.3. WTP-HAMS System Elements Functionality

This study is targeted at users with mobility impairment with a need for mobility scooters in environments such as care homes or modern shopping malls that are careful to cater to the disabled. Care homes are different from other workplaces due to its unique position

to be a workplace and also home to residences. It is therefore imperative that residents are treated with the utmost dignity and, health and safety of everyone are effectively managed. The Health and Safety Executive (HSE) and local authorities discussed recently in their regulations guide [163] to have investigated worker and resident incidences over time and have concluded on new safety standards for the management of health and safety. The HSE regulates homes with nursing whiles local authorities run care homes in England. Amongst their standard is the management slips, trips and falls of everyone especially residences by controlling environmental factors particularly floors and obstacles. 'Stop Falling' report from The Age [164] highlights that:

- In every minute about six people over the age of 65 suffer a fall.
- A fall which can cause serious injuries with high possibilities of leading to death is suffered by more than one in three (3.4 million) people over 65 every year.
- There is a rise in reported incidences of fractures from resulted falling every year, with at least 310,000 incidences of reported each year.

Choice of floor type in care homes is extremely critical when managing slips, trips and falls of residences. The floor surface recommended for care homes must have tread safety, slip resistance, low-level gloss and, dust free and easy cleaning capabilities. Even wooden floor tiles [165] best satisfy the recommendations and are amongst the most used floor types in care homes such as the case studies by A. W. Safety [166]. This is because they are more resistance, hygienic and easy to clean. This floor type also creates an inviting ambience in the rooms. The standard [163], advices that all floors should be clear of obstacles.

Therefore, this study considers wooden floor tiles similar to those used in care homes when localizing mobility scooters with anti-slip tyres.

Explained in 4.2, the proposed WTP-HAMS system combines results from exploited technologies (including Wi-Fi, accelerometer, magnetometer and wheel encoders) with existing and new techniques and models to significantly reduce positioning errors in an indoor environment with wooden floor tiles. Due to special recommendations by HSE [163] to use floor types which better manage slip, trips and falls like wooden floor tiles

[165], our indoor localisation research limits its scope to the following environmental and technological conditions including:

- Obstacle-free communal room with wooden anti-slip floor tiles.
- Four Wi-Fi routers / Access points (APs) fixed at known locations.
- One Neo4 mobility scooter [167] with solid puncture proof, non-marking anti-tip tyres.
- One Smartphone with accelerometer, magnetometer and Wi-Fi modalities.
- Two wheel encoders secured to the two rear wheels of the mobility scooter.
- The known start point of mobility scooter.

In an instance where the user on the mobility scooter travels from a known position to a new unknown position, proposed WTP-HAMS system calculates for the unknown position using a detailed conceptual flow illustrated in Figure 4-7. Mobility scooter used in this study is the Neo 4 with three anti-tips solid tyres. It has a turning radius of 110cm and a maximum travelling range of up to 10Km at 12 Amps and up to 21km at 18Amp depending on the conditions of use.

In a test environment with four fixed routers/APs, the Neo4 mobility scooter travels in translational motion from a known position to an unknown new position with two mounted wheel encoders and a smartphone. The smartphone is the device which collects, calculates and transfers received information from all connected technologies including four Wi-Fi routers/APs, accelerometer, magnetometer and two wheel encoders. According to the working scheme in Figure 4-1, each exploited technology is critical in providing *Relative position derivation using RSSI* and *Pose estimation with relative position using Odometry*, whose outcome and error shapes are combined to find new position estimates with reduced errors. An expansion of the working scheme is shown in Figure 4-7 below, where discussed algorithms techniques and models from 4.2 are designed into the WTP-HAMS system. (See Figure 4-8 Figure 4-9 and Figure 4-10 for associated algorithms, formulas and models from Figure 4-7)

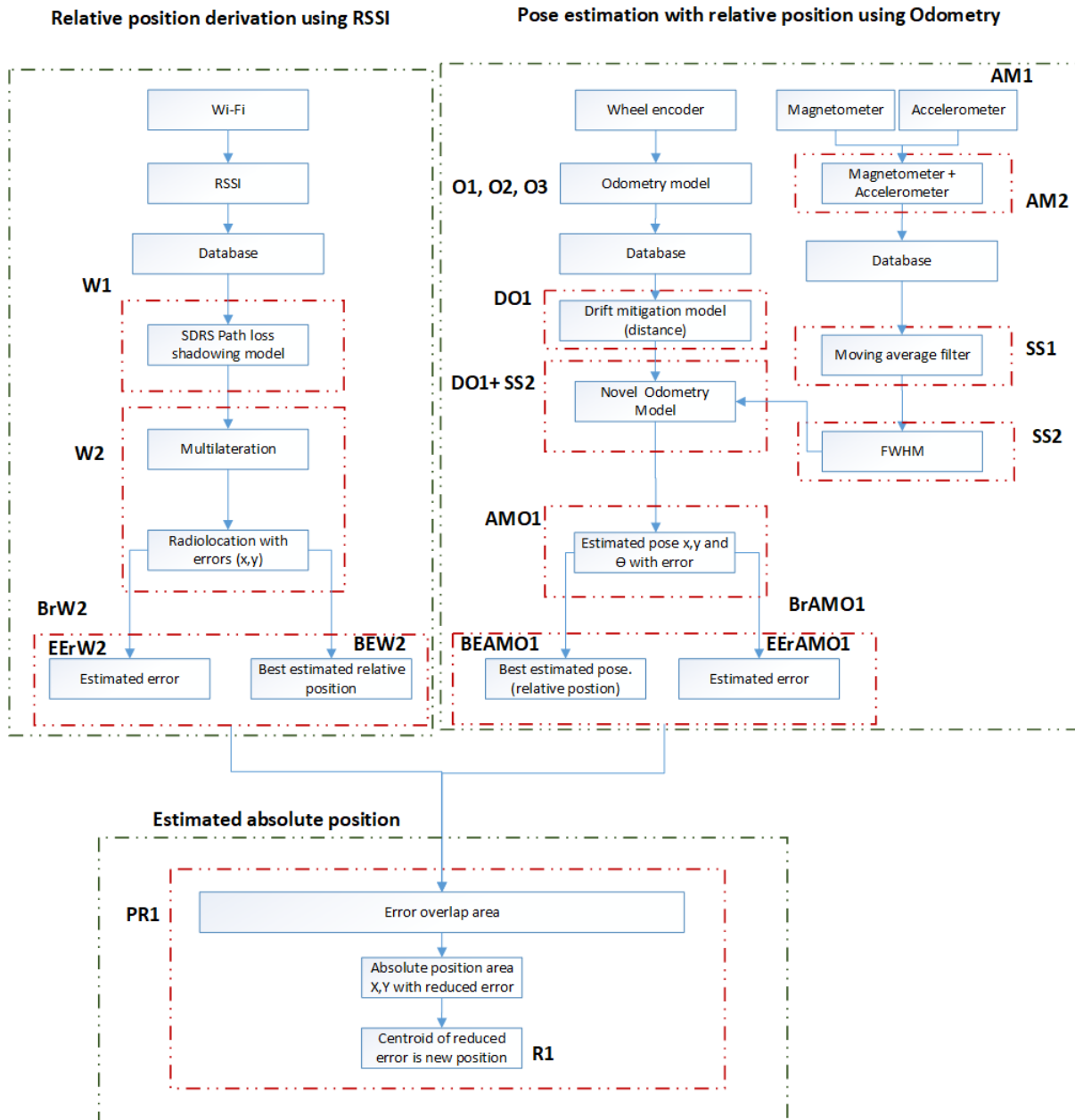


Figure 4-7 Flow chart displaying the WTP-HAMS system combining estimated relative positions and pose to improve position accuracy

Relative position derivation using RSSI

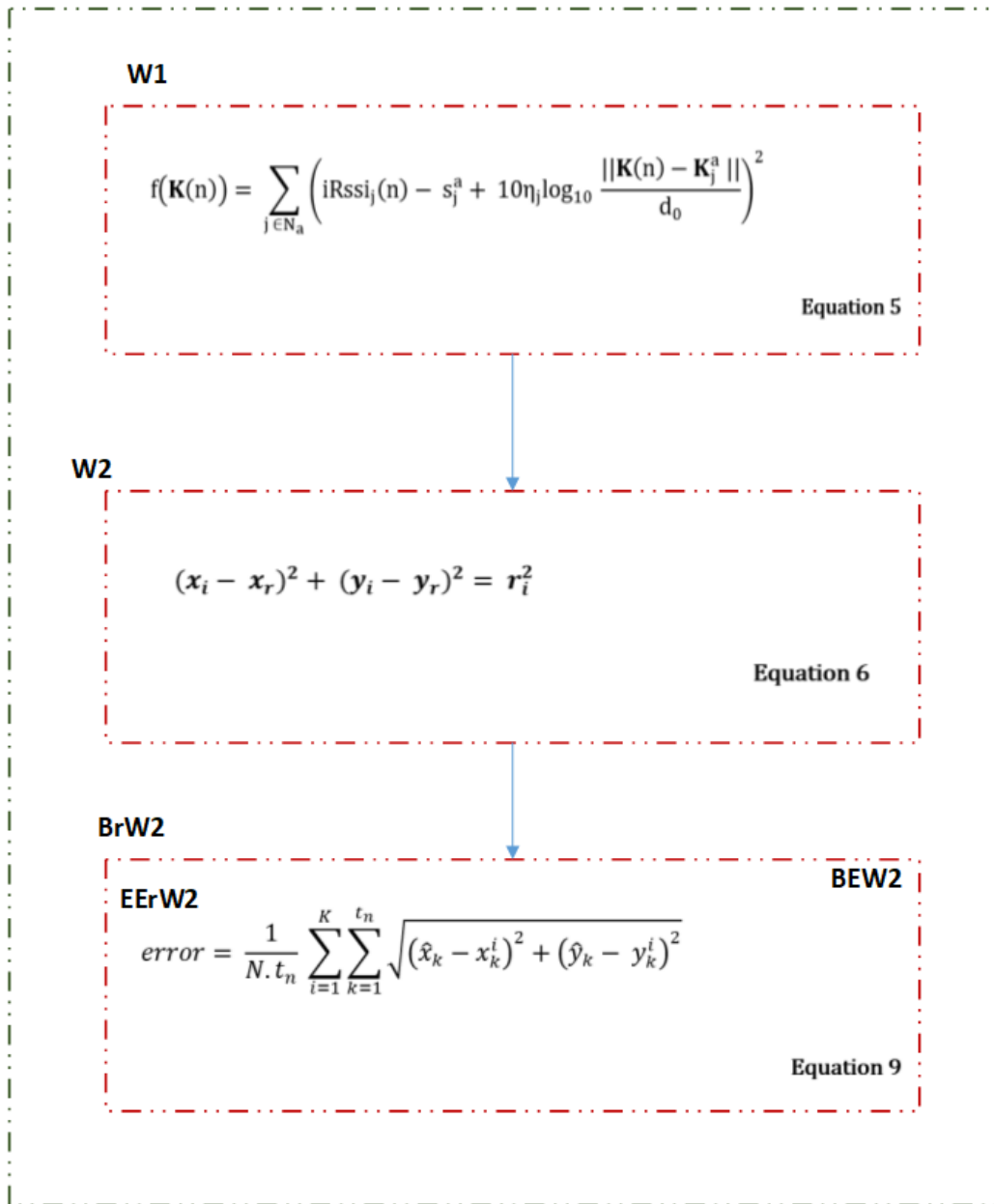


Figure 4-8 Associated formula or models for relative position based on the flow chart in Figure 4-8

Pose estimation with relative position using Odometry

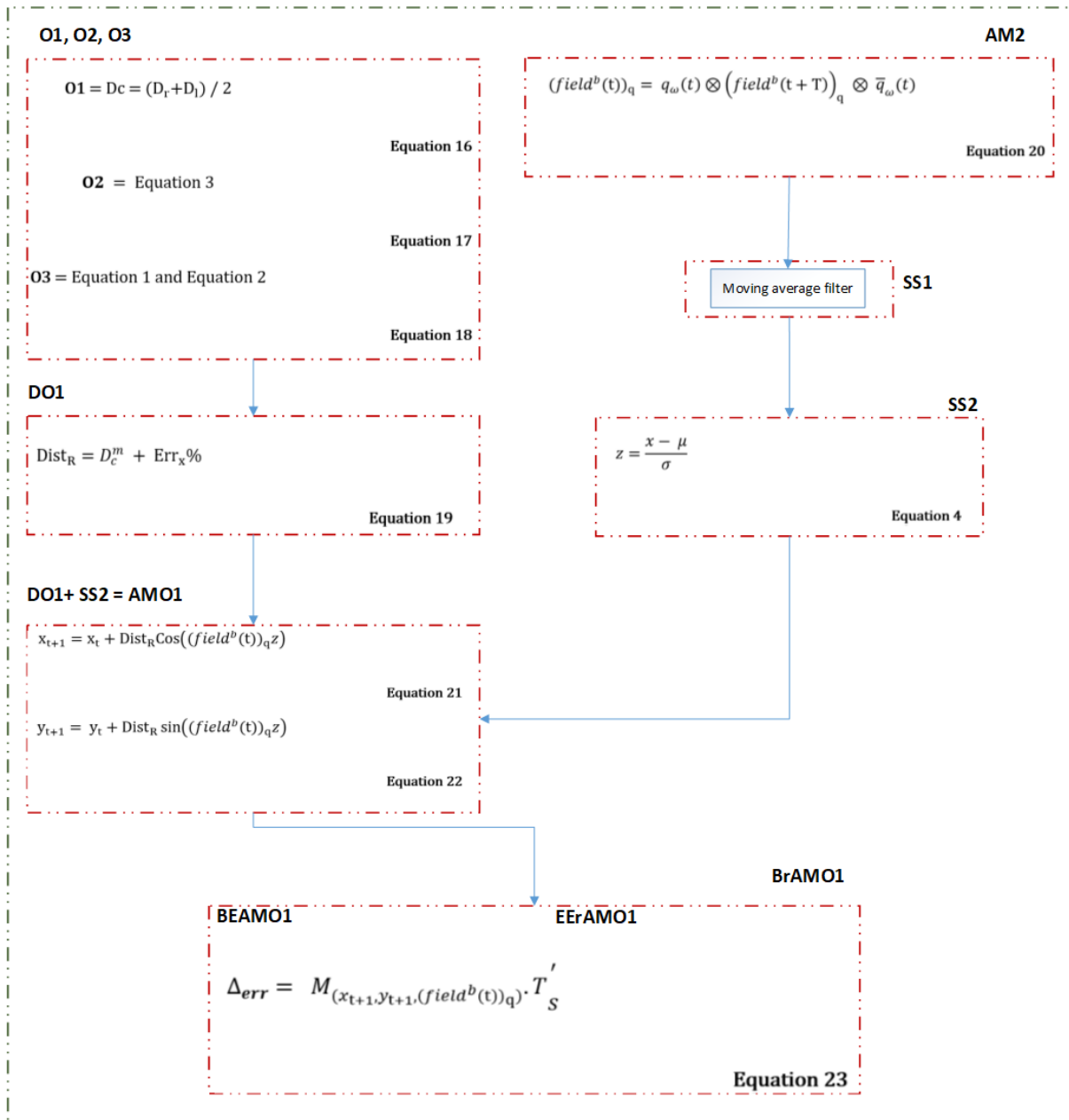


Figure 4-9 Associated formula or models for pose estimation based on the flow chart in Figure 4 8

Estimated absolute position

PR1

$$f(c, u) \cdot f(s, k) < 0$$

Equation 24

$$d_L = \text{dist}(O, L)$$

Equation 25

$$d_F = \text{dist}(O, F)$$

Equation 26

$$k_L = \sqrt{d_L^2 - p^2} < \text{dist}(L, F)$$

Equation 27

$$k_F = \sqrt{d_F^2 - p^2} < \text{dist}(L, F)$$

Equation 28

$$\int_A dA$$

R1

Figure 4-10 Associated formula or models for estimated absolute position based on the flow chart in Figure 4 8

In this study, *Relative position derivation using RSSI* exploits RSSI propagated from four Wi-Fi routers/APs. SDRS path-loss shadowing model Equation 5 is applied to RSSI emitted from each router to produce **W1** which is relative distances without position estimates. To generate position estimates **W2** (also referred to as radiolocation) with RSSI, multi-trilateration Equation 6 is employed to combine **W1** from all four routers/APs. Generated radiolocation **W2** in this instance, is the relative position of the mobility scooter with localisation errors from the ground truth. WTP-HAMS system stores best-estimated position **BEW2** in a database; this is the centre O of the error circle as shown in Figure 4-2. The localisation error **EErW2** is derived when Equation 9 is adapted to estimate the error position between **BEW2** and ground truth. An error circle **BrW2** is formed around **BEW2** and **EErW2** when the Euclidean distance from Equation 10 between **EErW2** and **BEW2** is calculated. This Euclidean distance is radius r of the error circle formed. The difference between **EErW2** and **BEW2**, show the position inaccuracies of Wi-Fi, therefore proving limitations of RSSI when determining accurate positions. WTP-HAMS system proposes to improve the position accuracy of Wi-Fi by combining **BrW2** with the second model, *pose estimation with unique odometry*.

Pose estimation with relative position using Odometry commences by permitting the smart Phone to collect real-time data outputs **O1** (travelled distance) and **O2** (heading estimates from wheel encoders) from the two wheel encoders and, **SS2** (improved heading estimate) from filtered outputs of fused accelerometer and magnetometer. **O1** and **O2** are collected because of their necessity when calculating odometry of a moving mobility scooter. Calculated odometry of the mobility scooter is achieved when **O1** and **O2** are combined in odometry model (*Equation 1 Equation 2 Equation 3*) to result in position estimation output **O3**. This outcome **O3** demonstrates systematic error in heading caused by drift in travelled distance **O1**.

WTP-HAMS system introduces a new drift mitigation model using Equation 19 to get a better distance travelled estimates $Dist_R$, identified as **DO1**. Although **DO1** demonstrates favourable travelled distance outcomes with reduced drift when compared to **O1**, it does not adequately compensate for directional errors **O2** experiences. Therefore, a

combination of **D01** and **O2** using *Equation 1**Equation 2* *Equation 3* still exhibits significant position errors due to angular heading errors of **O2** over distance and time.

The heading errors **O2** exhibits are mitigated with the introduction of **AM1**, whose fusion result is **AM2** using Equation 20. Moving average and FWHM will then be applied to **AM2** to result in **SS2** which proffers a better navigational/heading estimation of the smartphone mounted on the mobility scooter. It uses a high sampling rate to manage the growth of the probable heading error. The superiority of combined **D01** and **SS2** when compared to a combination **O1** and **O2** encourages our research to propose the substitution of **O1** with **D01** and **O2** with **AM2** in a novel odometry model demonstrated in *Equation 21* and *Equation 22*. The novel odometry model combines **D01** with **SS2** to result improved posed estimates **AM01** of the mobility scooter. This result has reduced error probabilities. The combination of **D01** and **SS2** in the proposed odometry model is achievable only after a special filter-sync process discussed in 4.2 is introduced by WTP-HAMS system. Introduced filter-Sync processing includes moving average filter and FWHM which smoothens and synchronizes **SS2** frequency spectrum with **D01** in respect to time. This converts the frame of the mobility scooter to obey global truths of navigation.

Heading Error Reduction Process

1. The mobility scooter moves from an initial position to a new position.
2. The wheel encoders calculate an estimated travelled distance (**O1**) and save it in an online database.
3. The synced accelerometer and magnetometer (**AM01**) outputs heading estimates.
4. The heading estimates will demonstrate an error rate that diverges in triangular form from start point towards the motion direction of the mobility scooter.
5. A high frequency of $0.33f$ will be applied to the error rate.
6. The applied high frequency will reset the measurement of the error rate to the centre of the triangular error. This is important because it readjusts the heading error to be closer to the ground truth.

The heading error reduction process is illustrated in Figure 4-11.

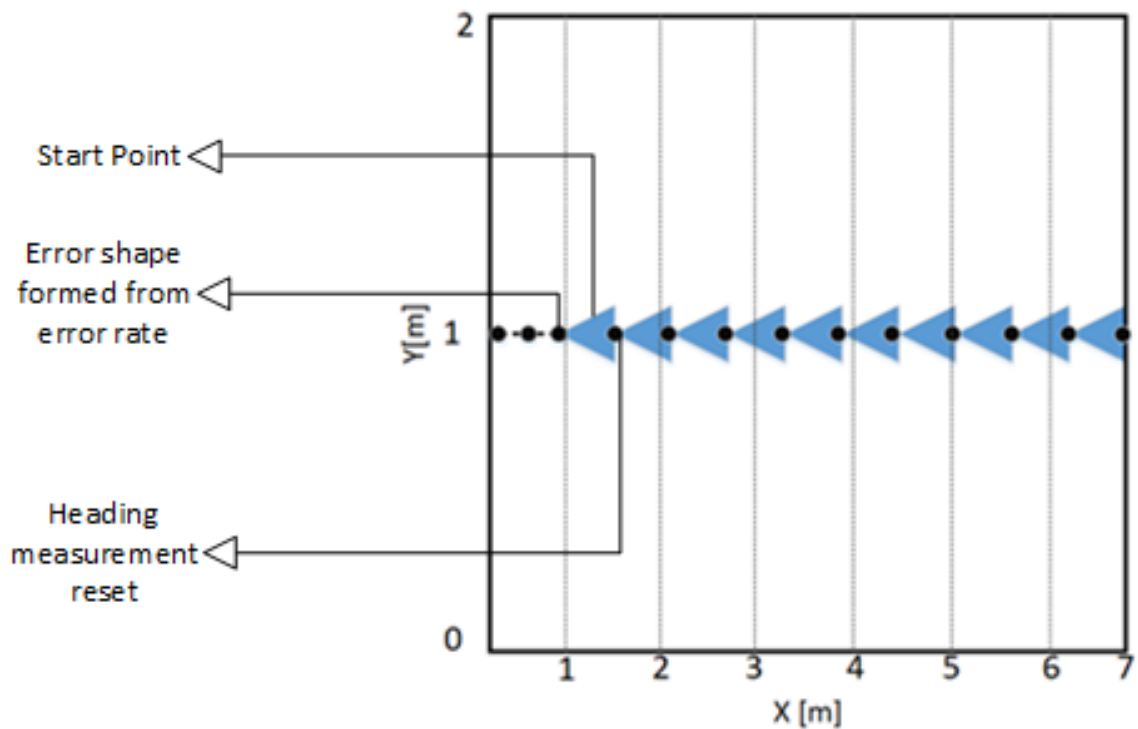


Figure 4-11 Heading error reduction in WTP-HAMS odometry showing triangular error shapes experienced in AMO1

The best-estimated pose of the mobility scooter is saved in a database as **BEAMO1** with its correspondent error **EErAMO**. **BEAMO1** and **EErAMO** are represented as **BrAMO1** in Figure 4-7.

The shape formed from **EErAMO** when **BEAMO1** is identified a triangular error shape controlled from growing too large by the high sampling rate of **AM2**. This is shown in Figure 4-11.

Stipulated from Figure 4-1 and Figure 4-7, the novel odometry model will show better pose estimates but its reference frame is the mobility scooter with world frame. For the tracked mobility scooter to be located in the test room, WTP-HAMS system proposes combining **BrAMO1** with **BrW2**, which has the advantage of the room reference frame.

The combination of the **AM01's** triangular error shapes **BrAM01** and **W2's** circular error shape **BrW2** results in an improved position area **R1**. **R1** is the area of convergence for both error shapes when instances expressed in Equation 24 - Equation 28 are obeyed. Then, the centroid of overlap is calculated using equations from solutions presented by U. S. River [80][162]. This resultant centroid will be the new and improved estimated position.

Localisation errors of WTP-HAMS system are determined using Equation 10 and Equation 11 to calculate Euclidean distance error between ground-truth and **R1**. WTP-HAMS system achieves its reduced position error goal under the following circumstances - If $R1 < 2m - 3m$, then WTP-HAMS system has improved RSSI based position estimates of SOTA [14]; If $R1 \leq 33cm$, then WTP-HAMS system has improved position accuracy of SOTA containing odometry combined with IMU in solution by A. Faralli et al [158] and RSSI in study conducted by S. Boonsriwai et al [14].

4.4. Analysis of Proposed Technology Solution

We identified a gap in the market, where typically, indoor localisation systems are designed for localising either pedestrians or robots. This neglected market has been on a steady rise as the high mortality rate [6][138][168] of people have increased and some older people are now using mobility scooters [167]. Therefore, we proposed an investigation that will localise elderly and mobility impaired mobility scooter users using familiar technologies such as smartphone [8]. It is our expectation that these tech-savvy users would appreciate and benefit from our proposed investigation.

Our proposed investigation is our methodology, which is the design of a novel WTP-HAMS system. WTP-HAMS system is a TT based hybrid system that uniquely combines the following –

- **Technologies –**

- *Wi-Fi* – which is advantageous due to its capability to provide position estimates with reference to room. Our investigation will consider and compare the following–
 - LOS versus NLoS for RSSI signal propagation environment.
 - Three versus four Wi-Fi routers for better position estimates.
- *Smartphone IMU modalities* – this will be beneficial because it will provide heading estimation with reference to the globe. This investigation will consider the following –
 - *Navigation heading estimation* – with two comparison
 - Combined accelerometer and magnetometer
 - Combined gyroscope, accelerometer and magnetometer
 - Smartphone pose with a comparison of orientation versus vertical phone orientation.
 - *Wheel encoders* – this will be beneficial in estimating mobility scooter pose with reference to the frame. This investigation will compare
 - Tradition distance travelled versus our proposed new drift mitigation model
 - Traditional odometry model to our proposed novel odometry model

- **Techniques –**

- *For Wi-Fi* –
 - *SDRS log-normal shadowing model* in Equation 5 for relative distance estimation between a Wi-Fi router and smartphone. This is important because it reduces errors in the propagated signals. In particular, errors caused by interferences such as shadowing and multipath.
 - *Multi-trilateration* in Equation 6 for RSSI based position estimation. This is considered over fingerprinting because multi-trilateration is lightweight and its latency period is significantly low. According to S. Boonsriwai et al [14], fingerprinting latency is about 2-3 seconds.

- *For smartphone IMU modalities*
 - Complementary fusion in Equation 20 for estimating navigation heading. This is important because the direction will improve the pose and position of the mobility scooter.
- *For wheel encoders*
 - *Traditional travelled distances* versus *our proposed new drift mitigation model* (in Equation 19). This will be important in improving travelled distances by adding a measured
 - *Traditional odometry* (in Equation 1, Equation 2 and Equation 3) versus *our proposed novel odometry model* (in Equation 21Equation 22). This will be important in improving the pose estimation of mobility scooter.
- **Novel methods –**
 - Centroid calculation of error overlap from *Multi-trilateration* (in Equation 27Equation 28 and error (in Equation 23) from *our proposed novel odometry model* using Equation 21Equation 22 based on check for overlap and centre using Equation 27Equation 28.

The unique combination of **technologies, techniques** and **novel models**, would aim to improve indoor localisation accuracy in real environments. In particular, the design of the proposed investigation will cover key elements including, accuracy, cost, energy efficiency and scalability.

Accuracy

This is a critical feature for all indoor localisation systems because it is important to localise users to centimetre or low meter level. This is beneficial especially in emergency situations where the life of the user is threatened and emergency services are trying to locate said, users.

In order to improve position accuracy, we propose to combine position estimates from Wi-Fi (**W2**) and combined wheel encoders and smartphone IMU modalities, specifically

accelerometer and magnetometer (**AM01**). To be precise, we combined, **W2** from multi-trilateration with **AM01** from the proposed novel odometry model that includes a combination of a proposed new drift mitigation model and navigation heading. To buttress further on the proposed novel odometry model, we expect wheel encoders will suffer drift that would cause significant errors, and that Wi-Fi will fail at providing navigation heading, therefore, we will opt to design a system that will provide users will better pose estimates by mitigating distance travelled errors using a proposed new drift mitigation model, as well as, get navigation heading from complementary fusion of accelerometer and magnetometer, to correct heading drift over travelled distance.

Before the improved position estimate **R1** will be derived, it is the plan to get the error shapes formed from the deviation between the position estimates (**W2** and **AM01**), and the ground truth. The idea is that the centre point at which both error shapes of **W2** and **AM01** overlap will be the new improved position estimate **R1**. This is because it is our expectation that **R1** will be better than results **W2** or **AM01**. Further expectation is that, will complement each other by improving the position of each other such that **AM01** will improve results of **W2** and **W2** will improve results of **AM01**.

We predict that our proposed investigation will outperform literature works on Wi-Fi by providing results within the error range of 0.35m – 1.35m. This is compared to literature works, that provide an error range of 1.5m – 3.1m for Wi-Fi [14][80][146]. If the average mean μ of the estimated error range 0.35m – 1.35m is 0.865, then it is our expectation that our proposed system will outperform SOTA by approximately 189%.

The proposed system would provide a range of capabilities especially in the pose estimate improvement of indoor vehicles moving in translational motion on a smooth wooden tiled floor.

Cost

This is another critical element research consider when designing a localisation system. A majority of existing systems in the literature are either expensive to develop or costly for users. This is especially in situations where additional infrastructure is needed, e.g. [137][109][110]. (See Table 3-5)

Our proposed system will be very cost effective for developers and users. This is possible because only ubiquitous, easy to access technologies will be exploited. These technologies include Wi-Fi, smartphone IMU modalities and wheel encoders. For developers, there will be no need to buy additional infrastructure in the development of our proposed system.

It is assumed that the users of our proposed system, will be mobility scooter users who own at least one smartphone and are in environments with Wi-Fi routers. This, therefore, will demonstrate that the user will not have to spend anything to use our WTP-HAMS system.

Energy efficiency

It is important that energy consumption is better managed, especially in our proposed system that includes a smartphone. This is because the battery life of the smartphone needs to be conserved for the user. Some literature overlook this important element in their design (see Table 3-5).

We propose to design a system that will do the following –

- Pause in background, when not in use,
- Give user complete control to initiate and terminate scan at will, instead of continuously scanning and listening for Wi-Fi, wheel encoders and smartphone IMU signals in an online state (further discussed in 5.1.1.1). This is important because it prevents the battery from getting drained quickly.

In addition to the list above, the system would conserve energy by processing the proposed mathematical computations and models in an offline server (further discussed in 5.1.1.3). Our methodology will be a lightweight solution that will conserve the battery life of the user's smartphone.

4.5. Research Development Plan

The development of this research is divided into 6 phases as illustrated in Table 4-1, where it would take 1394days (see Figure 4-12) to completely analyse the state-of-the-art, propose, design and develop an in indoor localisation system that would better address indoor localisation challenges. In particular, accuracy, cost and energy efficiency.

Task Name	Resource Names
Phase 1	SOTA
Phase 1	Identify the difference between Indoor and outdoor localisation
Phase 1	Analysis of Indoor localisation
Phase 1	Identify, design and propose a new classification system for hybrid localisation
Phase 1	Identify, design and propose an investigation based on SOTA
Phase 2	Designing the proposed investigation (WTP-HAMS system)
Phase 2	Planning the methodology
Phase 2	Propose application novelty
Phase 2	Propose novel mathematical models
Phase 3	Design the implementation of the methodology, including software and hardware development of the proposed WTP-HAMS system
Phase 3	Designing the software for the proposed WTP-HAMS system
Phase 3	Smartphone API
Phase 3	Mathematical computational processes in Matlab
Phase 3	Designing and developing the hardware for the proposed WTP-HAMS system
Phase 3	Wheel encoders
Phase 4	Experiments assessing the methodology
Phase 4	Design, plan and strategy of the experiments
Phase 4	Implementation and pilot experiment in room 1 based on the methodology
Phase 4	Extensive studies and trials of proposed Novel WTP-HAMS System in room 2. In particular focused study and comprehensive study
Phase 5	Results and analysis
Phase 6	Thesis writing

Table 4-1 Overview of the research development plan

Each phase is further described below -

Phase 1

- SOTA
 - Over 180 literature works are examined to fully understand the key challenges in this area. These included technology and technique limitations.
 - Identifying the difference between Indoor and outdoor localisation
 - In-depth analysis of Indoor localisation solutions
 - Identifying, designing and proposing a new classification system for hybrid localisation. This is because a standard does not exist to identify systems that fall under this type of localisation. (Discussed in Chapter 3)
 - Identifying, designing and proposing of a methodology based on SOTA. in particular, the proposed hybrid indoor localisation classification

Phase 2

- Designing the methodology, i.e. the novel WTP-HAMS system
 - Planning the methodology
 - Proposal and design of the novel application which includes the unique combination of Wi-Fi, smartphone IMU modalities and wheel encoders. (also discussed in Chapter 4)
 - Proposal and design of novel mathematical models which includes the new drift mitigation model and novel odometry model (also discussed in Chapter 4).

Phase 3

- Design the implementation of the methodology, including software and hardware development of the proposed WTP-HAMS system (discussed in Chapter 5)
 - Designing software for the proposed WTP-HAMS system

- Smartphone API for Samsung galaxy note 1 to receive data from transmitting sensors, including Wi-Fi routers, wheel encoders and smartphone IMU sensors.
 - Mathematical computational processes in Matlab for the received data from the smartphone.
 - Mbed data transmission to the smartphone
- Designing and developing the hardware for the proposed WTP-HAMS system
 - Designing the wheel encoders
 - Purchasing components for the wheel encoder development
 - 3D printed wheel encoder case

Phase 4

- Experiments assessing the methodology (discussed in Chapter 6)
 - Design, plan and strategy of the experiments
 - Implementation and pilot study in room 1 based on methodology. In particular Wi-Fi.
 - Extensive studies and trials of proposed Novel WTP-HAMS System in room 2. In particular focused study and comprehensive study

Phase 5

- Results and analysis (also discussed in Chapter 6)
 - Focus study
 - Comprehensive study

Phase 6

- Thesis writing

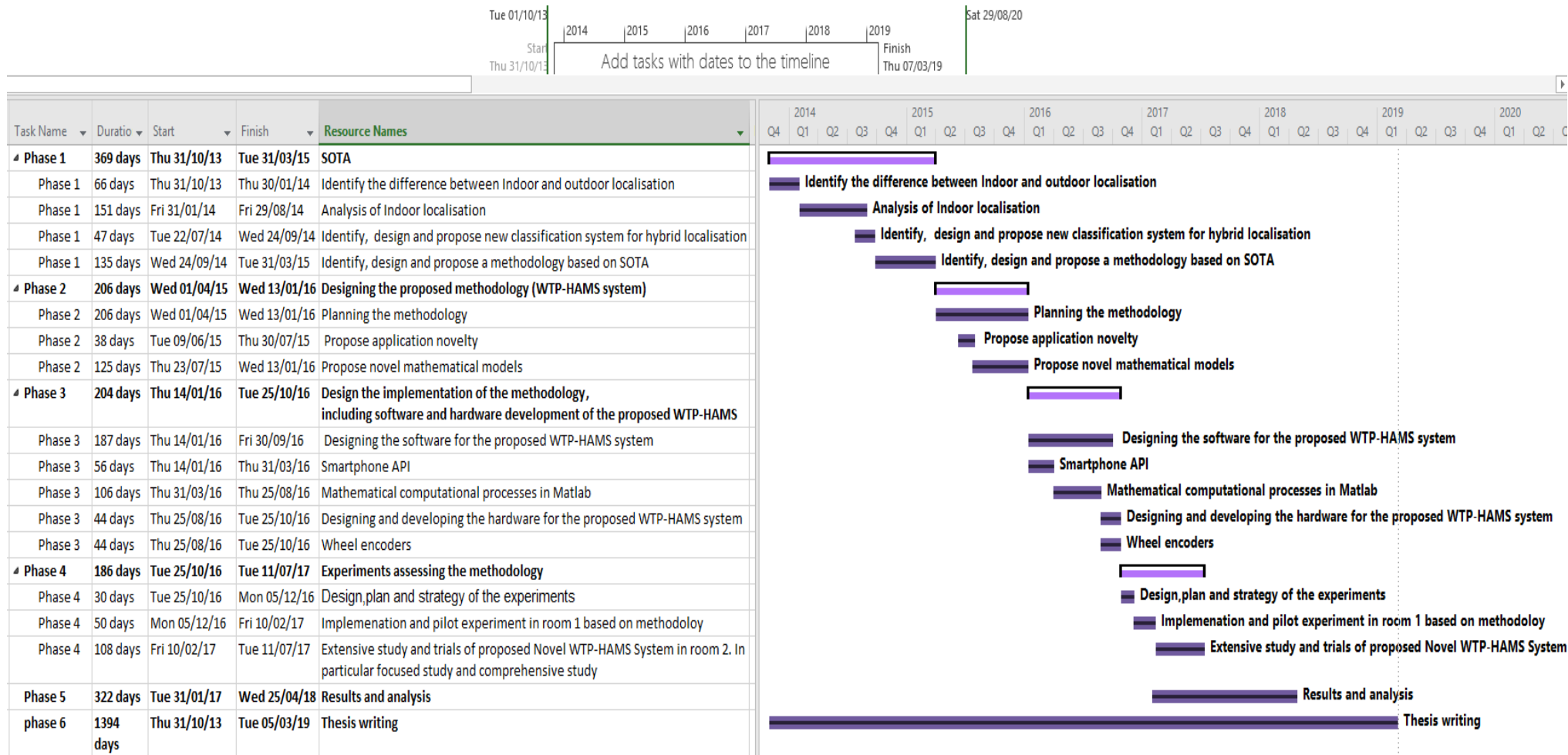


Figure 4-12 Research development plan with timelines

Chapter 5 System Implementation

This chapter discusses the software and hardware design, development and implementation of the proposed investigation. It describes the system requirement and proposes a system architecture that will operate in online and offline phases. These phases will include proposed mathematical models and concepts discussed in the methodology in Chapter 4.

5.1. WTP-HAMS System overview

The proposed investigation will comprise of the combination of Wi-Fi, wheel encoders, accelerometer and magnetometer as described in chapter 4. This system will implement a combination of SOTA adapted algorithms and models such as SDRS path-loss shadowing model [64][77], multi-trilateration [14], moving average filter [73], FWHM odometry model [70], and error overlap area model using shape intersection and overlap formula [161] with complementary innovative models including new drift mitigation model for improved travelled distance and novel odometry model to significantly reduce position errors.

The proposed WTP-HAMS system will be combining two models, *relative position derivation using RSSI technique* and *pose with relative position using innovative odometry* model to significantly reduced position error. To do this following is required:

- Neo 4 mobility scooter as a target object for localisation. It is an inexpensive mobility scooter preferred by users.
- Smartphone (SP) for interfacing between user and technology as well as having its inbuilt modalities exploited for indoor localisation purposes. Samsung galaxy note 1 is SP of choice due to its inexpensiveness, availability and easy usability by the elderly.

- The navigational heading of the mobility scooter from the fusion of inbuilt IMU modalities within SP. In particular, gyroscope, accelerometer and magnetometer sensors are considered.
- Estimate position with room reference using combined RSSI propagated from four and three Wi-Fi routers.
- Estimate travelled distance from the *new drift mitigation model*. This is calculations that will be done on raw distance travelled values from two wheel encoders mounted on both rear wheels of the mobility scooter.
- Improved pose estimates using the *proposed novel odometry model*, which combination of estimated relative travelled distance and directional or heading information in WTP-HAMS system unique odometry model.

5.2. WTP-HAMS System requirements

WTP-HAMS is an infrastructure reliant system, which consists of internal and external technologies. Internal technologies refer to relevant modalities of a smartphone (SP) which include accelerometer, magnetometer and Wi-Fi sensors while external technology describes the two wheel encoders mounted on two rear wheels of a mobility scooter. Both categories are further expatiated on in appendix A.

In our research, there are critical power and communication requirement expectations for the technologies used. Each explored technology operates independently and therefore requires specific data transmission protocol to communicate with the API on the SP that handles computation. The API displayed in Figure 5-1 provides WTP-HAMS system with synchronised data from all utilised internal and external technologies with respect to time. This, therefore, enables all technologies to function as a single unit when it transfers collected data for further analysis.



Figure 5-1 WTP-HAM API on SP displaying data extracted from internal and external technologies

Smart Phone Implementation for the Proposed Investigation

For experimental purposes, Samsung Galaxy Android smartphone is exploited because of its super AMOLED capacitive touch screen with physical dimensions of 146.9 x 83 x 9.7 mm (5.78 x 3.27 x 0.38 in) and a large screen with a resolution of 1280 x 800 pixels (~285 ppi pixel density). Similar to most smartphones, the Samsung Galaxy is a very portable ubiquitous device renowned for its elderly friendly features. This technology has 1061 components, however, WTP-HAMS system will be using only three of its modalities which include Wi-Fi, accelerometer and magnetometer sensors to achieve improved indoor localisation. Implementations of the aforementioned modalities are further expatiated on in Section 5.3.1.

Wheel Encoder Design and Development for the Proposed Investigation

The mobility scooter also referred to as MS possesses two low costing wheel encoders mounted on both rear wheels. Both wheel encoders are external technologies built with inexpensive MBED that require additional circuitry and MCU to communicate with the API on the SP when achieving **01**, **02**, and **03**.

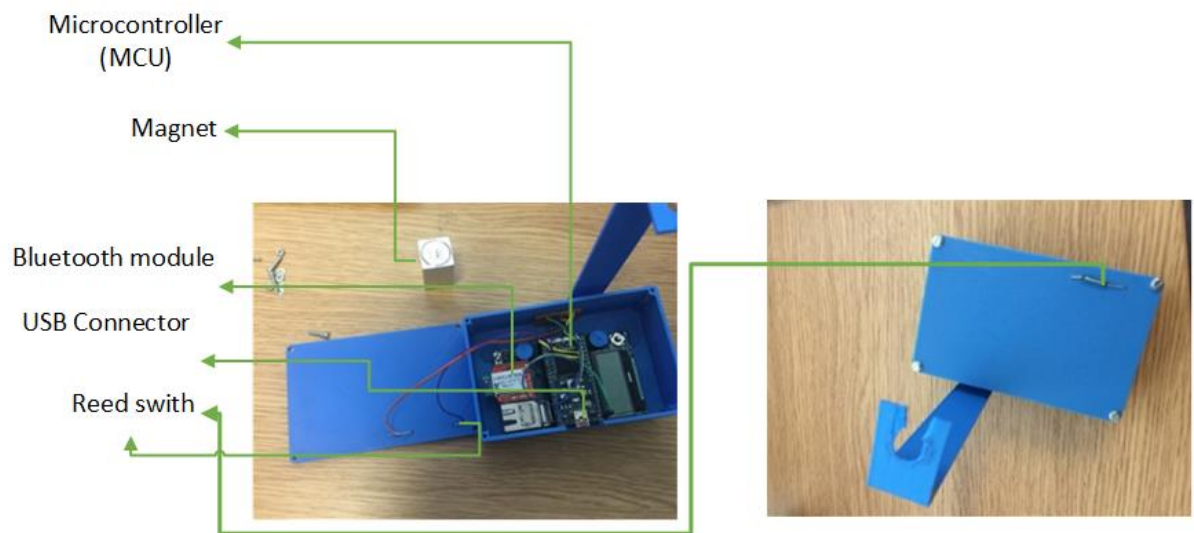


Figure 5-2 Developed wheel encoder components necessary for distance estimation

Each wheel encoder composes of three core components - an MBED, one reed switch and a magnet displayed in Figure 5-2. These three core components work together to capture the distance travelled when each wheel rotates as it travels along a path.

MBED is the preferred MCU for this investigation due to its, cost-effectiveness and operating system's programmable capabilities. MBED microcontroller unit (MCU) consumes low energy due to its inbuilt Bluetooth Low Energy (BLE) short-range feature for low power applications. BLE of the MBED communicates with the SP's inbuilt 3.0 high-speed Bluetooth module which is supported by 802.11 Wi-Fi radio for producing data speed of 24Mbps. The wheel encoders employ Bluetooth

communication protocol shown in Figure 5-3 to achieve maximum communication range of 10 meters at 2.5mW input power with a data rate of 3Mbps. In accordance with mbed online [37], higher BLE signal strength is obtained at shorter distances.

MBED Schematic and Data Transmission To SP For Wheel Encoder

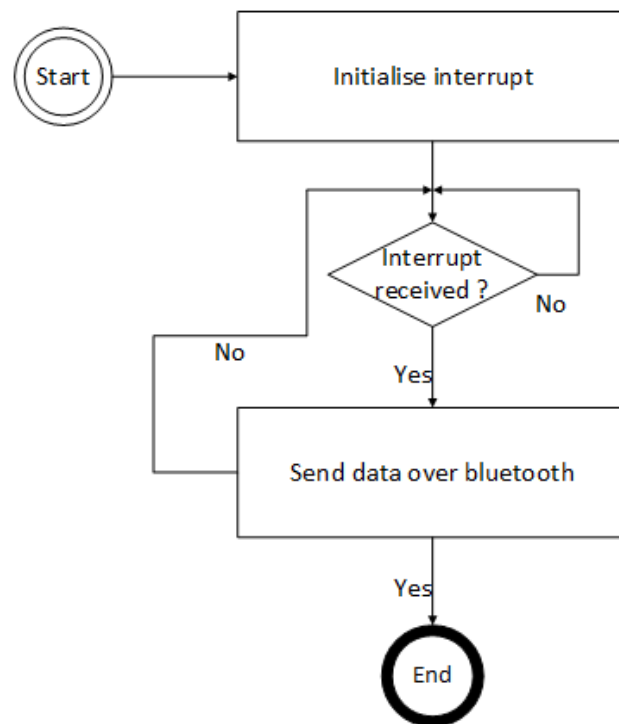


Figure 5-3 Wheel encoder system communication flow to SP

At **Start** in Figure 5-3, MBED in the indigenously designed wheel encoder is initiated when power is provided via its inbuilt USB connector. The wheel encoder's circuitry power source is an MBED USB connected external battery pack with the power of at most 2.5mW and current 10000mAh. This battery pack has a daily life span of at least eight hours when MBED firmware is running. Maximum power consumption of the MBED MCU is 300mA with a regulator of 3.3v. For the MCU to be operational, it requires an input voltage of about 3.3V – 9v as illustrated in Figure 5-4. The

current from the battery pack provides substantial power required for the wheel encoder to function for at least eight hours.

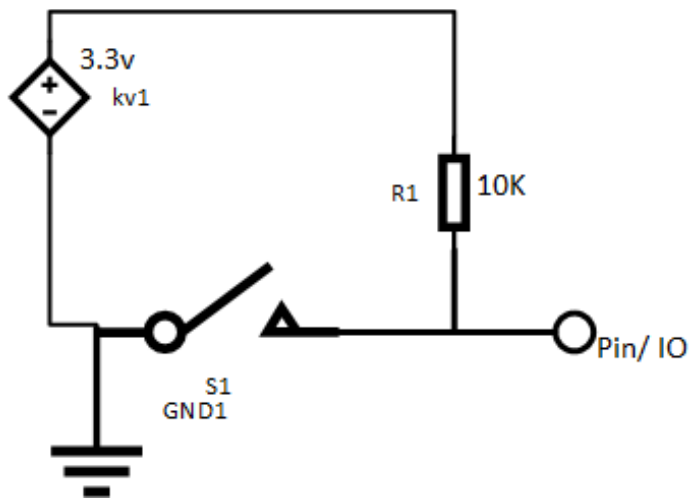


Figure 5-4 Wheel encoder circuit schematic

When each wheel rotates, **interrupt** is initialised to capture triggered ticks when the magnet on the tyre frame passes the reed switch connected to the encased MBED. This encased embed is placed opposite the tyre frame such as Figure 5-5. Due to specifications of the mobility scooter implemented in this research, each recorded tick is a complete rotation equivalent to 60cm distance travelled, *this is further* discussed in section 5.3.1.

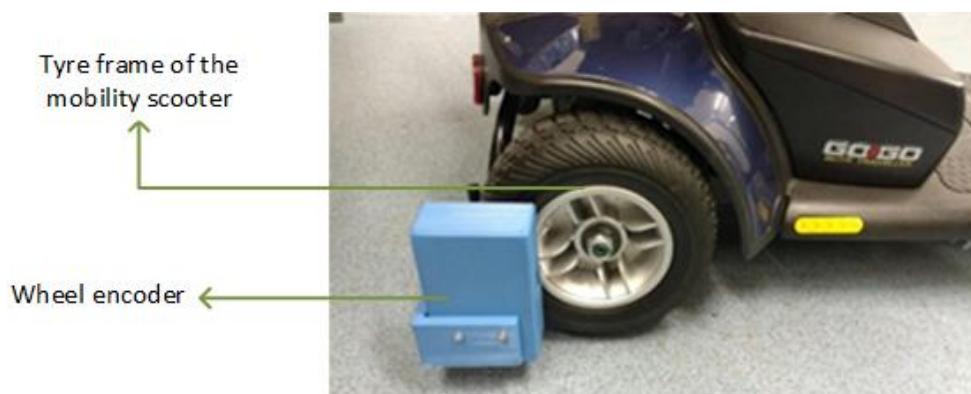


Figure 5-5 wheel encoder mounted onto the wheels of the mobility scooter

On each successfully received **interrupt**, a tick is transmitted to SP API via the Bluetooth communication protocol between SP and MBED as illustrated in Figure 5-6. If the **interrupt** is unsuccessful, MBED will show no changes in the SP API over Bluetooth protocol, therefore, will enforce a measurement repeat.

```
1  #include "mbed.h"
2
3  Serial bt(p9, p10);
4  InterruptIn magnet(p21);
5
6  void notifyPhone() {
7      wait(0.001); //add little delay to minimize effect of switch debouncing
8      bt.putc('i'); //send 'i' over bluetooth to phone
9  }
10
11 int main() {
12     bt.baud(115200); //setup baudrate
13     wait(1); //wait for bluetooth to initialize
14
15     //add interrupt on pin, for when magnet is detected
16     //and when magnet is detected run method 'notifyPhone'
17     magnet.fall(&notifyPhone);
18
19     while(1) ;
20 }
```

Figure 5-6 Bluetooth communication protocol between wheel encoder and SP

MBED reliant wheel encoders are much cheaper when compared to off-the-shelf wheel encoders. Besides its expensiveness, off-the-shelf wheel encoders have programming limitations unlike wheel encoders built for WTP-HAMS system provide controlled accessible data with can be synchronised with outputs from the internal technologies of the SP, as shown in Figure 5-6. Another advantage of building a wheel encoder for WTP-HAMS system is the possibility it provides to synchronise all data with relation to time. Time in the implementation of this study is UNIX timestamp which tracks time as running total of seconds. This employed timestamp selection has zero dependencies on time zones as it calculates the number of seconds between data collection date and Unix Epoch. Additionally, according to an article [169], Unix timestamp is advantageous in tracking and sorting information in dynamic and distributed application on the client side and online.

In summary, all relevant internal and external technologies explored in this study provide adequate data needed for WTP-HAMS system to achieve its purpose. Each technology is special because of its ubiquity, cost-effectiveness and programmability.

5.3. System Architecture

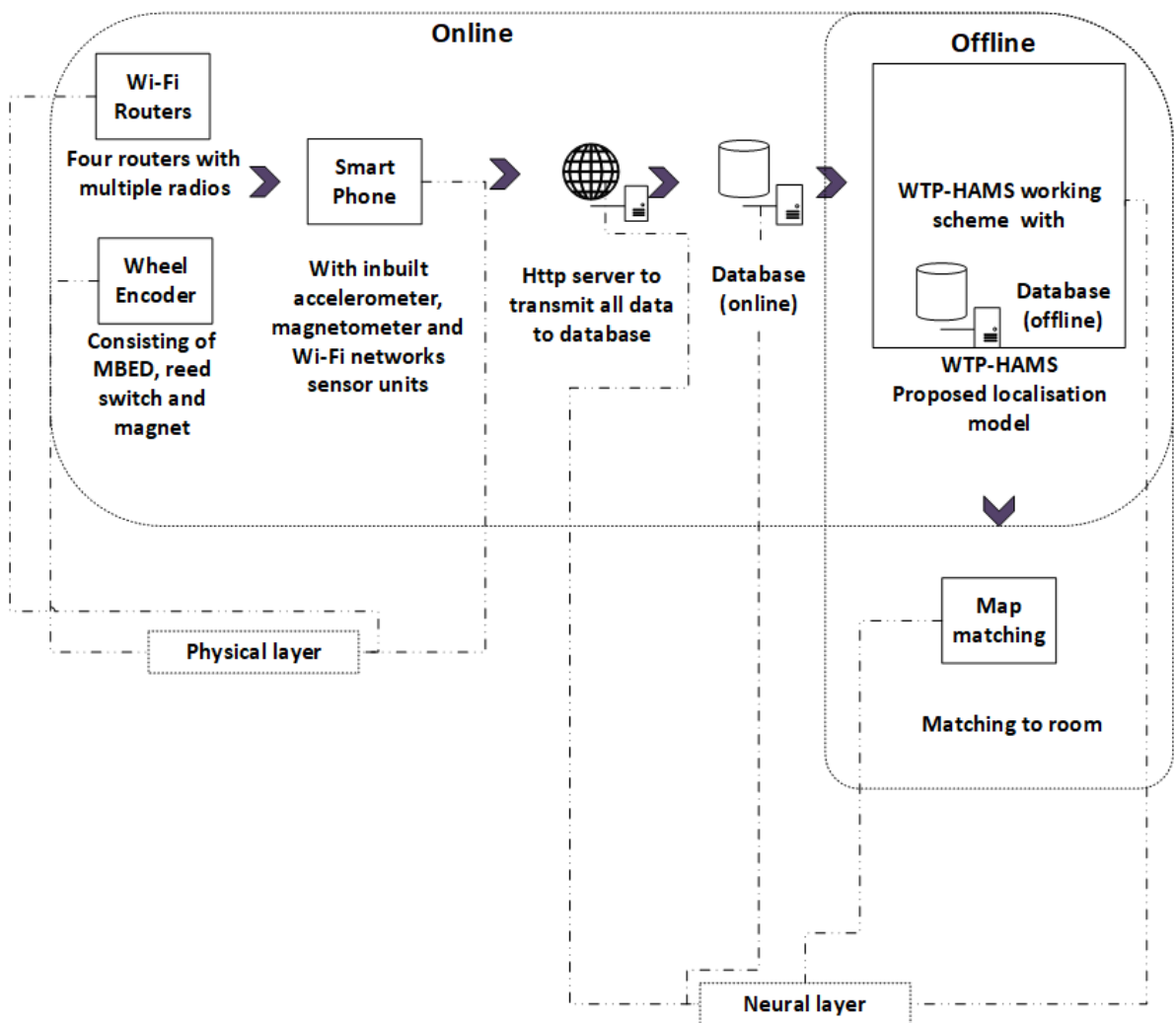


Figure 5-7 Proposed WTP-HAMS system Architecture

WTP-HAMS system architecture in Figure 5-7, best illustrates the system process flow as each technology perform their respective roles (as further expressed in Figure 4-7 and Appendix 1 in appendix A) to achieve better indoor localisation accuracy. The illustrated WTP-HAMS system architecture shows a categorisation of its system processes into *physical layer* and *neural layer*.

The physical layer refers to the infrastructures which include the internal and external technologies explained in 5.2. The internal and external technologies consist of wheel encoder, Wi-Fi routers and SP modalities which operate in real-time. This operation falls within the **online phase** of WTP-HAMS systems processes, which is further discussed in 5.1.1.1. Within the physical layer, Wi-Fi sensing receiving modality of SP propagates network signals transmitted from four Wi-Fi routers/APs when API scan instance is initiated. The purpose of this signal propagation is to provide data necessary for calculating estimated relative position **W2** from the working scheme in Figure 4-1 and its detailed counterpart in Figure 4-7. Also within the physical layer, wheel revolutions ticks measured by the wheel encoder is pushed to the API sitting on the SP via the Bluetooth communication protocol. Its objective is to provide distance travelled output required to calculate relative position **O3** described in working scheme in Figure 4-1 and its detailed counterpart in Figure 4-7. A final feature of the physical layer is the smartphone (SP) that accommodates its inbuilt accelerometer and magnetometer sensors. Data output from accelerometer and magnetometer are retrieved and combined within SP using a complementary fusion filter further explained in section 5.1.1.1. This is important because, it produces **AM2**, which is critical to our proposed investigation as it proposes to be an asset for improving our odometry model which will provide better pose estimates. Parallel to data push processes of Wi-Fi and wheel encoder outputs, SP retrieves outputs from its inbuilt IMU sensors (gyroscope, accelerometer and magnetometer) and displays on its API. SP is very essential in organising all data output from necessary exploited technologies as a single unit with reference to a similar UNIX time.

The neutral layer contains online and offline databases for data storage, server for data transfer and communication, WTP-HAMS localisation model for methodology implementation, computation and data analysis, and map matching for synchronising results with the floor plan of a measured room. Live data packets collected from participating technologies by SP at the physical layer and pushed to the online database sitting on the local host via HTTP server in real time. Real data is fundamental in this study because it proves the feasibility of this study to actualise improved indoor localisation with our proposed WTP-HAMS system in real-world scenarios.

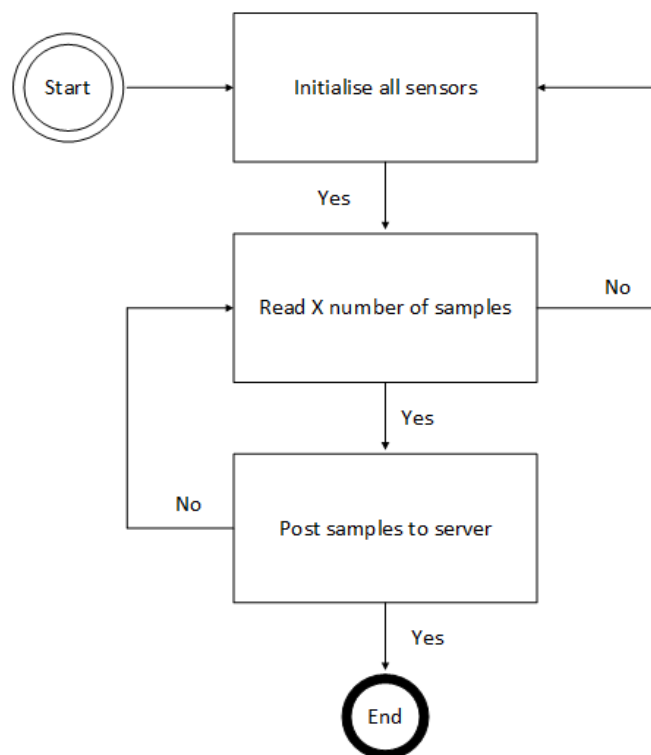


Figure 5-8 SP to the online database communication flow

SP pushes collected data to an online database through HTTP server as illustrated in Figure 5-8, when participating sensors are initialised by API within the SP is triggered. The communication flow between SP and server is created in three phases, including the initialise phase, read phase and post phase. The initialise phase prompts SP to initialise all sensors. On success, the read phase is executed. All

samples from all initialised sensors are read and pushed to the server on success. This populates the online database with real data sets with respect to real time. Collected real data is transferred from the online database to an offline database in MATLAB where algorithms and mathematical models of the proposed WTP-HAMS system are implemented. MATLAB is selected because of its high mathematical, computational and analytic prowess. Within the offline environment, the proposed localisation model further analyses the real data. Here, executable algorithms within Figure 4-7 excluding **AM2** is performed to produce **W1, W2, O2, O3, AMO1** and **R1**. These derivatives are stored in the offline database for map matching with a test environment floor plan. The mathematical algorithms and models in Figure 4-7 to produce **W1, W2, O2, O3, AMO1** and **R1** are calculated in section 5.1.1.3, where the goal of WTP-HAMS system is to generate improved absolute positions estimates with reduced errors when **R1** is realised in the offline phase using MATLAB. (See appendices A and B for offline and online screenshots).

5.3.1. WTP-HAMS system phase implementation

Implementation of the physical and neutral layers illustrated in Figure 5-7 are processed in two phases as indicated in 5.3. These phases include **online phase** and **offline phase**.

The online phase is the active application which is necessary for system training, data retrieval via server and light computation. While the offline phase is designed in MATLAB for the computation of mathematical models and algorithms on the data collected from the online phase. The localisation results are produced at the offline phase using real data from the online phase. Both phases are discussed further in 5.1.1.1 and 5.1.1.3 with the development and implementation breakdown of all necessary computation and data churning processes. Each phase is unique as they contain are core components necessary for determining absolute position estimate **R1**.

5.1.1.1 Online Phase

In this phase, real data is retrieved from participating sensors during live testing and saved in an online database. In particular, Wi-Fi, wheel encoders and smartphone IMU modalities. This phase happens when the API of the smartphone (SP) interfaces between the three technologies and the online database through a server. All three associated technologies are set as members of Wi-Fi and sensor managers within the SP, which we have titles as WiFiManager and SensorManager. WiFiManager governs Wi-Fi property data retrieval while SensorManager oversees data retrieval from wheel encoders and smartphone IMU modalities.

The API on SP is manually managed by the user. This is important because, SP battery life will be conserved and performance can be controlled, especially when retrieving data. Therefore, quick battery drainage will be prevented, because, when not in use, its foreground activity will be paused in SP background when API process is terminated.

The API, when triggered, initiates all the connected sensors, retrieves data from them and pushes all collected data to offline phase described in 5.1.1.3, where necessary models and algorithms are executed for position accuracy computation.

The online phase comprises of the following elements–

- SP API design and launch
- SP API environment set up
- Determining pitch, azimuth and roll of smartphone IMU modalities comprising of accelerometer, magnetometer and gyroscope

Each of these elements is discussed in the subsections below in detail.

SP API Design and Launch

SP API has three executable instances for application activity control, these include **START**, **STOP** and **RESUME**.

On **START**, a new array list of scanned samples is registered when either *Single Scan* or *mSCANButton* button is selected. The *Single Scan* registers sensor datasets from a set 5 seconds scan while *mSCANButton* listens and collects data over periods longer than 5 seconds. The *Single Scan* terminates its process automatically after 5 seconds scan duration, while the *mSCANButton* process is terminated by the user only when *mStopButton* is initialised. **STOP** terminates processes initiated by the *mSCANButton* and *Single Scan* buttons while still allowing SP API to actively listen to all connected sensors in the background. **RESUME** restores sensor listeners, especially when the SP API is launched.

SP API Environment Set Up

The executable instances **START**, **STOP** and **RESUME** reside in SP API environment. This environment is built to sniff and listen to received signals from connected sensors in the online phase. The application is set up with the required members to implement listeners which include `SensorEventListeners` and `RadioGroup.OnCheckedChangeListener` using a `SensorFusion Activity`. `SensorEventListeners` responds to modification in data received when a new sensor data is encapsulated from the four technologies measured in the SP. `RadioGroup.OnCheckedChangeListener` responds to selected options amongst the sensor alternatives attached to the radio group displayed on the SP interface. Both listeners contain two key listening parameters including **WiFiManager** and **sensorManager** which are initialised when start instance is triggered by a start button on the SP application interface. Each measured parameters are displayed as a string on the API.

- **WiFiManager**

WiFiManager accommodates world Wi-Fi channel standards by using 802.11a/h/j/n/ac/ax applied in all countries. This is because its channel bandwidth ranges from 10 MHz to 80 MHz frequency with the best-preferred frequency resting at 5 GHz.

After listeners are initialised, WiFiManager checks and registers unique channel frequencies with its distinctive received measured properties including BSSID, RSSI, SSID and frequency of each router as illustrated in Figure 5-9.

```
for (int i = 0; i < results.size(); ++i) {  
    mWifiInfo += "\r\n"; // "\r\n" = next line  
    mWifiInfo += "SSID: " + results.get(i).SSID + "\r\n";  
    mWifiInfo += "RSSI: " + results.get(i).level + "\r\n";  
    mWifiInfo += "BSSID: " + results.get(i).BSSID + "\r\n";  
    mWifiInfo += "Frequency: " + results.get(i).frequency + "\r\n";  
    //wifi_info += "Channel: " + results.get(i).frequency + "\r\n";  
    mWifiInfo += "Channel: " + getChannelFromFrequency(results.get(i).frequency) + "\r\n";  
}
```

Figure 5-9 Wi-Fi state in loop from the beginning to the size of each scanned result

Unique channel frequency assurance is necessary to ensure measured signals are not travelling on the same channel. Therefore, it is important that each router or Access Points (APs) is allowed to function effectively without interferences from the neighbouring router or Access Points (APs). Therefore, WiFiManager ensures that each Wi-Fi data from each channel frequency within APs is mapped with its distinctive properties. This is the initial step to mitigating Wi-Fi performance challenges, especially RSSI interferences.

WiFiManager scans and updates Wi-Fi data every 1.5 seconds after identifying available router or Access Points (APs). 1.5 seconds is the most suitable sampling rate as it gives SP enough time to acknowledge relevant Wi-Fi signals available. Collecting Wi-Fi properties is necessary because it provides data essential for

calculating estimated relative position using RSSI in the offline phase discussed in section 5.1.1.3.

- **SensorManager**

The SensorManager listens and pushes data from accelerometer, magnetometer, gyroscope and wheel encoders to accomplish the following –

- Orientation angle calculation of SP using accelerometer and magnetometer sensor **AM1** output fusion.
- Rotation vector output from a filtered gyroscope to compare with orientation angle output of fused accelerometer and magnetometer **AM1**.
- Travelled distance calculations on collected ticks from mobility scooter mounted wheel encoders when magnet interrupts the MBED MCU connected reed switch on wheel rotation.

SensorManager refreshes and pushes scanned results from the accelerometer, magnetometer and gyroscope in every 30 milliseconds using code snippet in Figure 5-10. This high sampling rate improves orientation angle estimates by managing heading uncertainties. It should be noted that the signal quality is dependent on sampling frequency and the rate at which the filtration method is called per second.

```
public static final int TIME_CONSTANT = 30;
public static final float FILTER_COEFFICIENT = 0.98f;
private Timer fuseTimer = new Timer();
```

Figure 5-10 High-frequency rates for SensorManager governing data retrieval from the accelerometer, magnetometer and gyroscope sensor

Determining Pitch, Azimuth and Roll of Smartphone IMU Modalities Comprising Of Accelerometer, Magnetometer and Gyroscope

Pitch (x), azimuth (y) and roll (z) from datasets recovered from the accelerometer, magnetometer and gyroscope sensors are collected and displayed on SP interface using Figure 5-11, before being pushed to the online database. To determine relevant pitch (x), azimuth (y) and roll (z) of the SP, the three exploited technologies implement AccMagOrientation matrix demonstrated in Figure 5-11 and gyroOrientation matrix shown in Figure 5-12 to determine best for heading estimation.

```
mRadioGroup = (RadioGroup) findViewById(R.id.radioGroup1);  
mAzimuthView = (TextView) findViewById(R.id.textView4);  
mPitchView = (TextView) findViewById(R.id.textView5);  
mRollView = (TextView) findViewById(R.id.textView6);  
mRadioGroup.setOnCheckedChangeListener(this);
```

Figure 5-11 display organisation of pitch (x), azimuth (y) and roll (z) of accelerometer, magnetometer and gyroscope post matrix implementation

First technology explored is the gyroscope sensor where it is observed to experience drift. To improve gyroscope drift, gyroOrientation matrix must overwrite initial gyroscope measurements. This, therefore, presents a rotation vector of SP as it rotates around its axis. This rotation vector is mandated to calculate the angular speed of SP orientation. Consequently recognising the behaviour of SP. Although output from implemented gyroOrientation matrix has reduced drift, it is insufficient for getting heading estimates. This is because as it only considers the rotation of SP without recognising direction SP is moving in.

```

gyroOrientation[0] = 0.0f;
gyroOrientation[1] = 0.0f;
gyroOrientation[2] = 0.0f;

gyroMatrix[0] = 1.0f; gyroMatrix[1] = 0.0f; gyroMatrix[2] = 0.0f;
gyroMatrix[3] = 0.0f; gyroMatrix[4] = 1.0f; gyroMatrix[5] = 0.0f;
gyroMatrix[6] = 0.0f; gyroMatrix[7] = 0.0f; gyroMatrix[8] = 1.0f;

```

Figure 5-12 gyroOrientation matrix calculating SP behaviour

The second explored technology include fused accelerometer and magnetometer sensor outputs. Output **AM2**, from the fusion of accelerometer and magnetometer sensors, occurs when AccMagOrientation matrix in Figure 5-13 is implemented. This achieves rotation angles which deliver absolute orientation of the SP. For example, instances where SP is lying flat on a surface or held up in hand, the filter coefficient of the signal quality for **AM2** returns stabilised x, y, and z output from negative-to-positive states. Compared to gyroscope output, this combination is advantageous in better determining SP orientation instances and also calculating heading angles to find direction SP when in motion. This output offers directional information which is combined with outputs from wheel encoders when determining pose with relative position estimates.

```

public void calculateAccMagOrientation() {
    if (SensorManager.getRotationMatrix(rotationMatrix, null, accel, magnet)) {
        SensorManager.getOrientation(rotationMatrix, accMagOrientation);
    }
}

```

Figure 5-13 orientation calculation from accelerometer/magnetometer fusion

A complementary fusion of gyroOrientation output with **AM2** is considered in this study. The intention is to improve SP orientation and rotation output through increased sensitivity of SP to gravitational influences which is achieved via the application of a sensor fusion illustrated in Figure 5-14. However, this is expected

to be ineffective due to system sensitivity which will invoke unwanted values. Thus, verifying that **AM2** is sufficient for providing more precise heading estimates.

```
class calculateFusedOrientationTask extends TimerTask
```

Figure 5-14 Fusing all IMU sensors

Distance Travelled Computation from Wheel Encoder

For wheel encoders, sensorManager identifies and converts rotation counts of the wheels to distance travelled estimates when mobility is in motion. This is mandatory when calculating pose estimates respect to relative travelled distance estimates. Here, distance travelled by the left and right wheels of the mobility scooter is calculated using Equation 29 to result in Figure 5-15.

$$\text{Circumference of the wheel} = 2\pi r \text{ (where 'r' is in cm)}$$

Equation 29

Where $2\pi r$ is the equation for calculating the outer circular circumference of the wheel and r is the radius of the outer the wheel in cm.

```
@Override  
public void pulseReceived() {  
    distance_travelled += 60;  
    mOdoInfoView.setText("Distance travelled: " + distance_travelled + "cm");  
}
```

Figure 5-15 travel distance of each wheel over time

In this instance, complete wheel rotation is equivalent to 60cm travelled distance which is also the circumference of the wheels. Distance travelled is calculated using a 9.6cm radius of the wheel's circumference. If speed is distance over time of each wheel revolution, it is assumed that it will take the mobility scooter 1 second for the wheel to complete one revolution equivalent to 60cm of ground. In a larger area, cm-level calculations will be tedious for the system and therefore would be required to calculate for the speed in m/hour as shown in Equation 16:

$$N \times 0.60 \times 3600/1000 \text{ (1 hour = 3600 secs; 1km = 1000m)}$$

$$= N \times 2.16 \text{ or } N \times 2.2$$

Equation 16

Where N represents the varying number of revolutions per second and 2.2 is constant.

5.1.1.2 Online process cycle completion

The output from WiFiManager and SensorManager are converted into a JSON array. The JSON array is saved in the online database with unique identification names and timestamps using code snippet in Figure 5-16 and Figure 5-17.

```
List<NameValuePair> http_data = new ServerSample().ToHTTPPostString(scanSamples);
http_data.add(new BasicNameValuePair( name: "WIFI", mWifiInfo));
http_data.add(new BasicNameValuePair( name: "Tag", mScanName.getText().toString()));
http_data.add(new BasicNameValuePair( name: "Size", Integer.toString(scanSamples.size())));

new HTTPAsync(http_data, new HTTPAsync.HTTPAsyncResponseListener() {
    @Override
    public void onPostExecute() {
        mStopButton.setEnabled(true);
        mScanButton.setEnabled(true);
    }
}).execute();
```

Figure 5-16 WiFiManager JSON array transfer to the database

```

for(ServerSample sample : list){
    nameValuePairs.add(new BasicNameValuePair( name: "AccelX["+i+"]", Double.toString(sample.AX)));
    nameValuePairs.add(new BasicNameValuePair( name: "AccelY["+i+"]", Double.toString(sample.AY)));
    nameValuePairs.add(new BasicNameValuePair( name: "AccelZ["+i+"]", Double.toString(sample.AZ)));
    nameValuePairs.add(new BasicNameValuePair( name: "GyroX["+i+"]", Double.toString(sample.GX)));
    nameValuePairs.add(new BasicNameValuePair( name: "GyroY["+i+"]", Double.toString(sample.GY)));
    nameValuePairs.add(new BasicNameValuePair( name: "GyroZ["+i+"]", Double.toString(sample.GZ)));
    nameValuePairs.add(new BasicNameValuePair( name: "MagX["+i+"]", Double.toString(sample.MX)));
    nameValuePairs.add(new BasicNameValuePair( name: "MagY["+i+"]", Double.toString(sample.MY)));
    nameValuePairs.add(new BasicNameValuePair( name: "MagZ["+i+"]", Double.toString(sample.MZ)));
    nameValuePairs.add(new BasicNameValuePair( name: "AccelMagX["+i+"]", Double.toString(sample.AMX)));
    nameValuePairs.add(new BasicNameValuePair( name: "AccelMagY["+i+"]", Double.toString(sample.AMY)));
    nameValuePairs.add(new BasicNameValuePair( name: "AccelMagZ["+i+"]", Double.toString(sample.AMZ)));
    nameValuePairs.add(new BasicNameValuePair( name: "GyroDE_X["+i+"]", Double.toString(sample.GDX)));
    nameValuePairs.add(new BasicNameValuePair( name: "GyroDE_Y["+i+"]", Double.toString(sample.GDY)));
    nameValuePairs.add(new BasicNameValuePair( name: "GyroDE_Z["+i+"]", Double.toString(sample.GDZ)));
    nameValuePairs.add(new BasicNameValuePair( name: "SF_X["+i+"]", Double.toString(sample.SFX)));
    nameValuePairs.add(new BasicNameValuePair( name: "SF_Y["+i+"]", Double.toString(sample.SFY)));
    nameValuePairs.add(new BasicNameValuePair( name: "SF_Z["+i+"]", Double.toString(sample.SFZ)));
    nameValuePairs.add(new BasicNameValuePair( name: "ODO["+i+"]", Double.toString(sample.ODO)));
    nameValuePairs.add(new BasicNameValuePair( name: "Timestamp["+i+"]", sample.timestamp));
}

```

Figure 5-17 SensorManager JSON array transfer to the database

5.1.1.3 Offline Phase

Offline phase handles mathematical calculations and algorithm applied to data received from the technologies at the online phase to derive the absolute position of the mobility scooter. The implementation of these models and algorithms are crucial in defining mathematical processes necessary in achieving **W1, W2, O2, O3, AMO1** and **R2** (see Figure 4-7) with respect to time.

A JSON array containing datasets from sensorManager and WiFiManager is transferred to an offline database designed in MATLAB. An extracted JSON array is arranged in a struct with correspondence to UNIX timestamp reference. This is because a timestamp is used to calculate absolute time for when data was collected by both members of SensorManager and WiFiManager. Absolute time is obtained when the difference between the current time and the first time is calculated using Figure 5-18. This is essential because it acts as the reference for each data point received over distance.

```
times=times-times(1);
```

Figure 5-18 Calculating for absolute time

Still, within the offline phase, MATLAB performs the following models and algorithms to achieve the overall purpose of this study -

- a) Adopted SDRS log-normal shadowing model [38][39] (Equation 5) on RSSI propagated from Wi-Fi to produce **W1**
- b) Multi-trilateration algorithms [14] (Equation 6) applied on **W1** get **W2**, which is estimated relative position using RSSI
- c) New drift mitigation model (Equation 19) proposed by WTP-HAMS system is used on estimated travelled distances received from the wheel encoders to get improved travelled distance estimates **DO1**.
- d) Odometry model [19] (Equation 1, Equation 2 and Equation 3) is applied on **O1** to get **O2** to get relative position estimates **O3** of the mobility scooter
- e) Novel WTP-HAMS odometry model (Equation 21Equation 22) combining **DO1** from wheel encoders with **SS2** from fused accelerometer and magnetometer (Equation 20) to get improved pose estimates with relative positions **AMO1**.
- f) Novel WTP-HAMS localisation system which uses geometric error shapes formed by combined **BrAMO1** and **BrW2** (Equation 25Equation 26) to find improved absolute position **R1**. This is true when error shapes of **W2** and **AMO1** intersect or overlap (Equation 27Equation 28).

All the calculation performances are grouped into three sections, namely, *estimated relative position using RSSI*, which is satisfied when performances **a** and **b** are fulfilled; *pose estimation with relative position using odometry*, that is achieved when **c**, **d** and **e** are performed; and *estimated absolute position with reduced error*, which is obtained when **f** is executed. These are further discussed below.

Estimated Relative Position Using RSSI

Relative position estimates using RSSI needs SDRS log-normal shadowing model [38][39] (Equation 5) and multi-trilateration [14] (Equation 6) algorithms to be implemented sequentially. Equation 4 is applied to RSSI collected from measured APs to obtain **W1**. This thesis demonstrates how **W1** is derived from three and four routers/APs present in a test environment. Identifying the locations of these routers/APs is important in creating outline boundary needed for effective mapping of estimated distances from the ground truth. Each router/APs is identifiable in the offline phase by its unique mac address as shown in Figure 5-19.

```
macA = '00:11:92:10:40:00';  
macB = '00:19:92:12:07:61';  
macC = '24:0d:c2:aa:86:71';  
macD = 'ec:43:f6:6a:8f:70';  
macE = '64:70:02:eb:d4:66';
```

Figure 5-19 Mac addresses identifying unique APs for RSSI propagation

The mac addresses in Figure 5-19 belong to the five identifiable Wi-Fi router/APs present in a test room. Identifying Mac addresses of relevant routers/APs filters RSSI readings from other measured but unnecessary routers. RSSI from relevant APs are measured signal power with a certain degree of noise caused by shadowing effects. SDRS log-normal shadowing model filters noise experienced in each RSSI while, also calculating for distance estimates relative to relevant APs.

In our investigation, the Gaussian variance of -36 dBm is used when considering noise experiences within RSSI. In this study, conversion of power to relative distance estimates **W1**, is resulted when Gaussian variance 36 dBm is combined with free space exponent of 2.2 based on environment dynamics and RSS power at 1m as shown in code snippet Figure 5-20.

```
function [dist] = get_distance(rssi, variance)
    sj = -36;
    n = 2.2;
    dist = 10 ^ ((sj - rssi + variance) / (10 * n));
```

Figure 5-20 SDRS log-normal shadowing model to get relative RSSI distance

It is expected that **W1** will be meter level distance estimates relative to the room, however, it does not provide position estimate. Therefore, multi-trilateration (Equation 6) is adapted to combine all distance estimates from relevant routers/APs to get relative position estimates **W2**. Multi-trilateration (Equation 6) code snippet shown in Figure 5-21 is written to calculate for relative position estimate **W2** using **W1** calculated from each RSSI of relevant routers/APs.

```
D = zeros(BeaconN -1, 2);
b = zeros(BeaconN -1, 1);
]for i = 1 : BeaconN -1
    D(i, :) = [ B(1,1) - B(i+1, 1), B(1, 2) - B(i+1, 2) ];
    b(i) = B(1,1)^2 - B(i+1,1)^2 + B(1,2)^2 - B(i+1,2)^2 - B(1,3)^2 + B(i+1,3)^2;
end
D = 2 * D;
DT = D';
Q = (DT * D) \ DT * b;
x = Q(1);
y = Q(2);
```

Figure 5-21 multi-trilateration computation for four APs/router

Here in Figure 5-21, **b** represents the beacon matrix that considers x,y coordinates of each router; BeaconN is the number of routers; [x,y] represent x,y coordinates of the mobility scooter using RSSI; and Q is the algorithm calculating the point at which all estimated distances from the APs meet.

The convergent point for all distance estimates is **W2** with errors. In our investigation, an average for x,y value per **W2** from over 100 iterations is selected as best relative position estimation **BEW2** with its corresponding average error

estimate **EErW2** calculated and saved in the offline database. **EErW2** is radius highlighting estimated variation between **BEW2** and ground truth to form a circle **BrW2** that concludes *relative position estimation using RSSI*.

Pose Estimation with Relative Position Using Odometry

Pose estimation with relative position is calculated using estimated distance travelled approximations saved within the extracted JSON array read by MATLAB. It is established by researches [19][170] that drift sets in as the mobility scooter travels longer distances, therefore, our proposed WTP-HAMS system proposes new drift mitigation model (Equation 23) be implemented on the received travelled distance approximates to determine new **O1**. New **O1** in this study represents improved travelled distance estimates that are calculated using received travelled distance approximates from each wheel.

First off, Equation 1, Equation 2 and Equation 3 are implemented to calculate the pose of the mobility scooter formula from research by A. Jha and M. Kumar [19]. It is important to understand drift from the wheel encoders. However, because it is expected that drift will be experienced, the proposed *new drift mitigation model* (Equation 19) is implemented on the D_C (**O1**), where a maximum percentage error is added to its overall travelled distance. This reduces the drift distance travelled. However, the heading errors will persist because the traditional odometry (Equation 1, Equation 2 and Equation 3) is dependent on travelled distances of both wheels described in the code snippet below in Figure 5-22.

```
D_L = m_per_tick * (left_ticks-prev_left_ticks);  
  
D_R = m_per_tick * (right_ticks-prev_right_ticks);  
  
theta_dt = (D_R - D_L)/L;
```

Figure 5-22 distance travelled computation based on SOTA

Where D_L is the distance travelled by the left wheel; D_R is the distance travelled by the right wheel; D_C is the distance travelled by the centre of the scooter.

The drift experiences in the heading navigation is expected to cause significant pose and positioning errors, therefore, the **AM1** of the smartphone IMU modalities is proposed to offer heading navigation solution. This is because **AM1** reduces directional errors **O2** provides by producing better accurate heading estimates.

To implement the proposed novel odometry model that will improve pose estimation, **O2** is substituted with the improved AccMagOrientation (**AM2**) (Equation 24) from the online phase. This is accelerometer and magnetometer fusion, which is selected because it considers the orientation of the smartphone as well as provides heading navigation angles. (See code snippet in Figure 5-23).

```
theta_global=get_column(filetext2, "AMY");  
  
plot (theta_global)  
if theta_global> 0.00001  
    target_bearing_theta_global = 90.0 - atan(y/x);  
elseif
```

Figure 5-23 identifying AM2 with respect to the globe

However, the frequency spectrum of **AM1** is inconsistent with multiple peaks. To smoothen this frequency spectrum, moving average filter of 2, 20 and 50 spans are considered, and, 50 spans are selected. This is because 50 spans produce most useable dataset. This is identified as **SS1**.

The smoothened signal (**SS1**) is then set to identify and synchronise with the initiation, acceleration and deceleration of the mobility scooter through the employment of FWHM (Equation 4). The resultant is **SS2**, which produces better accurate directional information with significantly reduced heading error. **SS2** is vital in our investigations as it presents better navigation heading.

Then, the *pose estimation with relative position* is calculated for, by combining the results from the new drift mitigation model (O1) with AM2 in a proposed novel odometry model (Equation 21Equation 22). This is important because, it produces AMO1, which is the combination that will get the relative pose and position estimate with significantly reduced errors. The implementation is shown in the code snippet in Figure 5-24.

<code>x_dt = D_C * cos(theta);</code>	Equation 21	AMO1
<code>y_dt = D_C * sin(theta);</code>	Equation 22	
<code>theta * (180.0/pi);</code>	Equation 20	AM2

Figure 5-24 Odometry model for position estimation with error

Similar to estimated relative position using RSSI, best-estimated pose with relative position (**BEAMO1**) from **AMO1** and estimated errors (**EErAMO1**) are saved in the database, after Equation 26 is implemented. It should be noted that **BEAMO1** is obtained from an average of 1000 relative position samples of collected data while **EErAMO1** is the variation from the true position when Equation 26 is applied. Both **EErAMO1** and **BEAMO1** when united in Equation 23 form error triangles between the true position and **BEAMO1**. This combination to form error triangles is identified as **BrAMO1**.

Estimate Absolute Position R1 with Reduced Error

The purpose of this investigation, which is the improvement of indoor localisation, is achieved when new absolute position **R1** is originated. In particular, this is the centroid of the calculated position area estimate from Equation 27Equation 28. This is true because the centroid is in the shaded area where **BrW2** (Equation 25) and **BrAMO1** (Equation 26) overlap. Especially, when the system implements Equation 27 and Equation 28 to confirm an overlap has occurred. It should be known, that,

the shaded area is the improved estimation position area with reduced error and its centre is the new position **R1** with significantly reduced error.

The position error of **R1** is then compared with ground truth using Equation 10 and Equation 11. This is important to measure the improvement of the proposed WTP-HAMS system. In particular, validate our proposed investigation that plans to provide better accuracy when compared to SOTA.

5.4. Summary and Analysis

The proposed investigation presents a lightweight system that implements several mathematical models in an innovative technique to achieve indoor position accuracy improvement. This is because; it is an innovative combination of position estimation from RSSI and pose estimation with relative position using the proposed novel odometry model, to get the centroid **R1**. Importantly, the centroid **R1** is an improved absolute position area with reduced position error.

Position estimation using RSSI is obtained from the processing the Wi-Fi signals collected by the API of the smartphone in the online phase. This system then pushes the signals to an online database via a server. This online database, consequently, pushes the data to an offline MATLAB database where calculations are performed. The first performed calculation is Equation 5 where the signal strength of the Wi-Fi is translated into distance measurements. The second performance is Equation 6, where the distance measurements from the considered 3 and 4 routers, are combined to estimate position **BEW2**. This calculation takes less than a second. It is an advantage to our system because; its latency is low, especially when compared to 2-3seconds latency from fingerprinting methods adopted by SOTA [14]. The position error **EErW2** gotten when Equation 9 is implemented, makes forming the error shapes achievable. In particular, the circle formed around the estimated position and ground truth. This may also be influenced by LOS or NLoS instances. RSSI position estimation is important because it provides a room reference frame.

Pose estimation using the proposed novel odometry model is the combination of proposed new drift mitigation model on travelled distance from wheel encoders and navigation heading from combined IMU sensors, in particular, accelerometer and magnetometer. These technologies (wheel encoders and smartphone IMU sensors) send data packets to the smartphone concurrently with the exploited Wi-Fi routers. This system then pushes the data alongside RSSI signals to an online database via a server. This online database, consequently, pushes the received data to an offline MATLAB database where calculations are performed. In particular, the proposed new drift mitigation model and novel odometry model.

The first performed is the traditional odometry model from Equation 1, Equation 2 and Equation 3, where it was expected that drift would occur. In particular, in the distance travelled based on Equation 29. Therefore, a new drift mitigation model (Equation 19) was proposed. This was important because it would correct distance travelled errors. However, it defaulted in correcting heading errors. Therefore, a novel odometry model (Equation 21Equation 22) was proposed to get **AM01**. In particular, it included the combination of distance-travelled estimates with reduced drift and heading navigation **AM1** from smartphone IMU sensors. This was important because the combination of **AM1** is **AM2** when Equation 20 is applied, provides better navigation heading values, as well as, provides the orientation of the smartphone. In particular, it provides better navigation heading when compared to direction estimates **O2** from traditional odometry based on the original travelled distance estimates. Although **AM2** presents better navigation heading, it needs to be synchronised with the drift reduced travelled-distance estimates. Therefore, a unique FWHM process in Equation 4 is implemented to smoothen out the multiple peaks of **AM2**. FWHM synchronises the waveform of **AM2** synchronised with the drift reduced travelled-distance estimates, by identifying points of initialisation, acceleration and deceleration over drift corrected travel distance of the mobility scooter and time. After the synchronisation is complete, then the estimated values from **SS2** and drift corrected distance travelled can be combined in the proposed novel odometry model. The expectation is that the proposed novel odometry model will significantly outperform the traditional odometry model. To check the

expectation, position error **E_{Er}AM01** of the estimated pose with relative position **BEAM01** from ground truth is calculated using Equation 23. Here, it is expected that the error shape will be triangular, especially because of the high sampling rate of 0.33f. This proposed novel odometry is important because it is expected to correct the errors of RSSI.

Finally, a check is carried out find if error shapes triangle from **E_{Er}AM01** of **BEAM01** and circle from **BEW2** of **E_{Er}W2** overlap. If both circular and triangular error shapes overlap, then a centroid **R1** is calculated and is the new estimated position. This is illustrated in Figure 4-6, where the improved position area, which is the shaded overlap area, shows the new position estimate **R1**, which is the centre of the shaded area.

It is our proposal that a series of studies be carried out to test our methodology, including the proposed software and hardware system implementation. In particular, the following will be investigated –

- The influence of LOS and NLoS on RSSI
- Which provides better position estimates for Wi-Fi, a combination of 3 routers or 4 routers
- Comparing navigation heading results from two configurations of smartphone IMU modalities
 - Accelerometer, gyroscope and magnetometer
 - Accelerometer and magnetometer
- Determining if smartphone orientation will impact results, in particular, horizontal versus vertical orientation
- Finding out where the smartphone will be best placed with consideration to the following
 - In hand
 - On mobility scooter
 - On mobility floor

- Examining how best our proposed new drift mitigation model improves travelled-distance.
- Investigating the proposed novel odometry, especially in the improvement of pose estimation of the tracked mobility scooter user.
- A comprehensive study that combines all the results from RSSI and novel odometry model. This is important to demonstrate how our proposed WTP-HAMS system improves position accuracy.

Chapter 6 Experimentation

This chapter aims at designing and evaluating studies to test the proposed WTP-HAMS system described in the methodology in chapter 4. Also contained in this chapter, are specific studies of each technology exploited by our proposed WTP-HAMS system. The exploited technologies include Wi-Fi, wheel encoders and smartphone IMU modalities – accelerometer and magnetometer sensors. The major reasons for our experimentations are to measure the accuracy of the proposed WTP-HAMS system.

Because of the extension of the experimentation described in this chapter, the content of the presented section is outlined below:

Section 6.1 presents a design overview of our studies in terms of experimental strategy and implementation of our methodology. It also presents an overview containing the advantages and limitations of the exploited technologies in our methodology.

Section 6.2 breaks down the experimental strategy for a focused and comprehensive study with supporting illustrations. It includes plans for five sub-studies under Wi-Fi, smartphone IMU modalities and wheel encoders.

Section 6.3 details the strategies and conditions for conducting studies on Wi-Fi and its purpose in our proposed system. Its studies are grouped into first and second studies which respectively includes the comparison of LOS vs NLoS and 3 vs 4 routers for position estimation using multi-trilateration.

Section 6.4 in-depth study and strategy discussion for smartphone IMU modalities and its particular benefit in our proposed methodology. This is grouped into third and fourth studies which respectively includes identifying best navigation heading and smartphone pose for our system.

Section 6.5 plans and examines a strategy for a detailed study of wheel encoders and its specific advantage in our proposed system. We allocated it to a fifth study which includes relative pose accuracy.

Section 6.6 develops a strategy to examine a comprehensive study of our proposed system using outcomes from previous sections 6.3 - 6.5.

Section 6.7 the plans and strategies of the studies discussed and recommended in 6.3 - 6.6 are implemented in this section.

Section 6.7.4 this section includes our results discussions and summary of the experiments of our proposed WTP-HAMS system. It also compares our results to relevant literature works.

Section 7.3 this concludes our chapter with personal and technical lessons learnt when carrying our studies.

6.1. Design

In order to design the proposed system experimentation and to best address the advantages and limitation of each relevant sensor, it is proposed to analyse the different characteristics of each sensor. Figure 6-1 illustrates the main advantages and limitations based on the state of the art.

		Representation	Description
	+	+	Absolute position
		+	The global reference frame is room
		+	economical
		+	Readily available, therefore ubiquitous
		+	Easily accessible
		+	
		+	
		+	
		+	
		+	
	+	+	Good heading/navigation estimate
		+	High accuracy with 1-2 degrees error
		+	A global reference for orientation only
		+	Absolute position estimation for tracked pedestrians
		+	
		+	
	+	+	Travelled distance estimation
		+	Better position accuracy possibility dependent on the path
		+	
		+	
		+	Relative position estimation with reference to mobility scooter frame
		+	Drift (accumulated errors)

Figure 6-1 Purpose for experimenting on Wi-Fi, smartphone modalities including IMU sensors - accelerometer, magnetometer and wheel encoder based on evaluations by the State-of-The-Art (SOTA)

We will begin the experiments with a design, which includes

- **Experimental strategy** – this is the planning stage to strategize on how our experiments will be carried out. It includes -
 - Focused study – studies the individual technologies proposed in our methodology and how they will be implemented in our experiments. It includes studies for Wi-Fi, smartphone IMU modalities and wheel encoders. They are grouped into Pilot test phase and Main test phase.
 - Comprehensive study – studies the validity and viability of our proposed methodology, especially in indoor position improvement.
- **Experimental implementation** includes the experimental setup, procedure, results and analysis of all the studies carried out in the focused and comprehensive studies.

6.2. Experimental Strategy

After identifying the purpose of our experiments, we designed a strategic approach to assess our proposed WTP-HAMS system. This is important to evaluate our methodology, in particular, a **focused study** evaluating each technology on its own, to get insight on how best to run a more **comprehensive test**. This is illustrated in Appendix 2.

It is proposed that we carry out a **focused study** and a **comprehensive test**.

6.2.1. Focused study

The **focused study** individually assesses Wi-Fi, smartphone modalities – IMU sensors and wheel encoders. This is important to build our proposed **comprehensive test**.

Our experimental strategy for the **focused study** is to group our studies into two phases, namely, **pilot test phase** and **main test phase**.

Pilot Test Phase

The **pilot test phase** examines the signal quality of Wi-Fi in a small-congested room. It includes the use of a smartphone to collect all sensor data from the one Wi-Fi router. The purpose is to conduct a **first study**, which aims at understanding the effects of the line of sight (LOS) and None Line of Sight (NLOS) of routers in a controlled environment (*room 1*).

This is critical because the outcomes from the **pilot test phase** will determine the instance our subsequent tests we will adopt when conducting position experiments using multi-trilateration of 3 and 4 routers in the **main test phase**. This is highlighted in 6.1 and expatiated on in sections 6.3.1 and 6.7.2.

Main Test Phase

The **main test phase** studies the independent advantages of Wi-Fi, Smartphone IMU modalities and wheel encoders (shown in Appendix 2) in a medium sized representative environment (*room 2*) with a smooth wooden tiled floor. This is important because it provides an effective understanding and adequate measurement of position, direction and pose of our implemented smartphone and mobility scooter in room 2.

It is critical we divide the main test phase into four studies, where one of this study is based on results from the **first study** in the **pilot test phase**. Therefore, we opted to continue the study count from the **second study**.

The studies in the **main test phase** include –

Second study– two core tests are carried out to determine the best router number and configuration best needed to get position estimate in room 2. The router number and configuration we will consider for testing best position estimation with Wi-Fi are three-router configuration (config 1) versus four routers configuration (config 2).

This study is highlighted in Appendix 2 (Appendix B) and expatiated on in sections 6.3.2 and 6.7.2.

Third study–we experiment for navigation heading using two major tests, including our proposal to combine *accelerometer and magnetometer* sensors and SOTA recommendation to combine *gyroscope, accelerometer and magnetometer* sensors. This is important for us to compare both studies and find out the most accurate combination sufficient for our system.

This is highlighted in Appendix 2 (Appendix B) and expatiated on in sections 6.4.1 and 6.7.2.

Fourth study– we investigate for the best suitable smartphone pose in our system by testing two smartphone orientations including vertical and horizontal orientations. This is critical in choosing the most efficient and conducive orientation for the user. In addition, it is very important we identify the best orientation because it influences the result of the ***third study***. Therefore, it is expected that the best orientation in our ***fourth study*** will positively influence the ***third study*** when getting the best heading navigation.

This is highlighted in Appendix 2 (Appendix B) and expatiated on in sections 6.4.1 and 6.7.2.

Fifth study– in this study, we examine results from our proposed new drift mitigation model and combine it with results from ***third*** and ***fourth studies***. This combination is necessary for the testing of our proposed odometry model. Most importantly for the derivation of improved relative position estimates.

This is highlighted in Appendix 2 (Appendix B) and expatiated on in sections 6.5.1 and 6.7.2.

6.2.2. Comprehensive study

This study involves experiments using the proposed methodology, which is our WTP-HAMS system. Technological and environmental conditions and instances will be recommended for testing based on outcomes from **first – fifth studies**. It is important to validate our proposal that WTP-HAMS system will improve position accuracy.

This is highlighted in Appendix 2 (Appendix B) and expatiated on in sections 6.6 and 6.7.3.

6.3. Wi-Fi

Wi-Fi is selected for experimentation as relevant papers referred to in chapters 2 and 3 including a Wi-Fi sensing survey [59], discuss advantages of Wi-Fi in its ubiquity, cost-effectiveness, non-invasiveness and technology deployment ease. It is evaluated based on papers discussed in chapters 2 and 3, with emphasis on representative paper by S. Boonsriwai et al and S. He et al [14][106], where it is examined and reported that the granularity of position estimation may be limited to room level due to signal order from stationed Wi-Fi APs. This confines position reading within the measured area like room and therefore, making room the global reference. S. Boonsriwai et al[14], investigated the calculation of a user's relative position to Wi-Fi APs using multi-trilateration methods. It is our understanding from the investigation of journals and conferences on Wi-Fi-based indoor localisation that though calculated positions are relative to Wi-Fi APs/routers at fixed positions, its position measurement is within a room absolute to the global frame. Therefore, position estimates from Wi-Fi can be regarded as absolute if the room with fixed Wi-Fi APs/routers is assumed to be the global reference frame for the tracked object. With consideration to the above, the experimentation will look into studying the following: (1) LOS versus NLoS; (2) Position accuracy based on multi-trilateration.

6.3.1. First Study: LOS versus NLOS

Several literature works [29][62][59][171][14][172][173] evaluate Wi-Fi with a demonstration on how distance inaccuracies are affected in cases of None-Line-Of-Sight (NLoS) and clear Line-Of-Sight (LOS). In representative paper S. Boonsriwai et al [14], LOS shows an error of approximately 4.236m and 2.816m when three and four routers are considered respectively while NLoS show error of 5.690m and 6.156m when three and four routers are considered respectively in an area with wall partitions and poor signal propagation. It should be noted that NLoS influence is highly dependent on the number of obstacles between the device and APs, this is not indicated by the literature works mentioned above.

It is proposed that we follow the approach seen in the Literature with testing out both LOS and NLoS. This is important because the system performance depends on many elements (among them: environment configuration, and human interference), and therefore the outcome of SOTA experiments do not necessarily apply to all environments. We expect LOS will perform better and therefore we will rely on it and run more focused trials with LOS only, but we wish to start with a first step which is the **first Study** that includes LOS versus NLoS.

The **first study** includes a *small-congested environment* and *one router only*.

- A small-congested environment (*room 1*) is proposed because it allows for testing with LOS and NLoS situations. In particular, the situation of NLoS will mainly arise by people moving around. It is expected NLoS will perform worse, and it will be of particular interest to measure the deviation from LOS and possibly get indications about how the Wi-Fi behaviour will change based on specific arising situations, e.g. how people's movements (and still positions) will affect distance estimation.
- One router only is proposed because this setup is deemed representative and no relevant observations are expected from using more routers.

Furthermore, the one router only situation is deemed leading to a neater outcome.

6.3.2. Second Study: Position Accuracy Based On Multi-Trilateration

One of Wi-Fi limitations argued in representative papers [14][174] is position accuracy of multi-trilateration. This position inaccuracy is influenced by the conditions discussed in the **first study**, and especially the number of routers/APs. Literature works, particularly S. Boonsriwai et al [14] examined the influence on position accuracy when one to nine number of Wi-Fi routers/APs are involved. It is their remark that the number of routers affects positioning process performance. Their findings show that an increase in the number of routers to 5 or 6 provide a higher possibility for position inaccuracy due to the selection of low-quality signals during the ranging calculation. In other words, poor signals from the router will negatively affect the calculation. Their recommendation is that best position approximation is achievable when the number of routers is 3 or 4.

It is proposed we obey the recommendation by SOTA with testing for both 3 and 4 routers/APs. This is critical because the performance of WTP-HAMS system is dependent on the following elements like room size, environment configuration, router position and conditions in the **first study**. Therefore, the outcome of SOTA experiments does not necessarily apply to all environments. It is our expectation that the 4 router combination will produce better results. Therefore further focused trials for the experiment are planned, which will rely on *number of routers* = 4. However, before experimenting with 4 routers, we propose to also test with 3 routers. This test is included in the experiment's **second study**.

The **second study** includes a *medium sized uncongested environment* and, *three to four routers only*.

- A medium sized uncongested environment (*room 2*) is proposed because it allows for better testing of situations for three routers/APs and four routers/APs. Particularly, three routers/APs will not be best suitable due to signal propagation influence caused by room size. It is expected that four router/APs will perform better, and it will be of particular interest to measure the deviation of from three routers/AP. The purpose is to get indications about how three and four routers/APs will influence position estimation accuracy in our environment based on smartphone position in the instance where the smartphone is on the arm of the mobility scooter.
- Three routers/APs is proposed for the initial trial because it is the standard for trilateration and therefore needs to be investigated in our environment.
- Four routers/APs is proposed for the next trial because this setup is expected to provide better position accuracy in our test environment.

6.4. Smartphone IMU Modalities

Smartphone IMU modalities (accelerometer, magnetometer and gyroscope sensors) are chosen for experimentation because we have observed a trend by SOTA [64][145][109][158][175], that it is best for estimating heading. This is discussed in chapters 2 and 3. With consideration to the above, the experimentation will look into studying the following:

- Navigation Heading
- Smartphone Pose

6.4.1. Third Study: Navigation Heading

The representative papers mentioned above, experiment with IMU sensors to demonstrate how heading can be estimated on tracked pedestrians. This is of particular interest to us because SOTA investigates IMU influences on pedestrian motion, but our system is focused on transitional motion.

It is our proposal that we test out heading estimation of the smartphone when mobility scooter is moving in translational motion. This is important because the performance of our system is dependent on the combination of two out of three IMU sensor combination, and therefore the outcome of SOTA experiments do not essentially apply to translational motion. We expect accelerometer only will not be sufficient for measuring distance in translational motion and gyroscope drift will greatly influence our system, therefore we wish to investigate this aspect through a **third study** that includes accelerometer, magnetometer and gyroscope.

The **third study** includes *a smartphone* and *smooth wooden tiled floor*.

- A smartphone is proposed because it is ubiquitous and therefore less expensive. In addition, it contains critical sensors (accelerometer, magnetometer and gyroscope sensors) needed for system testing. It is our expectation that *configuration one* which is, the combination of accelerometer and magnetometer, will outperform *configuration two* that is, combined accelerometer, magnetometer and gyroscope. Therefore, it is our interest that we measure the noise level of the two configurations.
- A smooth wooden floor is chosen because it allows better testing for waveform patterns from IMU sensors when in translational motion. Furthermore, this flooring type is recommended for the target audience by regulatory bodies in SOTA [163] [164].

6.4.2. Fourth Study: Smartphone Pose

Representative papers [171] [176] experiment with smartphones because of its inbuilt IMU and ability to allow all connected systems to be referenced in a timely manner. It is their observation that poor time synchronisation will cause drift, therefore, time synchronisation is recommended to mitigate it.

Furthermore, it is recommendation [171] [176] that the smartphone is set up in a vertical orientation in their experimentation. It is of interest to us because SOTA investigates phone frame to navigational frame impact on only pedestrian motion when the user has phone placed vertically in a pocket or phone holder in a car, but our system is focused on that of transitional motion.

It is our proposal that we follow SOTA approach in experimenting with smartphone time synchronisation and phone orientation. This is vital because our proposed WTP-HAMS system relies on elements including UNIX time and smartphone orientation. We expect the UNIX time will provide global time-frame. Also, we expect horizontal orientation will perform better and therefore perform focused trials with a horizontal orientation. We commenced with the **fourth study**, which includes vertical and horizontal orientations.

Fourth study includes *a UNIX time timestamp and smartphone orientations*

- UNIX timestamp is proposed because it allows for global tracking and sorting of dated information from connected sensors within a dynamic system. Particularly useful situations where the system is tested in different time zones. It is our expectation dates will remain true to the country's time zone.
- The smartphone orientation is proposed to test vertical and horizontal orientations. Particular situations, which may arise, are sensor readings from axes with reference to smartphone frame and translational motion. It is our opinion that horizontal orientation, (representing the smartphone placed horizontally on the mobility scooter arm), is more practical as user

will need both hands to steer the mobility scooter and this configuration is also considered more stable (while if the phone is held vertically it could greatly be influenced by hand's movements). Furthermore, holding the smartphone vertically may call for a vertical holder to be designed. It is proposed to test with both the orientations to assess heading direction accuracy in translational motion.

Particularly, we test to know the influence of the orientations will have on our system based on the following instances -

- In the user's hand
- Mobility scooter arm
- Mobility scooter floor

6.5. Wheel Encoders

Wheel encoders are selected for experimentation because representative papers [19] [177] in SOTA discuss its advantage in measuring travelled distances of tracked objects moving in translational motion. This is discussed in chapters 2 and 3. From investigations of journals and conferences on indoor localisation based on wheel encoders, calculate for poses relative to the mobility scooter frame. This therefore makes the mobility scooter the reference frame. With consideration to the above, the experimentation will look into studying the following: (1) Relative Pose Accuracy.

6.5.1. Fifth Study: Relative Pose Accuracy

One of the major limitations of wheel encoders discussed in representative papers [19] [65][178], is drift relative to distance travelled. Representative paper [5] show an odometry based pose error of 3m – 5m. Pose error is caused by an accumulated error in travelled distance from both wheels.

Therefore, it is our proposal we compare traditional SOTA approach with our **proposed novel odometry model**, to assess drift experienced by our system in our test environment. This is important because our system relies on the number of encoders, size of wheels, driving path and type of floor surface. It is our expectation that our **proposed novel odometry model** will perform better than traditional methods from representative papers. This test is therefore commenced with the **fifth study** which includes distance travelled with our proposed drift mitigation model and pose error correction.

Fifth study includes *a wooden tiled floor, two wheel encoders, straight driving path, our proposed new drift mitigation model and conditions from phase 4*

- A wooden tiled floor is proposed because it is recommended by the recommended body in literature papers [163] [164]. It is particularly relevant to the target audience and therefore of exact interest to us that experiments be done with wooden tiled floor.
- Two wheel encoders are proposed because they are sufficient for many applications and could easily be modified into three or four-wheeled devices. If this modification is required, the additional redundant wheel may be added. Two wheel encoders are advantageous to our experiment because the pivot point of the turning radius is the rear axle.
- The straight driving path is proposed to follow the assumption from SOTA [178], [19] to measure the equal travelled distance of each measured wheel. This is deemed adequate to lead to a tidier outcome.
- Our proposed new drift mitigation model is proposed to correct travelled distance error caused by drift. This is important to improve the pose of the mobility scooter.
- Conditions from the **fourth study** are proposed because it allows for improved pose measurement situation. Particularly, in situations where our **proposed novel odometry model** is applied. It is expected that the combinations from the **fourth study** with the **fifth study** would have better pose with heading estimates true to the global frame.

6.6. Comprehensive Study

It is important that the limitations of each technology critical to our methodology be studied. This includes Wi-Fi, wheel encoders, and smartphone modalities – accelerometer and magnetometer. Particularly within our test environment which is the representative standard for our target audience. It is expected that the limitations discussed for each technology will negatively affect position accuracy, therefore, sets of conducted studies, summarised in illustrated in *Table 6-1*, ascertain the best configuration for our experiments.

Critical elements of the experiments				
Technology	Environmental and technological Configuration	Studies/investigations	Study Section	Recommendation for comprehensive test
Wi-Fi	Router Number	1 router vs 3 routers vs 4 routers	First and Second study	4 routers
	Room size	Small room vs medium room	First and Second study	Medium room
	Room configuration	LOS vs NLOS	First study	LOS
Smartphone modalities - IMU	Motion type	Pedestrian vs transational	Third study	Translational
	Floor type	Smooth wooden tiled floor	Third study	Smooth wooden tiled floor
	IMU combination for heading	Accelerometer + gyroscope + magnetometer vs accelerometer + magnetometer	Third study	Accelerometer + magnetometer
	Smartphone orientation	Vertical vs Horizontal	Fourth study	Horizontal
	Time synchronization	Unix Timestamp	Fourth study	Unix Timestamp
Wheel encoders on Mobility Scooter	Number of wheel encoders	2 wheel encoders	Fifth study	2 wheel encoders
	Driving path	Straight path	Fifth study	Straight path
	Floor type	Smooth wooden tiled floor	Fifth study	Smooth wooden tiled floor

Table 6-1 Critical elements of the evaluation methods and setup

First and second studies in *Table 6-1* are focused on Wi-Fi, where it is proposed that we follow the literature approach and test for *LOS and NLoS* and *Position accuracy based on multi-trilateration*. Discussed above, this is important because the performance of the system is dependent on the number of routers, room size and room configuration. Outcomes from the **first and second studies** are vital for decisions made in our Comprehensive study. Our decision for Comprehensive studying includes 4 routers, a medium room and LOS. This is further discussed in the **Comprehensive study** paragraph below.

Third and fourth studies in *Table 6-1* are concentrated on smartphone IMU modalities, where it is proposed that we follow SOTA approach in testing *Navigation*

heading and *Smartphone pose*. This is important because the performance of the system is dependent on smartphone orientation, IMU sensor combination, motion type, time synchronisation and floor type. Outcomes from **third and fourth studies** are critical for choices made in our Comprehensive study. Our decision for Comprehensive studying includes smooth wooden tiled floor, horizontal smartphone orientation, UNIX timestamp and combination of accelerometer and magnetometer. This is further discussed in the **Comprehensive study** paragraph below.

Fifth study in *Table 6-1* is centred on wheel encoders, where it is proposed that we follow the state-of-the-art approach in investigating *Relative pose accuracy*. This is important because the performance of the system is dependent on a mobility scooter, number of wheel encoders, driving path and floor type. Outcomes from the **fifth study** are vital for decisions made in our Comprehensive study. Our decision for Comprehensive studying includes two wheel encoders, straight paths and smooth wooden tiled floor. This is further discussed in the **Comprehensive study** paragraph below.

Based on the outcomes from the **first – fifth study**, it is proposed we configure a **Comprehensive study**. This is important because our system relies on 2 wheel encoders mounted on a mobility scooter, moving along the surface of a smooth wooden floor in translational motion along a straight path, within a medium sized room with 4 routers and LOS. In particular, UNIX timestamp is used to synchronise all data including combined accelerometer and magnetometer of a smartphone. Critical elements of the **Comprehensive study** is shown in Table 6-2.

Recommendation for comprehensive test
4 routers
Medium room
LOS
Translational
Smooth wooden tiled floor
Accelerometer + magnetometer
Horizontal
Unix Timestamp
2 wheel encoders
Straight path

Table 6-2 Critical elements for Comprehensive study

It is our plan to map out our medium sized room and design a grid. This is important for managing room boundaries. With an assumption that both wheels travel at equal distances, sets of 50 iterations are carried out in two states – **stationary** and **moving**. We expect our system will be sufficient for estimating better position accuracy, and therefore, results are analysed using statistical and graphical evaluation methods.

6.7. Experiment Implementation and Results Analysis

In this section, we discuss how we implemented our experiment design. Our experiments were performed in two phases namely: Pilot test phase and Main test phase.

6.7.1. Pilot Test Phase

Pilot test phase investigates the performance of Wi-Fi related elements in the **first study** including testing for LOS and NLoS in a small sized room with one router. In particular, *experimental setup*, and *implementation procedure* are important to this phase. Results are critical for the main test. This is important because it determines LOS is best suitable for our system. This is discussed in 6.5.1.1. below.

Experimental Set Up

Investigations are conducted in a 480cm x 322cm room (*room 1*) with 1 router/APs at the University of Hertfordshire. Where we use one Samsung Galaxy Note 1 smartphone to collect RSSI signals from the one router at fifteen reference points (RP) as illustrated in Figure 6-2. The purpose is to investigate the dynamics of RSSI profiles in small-congested space in LOS and NLoS instances.

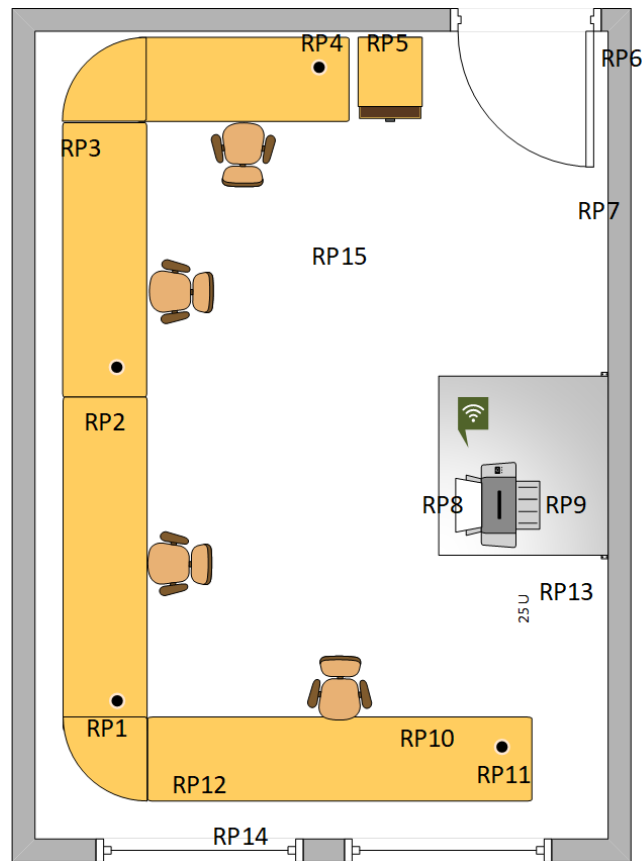


Figure 6-2 To scale representation of the test environment (room 1) for testing LOS and NLoS

It was expected the smartphone would pick up signals from nearby routers; therefore, it was important that we designed a system that will identify relevant router only based on its mac address. In our case, our smartphone picked up signals from over 23 different mac addresses.

We tested for performance of LOS and NLoS for our one identified router, and then analysed its influence on relative distance when Equation 5 is applied. This is discussed in the experimental procedure section.

Procedure

This section includes implementation procedure for LOS and NLoS in 480cm x 322cm room with 1 router/APs.

First, we designed an android application that listens and collects Wi-Fi signals from our one router only. Then, we calibrate the RSSI signal reading of the phone using the closest and furthest distance from the router. This is important to train the system on the difference between signal at the strongest point and at the weakest point. This is done in the online phase discussed in chapter 5.

Next, we placed the smartphone at the reference positions and collected readings with LOS and NLoS instances for one minute. Each reading collects an average of 4 RSSI signal data output per reference point per iteration. In our experiments, the average of the signal data output is used as final signal information to be processed.

The final signal is input into Equation 5 and calculated in our offline phase. This is important because it results in relative distances between router and smartphone in both LOS and NLoS instances.

In LOS instance, smartphone collected Wi-Fi signal data with a clear line of sight between it and the router. The RSSI data signal is collected at RPs 3 – 9, 13 and 15.

In NLoS instance, smartphone collected Wi-Fi signal data with interferences such as *computer monitors, CPU and humans*, between it and the router. The RSSI data signal is collected at RPs 1- 2, 10-12 and 14. Then, further investigations are conducted on NLoS instance RP 1 – 2 and 10 – 12 without interferences.

The results of the implementation for LOS and NLoS are discussed in the results and analysis section below.

Results and Analysis

The experiment was done to check the effects of LOS and NLoS of Wi-Fi signals on relative distance in a small-congested room with RP 1-15. Table 6-3 presents relative distance results gotten from RSSI after Equation 5 is applied.

We observed that LOS performed better than NLoS. This is in-line with our expectations during the design of the trials. Compared to LOS, the deviation of RSSI derived distance from the true distance is significant for NLoS. The true distance is measured between RP and router using a traditional measuring tape.

RSSI Derived Distance and Actual Distance Comparison Table

Reference point	RSSI derived distance (m)	True distance measurement (m)	Deviation from actual distance (m)	Instance
RP 1	0.93	4.8	3.87	NLoS
RP 2	0.73	2.84	2.11	NLoS
RP 3	3.7	4.1	0.4	LOS
RP 4	1.18	1.89	0.71	LOS
RP 5	0.96	1.46	0.5	LOS
RP 6	1.1	1.65	0.55	LOS
RP 7	0.27	0.43	0.16	LOS
RP 8	0.013	0.023	0.01	LOS
RP 9	0.06	0.12	0.06	LOS
RP 10	0.72	1.8	1.08	NLoS
RP 11	1.28	2.86	1.58	NLoS
RP 12	1.83	2.83	1	NLoS
RP 13	1.81	1.78	0.03	LOS
RP 14	1.66	4.03	2.37	NLoS
RP 15	0.71	1.1	0.39	LOS

Table 6-3 Distance accuracy deviation between true distance and relative RSSI distance estimates

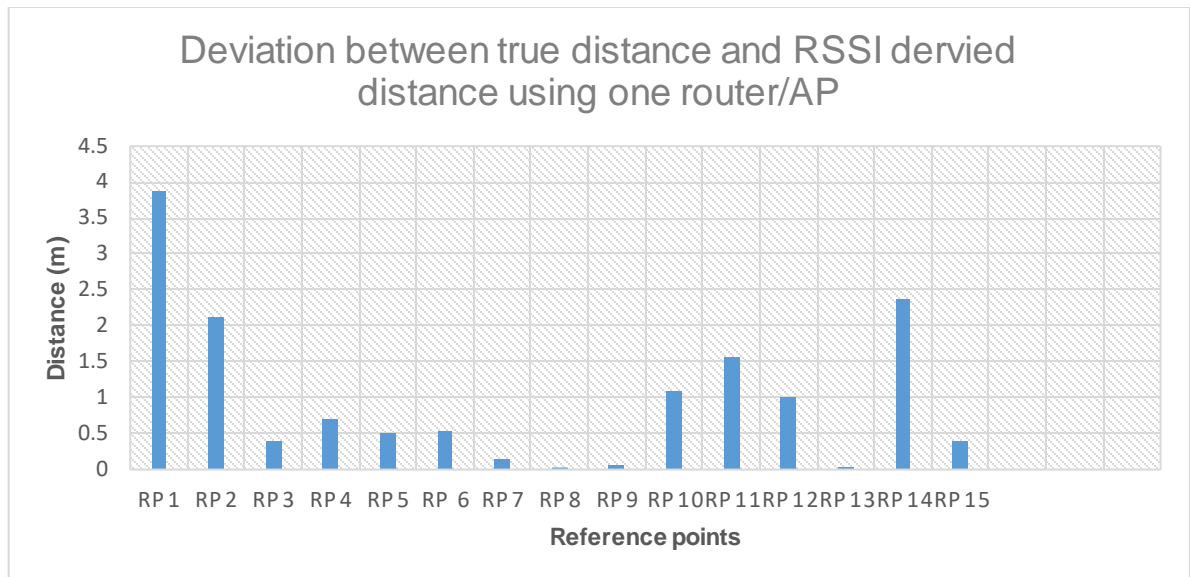


Figure 6-3 graphical analysis of dataset showing deviation of the estimated distance from the ground truth.

At RP 8, results are best because the smartphone is 0.023 m away from the router, in particular, in LOS instance with no interferences.

Results were worse at RP 1 when the smartphone was 4.8m away from the router. The poor result is because of the interference caused by a CPU blocking the line of sight. We expected an error from NLoS but this result is quite significant.

Human interferences are investigated at RP 2, with the smartphone 1.8m away from the router. One person constantly moved in-between RP 2 and the router. Thought the results are not as high as that of RP1, it is quite significant.

Our observations from the trial show that best results are gotten in LOS when the signal is strong and noise is almost non-existent. Table 6-4

Furthermore, it also proves that material in congested rooms significantly affects RSSI quality during propagation. The following below is true in this instance:

A1.	Strong signal - noise	=	High RSSI & high LQI	RP 7, 8, 9 and 13
A2.	Weak signal + noise presence	=	Low RSSI & low LQI	RP 1, 2, 11 and 14
A3.	Strong signal in a noisy environment	=	High RSSI & low LQI	RP 3, 4, 5, 6, 12 and 15
A4.	Strong noise	=	High RSSI & low LQI	RP 1, 2, 10 and 14

Table 6-4 LOS and NLoS influences based on RSSI and its LQI

A1 is the best result with small errors. This was observed to be true when SP was in LOS at less than a meter away from one router.

A3 showed good outcomes with moderate errors. This was observed when SP was in LOS at distances within 1m – 5m from the router.

A2 and **A4** displayed worse results with high errors. This was observed when SP was in NLoS at distances within 1m – 5m from the router. Most importantly, errors from less than 2m distances was caused by human interferences and inanimate objects like CPU and monitors. Therefore, NLoS introduces too many uncontrollable errors and therefore not suitable in the experimentation of our system noise as it is will affect the position accuracy of our system.

It is our observation that best results are from instances that fell within **A1** and **A3**. Therefore, our system will include only instances of **A1** and **A3** for Wi-Fi.

6.7.2. Main test phase

Main test phase tries out the designs from the **third, fourth and fifth studies**, plus the Comprehensive study. This test is performed with focus on the following:

- A medium sized environment (*room 2*)
- 3 versus 4 routers for best position accuracy using results **study 1 in focus test phase** specifically LOS in conditions **A1** and **A3**.
- A mobility scooter with two wheel encoders travelling in translational motion on a smooth wooden floor.
- Smartphone orientation and IMU combination of accelerometer, gyroscope and magnetometer versus our proposed accelerometer and magnetometer

The purpose of this main test is to investigate better position estimation using LOS in **A1** and **A3** conditions, navigation heading, smartphone pose, relative pose accuracy and position accuracy of our proposed WTP-HAMS system. It is our expectation that our proposed WTP-HAMS system will outperform representative literature works mentioned in 6.3, 6.4 and 6.5.

In particular, *experimental setup*, and *procedure* are critical in this phase. The outcomes are important for the experimentation of the system. This is important because the system relies on the design in the **Comprehensive study**. This is discussed below.

Experimental Set Up

Experiments were conducted in a medium-sized hall located within the University of Hertfordshire which is measured at 10.07m x 9m. The test environment is divided into a grid of 8 x 3 with 24 reference points (*see* Figure 6-4).

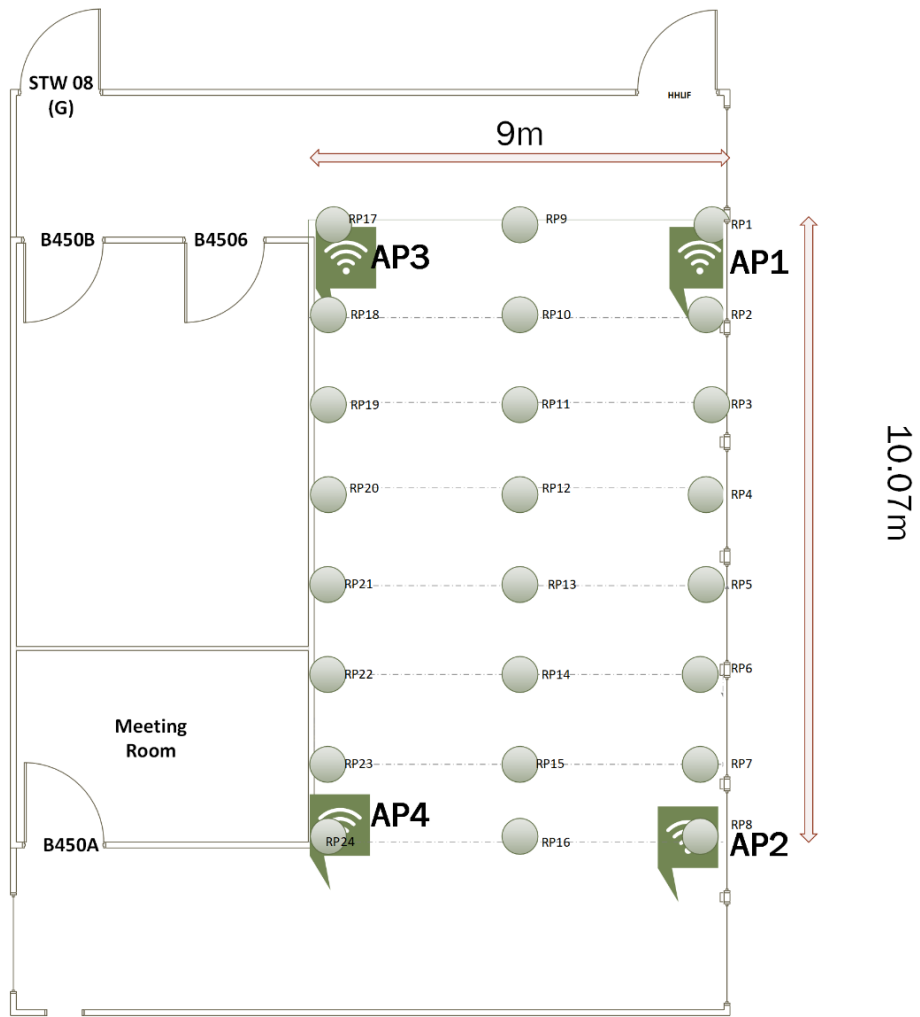


Figure 6-4 schematic map of the experimental site (room 2) and reference point distribution

Properties	Description
	Reference points
	Access points
	True vertical distances between references points
	True horizontal distances between references points

Table 6-5 representation table of the schematic map in Figure 6.2-3

Here, we use one Samsung Galaxy Note 1 smartphone to collect the following:

- RSSI signals from 3 and 4 routers
- Distance travelled from two wheel encoders
- IMU sensor data

The reason for using one smartphone is to guarantee consistency and consolidation of datasets. For our system, the following are expected:

- I. For position accuracy based on multi-trilateration, in instances of **A1** and **A3** our recommended 4 routers will outperform 3 routers
- II. For navigation heading, accelerometer combined with magnetometer will outperform SOTA in 6.4.1 which combines accelerometer with magnetometer and gyroscope
- III. For smartphone pose, horizontal will outperform vertical used in literature work mentioned in 6.4.2
- IV. For the relative pose, our proposed odometry model will outperform SOTA in 6.5.1 which uses traditional odometry
- V. For improved position accuracy, our proposed WTP-HAMS system will outperform results from literature works mentioned in 6.3, 6.4 and 6.5

We will test the performances of **I – IV** listed above, and, combine their results. We combined the results from **I – IV** because we need them to experiment with our proposed WTP-HAMS system, which is highlighted as **V** in the above. These are discussed in the implementation section below.

Procedure

This section contains experimental implementations for the above **I – V** expectations in the 10.07m x 9m medium-sized hall (*room 2*).

We tested the conditions and expectations in the five studies described in the strategy and planning stages.

Second study tested and compared position accuracy based on multi-trilateration from combined 3 and 4 routers.

Third study investigated for navigation heading using a combination of smartphone IMU modalities that includes accelerometer, magnetometer and gyroscopes.

Fourth study tried out horizontal and vertical orientations of the smartphone to prove smartphone orientation best for our system is horizontal orientation.

Fifth study assesses relative pose accuracy of our proposed odometry model, which includes our new drift mitigation model and results in the *fourth study*, which is the combination of accelerometer and magnetometer for navigation heading. These stages are further expatiated on below.

- **Second Study - Position Accuracy Based on Multi-Trilateration**

This stage follows recommendations from the **pilot test phase** by experimenting in **A1** and **A3** conditions. We compared position results from testing two-router configuration including *config 1* for *three routers* and *config 2* for *four routers*. The purpose is to prove 4 routers combined is better than 3 routers combined when finding position accuracy based on multi-trilateration.

Config 1 – Three Routers

In our test room, three known routers **AP2**, **AP3** and **AP4** from Figure 6-4 are selected. This is important because it is an appropriate representation of the SOTA. We then proceeded to collect Wi-Fi data from **RP1 – RP8** in a **stationary state**. The collected data was sent to the offline phase for multi-trilateration implementation.

We carried out at least 50 iterations at each reference point (RP) using a sampling rate of 1.5 seconds. In particular reference point 1 (RP1), because it did not have a close router within its range. Also, it served as best position comparable to that of four routers.

Results and Analysis of Config 1 – Three Routers

We considered the minimum, average and maximum values of the 50 iterations in our multi-trilateration calculations. It was our observation that the minimum values provided the best results.

Router	Router position x	Router position y	Router position x in m	Router position y in m	Actual distance	Estimated distance from multilateration (min values)	Estimated position at x	Estimated position at Y
AP2	7	1	10.07	0	10.07	14.4632	-2	-33.72
AP3	1	3	0	-9.07	9.07	10.02442299		
AP4	7	3	10.07	-9.07	13.55	7.554974945		

Table 6-6 Comparison table comparing true position to estimated relative position using three routers at RP1

The position outcome at **RP1** using three routers is $[-2, -33.72]$ at x and y coordinates as indicated in Table 6-5. Taking into account the ground truth of RP1 position, we calculated a position error is 9m using Euclidean distance between ground truth and estimated position. This result was similar when we conducted the same tests in the other 7 reference points.

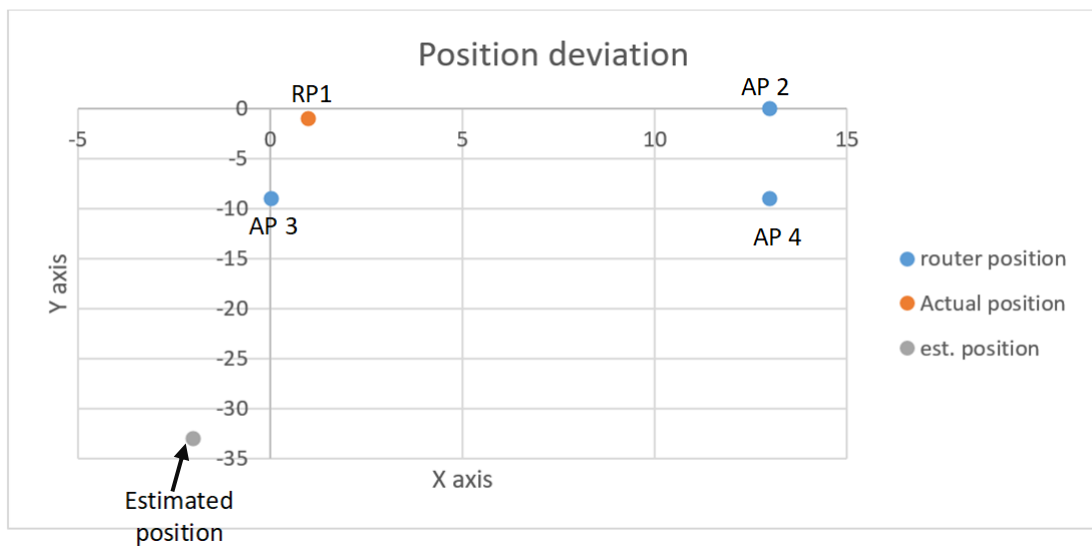


Figure 6-5 Graphical illustration showing deviation of estimated position from the true position in the test room with three routers/APs

It is our belief that this significant error occurred because signal data was insufficient. This was due to unavailability of close enough routers to correct the

other signals. Although we ensured room 2 was in LOS condition, we speculate that the signal loss of routers **AP2** and **AP3** negatively influenced our results. Therefore, it is our observation that the errors are because of LOS between routers **AP2** and **AP3**, and the smartphone fall within the instance **A2** (weak signal + noise presence) at when collecting reading at **RP1**.

Config 2 – Four Routers

In our test room, we used four known routers **AP1**, **AP2**, **AP3** and **AP4** from Figure 6-4 for our set up. This is important because it validates how 4 router combination is best for our system. Similar to **config 1**, we conducted at least 50 iterations at 1.5 seconds and collected Wi-Fi data from **RP1 – RP8** in a **stationary state**.

All collected data was sent to the offline phase for multi-trilateration implementation in Matlab (*see section 5.1.1.3 in chapter 5*).

When running the collected RSSI data through the multi-trilateration processes in Matlab, we tested the following for all samples from the 50 iterations per reference point: average, maximum values and minimum values.

Results and Analysis of Config 2 – Four Routers

First, we tested with the average, which resulted in a position error of 16.5m. Then, we tested with maximum values; this resulted in an error of 50.3m. Finally, we tested with minimum values, whose outcome was 0.5228m. These are shown in Table 6-7.

Position	Minimum values (m)	Average values (m)	Maximum values (m)
Error	0.5228	16.5	50.3
Rating	Best	Poor	Very poor

Table 6-7 Comparison table for RSSI min, average and max outcomes

Both average and maximum outcomes performed very poorly and therefore not suitable for our system. It is our recommendation that the average of the recurring minimum RSSI values be considered as its results have fewer errors.

Router	Router position x	Router position y	Router position x in m	Router position y in m	Actual distance	Estimated distance from multilateration (min_values)	Estimated position at x	Estimated position at Y
AP1	1	1	0	0	0	0.124577	1	-3
AP2	7	1	10.07	0	10.07	14.4632		
AP3	1	3	0	-9.07	9.07	10.02442299		
AP4	7	3	10.07	-9.07	13.55	7.554974945		

Table 6-8 Comparison table comparing true position to estimated relative position using four routers at RP1

Position accuracy result using minimum RSSI values from four routers is [1, -3] at x, y coordinates as indicated in Table 6-8. Taking into account the true RP position, we calculated a position error of 0.5228m with respect to the Euclidean distance between true position and estimated position.

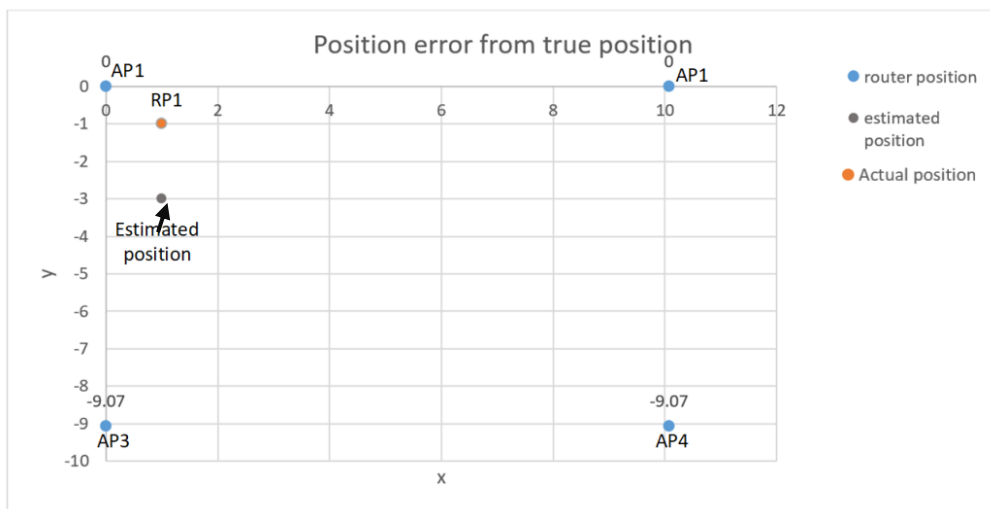


Figure 6-6 Graphical illustration showing deviation of estimated position from the true position in the test room with four routers/APs

This test proved our expectations to be true because four routers outperformed three routers in the same test environment shown in Figure 6-4.

Comparing our outcome from four routers to that of three routers, it is our observation that at **RP1, AP1** which falls within **A1 (*strong - noise*)** and it compensated for the lost signals from **AP2, AP3** and **AP4** which falls within **A3** (strong signal in noisy environment) instance based on results from the **first study**.

When compared to three-router configuration, our suggested four-router combination is best for our system because it ensured better position outcomes with Wi-Fi.

- **Fourth Study - Smartphone Orientation**

At this stage, we test to find the best orientation of the smartphone used in our experiments. This is important to our system because we want to design a practical system for the users. We considered two orientations including horizontal and vertical.

In horizontal orientation, we tested the smartphone orientation on two parts of the mobility scooter this included – the **arm** and the **floor** of the mobility scooter. It was expected that the **arm** would perform better because of its practicality.

In vertical orientation, the smartphone was held perpendicular to the ground with the screen directly facing the user. This was expected to perform poorly because of its impracticality.

Results and analysis of Fourth Study - Smartphone Orientation

In vertical orientation, with the smartphone in the user's hand, we observed that it was impractical and dangerous for the user to efficiently and successfully drive the

mobility scooter with just one hand. This is important because the safety of the user is critical, and, the uncontrollable jerking of the user's hand will negatively influence our results when calculating navigation heading in below.

In horizontal orientation, the **arm** and the **floor** of the mobility scooter were tested.

For the **arm**, the smartphone was placed on the arm of the mobility scooter in a horizontal orientation. This presented a much safer option when compared to holding the smartphone while driving. It was observed to play a critical role in supporting the calculation of navigation heading in . In particular, the padding on the **arm** cushioned vibrations experienced by the mobility scooter as it travelled across reference points.

For the **floor**, the smartphone was placed on the floor of the mobility scooter in the horizontal orientation. This presented itself to be an impractical and uncomfortable solution because the smartphone rested between the user's feet and will require the user to fully turn their head downwards to view smartphone screen when in motion. Also, the **floor** position was observed to have high errors because of the negative influences on the sensors, this was caused by user's voluntary and involuntary foot movements and vibrations from the mobility scooter in motion.

It is our recommendation that we place the smartphone on the **arm** of the mobility scooter when carrying out further experiments, especially navigation heading in the **third study**.

- **Third Study – Navigation Heading**

At this stage, we place the smartphone on the **arm** of our mobility scooter while we evaluated our proposed combination of accelerometer and magnetometer sensors. We compared our proposed combination with the SOTA recommendation of combining accelerometer, gyroscope and magnetometer sensors. This was important because we are calculating for navigation heading of a smartphone placed on the mobility scooter travelling on a smooth wooden floor.

We already expect that accelerometer only, magnetometer only and gyroscope only will be insufficient for heading navigation. This is because of the following –

- Accelerometer only calculates for acceleration and rotation of the phone
- Gyroscope only calculates for rotation of the phone
- Magnetometer only calculates for direction

During our experiment, the smartphone was placed in horizontal orientation on the handle of the mobility scooter with its screen facing upwards. This is important because it was the most practical position to place the phone in real life situations.

We experimented for noise analysis of each IMU sensor using our android application discussed in 5.1.1.1. The application measured sensor values from the Samsung Galaxy note 1 inbuilt IMU sensors (accelerometer, gyroscope and magnetometer) every 30ms for exactly four minutes in **stationary** and **moving** instances.

In stationary instance, we collected over 4000 datasets from one iteration with the mobility scooter staying in just one RP over a period of four minutes. It should be known that at least 50 iterations were carried out at each RP.

In moving instance, we collected over 5000 datasets from one iteration with the mobility scooter moving from one RP to another over a period of four minutes. Similar to stationary instance, at least 50 iterations were carried out for each travel between RPs.

Results and analysis of the Third study – Navigation Heading

This was important to analyse data noise from each IMU sensor in stationary and moving instances. Also, it was critical we compare outcomes from combining all three IMU sensors with our proposed magnetometer and accelerometer combination for heading navigation.

Stationary Instance for Each IMU Sensor

As expected, IMU sensors are quite accurate when in a stationary instance. The magnetometer measures values related directly to the orientation of the smartphone, but the accelerometer and gyroscope do not receive input. However, the z-axis of the accelerometer is influenced because of its gravity component. This is a response to its inertial frame as indicated in the representative graph Figure 6-7.

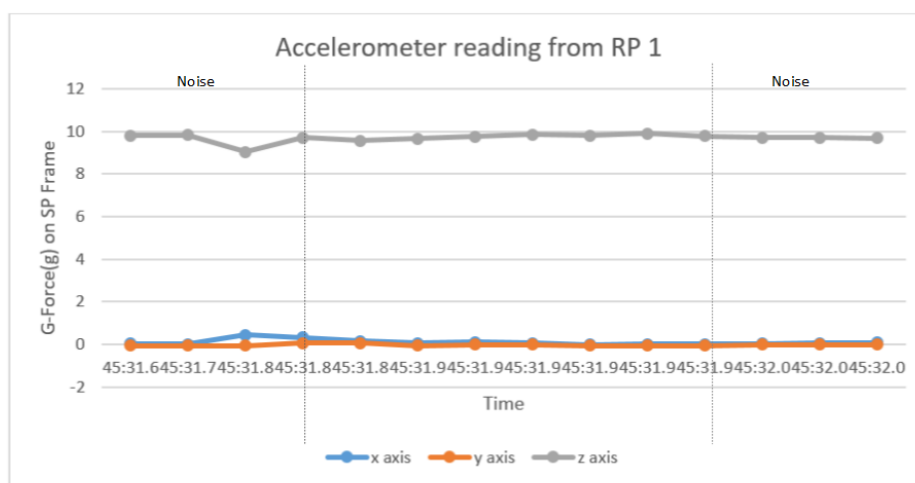


Figure 6-7 Accelerometer measurements indicating inactivity when SP is stationary

Moving Instance for Magnetometer, Accelerometer and Gyroscope

In this test, the mobility scooter travelled 1.98m from **RP1** to **RP8**. We evaluated results from magnetometer, gyroscope and accelerometer sensors. Magnetometer only was not considered in the experiments because it is expected it will analyse reference direction towards gravity. However, it was our observations that data values from the gyroscope and accelerometer sensors contained too much noise.

Gyroscope Only

Gyroscopes are known to suffer from drift (see chapter 2); therefore, we tested the system with drift eliminated gyroscope outputs in Figure 6-8. The results show how SP rotates about its axis but does not provide enough information to determine heading direction. Instead, the results are observed to be unsatisfactory as they exhibited an output frequency spectrum with significantly increased amplitudes and noise.

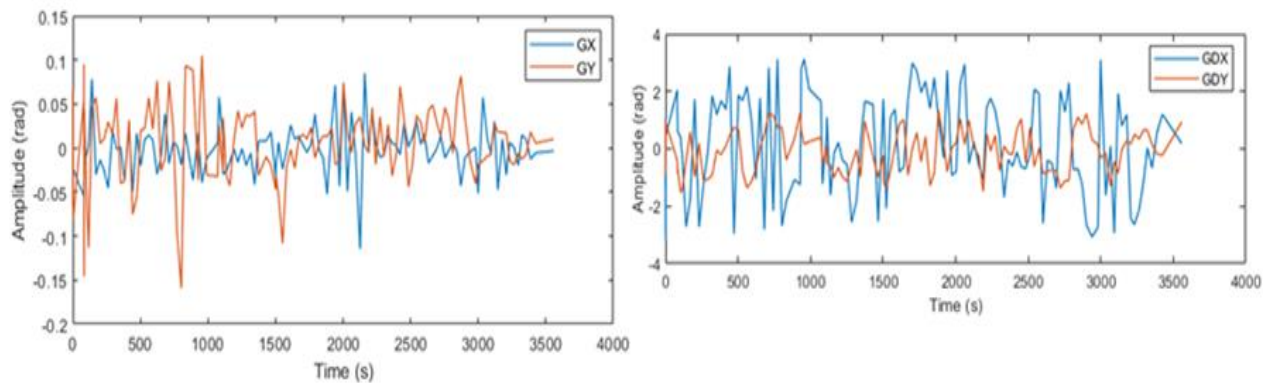


Figure 6-8 gyroscope (G) and drift eliminated gyroscope (GD) output frequency spectrum with high amplitude and noise

Accelerometer Only

Accelerometer sensors only are expected to show cyclical changes in pedestrians as true peaks are used in SOTA calculations. However, our experiments showed a frequency spectrum with multiple high amplitudes and noisy vibrations smartphones experienced during **moving instance**. Although this outcome was unsatisfactory, we were able to observe that it identified the axis the smartphone was orientated towards.

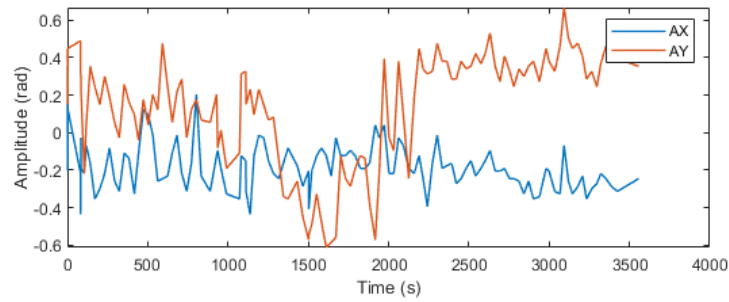


Figure 6-9 Accelerometer output frequency spectrum with high amplitude and noise

Therefore, it is our proposal that the advantage of accelerometer in identifying smartphone orientation be combined with the advantage of magnetometer in measuring direction.

Combining Accelerometer with Magnetometer

Accelerometer identifies the orientation of SP in relation to SP frame and magnetometer provides orientation in relation to earth magnetic fields. The combination of both sensors aligns the behaviour of SP on the mobility scooter as it travels in different directions in relation to the earth's magnetic field. Results of our experiments are promising as it shows 95% accuracy with 5% error caused by vibrations influencing SP orientation. The results show electromagnetic influences on the Y-axis of SP (indicated as **AMY**) as the mobility scooter at 90°.

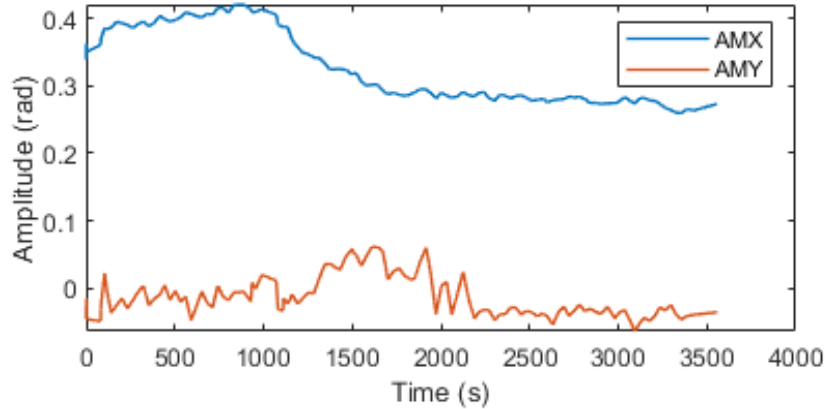


Figure 6-10 Frequency spectrum of fused accelerometer and magnetometer sensors demonstrating travel over time

The frequency spectrum of our fusion (*demonstrated in Figure 6-10*) is more favourable when compared to output from accelerometer only or gyroscope only in Figure 6-9 and Figure 6-8 respectively. It is our observation that the proposed combination of accelerometer with magnetometer drastically reduced noise and amplitude levels experienced in accelerometer. Thereby producing more accurate heading information of our SP mounted horizontally on a mobility scooter travelling at 90°.

We compared the SOTA combination of all IMU sensors with our proposed combination of accelerometer with magnetometer only in our test environment. Although we expect that the SOTA integration with gyroscope sensor value will not favour our system, we still tried it out to result in Figure 6-11.

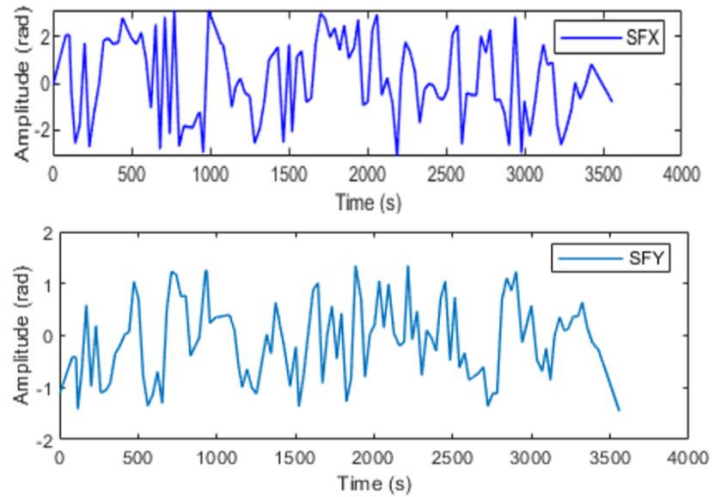


Figure 6-11 Sensor fusion outcome on x and y-axis of the smartphone (SP)

The results from the combination of all IMU sensor value are indicated as SFX and SFY in our experiments. It is our observation that the output datasets are impracticable as they exhibit hypersensitivity of the system. This hypersensitivity induces errors and therefore, is not best for our system.

Compared to **SFY**, **GDY**, **AY** and **GY**, our proposed **AMY** performed better because it exhibited significantly reduced amplitudes and noise in the frequency wavelengths. This is important because it provided more accuracy heading values. This is shown in the comparison displays Figure 6-12.

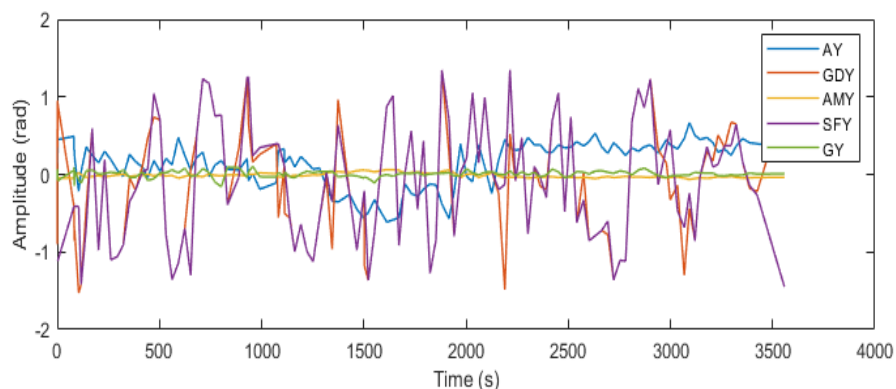


Figure 6-12 Accelerometer and magnetometer combination (AMY) is best for deriving heading direction in our system

- **Fifth Study - Relative Pose Accuracy**

Two wheel encoders are designed and installed on both wheels of the mobility scooter. Our test begins with the mobility scooter at an initial position set as $[0, 0]$ at the x and y corner of the room. We then proceeded to calculate for travel distances using the tick counts of both wheels as they rotated past both wheel encoders when the mobility scooter travelled from the corner of the room in a straight line to reference points.

In our test, the measured diameter of the wheels is 60cm, which is equivalent to one complete rotation when a tick is read by the wheel encoder sensors.

In this study, we tested four situations –

- Calculating travelled distance from the wheel encoders
- Calculating relative pose from SOTA using two wheel encoders
- Improving travelled distance of SOTA using our proposed new drift mitigation model
- Using our novel odometry model to get improved relative pose accuracy

The above test situations are grouped as *APA centred test* and *APA main test*, where,

APA centred test centred tests on travelled distances from the wheel encoders and implementation of relative pose computation from literature.

APA main test focused on trials using our proposed new drift mitigation model and novel odometry model. This was important to improve travelled distance and relative pose accuracy.

APA Centred Test – Travelled Distance and Relative Pose According to Literature

We carried out at least 50 iterations of the mobility scooter travelling between each reference points (RP) and from the start point to end point using a sampling rate of 30ms. At the start point, the travelled distance was set to be 0 cm. Travelled distance is observed to be accurate when mobility scooter travels in a straight line for a short period of time. However, drift sets in when mobility scooter starts to travel for longer periods of time.

It was our observation that error set in when the mobility scooter moved from the start point and increased steadily as the mobility scooter travelled across the smooth wooden tiled floor to the endpoint.

Results and analysis of Fifth study - APA centred test

We considered the reoccurring minimum and maximum distance estimates and observed that for a total travelled distance of 10.07m, there was a 2.87m error with 7.2m as its minimum distance travelled and an error of 1.07m with 9m maximum distance travelled. These are shown in Table 6-9

Actual distance from start point	Estimated distance travelled from start point wheel encoders	
	min	max
1.98	1.8	1.8
3.68	3	3.6
5.33	4.2	5.4
7.01	6	7.8
8.7	6.6	8.4
10.07	7.2	9

Table 6-9 minimum and maximum travelled distance from the start point to endpoint

We observed consistency in the values for min and max distance travelled estimates.

When all travelled distance outcomes including min and max values were used in Equation 1, Equation 2 and Equation 3 from literature, to calculate the relative pose of the mobility scooter, there was high position inaccuracy. This was due to the steady growing drift.

As expected, we observed that the system demonstrated a moving average drift of 19% percentage error when considering lower estimated travel distance values from the start point, 6.32% percentage error when considering higher estimated travel distance values from start point and 12.8% percentage error when considering the average of estimated travel distance values from the start point. This is shown in Table 6-10

Actual distance from start point	Percentage error		Average percentage error
	min	max	min and max
1.98	9.1	9.1	9.1
3.68	18.5	2.2	10.35
5.33	21.2	1.3	11.25
7.01	14.4	11.3	12.85
8.7	24.1	3.4	13.75
10.07	28.5	10.6	19.55
Moving average	19.3	6.316666667	12.80833333

Table 6-10 Comparing percentage error of drift for travelled distance considering the minimum, maximum and average values

The moving average of the maximum percentage error is significantly lower than that of the minimum percentage error and average percentage error.

This shows that maximum values perform best and will be best appropriate in our proposed new drift mitigation model and novel odometry model.

APA Main Test – Our Proposed New Drift Mitigation Model

We tested out our proposed new drift mitigation model and novel odometer model using outcomes for maximum reoccurring values. Our designed simple drift mitigation model in Equation 19 is applied. In our test, we measured a distance eD_x by driving the mobility scooter from one reference point to another. This was important to get the new estimated travelled distance.

Then, we added the new estimated travelled distance to our maximum percentage error $Err_x\%$. This was important to produce improved distance estimates $Dist_R$.

Results and analysis of APA main test – our proposed new drift mitigation model

The results from using the new drift mitigation model displayed a 5% maximum improvement in the drift with the observation that in a travelled distance of 10.07m, the new estimates from minimum is 7.49m and 9.1m from the maximum. These are displayed in Table 6-11.

Actual distance from the start point	New drift mitigation model			
Accumulated	min	max	average percentage error (min)	average percentage error (max)
1.8	1.89	1.89	1.89	1.89
3.68	3.19	3.62	3.1	3.7
5.33	4.4	5.4	4.31	5.51
7.01	6.14	7.91	6.13	7.93
8.7	6.84	8.4	6.74	8.53
10.07	7.49	9.1	7.4	9.2

Table 6-11 Results showing improved travelled distance using our drift mitigation model for minimum, maximum and average travelled distance estimates

We detected that our new drift model presented more accurate result close to actual distance when maximum values were considered. This was essential in providing a

controlled robust model, which effectively improves the system through drift mitigation, and estimates better travelled distances, especially in instances where distances travelled are larger.

APA Main Test – Novel Odometry Model

We tested for improved relative pose accuracy of the mobility scooter using our proposed novel odometry model, which included the combination of maximum travelled distance from our proposed drift mitigation model on wheel encoder outputs with results from our proposed combined accelerometer and magnetometer sensors of the smartphone. This is achieved using Equation 21 and Equation 22.

This is important for the following -

- For new drift mitigation model to get initial and subsequent distances closer to ground truth for the mobility scooter
- For proposed combined accelerometer and magnetometer outputs (**AMY**) to provide orientation and navigation heading for smartphone and mobility scooter.

When we tested, we observed that navigation heading results from the combined accelerometer and magnetometer outputs contained a small amount of noise. We considered applying moving average filter using Matlab default of 2 spans, and our suggestion of 20 and 50 spans.

Results and Analysis of APA Main Test – Novel Odometry Model

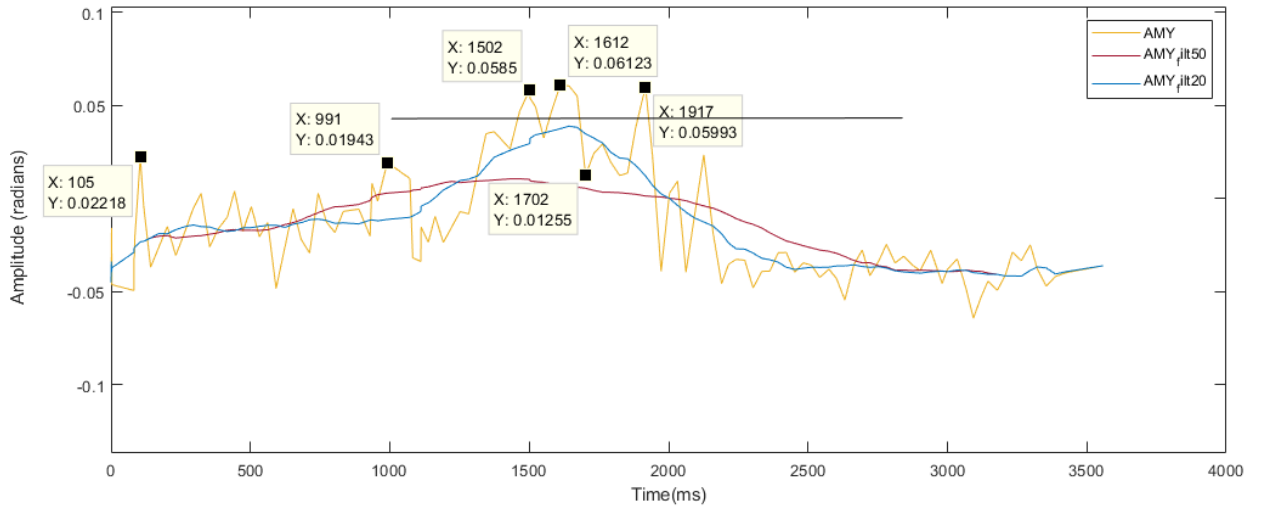


Figure 6-13 FWHM applied to AMY frequency spectrum identifying acceleration, change and deceleration

Matlab 2 span and 20 spans were unsuitable for our test because it displayed multiple peaks which make the frequency spectrum difficult to use by FWHM as shown in Figure 6-13.

We chose to reduce the noise by smoothing the frequency spectrum by 50 spans moving average filter. This was selected because it retained the resolution of the system while averaging every 50 samples to result in 50% noise and amplitude reduction. This provided better results for FWHM to work with as demonstrated in Figure 6-13.

FWHM is important because it synchronises new maximum travelled distance estimates $Dist_R$ with **AMY** to enable the system to identify acceleration, change and deceleration of the heading navigation over a new travelled distance $Dist_R$.

Then we calculated for relative pose using our proposed novel odometry model which combines Dist_R and **AMY**.

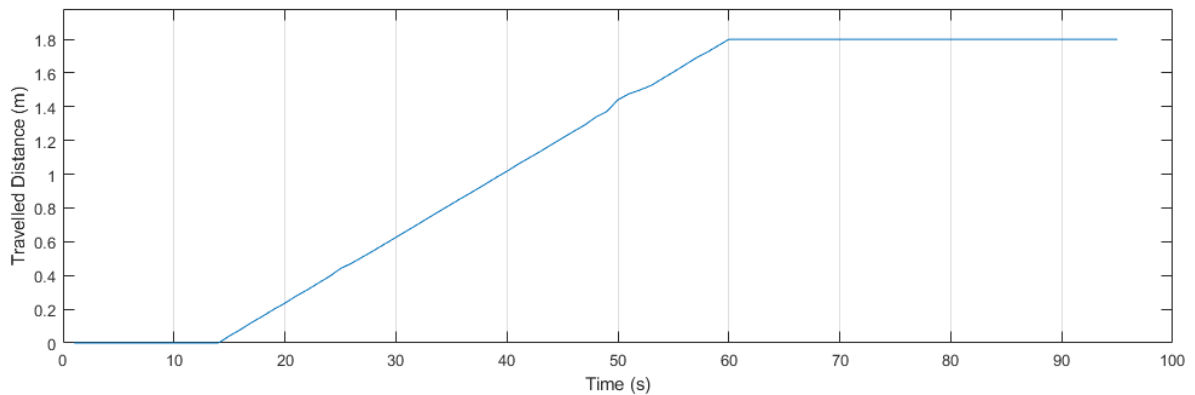


Figure 6-14 Relative pose accuracy using our proposed novel odometry model

We observed that the high sampling rates of **AMY** corrected our heading navigation error by resetting the system to read from a new position for 30ms only. Each sample session is completed before commencing with a new session.

The result of applying our proposed novel odometry model is a cumulative error of 4% between reference points. Compared to literature by J. Zolghadr and Y. Cai [176] that results 33cm and 51cm pose error, our tests demonstrate an average error of 9cm which is an improved relative pose.

- **Comprehensive Study - System Assessment Of Methodology (Proposed WTP- HAMS System)**

We proposed to combine the results and error shapes based on results from *config 2 – four routers* in the **first study** with results from *APA main test – novel odometry model* in the **fifth study**.

Here, we tested the whole system using 50 iterations between each reference points. In a live environment, we placed the smartphone on the arm of the mobility scooter and travelled between the reference points. The smartphone collected and

consolidated data gotten from smartphone modalities including accelerometer and magnetometer, Wi-Fi and two wheel encoders. These are done in an online phase, discussed in section 5.1.1.1.

The system proceeds to implement the following considerations and results from the previous five studies when conducting the comprehensive study.

- **First study** – LOS in **A1** (strong signal - noise) and **A3** (strong signal in a noisy environment) instances
- **Second study** – config 2 (four routers) for better absolute position
- **Third study** –**AMY** for navigation heading
- **Fourth study** – horizontal orientation
- **Fifth study** – proposed novel odometry model for improved relative pose accuracy

All the collected data and calculations are done in Matlab during the offline phase discussed in section 5.1.1.3.

The system assessment includes the combination of all the stages, especially the combination of the error shapes from **second** and **fifth studies**. The **second study** uses config 2 (four routers) to cast a circular error shape and the **fifth study** uses the proposed novel odometry model to result in a triangular error shape in our experiments. We used Matlab to calculate the centroid of the error overlap, which is the new absolute position (see Figure 6-15).

Results and Analysis of Comprehensive Study

The result from our proposed WTP-HAMS system in room 2 is a new and improved absolute position of 1.35 at x and -2 at y with an average error range of 0.35m – 1.35m (illustrated in Figure 6-15).

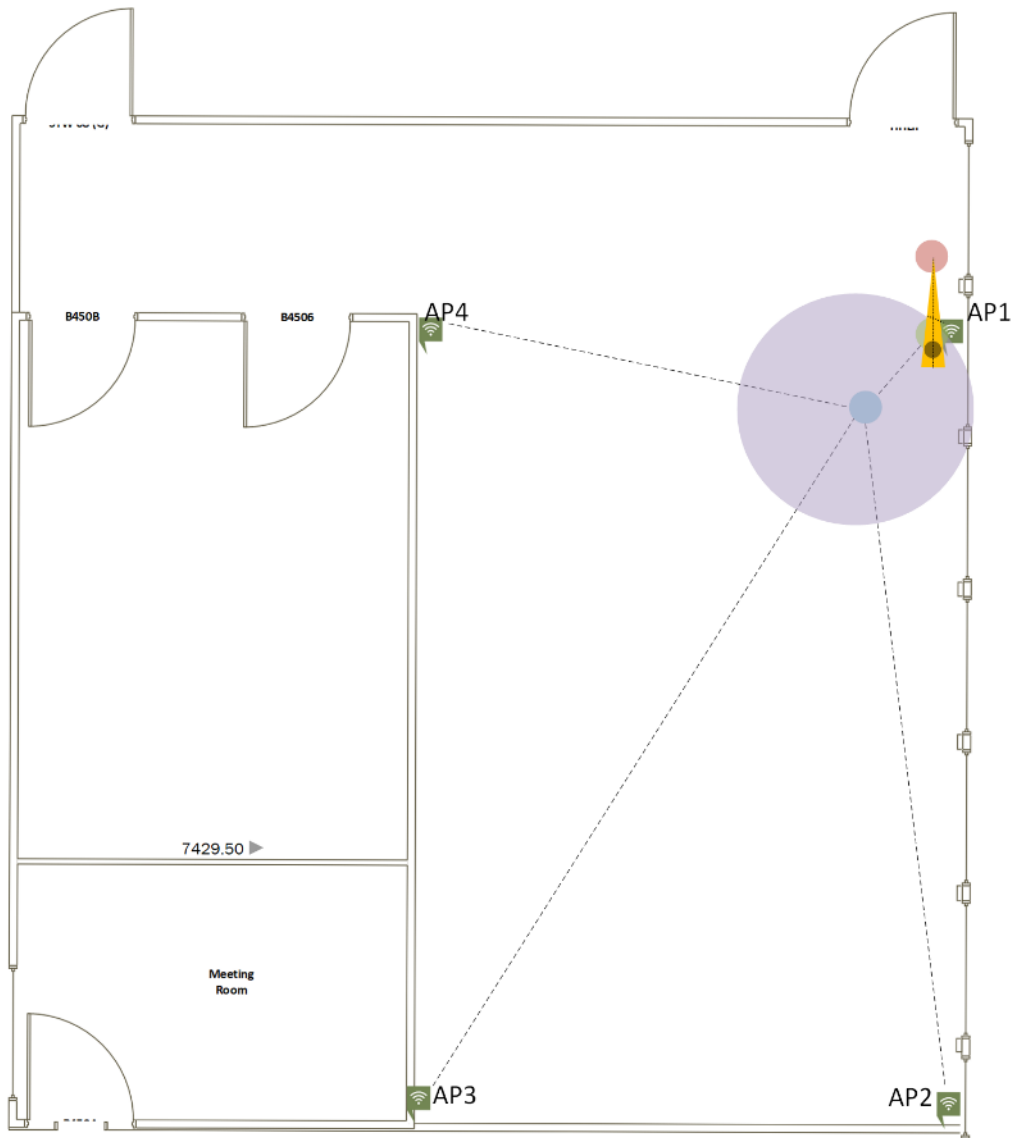


Figure 6-15 Proposed WTP-HAMS system showing improved localisation for the mobility scooter with a mounted smartphone in horizontal orientation with LOS in room 2

Representation	Description
	Ground truth RP1
	Relative Pose using our proposed odometry Model (Fifth study)
	Estimated position using Config 2 – four routers (Second study)
	Estimated position error from Config 2 – four routers (Second study)
	Estimated new absolute position using our proposed WTP-HAMS system (comprehensive study)
	Estimated position error from our proposed new odometry model (Third & Fourth studies)

Table 6-12 Descriptive table for Figure 6-15

Using on our comprehensive study, we compared the results of WTP-HAMS system to the results in our **second - fifth studies** as shown in Table 6-13.

Technique	Purpose	Outcome		
		x	y	Error
True position/ground truth	N/A	1	1	0
Estimated position using Config 1 –three routers (Second study)	Position estimation based on RSSI	-2	-33.72	9m
Estimated position using Config 2 –four routers (Second study)	Position estimation based on RSSI	1	-3	0.5228m
Proposed navigation heading (Third and Fourth study)	Heading and direction based on accelerometer and magnetometer	N/A	N/A	5%
Proposed new drift mitigation model (Fifth study)	Distance travelled based on wheel encoders	N/A	N/A	9.20%
Proposed novel proposed odometry model (Fifth study)	Relative position estimation based on a combination of proposed new drift mitigation model and proposed navigation heading	0.9	-2	4%
Proposed WTP-HAMS system (Comprehensive study)	Improved absolute position	1.35	-2	0.35m – 1.35m

Table 6-13 Results of all proposed studies to achieve improved position accuracy using our proposed WTP-HAMS system

In the instance of LOS in room 2, our proposed WTP-HAMS system performs better than the other five studies. This is because it results in position estimation closest to the ground truth.

Comparing Results of Comprehensive Study with Second Study Only

We observed that our WTP-HAMS system improved the results of the **second study** by about 96.2%. Comparing results from our proposed WTP-HAMS system to the **second study**, we calculated an error range of 0.35m -1.35m in our comprehensive study using our proposed WTP-HAMS system, while for the **second study** we calculated an error of 9m using config 1 of three routers and an error of 0.5228m error using config 2. As expected, config 2 outperformed config 1. This is because

config 2 has a sufficient number of routers to mitigate errors caused by signal loss, noise or poor propagation.

Although results from config 2 outperform config 1, it is still limited in its LOS instances of **A1** (strong signal - noise) and **A3** (strong signal in a noisy environment). Therefore, it can have bigger errors if applied in environments in **A2** (weak signal + noise presence) and **A4** (strong noise) instance.

Considering the best error result 0.35m of our proposed WTP-HAMS system, we calculated an error difference of 8.65m using config 1 and 0.1728m using config 2. Considering the worst error result 1.35m of our proposed WTP-HAMS system, we calculated an error difference of 7.65m using config 1 and 0.8275m using config 2.

Analysing the error differences between the best and worst error results it is our recommendation that four routers combination is best.

Comparing Results of Comprehensive Study with Fifth Study Only

As previously discussed, the **fifth study** combines results from **third** and **fourth studies** to result in a 4% error when in motion state and *APA main test - novel odometry model* is used.

The error in the **fifth study** is smaller than that from the **second study**. It is observed to demonstrate more accurate results because of the 95% accuracy of heading navigation that proposed the combination of accelerometer and magnetometer, and also, the 9.20% error simple drift mitigation model we proposed mitigates for every 10.07m travelled.

As expected our proposed novel odometry model with 4% error outperformed SOTA whose error was 33cm – 51cm. We suspect referenced literature work had small error because they experimented in areas with small dimensions.

The result from our proposed novel odometry model in the **fifth study** is very promising and it is used to correct the results from config 2 in the **second study**. This correction happens when results including error shapes of both **second** and **fifth studies** overlap in our proposed system.

Our proposed WTP-HAMS system has an error range of 0.35m – 1.35m, which from our observations is better than the 4% error the proposed novel odometry model results. Analysing the results from the proposed novel odometry model, we calculated the WTP-HAMS system's improvement on it by 25%.

6.7.3. Summary of Comprehensive Study Findings

In conclusion, position results from the **second study** only and **fifth study** only do not provide high accuracy when compared the results from our **comprehensive study** (our proposed WTP-HAMS system). Our proposed WTP-HAMS system outperformed the **second** and **fifth studies** in position accuracy.

We observed that our WTP-HAMS system not only provided better position accuracy, it also improved results of the **second study** by about 96.2% and, also improved results of the **fifth study** by about 25% (as shown in Table 6-14).

Proposed WTP-HAMS system	Position improvement
Improved RSSI based position results in Second study	96.20%
Improved our proposed novel odometry based results in Fifth study	25%

Table 6-14 WTP-HAMS system improvement on RSSI and odometry

6.7.4. Overall Results and Analysis

We assessed the methodology of our WTP-HAMS system and validated its feasibility in live environments.

Comparing our results to that of representative literature (shown in Table 6-15), it is evident that our system performs better.

Technology/System	Description	Accuracy error
RSSI [14] [64] [65]	Nine Wi-Fi routers/APs	1.5m – 3.1m
IMU + MILPS [145]	IMU includes three axial accelerometer, gyroscope, magnetometer and a digital pressure sensor	1-2m
	MILPS consists of three magnetic coils	
Odometry only [19]	Synchro Drive Robot	3m - 5m
Odometry + IMU [109]	Two Roomba robot with two wheel encoders each	0.33m and 0.51m
	IMU includes accelerometers, gyroscopes and magnetometer	
Proposed WTP-HAMS system which include RSSI + odometry + IMU	First study (LOS instance)	N/A
	Second study (config 2 - four routers)	0.5228m
	Third and fourth study (Proposed navigation heading including combined accelerometer and magnetometer of smartphone modalities in horizontal orientation)	5%
	Fifth study (Proposed new drift mitigation model)	9.20%
	Fifth study (Proposed novel proposed odometry model)	4%
	Comprehensive study (combine results from all five studies)	0.35m – 1.35m

Table 6-15 Comparing WTP-HAMS to literature works

For our system to perform effectively and result in a low position error of 0.35m – 1.35m, it must adhere to the descriptions shown in Table 6-15 above. In particular,

- The combination of four routers in LOS instance under conditions **A1** (strong signal - noise) and **A3** (strong signal in a noisy environment). This is important to get good position estimates with an error of 0.5228m.
- The combination of accelerometer and magnetometer outputs of a smartphone in a horizontal orientation. This provided a high heading navigation accuracy of 95%.
- Proposed simple new drift mitigation model, which improved drift in distance by 5% when error percentage $Err_x\%$ is added to raw travelled distance estimates. In our case, we added maximum $Err_x\%$ to result $Dist_R$.
- Proposed novel odometry model, which combined $Dist_R$ with the outcome from heading navigation to result in a 4% position error.

Chapter 7 Conclusion and Future Work

The chapter summaries our proposed investigations. In particular, our proposed novel WTP-HAMS system, which combines techniques from literature with proposed novel techniques to improve indoor position accuracy in representative environments used in care homes. It highlights improvements to standard techniques with details on the investigational test and corresponding results. This chapter presents the conclusion and feasible future research directions. Contained in this chapter a summary of the content of each chapter, briefly describing the novel contributions. Furthermore, this chapter outlines the deductions made from obtained results, justifying experimentations conducted. Finally, it expresses views on further work and future direction of this research.

7.1. Thesis Summary

Efficient, cost-effective and accurate indoor localisation is an area of high demand. Some of the key motivations and fundamental to its development are health care, security, navigation and assisted living for elderly persons and persons with mobility impairment who use mobility scooters. The research in this thesis aspires to target these motivations by exploiting ubiquitous technology, improving current methodologies in RSSI and odometry based localisation, and combining both improved methodologies. The goal is to provide a convenient and scalable approach to indoor localisation. Chapter 1 concisely defines the problem domain, which supports the research drive to enhance the current state of the indoor localisation, facilitating the combination of technologies – Wi-Fi, wheel encoders and accelerometer and magnetometer to improve position accuracy error.

Chapter 2 provides background knowledge to on localisation as it discusses current technologies, techniques and methods adopted for localisation purposes. It described the categorisation of localisation, their objectives and propagation methods. This chapter discusses communication protocols as it introduces indoor localisation and various filtration algorithms and models adopted for the research.

The chapter discusses the technologies and techniques used for this research. The chapter defines the terminologies used throughout the thesis

Chapter 3 expands on the indoor localisation. It emphasises on the current state of the art for indoor localisation, describing emerging architectures, complementary technologies and protocols relating to sensor combination for indoor localisation. It explains the challenges faced when identifying tracked objects to precision. The gap in catering to the target audience is demonstrated in the chapter. It demonstrates how state of the art implement methods, technologies and techniques discussed in chapter 2 to achieve indoor localisation. The chapter presents original categorisations as it analyses the most recent relevant state-of-the-art systems, methodologies and techniques that exhibit high localisation accuracy results. It goes on to define indoor localisation challenges within each category and also identify the advantages of the new category. This chapter discusses the most relevant technologies and techniques used for this research.

Chapter 4 presents a comprehensive description of our methodology, which is a proposed novel TT based hybrid localisation solution, WTP-HAMS system designed for this research. The emphasis is on the accuracy, cost-effectiveness, scalability and robustness of indoor localisation. The chapter commences by outlining the objectives of the WTP-HAMS and its technology requirements in terms of power usage, measurement properties and data transmission. It goes on to discuss the hardware and software components necessary for realising the object of this research. The drive for cost-effectiveness encouraged the exploration of ubiquitous technologies. The necessity for accuracy, scalability and robustness encouraged a novel system involving an innovative combination of existing techniques with one original model and one original technique. Existing techniques include SDRS path-loss shadowing model, triangulation, accelerometer and magnetometer fusion model, odometry. The existing techniques determine relative distances, positions and direction while the original model is the drift mitigation model to improve relative travelled distance and the original technique is the combination of accelerometer and magnetometer fusion model, and odometry to improve pose

with relative position. Therefore, this chapter proposed a new drift mitigation model, a novel odometry model and a unique system that combines RSSI outputs with the estimates from the proposed novel odometer model to get new position estimates. These are thoroughly described with equations and diagrams. It then summaries our unique contribution to knowledge. Finally, the design of our research development plan.

Chapter 5 explains the implementation of techniques and methods described in chapters 2 and 3 as it is used in developing the novel WTP-HAMS that is discussed in chapter 4. This chapter expatiates on WTP-HAMS system as it discussed the combination of techniques in the system architecture and conceptual flow. This is thoroughly defined with the use of flow charts justifying the use of certain techniques and models based on the overall system performance. It explains the system behaviour and development process with respect to technologies used. In particular, Wi-Fi, wheel encoders, accelerometer and magnetometer. It includes the designing and development of the implemented mathematical models need to achieve estimated relative position using RSSI, pose estimation with relative position using odometry and improved estimated absolute position. All supported features of WTP-HAMS are described in this chapter with respect to functionalities, modes of operation and expected outcomes at online and offline phases.

Chapter 6 presents an in-depth description of studies conducted to achieve the overall aim of the research, which is a reduced position accuracy error. The chapter analysis the purposed system, WTP-HAMS as it is examined in two test environments – small-congested room and medium sized room. In particular, it discusses focused and comprehensive studies, which were important in identifying the right conditions required for our proposed WTP-HAMS system to achieve its improved position accuracy. It evaluates and analyses the outcomes of each study, especially in the two test environments. Also, limitations of the SOTA is tested and mitigation models are proposed to address the limitations. These include,

- Position errors larger for 3 routers as opposed the 4 routers.

- Proposed new drift mitigation model to produce better-travelled distance estimates
- Proposed novel odometry model to produce better pose estimates, as opposed to traditional odometry model
- Unique error combination that considers the centroid of error overlap from position estimate from RSSI and Proposed novel odometry model to be the new position

The chapter then makes another assessment that justifies WTP-HAMS system. This is the trails of the proposed system in room 2 with expected outcomes. Finally, the chapter analyses each study as it discusses and compares the position improvement of our proposed investigation to the state of the art. This is important because, the objective for proposing WTP-HAMS system is to achieve a cost-effective, accurate positioning system that consumes low power due to its lightweight computation process. Furthermore, the proposed WTP-HAMS system demonstrates how odometer can improve RSSI positioning estimate.

7.2. Outcomes

WTP-HAMS is a cost-effective novel system that exploits a combination of ubiquitous technologies including four Wi-Fi routers/APs, two wheel encoders mounted on the two rear wheels of a mobility scooter and smartphone modalities such as accelerometer and magnetometer to reduce position get improved position accuracy in a room.

Wi-Fi is advantageous due to its capability of providing position estimates with reference to room. This research combines four Wi-Fi routers/APs instead of three Wi-Fi routers/APs because it gives better position estimates with smaller error radiuses. Although the combination of four routers/APs estimates favourable positioning information, its outcome was insufficient because of its high position errors caused by signal shadowing effects and NLOS respectively. Signal shadowing effect is mitigated in the SDRS log-normal shadowing model [64] and NLOS is better

managed with the good placement of the smartphone in clear visibility from the router. Still, Wi-Fi is insufficient; therefore, complementary technologies including two wheel encoders, and, fused accelerometer and magnetometer technologies are employed to improve position accuracy.

The ubiquity of Wi-Fi, accelerometer and wheel encoders has encouraged researchers to exploit the technologies for indoor localisation purposes. These technologies are popular in localising target objects within a building. Although Wi-Fi is popular, state of the art exploration of the technology demonstrates the limitations in Chapters 2 and 3. These limitations stem from Wi-Fi high sensitivity to interferences. Discussed in chapter 3, are studies aiming to mitigate Wi-Fi sensitivity by introducing additional filtration and predictive elements that require complex computations. Unlike the state of the art that employs Kalman filtering on estimated positions derived by triangulating estimated distances of three routers to achieve 2m – 3m error, our proposed WTPHAMS system employs multi-trilateration of four routers to get accuracy error of 0.5228m, which is better SOTA as shown in Table 7-1.

Table 7-1 In-depth comparison of the SOTA to our proposed WTP-HAMS system

Research Solution	Exploited Technology	Tracked Object	Techniques, Methods and Models	Experimental conditions	Outcomes	Cost	Best accuracy error
RSSI [14] [64] [65]	Smartphone IMU Wi-Fi [64]	Pedestrians	Sequential Monte Carlo Kalman filter for IMU SDRS log-normal shadowing model Path Loss Exponent Decision Kalman Filter for SDRS	Room configuration - NLoS and LOS Room size - 15m wide corridor Path - N/A Floor type - N/A Experiment iterations - 100 Router no - Fourteen routers Motion type - Pedestrians Smartphone orientation - Unknown Number of wheel encoders - N/A Heading estimation – Yes, with combined accelerometer and gyroscope	Simulated testing, therefore no guarantee it is applicable in a real-world environment. High position error More infrastructure is required This solution provides position only	Expensive	1.5m - 3.1m
	Wi-Fi Smartphone [14][65]	Pedestrians	Multi-trilateration	Room configuration - NLoS and LOS Room size - 1 medium sized room measured at 1:2 unit/meters Path - N/A Floor type - N/A Experiment iterations - 50 Router no - Three - Nine routers Motion type - Pedestrians Smartphone orientation - Unknown Number of wheel encoders - N/A Heading estimation – N/A	Real environment testing. The best result is when four routers are combined. Position error is high and therefore, inaccurate. Excessive infrastructure needed Provides position only	Expensive	4.236m
MILPS [145]	IMU (three axial accelerometer, gyroscope, magnetometer) Digital pressure sensor	Mobile Cart	Trilateration Dead reckoning Extended Kalman filter Sensor fusion	Room configuration - N/A Room size - 2m x 4m Path - Curved Floor type - Smooth Experiment iterations - 50 Reference point no - Three magnetic coils Motion type - Curvilinear IMU orientation - Horizontal Number of wheel encoders - N/A Heading estimation – N/A	Minimal infrastructure and complexity Real environment testing MILPS is not readily available	Moderate	1m- 2m

<p>Odometry only [19]</p>	<p><i>IR range sensors</i> <i>Wheel encoder</i></p>	<p><i>Simulated mobile robot</i></p>	<p><i>Kinematics model - Taylor's series expansion</i></p>	<p><i>Room configuration - Unknown and dynamic</i> <i>Room size - N/A</i> <i>Path - Rectilinear</i> <i>Floor type - Smooth floor</i> <i>Experiment iterations - N/A</i> <i>Router no - N/A</i> <i>Motion type - Translational</i> <i>Smartphone orientation - N/A</i> <i>Number of wheel encoders - Two wheel encoders and five IR range sensors</i> <i>Heading estimation – Yes, estimated by the wheel encoders</i></p>	<p>Simulated experiments, there is no guarantee the solution will work in a real-world environment.</p> <p>Exploits the tradeoff between the linear and angular velocity of the mobile robot.</p> <p>IR range sensor is limiting because its effective distance is 0.04m - 0.3m</p> <p>The solution is designed to be applied in wheelchairs within hospitals</p> <p>Error is visibly high due to drift</p> <p>The outcomes from their solution are travelled distance and pose</p>	<p>High</p>	<p>3m - 5m</p>
<p>Odometry + IMU + Camera vision [109]</p>	<p><i>IMU (Accelerometer, gyroscopes and magnetometer)</i> <i>Camera</i> <i>Wheel encoders</i></p>	<p><i>Two Roomba robot</i></p>	<p><i>Feature-based technique - SURF</i> <i>Odometry</i> <i>Two Kalman filters</i> <i>Two Extended Kalman filter on IMU</i> <i>Morphological operations - erosion and dilation</i></p>	<p><i>Room configuration - Unknown and dynamic</i> <i>Room size - 7m x 3m</i> <i>Path - Rectilinear</i> <i>Floor type - Flat smooth surface</i> <i>Experiment iterations - N/A</i> <i>Camera no - Two high-quality cameras</i> <i>Motion type - Translational</i> <i>Smartphone orientation - N/A</i> <i>Number of wheel encoders - Two wheel encoders</i> <i>Heading estimation – Yes, estimated by the cameras</i></p>	<p>Real environment testing.</p> <p>The best result is when four routers are combined.</p> <p>Presents Pose of the robot</p> <p>Extra infrastructure such as cameras are needed</p> <p>Experiences drift from the odometry</p> <p>The system requires multiple cameras</p> <p>The camera is not as ubiquitous as Wi-Fi and wheel encoders</p> <p>Brightness can significantly influence results from the camera</p>	<p>Expensive</p>	<p>0.33m and 0.51m (odometry + IMU)</p> <p>0.01m - 0.10m (odometry + IMU + camera vision)</p>

<p>WTP-HAMS system (The proposed solution)</p>	<p>Wi-Fi</p> <p>Smartphone with inbuilt Wi-Fi modalities, accelerometer and magnetometer sensors</p> <p>Wheel encoders</p>	<p><i>Mobility scooter</i></p>	<p><i>SDRS Log-normal Shadowing Model [64][77]</i></p> <p><i>Trilateration [14][65]</i></p> <p><i>IMU sensor fusion - Magnetic angular rate update (MARU) and acceleration gradient update (AGU) of MAGYQ filter [160]</i></p> <p><i>FWHM on fused IMU data signal [72] [73]</i></p> <p><i>Proposed new Drift mitigation model</i></p> <p><i>Proposed novel Odometry model</i></p> <p><i>Error propagation - ALE [78]</i></p> <p><i>Euclidean distance error [14][79][65]</i></p> <p><i>Shape intersection and overlap checks [161]</i></p> <p><i>Centroid calculation [80]</i></p>	<p><i>Room configuration - NLoS and LOS</i></p> <p><i>Room size - Room 1 is 480cm x 322cm and Room 2 is 10.07m x 9m</i></p> <p><i>Path - Rectilinear</i></p> <p><i>Floor type - Smooth wooden tiled floor</i></p> <p><i>Experiment iterations - 50 per study</i></p> <p><i>Router no - Four routers</i></p> <p><i>Motion type - Translational</i></p> <p><i>Smartphone orientation - Horizontal vs Vertical</i></p> <p><i>Number of wheel encoders - Two wheel encoders</i></p> <p><i>Heading estimation – Yes, from combined accelerometer and gyroscope with a high sampling rate</i></p>	<p>Drift is significantly reduced</p> <p>Improved position estimates when compared to SOTA [14][64][65] [145]</p> <p>Real environment experimentations</p> <p>Pose and Position error is very low</p> <p>No additional infrastructure is needed, therefore, makes WTP-HAMS an economical solution</p> <p>Due to the ubiquitous nature of the exploited technologies, this solution can be scalable</p>	<p>Low</p>	<p>0.63m – 1.35m</p>
---	--	--------------------------------	---	---	--	------------	----------------------

The outcome shown in Table 7-1 is discussed and demonstrated in Chapter 6. When compared to the state of the art, Chapter 6 shows the adaptation of multi-trilateration is best for our proposed system WTP-HAMS. This is because it uses fewer filtration elements on Wi-Fi and short latency of less than 1 second to perform its calculations.

The accelerometer is another popular technology investigated for indoor localisation. Chapter 3 displays how accelerometers play major roles in localising pedestrians and monitoring vibrations majorly. This is corroborated in chapter 6 where accelerometer only output proved insufficient for localising a mobility scooter travelling in translational motion on a smooth surface. This did not deter the research; instead, it encouraged the repurposing of the accelerometer for determining the orientation of the smartphone in chapters 4-6. Especially when combined with direction from magnetometer. Development is taken a step further in chapters 4-5 where accelerometers are combined with a magnetometer to achieve navigational information in chapter 6.

Wheel encoders are popularly used in robotics for localising robots through odometry. This is discussed in chapters 2-3 as it shows the benefits of wheel encoders in building robot control systems. Drift is a constant occurrence with wheel encoders and studies have attempted mitigating this using complex mathematical prediction models such as extended Kalman filter. The proposed investigations use wheel encoders to get travelled distances. Unlike the prediction model needed in robotics, the proposed system does not need to predict the next position of the mobility scooter because it is manually controlled by the user and users are unpredictable. However, drift is still experienced in the distance travelled and the direction of travel. Our proposed WTP-HAMS system mitigates for distance-travelled drift by proposing and implementing a new drift mitigation model that improved the outcome of travelled distance by about 9%.

The heading was calculated from the distance-travelled as demonstrated in chapters 2 and 6. However, its results were riddled with a systematic drift caused

by accumulated travelled distance errors affecting heading. It showed an exponential relative heading error increase as the mobility scooter travelled over distance. Therefore, we proposed to replace the heading estimates from the travelled distance, with, combined accelerometer and magnetometer sensors. This is because combined accelerometer and magnetometer sensors of the smartphone, give better navigation heading estimates. This navigation heading was then combined with the distance travelled in a proposed novel odometry model to result in improved pose estimates of the mobility scooter with an average error of 9cm, which is better than results shown in SOTA Table 7-1. This is achievable because of the high sampling rate of the data from combined accelerometer and magnetometer sensors. In particular, it reduced the possibility of relative growing error, thus, providing improved heading error. The outcome demonstrates our proposed system better controls drift and provide good accuracy when the following necessary factors exist:

- Environmental factors such as wooden floor tiles that reduce the probability of slippage and tips.
- Infrastructural conditions such as thread free anti-tip tyres of the mobility scooter buffer the inconsistencies mobility scooter might feel when in motion
- Computational factors in Equation 21 and Equation 22 that combine estimates of improved distance travelled with fused accelerometer and magnetometer outputs to provide better pose estimates.

These are discussed in chapters 4-6.

The proposed WTP-HAMS system is thoroughly studied, assessed and validated in chapter 6. This is because it combines the improved outcomes of Wi-Fi, wheel encoders, accelerometer and magnetometer sensors to produce improved absolute position estimates with reduced errors. Analyses of the outcomes show commendable improvements of an error range of 0.35m – 1.35m when compared to state of the art shown in Table 7-1. This improvement is achieved through the exploitation of error shapes exhibited by the outcomes. The error shape of RSSI constrains the error from odometry from going beyond the error boundaries. While

the combination of errors show how odometry improves RSSI based localisation. These are discussed and demonstrated in chapter 6.

The proposed WTP-HAMS system will be valuable when localising mobility scooters users in commercial buildings like care homes with the recommend wooden tiled floors and four Wi-Fi routers that can be assessable for users who use smartphones. Although the application seems very specific, it is possible that the system can be used in other health care environments. These are discussed in chapters 1 and 2.

7.3. Lessons Learned

The assessments of the aforementioned studies implemented for validating our proposed WTP-HAMS system enabled us to closely observe and evaluate all deployed technologies in our representative test environments. All though studies did not cover everything pertaining to the technologies, it focused on their key advantages to our system. Therefore, based on the analysis of our results and the experience gained from the studies, we can safely draw some conclusions. These conclusions are grouped into

- Personal lessons
- Technical lessons

7.3.1. Technical Lessons

Indoor Localisation Challenges Still Persists

Despite continuous investigations in this area, indoor localisation challenge persists. Our investigations show that in indoor environments, there is no technology or combination of technologies that have successfully recreated the outdoor GPS experience of 95% confidence and 3m accuracy.

Although our system WTP-HAMS resulted with an error range of 0.35m – 1.35m, it should be known that result is from areas with specific parameters including 4 routers, 2 wheel encoders on a mobility scooter moving in translational motion on a straight path, a smartphone with accelerometer and magnetometer sensors, and an uncluttered medium sized room with smooth wooden tiled floors.

Our WTP-HAMS system achievement of 0.35m -1.35m range error is a subset of existing localisation solutions that offer 1.5m -3.1m accuracy. Although we believe our error range is sufficient for localising a 2ft 31 inches long mobility scooter in a medium sized room, our achievement is a step closer to realising the ideal indoor localisation vision, which is no error with a high confidence level.

We see that employed technologies in our proposed WTP-HAMS system do not provide the same localisation error even though reading and testing is done at the same point. Significant accuracy variations from each employed technology raise concerns about the error consistency of our system.

Error Is Not Always Bad

In our findings, we have discovered that error is not always bad. From our studies, outcomes especially the errors from **second** and **fifth studies** were critical in achieving our overall objective of the research, which is, proposing and designing our WTP-HAMS system to improve indoor position accuracy.

We identified that error can be an advantage, especially in our instance where the error shapes the employed technologies or techniques cast are very different. Our realisation of the clear and constant distinction between the error shape of the **second study** and that of the **fifth study** made our testing the more provoking. Specifically, the **second study** error shape is circular and the **fifth study** error shape is triangular. The difference in the shapes made it so much easier to calculate the centroid (new position) when both error shapes overlap.

We have learnt that dependent on the system and the type of error shapes it casts, errors can be an advantage.

Better Accuracy from Individual Technologies Equals Improved Localisation Accuracy

We observed the more accurate study, which is **fifth study** (*proposed odometry model combining results from wheel encoders and fused accelerometer and magnetometer sensor outputs*) significantly improved the results of the less accurate study, which is the **second study** (position estimation using multi-trilateration of 4 routers).

Although the **fifth study** used technologies known to provide more accurate results, it was still prone to growing errors that influenced output. The combination of the **fifth study** with our **second study** subsequently corrected position results in our **fifth study**.

We learned that the more accurate the technology is the more accurate our position estimation will be using our WTP-HAMS system.

Environment Influences Results

Literature works have already demonstrated how localisation accuracy can be negatively impacted due to the presence of large objects and human presence for Wi-Fi, and vibrations from wheel encoders due to floor roughness. Generally, indoor localisation evaluation is done in a static environment.

Therefore, for Wi-Fi, we evaluated our environment in the **first study** by modifying our room 1 in two settings: NLoS instance with objects and human presence and LOS instance with no objects and no human presence. We learned that NLoS can experience error up to 3.87m (see Table 6-3) and LOS can experience an error of up to 1m. Although both errors are high, NLoS is considerably worse than LOS. Though

we implemented and tested in LOS instance, it should be known that the increase in position accuracy error is heavily reliant on implementation and environmental conditions.

Technology Configuration Influences Accuracy

We learned from literature works that technology or technology combination is very important as it affects position accuracy.

Therefore, our system required the following technology configuration - 4 Wi-Fi routers in LOS instance, 2 wheel encoders and a combination of accelerometer and magnetometer of a smartphone (see Table 6-2).

For Wi-Fi in LOS instance, when we modified the Wi-Fi number from 3 routers to 4 routers in the same test room, there was an improvement in position accuracy by about 94%.

For wheel encoders, distance travelled of a mobility scooter is best calculated for when using outputs from two wheel encoders mounted on either side of the rear wheels. The front wheel was not included because we deduced that a wheel encoder output from it could negatively influence position results especially when our proposed novel odometry model (Equation 21 and Equation 22) is implemented.

For smartphone IMU modalities – accelerometer and magnetometer sensors, we learned that the orientation of the smartphone greatly influences the heading navigation computation. We quickly identified axis with more positive heading responses when in a horizontal orientation. Also, we learnt very quickly based on results from literature and our WTP-HAMS system, that the way IMU works for pedestrians differ greatly from a translational moving mobility scooter on a smooth wooden tiled floor. Importantly, for pedestrians, the multiple peaks are translated as a human moving point while for motion in translation a single peak is best to translate to initiation, acceleration, steady movement and deceleration.

The smartphone was the most inexpensive and easily accessible technology that could synchronise all dataset from exploited technologies to time.

Each technology plays a major role; therefore, it is important they are all considered when designing our WTP-HAMS system.

Indoor Localisation Does Not Have to Be Expensive or Complex

One of our key objectives was to find an inexpensive means of achieving indoor localisation. Therefore, we used already existing technologies such as Wi-Fi and smartphone with its modalities. This is already easily accessible and ubiquitous in today's society.

We designed and developed inexpensive custom wheel encoders for our trials because our mobility scooter needed a distance travel counter. Development cost us £18.14 excluding the cost of a 3D printer.

We carefully evaluated the cost implications for a user who uses a mobility scooter with inbuilt odometer and a smartphone in an environment like ours (i.e. smooth wooden tiled floor room with 4 routers), it is our conclusion that it will be practically inexpensive to use.

7.3.2. Personal Lessons

Writing Early

We learnt how critical it was to document every detail of the research including ideas, plans, strategy, studies, results consisting of successful test and limitations. Early documentation of our proposed research methodology, plans, ideas and processes using visual representations such as flow diagrams, tables and graphs helped clarify our objectives.

Our thesis development included two years of progression development reports (which included thorough comprehensive literature reviews, background knowledge and design of our proposed methodology) and two additional years of more experiments and progression updates (which included a development and refinement of our proposed methodology, testing and analyses of results from all studies used for achieving our methodology).

An important lesson to take home is not to leave the writing to the last minute, as important information will be omitted.

7.4. Future Directions

Though error mitigation is described in Section 7.2., it hints at the possible area for further explorations on the drift mitigation model and absolute position estimation model. The system relies on the theory that errors exhibited from Wi-Fi can be improved by odometry outcomes. This odometry is a combination of outcomes from wheel encoders, accelerometer and magnetometer. Numerous investigations suggest that directional information from accelerometer and magnetometer combination is better than that from wheel encoders. It further examines the drift experiences of the wheel encoders when measuring travelled distance with employed drift mitigation model. Though drift is mitigated, it is not eradicated completely. However, we tested out smooth wooden floor surfaces only to get a pose error of 9cm. Therefore, we suggest that our proposed novel odometry model be further explored on rough surfaces and uneven floors. The reason will be to investigate the robustness and scalability of our proposed novel odometry model in different environments. This will likely present a sturdier system that might not require Wi-Fi to constrain or improve it. In addition, it creates the opportunity to tackle the mitigation of drift that will be evident because of larger distances or rougher surfaces.

Already, we have demonstrated that combing the resulted improved distance estimate with heading information from accelerometer and magnetometer would

generate better pose estimates. Another area of exploration is the further development of the drift mitigation model itself. Currently, the system manually adds to the percentage error to the estimated travelled distance to improve travelled distance error. It will be interesting to explore the potentials for the system to intuitively add or subtract the percentage errors to travelled distance estimate for a more scalable system resulting in new improved travelled distance estimate.

Another possible advancement to the research is achieving real-time indoor positioning to mobility scooter user when in motion within commercial buildings. This can be achieved with the transfer of the current offline phase described in Chapters 4 and 5 to an online environment that updates data in real time as it calculates for new absolute positions. It is our speculation that this might slow down the system; however, it will be of benefit to users to see their current location on their smartphone in real time. This is important because it will enhance the practicality of our system.

Also, it has to be considered that the high quantity of data that would be obtained over several kilometres will require complex compression and data formatting algorithms to shrink stored data. It is important that these algorithms must maintain sufficient information to calculate a new absolute position estimate of the mobility scooter. However, this is a big data challenge and beyond the scope of this research.

Final future work in the possibility of creating an error model designed a repurposed speaker recognition normalisation system. We believe, that this model store new estimated position as true position as it checks against saved false data to inform the user of their current location in real time. The challenge is in aligning the trained model with the test model. We believe this will provide a lightweight alternative to existing fingerprinting methods. This challenge, however, is beyond the scope of this research.

References

- [1] D. Zhang, F. Xia, Z. Yang, L. Yao, and W. Zhao, "Localization technologies for indoor human tracking," *2010 5th Int. Conf. Futur. Inf. Technol. Futur. 2010 - Proc.*, no. 60903153, 2010.
- [2] W. D. Rencken, "Autonomous sonar navigation in indoor, unknown and unstructured environments," *Proc. IEEE/RSJ Int. Conf. Intell. Robot. Syst.*, vol. 1, pp. 431–438.
- [3] R. McConville, D. Byrne, I. Craddock, R. Piechocki, J. Pope, and R. Santos-Rodriguez, "Understanding the quality of calibrations for indoor localisation," *2018 IEEE 4th World Forum Internet Things*, no. February, pp. 676–681, 2018.
- [4] K. Chintalapudi, "Indoor Localization Without the Pain," pp. 173–184.
- [5] "Accurate relative localization using odometry - IEEE Conference Publication." .
- [6] ONU, "World population, ageing," *Suggest. Cit. United Nations, Dep. Econ. Soc. Aff. Popul. Div. (2015). World Popul. Ageing*, vol. United Nat, no. (ST/ESA/SER.A/390, p. 164, 2015.
- [7] Department of Health, "Guide to the Healthcare System in England," *Natl. Heal. Serv.*, no. May, pp. 1–36, 2013.
- [8] www.statista.com, "Do you personally use a smartphone?* - by age," *Statista*, 2019. [Online]. Available: <https://www.statista.com/statistics/300402/smartphone-usage-in-the-uk-by-age/>.
- [9] A. Canedo-Rodríguez, V. Álvarez-Santos, C. V. Regueiro, R. Iglesias, S. Barro, and J. Presedo, "Particle filter robot localisation through robust fusion of laser, WiFi, compass, and a network of external cameras," *Inf. Fusion*, vol. 27, pp. 170–188, 2016.
- [10] M. Signal, L. Thresholds, A. P. Placement, A. P. Separation, D. L. Readiness, D. Coexistence, A. Location, D. Jitter, M. Location, A. Designs, A. Considerations, and I. L. Quality, "Best Practices—Location-Aware WLAN Design Considerations," pp. 5–68.
- [11] Alex Mariakakis et al, "SAIL: Single Access Point-Based Indoor Localization," *ACM Trans. Embed. Comput. Syst.*, 2014.
- [12] D. Omkar and P. S. S. Koul, "Indoor Localization and Tracking using Wi-Fi Access Points," vol. 47, no. May, pp. 263–269, 2017.

- [13] J. Yang and Y. Chen, "Indoor Localization Using Improved RSS-Based Lateration Methods.pdf," *IEEE Glob. Commun. Conf.*, vol. 4, 2009.
- [14] S. Boonsriwai and A. Apavatjirut, "Indoor WIFI localization on mobile devices," *2013 10th Int. Conf. Electr. Eng. Comput. Telecommun. Inf. Technol. ECTI-CON 2013*, 2013.
- [15] A. S. Paul and E. a. Wan, "Wi-Fi based indoor localization and tracking using sigma-point Kalman filtering methods," *2008 IEEE/ION Position, Locat. Navig. Symp.*, no. June, pp. 646–659, 2008.
- [16] S. Mazuelas, A. Bahillo, R. M. Lorenzo, P. Fernandez, F. A. Lago, E. Garcia, J. Blas, and E. J. Abril, "Robust indoor positioning provided by real-time rssi values in unmodified WLAN networks," *IEEE J. Sel. Top. Signal Process.*, vol. 3, no. 5, pp. 821–831, 2009.
- [17] J. Cheng, Z. Song, Q. Ye, and H. Du, "MIL: A mobile indoor localization scheme based on matrix completion," *IEEE Int. Conf. Commun. ICC2016*, pp. 1–5, 2016.
- [18] Z. Tian, X. Fang, M. Zhou, and L. Li, "Smartphone-based indoor integrated WiFi/MEMS positioning algorithm in a multi-floor environment," *Micromachines*, vol. 6, no. 3, pp. 347–363, 2015.
- [19] A. Jha and M. Kumar, "Two wheels differential type odometry for mobile robots," *Proc. - 2014 3rd Int. Conf. Reliab. Infocom Technol. Optim. Trends Futur. Dir. ICRITO 2014*, 2015.
- [20] R. Mehra and A. Singh, "Real time RSSI error reduction in distance estimation using RLS algorithm," *Proc. 2013 3rd IEEE Int. Adv. Comput. Conf. IACC 2013*, no. February 2013, pp. 661–665, 2013.
- [21] E. Burke, "'The only thing necessary for the triumph of evil is for good men to do nothing.' Edmund Burke (1729-1797)," 2014.
- [22] O. Woodman and R. Harle, "Pedestrian localisation for indoor environments," *Proc. 10th Int. Conf. Ubiquitous Comput. - UbiComp '08*, p. 114, 2008.
- [23] G. Sun, J. Chen, W. Guo, and K. J. R. Liu, "Signal processing techniques in network-aided positioning: A survey of state-of-the-art positioning designs," *IEEE Signal Process. Mag.*, vol. 22, no. 4, pp. 12–23, 2005.
- [24] G. Deak, K. Curran, and J. Condell, "A survey of active and passive indoor localisation systems," *Computer Communications*, vol. 35, no. 16. pp. 1939–1954, 2012.
- [25] K.-F. Ssu, C.-H. Ou, and H. C. Jiau, "Localization With Mobile Anchor Points in Wireless Sensor Networks," *Ieee Trans. Veh. Technol.*, vol. 54, no. 3, pp. 1187–1197, 2005.

- [26] X. Ge, B. Yang, J. Ye, G. Mao, C. X. Wang, and T. Han, "Spatial spectrum and energy efficiency of random cellular networks," *IEEE Trans. Commun.*, 2015.
- [27] F. Rebecchi, M. Dias de Amorim, V. Conan, A. Passarella, R. Bruno, and M. Conti, "Data Offloading Techniques in Cellular Networks: A Survey," *IEEE Commun. Surv. Tutorials*, 2015.
- [28] M. Yassin and E. Rachid, "A survey of positioning techniques and location based services in wireless networks," in *2015 IEEE International Conference on Signal Processing, Informatics, Communication and Energy Systems (SPICES)*, 2015.
- [29] G. Deak, K. Curran, and J. Condell, "A survey of active and passive indoor localisation systems," *Comput. Commun.*, vol. 35, no. 16, pp. 1939–1954, 2012.
- [30] A. Bensky, "Wireless Positioning Technologies and Applications, Second Edition - Alan Bensky - Google Books." p. 424, 2008.
- [31] C. Li and Z. Weihua, "Hybrid TDOA/AOA mobile user location for wideband CDMA cellular systems," *IEEE Trans. Wirel. Commun.*, vol. 1, no. 3, pp. 439–447, 2002.
- [32] U. N. Kar and D. K. Sanyal, "An overview of device-to-device communication in cellular networks," *ICT Express*, 2018.
- [33] A. Asadi, Q. Wang, and V. Mancuso, "A survey on device-to-device communication in cellular networks," *IEEE Commun. Surv. Tutorials*, 2014.
- [34] C. H. Lim, Y. Wan, B. P. Ng, and C. M. S. See, "A real-time indoor WiFi localization system utilizing smart antennas," *IEEE Trans. Consum. Electron.*, vol. 53, no. 2, pp. 618–622, 2007.
- [35] G. Sun, J. Chen, W. Guo, and K. J. R. Liu, "Signal processing techniques in network-aided positioning: A survey of state-of-the-art positioning designs," *IEEE Signal Process. Mag.*, 2005.
- [36] D. Niculescu and B. Nath, "Ad-hoc positioning system (APS) using AOA," *Int. Conf. Comput. Commun.*, vol. 00, no. C, pp. 1734–1743, 2003.
- [37] mbed, "mbed LPC1768," *mbed*. [Online]. Available: <https://developer.mbed.org/platforms/mbed-LPC1768/>.
- [38] R. Mehra and A. Singh, "Real time RSSI error reduction in distance estimation using RLS algorithm," *Proceedings of the 2013 3rd IEEE International Advance Computing Conference, IACC 2013*. pp. 661–665, 2013.
- [39] By and M. Viswanathan, "Simulation of Digital Communication Systems using Matlab," p. 292, 2013.

- [40] Y. Gu, A. Lo, and I. Niemegeers, "A survey of indoor positioning systems for wireless personal networks," *IEEE Commun. Surv. Tutorials*, vol. 11, no. 1, pp. 13–32, 2009.
- [41] M. A. Al-Ammar, S. Alhadhrami, A. Al-Salman, A. Alarifi, H. S. Al-Khalifa, A. Alnafessah, and M. Alsaleh, "Comparative survey of indoor positioning technologies, techniques, and algorithms," in *Proceedings - 2014 International Conference on Cyberworlds, CW 2014*, 2014, pp. 245–252.
- [42] Erin-Ee-Lin La et al, "ENHANCED RSSI-BASED HIGH ACCURACY REAL-TIME USER LOCATION TRACKING SYSTEM FOR INDOOR AND OUTDOOR ENVIRONMENTS," *Int. J. SMART Sens. Intell. Syst.*, pp. 534–548, 2008.
- [43] H. Balakrishnan, T. Supervisor, and A. C. Smith, "The Cricket Indoor Location System," *Architecture*, vol. 16, no. 2001, p. 199, 2005.
- [44] E. Mok and G. Retscher, "Location determination using WiFi fingerprinting versus WiFi trilateration," *J. Locat. Based Serv.*, vol. 1, no. 2, pp. 145–159, 2007.
- [45] M. Youssef, M. Mah, and A. Agrawala, "Challenges: Device-free Passive Localization for Wireless Environments," *Proc. 13th Annu. ACM Int. Conf. Mob. Comput. Netw. - MobiCom '07*, p. 222, 2007.
- [46] Space-based positioning navigation and timing nation executive Committee, "Official U.S. government information about the Global Positioning System (GPS) and related topic," *NOAA*, 2017. [Online]. Available: <http://www.gps.gov/systems/gps/space/>.
- [47] E. B. Quist and R. W. Beard, "Radar Odometry on Small Unmanned Aircraft," *AIAA Guid. Navig. Control Conf.*, vol. 52, no. 1, pp. 1–18, 2013.
- [48] G. Pipelidis, O. R. M. Rad, D. Iwaszczuk, C. Prehofer, and U. Hugentobler, "Dynamic vertical mapping with crowdsourced smartphone sensor data," *Sensors (Switzerland)*, vol. 18, no. 2, pp. 1–25, 2018.
- [49] S. Panzieri, F. Pascucci, and G. Ulivi, "An outdoor navigation system using GPS and inertial platform," *IEEE/ASME Trans. Mechatronics*, vol. 7, no. 2, pp. 134–142, 2002.
- [50] A. Bondavalli, A. Ceccarelli, F. Gogaj, A. Seminatore, and M. Vadursi, "Experimental assessment of low-cost GPS-based localization in railway worksite-like scenarios," *Meas. J. Int. Meas. Confed.*, vol. 46, no. 1, pp. 456–466, 2013.
- [51] J. Chon and H. Cha, "LifeMap: A smartphone-based context provider for location-based services," *IEEE Pervasive Comput.*, vol. 10, no. 2, pp. 58–67, 2011.
- [52] Ofcom, "Ofcom Location information for emergency calls from mobile

- phones,” *Ofcom*, 2014. [Online]. Available: https://www.ofcom.org.uk/_data/assets/pdf_file/0023/83075/emergency_mobile_location_information_statement.pdf. [Accessed: 04-Jul-2017].
- [53] R. Kümmerle, G. Grisetti, and W. Burgard, “Simultaneous calibration, localization, and mapping,” *IEEE Int. Conf. Intell. Robot. Syst.*, pp. 3716–3721, 2011.
- [54] Seongwoo Jang, Kyungjae Ahn, Jongseong Lee, and Yeonsik Kang, “A study on integration of particle filter and dead reckoning for efficient localization of automated guided vehicles,” *2015 IEEE Int. Symp. Robot. Intell. Sensors*, pp. 81–86, 2015.
- [55] Y. Pei and L. Kleeman, “A novel odometry model for wheeled mobile robots incorporating linear acceleration,” *2017 IEEE Int. Conf. Mechatronics Autom. ICMA 2017*, pp. 1396–1403, 2017.
- [56] J. Xiao, Z. Zhou, Y. Yi, and L. M. Ni, “A Survey on Wireless Indoor Localization from the Device Perspective,” *ACM Comput. Surv.*, vol. 49, no. 2, pp. 1–31, 2016.
- [57] J. Xiong and K. Jamieson, “Towards Fine-Grained Radio-Based Indoor Location Categories and Subject Descriptors,” 2010.
- [58] C. Yang and H. R. Shao, “WiFi-based indoor positioning,” *IEEE Commun. Mag.*, vol. 53, no. 3, pp. 150–157, 2015.
- [59] H. Jiang, C. Cai, X. Ma, Y. Yang, and J. Liu, “Smart Home Based on WiFi Sensing: A Survey,” *IEEE Access*, vol. 6, pp. 13317–13325, 2018.
- [60] E. Mok and G. Retscher, “Location determination using WiFi fingerprinting versus WiFi trilateration,” *J. Locat. Based Serv.*, vol. 1, no. 2, pp. 145–159, 2007.
- [61] J. Hong and T. Ohtsuki, “Signal eigenvector-based device-free passive localization using array sensor,” *IEEE Trans. Veh. Technol.*, vol. 64, no. 4, pp. 1354–1363, 2015.
- [62] L. Jiang, “a Wlan Fingerprinting Based Indoor Localization Technique,” *Univ. Nebraska*, 2012.
- [63] N. D. Lane, E. Miluzzo, H. Lu, D. Peebles, T. Choudhury, and A. T. Campbell, “A survey of mobile phone sensing,” *IEEE Commun. Mag.*, vol. 48, no. 9, pp. 140–150, 2010.
- [64] W. W. L. Li, R. A. Iltis, and M. Z. Win, “A smartphone localization algorithm using RSSI and inertial sensor measurement fusion,” *GLOBECOM - IEEE Glob. Telecommun. Conf.*, pp. 3335–3340, 2013.
- [65] M. E. Rusli, M. Ali, N. Jamil, and M. M. Din, “An Improved Indoor Positioning

Algorithm Based on RSSI-Trilateration Technique for Internet of Things (IOT)," *2016 Int. Conf. Comput. Commun. Eng.*, pp. 72–77, 2016.

- [66] R. Harle, "A survey of indoor inertial positioning systems for pedestrians," *IEEE Commun. Surv. Tutorials*, vol. 15, no. 3, pp. 1281–1293, 2013.
- [67] Z. YANG, C. WU, Z. ZHOU, X. ZHANG, X. WANG, and U. LIU, "Mobility Increases Localizability: A Survey on Wireless Indoor Localization using Inertial Sensors," *ACM*, p. 34, 2015.
- [68] R. Henken and M. A. Wiering, "Indoor-localization using a mobile phone," 2014.
- [69] W. Zijlstra, "Android sensor fusion tutorial." pp. 1–15, 2014.
- [70] S. Cai, Y. Wu, N. Xiang, Z. Zhong, J. He, L. Shi, and F. Xu, "Detrending knee joint vibration signals with a cascade moving average filter," *Proc. Annu. Int. Conf. IEEE Eng. Med. Biol. Soc. EMBS*, pp. 4357–4360, 2012.
- [71] M. N. Pontuschka, I. M. Da Fonseca, and M. A. A. Melo, "Experiment on signal filter combinations for the analysis of information from inertial measurement units in AOCs," *J. Phys. Conf. Ser.*, vol. 641, no. 1, 2015.
- [72] "Statistics and the Treatment of Experimental Data." .
- [73] M. Galotto and P. Ulloa, "statistical characterisation of acceleration levels of random vibrations during transport," *Packag. Technol. Sci.*, vol. 23, no. May, pp. 253–266, 2010.
- [74] N. I. C. R. P. H. F. M. S. M. Inagaki, "Specification for a standard procedure of X-ray." Elsevier.
- [75] Elizabeth G. Armstrong; Corina Sandu; Saied Taheri, "Investigation into use of piezoelectric sensors in a wheeled robot tire for surface characterization." Elsevier, pp. 75–90, 2015.
- [76] A. Wu and Z. Zeng, "Dynamic behaviors of memristor-based recurrent neural networks with time-varying delays," *Neural Networks*, vol. 36, pp. 1–10, 2012.
- [77] R. A. Iltis and S. Barbara, "System-Level Algorithm Design for Radionavigation," 2016.
- [78] L. Cheng, H. Wu, C. Wu, and Y. Zhang, "Indoor mobile localization in wireless sensor network under unknown NLOS errors," *Int. J. Distrib. Sens. Networks*, vol. 2013, 2013.
- [79] H. Aksu, D. Aksoy, and I. Korpeoglu, "A study of localization metrics: Evaluation of position errors in wireless sensor networks," *Comput. Networks*, vol. 55, no. 15, pp. 3562–3577, 2011.

- [80] U. S. River, "D - 3 4 300," pp. 879–1009, 2016.
- [81] J. S. Ju, Y. Shin, and E. Y. Kim, "Intelligent wheelchair using head tilt and mouth shape," *Electron. Lett.*, vol. 45, no. 17, p. 873, 2009.
- [82] T. Carlson and Y. Demiris, "Human-wheelchair collaboration through prediction of intention and adaptive assistance," *Proc. - IEEE Int. Conf. Robot Autom.*, pp. 3926–3931, 2008.
- [83] B. Cheng, R. Du, B. Yang, W. Yu, C. Chen, and X. Guan, "An accurate GPS-based localization in wireless sensor networks: A GM-WLS method," in *Proceedings of the International Conference on Parallel Processing Workshops*, 2011, pp. 33–41.
- [84] G. Reina, A. Vargas, K. Nagatani, and K. Yoshida, "Adaptive Kalman Filtering for GPS-based Mobile Robot Localization," *2007 IEEE Int. Work. Safety, Secur. Rescue Robot.*, pp. 1–6, 2007.
- [85] Z. Tao, P. Bonnifait, V. Fremont, and J. Ibanez-Guzman, "Mapping and localization using GPS, lane markings and proprioceptive sensors," in *IEEE International Conference on Intelligent Robots and Systems*, 2013, pp. 406–412.
- [86] S. Nirjon, J. Liu, G. Dejean, B. Priyantha, Y. Jin, and T. Hart, "COIN-GPS : Indoor Localization from Direct GPS Receiving," *MobiSys '14*, pp. 301–314, 2014.
- [87] S. Weiss, D. Scaramuzza, and R. Siegwart, "Monocular-SLAM-based navigation for autonomous micro helicopters in GPS-denied environments," *J. F. Robot.*, vol. 28, no. 6, pp. 854–874, 2011.
- [88] K. Wu, J. Xiao, Y. Yi, D. Chen, X. Luo, and L. M. Ni, "CSI-based indoor localization," *IEEE Trans. Parallel Distrib. Syst.*, vol. 24, no. 7, pp. 1300–1309, 2013.
- [89] C. Wu, Z. Yang, and Y. Liu, "Smartphones based crowdsourcing for indoor localization," *IEEE Trans. Mob. Comput.*, vol. 14, no. 2, pp. 444–457, 2015.
- [90] F. Brachmann, "A comparative analysis of standardized technologies for providing indoor geolocation functionality," in *CINTI 2012 - 13th IEEE International Symposium on Computational Intelligence and Informatics, Proceedings*, 2012, pp. 127–130.
- [91] E. S. Bridge, K. Thorup, M. S. Bowlin, P. B. Chilson, R. H. Diehl, R. W. Fléron, P. Hartl, R. Kays, J. F. Kelly, W. D. Robinson, and M. Wikelski, "Technology on the Move: Recent and Forthcoming Innovations for Tracking Migratory Birds," *Bioscience*, vol. 61, no. 9, pp. 689–698, 2011.
- [92] K. Kim and M. Kim, "RFID-based location-sensing system for safety management," *Pers. Ubiquitous Comput.*, vol. 16, no. 3, pp. 235–243, 2012.

- [93] Z. Feng, Y. Zhu, Q. Zhang, L. M. Ni, and A. V. Vasilakos, "TRAC: Truthful auction for location-aware collaborative sensing in mobile crowdsourcing," in *Proceedings - IEEE INFOCOM*, 2014, pp. 1231–1239.
- [94] L. Liu, Z. Liu, and B. E. Barrowes, "Through-Wall Bio-Radiolocation With UWB Impulse Radar: Observation, Simulation and Signal Extraction," *IEEE J. Sel. Top. Appl. Earth Obs. Remote Sens.*, vol. 4, no. 4, pp. 791–798, 2011.
- [95] F. Papi, D. Tarchi, M. Vespe, F. Oliveri, and G. Aulicino, "Radiolocation and tracking of automatic identification system signals," in *IEEE Workshop on Statistical Signal Processing Proceedings*, 2014, pp. 504–507.
- [96] S. Abbate, M. Avvenuti, F. Bonatesta, G. Cola, P. Corsini, and A. Vecchio, "A smartphone-based fall detection system," *Pervasive Mob. Comput.*, vol. 8, no. 6, pp. 883–899, 2012.
- [97] B. Alsinglawi, M. Elkhodr, Q. V. Nguyen, U. Gunawardana, A. Maeder, and S. Simoff, "RFID Localisation for Internet of Things Smart Homes : A Survey," *Int. J. Comput. Networks Commun.*, vol. 9, no. 1, pp. 81–99, 2017.
- [98] B. Fu, F. Kirchbuchner, J. von Wilmsdorff, T. Grosse-Puppendahl, A. Braun, and A. Kuijper, *Indoor localization based on passive electric field sensing*, vol. 10217 LNCS. 2017.
- [99] T. Vuorela, P. Peltola, J. Vanhala, and C. Engineering, "a review on device-free passive indoor positionin methods," vol. 8, no. 1, pp. 71–94, 2014.
- [100] Y. Sun, Z. Zhou, S. Tang, X. K. Ding, J. Yin, and Q. Wan, "3D Hybrid TOA-AOA Source Localization Using an Active and a Passive Station," pp. 257–260, 2016.
- [101] Nasrullah Pirzadaa, M Yunus Nayanb, Fazli Subhanc, M Fadzil Hassan d, Muhammad Amir Khan, "Comparative Analysis of Active and Passive Indoor Localization Systems," *Elsevier*, 2013.
- [102] J.O. Smith et al, "The spherical interpolation method for closed-form passive source localization using range difference measurements," pp. 471–474.
- [103] N. Pirzada, M. Y. Nayan, F. Subhan, M. F. Hassan, and M. A. Khan, "Comparative Analysis of Active and Passive Indoor Localization Systems," *AASRI Procedia*, vol. 5, pp. 92–97, 2013.
- [104] M. Terán, J. Aranda, H. Carrillo, D. Mendez, and C. Parra, "IoT-based system for indoor location using bluetooth low energy," in *2017 IEEE Colombian Conference on Communications and Computing (COLCOM)*, 2017, pp. 1–6.
- [105] A. Ward, A. Jones, and A. Hopper, "A new location technique for the active office," *IEEE Pers. Commun.*, vol. 4, no. 5, pp. 42–47, 1997.
- [106] S. He and S. H. G. Chan, "Wi-Fi fingerprint-based indoor positioning: Recent

- advances and comparisons," *IEEE Communications Surveys and Tutorials*, vol. 18, no. 1. pp. 466–490, 2016.
- [107] A. Correa, M. Barcelo, A. Morell, and J. L. Vicario, "A review of pedestrian indoor positioning systems for mass market applications," *Sensors (Switzerland)*, vol. 17, no. 8. 2017.
- [108] D. Konings, A. Budel, F. Alam, and F. Noble, "Entity tracking within a Zigbee based smart home," in *M2VIP 2016 - Proceedings of 23rd International Conference on Mechatronics and Machine Vision in Practice*, 2017.
- [109] M. Alatise and G. Hancke, "Pose Estimation of a Mobile Robot Based on Fusion of IMU Data and Vision Data Using an Extended Kalman Filter," *Sensors*, vol. 17, no. 10, p. 2164, 2017.
- [110] R. Mautz, "Indoor Positioning Technologies," *Inst. Geod. Photogramm. Dep. Civil, Environ. Geomat. Eng. ETH Zurich*, no. February 2012, p. 127, 2012.
- [111] L. Mainetti, L. Patrono, and I. Sergi, "A survey on indoor positioning systems," in *2014 22nd International Conference on Software, Telecommunications and Computer Networks (SoftCOM)*, 2014, pp. 111–120.
- [112] S. N. Patel, M. S. Reynolds, and G. D. Abowd, "Detecting human movement by differential air pressure sensing in HVAC system ductwork: An exploration in infrastructure mediated sensing," in *Lecture Notes in Computer Science (including subseries Lecture Notes in Artificial Intelligence and Lecture Notes in Bioinformatics)*, 2008, vol. 5013 LNCS, pp. 1–18.
- [113] J. Parviainen, J. Kantola, and J. Collin, "Differential barometry in personal navigation," in *Record - IEEE PLANS, Position Location and Navigation Symposium*, 2008, pp. 148–152.
- [114] A. Schmitz-Peiffer, A. Nuckelt, M. Middendorf, and M. Burazanis, "A new navigation system for indoor positioning (InLite)," in *2010 International Conference on Indoor Positioning and Indoor Navigation, IPIN 2010 - Conference Proceedings*, 2010.
- [115] J. Hightower and G. Borriello, "Location Sensing Techniques," *IEEE*, pp. 57–66, 2001.
- [116] A. Braun, H. Heggen, and R. Wichert, "CapFloor - A flexible capacitive indoor localization system," in *Communications in Computer and Information Science*, 2012, vol. 309 CCIS, pp. 26–35.
- [117] M. M.R., A. M., S. C., and B. A., "Safety Services in Smart Environments Using Depth Cameras. In: Braun A., Wichert R., Maña A. (eds) Ambient Intelligence. Aml 2017. Lecture Notes in Computer Science," *Springer, Cham*, vol. 10217, pp. 80–93, 2017.

- [118] M. Andries, O. Simonin, and F. Charpillet, "Localization of Humans, Objects, and Robots Interacting on Load-Sensing Floors," *IEEE Sens. J.*, vol. 16, no. 4, pp. 1026–1037, 2016.
- [119] S. Pirttikangas, J. Suutala, and J. Riekkii, "Footstep_identification_from_pressure_signals_usin.pdf," no. May 2014, 2003.
- [120] R. J. Orr and G. D. Abowd, "The Smart Floor : A Mechanism for Natural User Identification and Tracking," in *Conference on Human Factors in Computing Systems*, 2000, pp. 275–276.
- [121] M. D. Addlesee, A. Jones, F. Livesey, and F. Samaria, "The ORL active floor," *IEEE Pers. Commun.*, vol. 4, no. 5, pp. 35–41, 1997.
- [122] S. P. S. Park and S. Hashimoto, "Autonomous Mobile Robot Navigation Using Passive RFID in Indoor Environment," *IEEE Trans. Ind. Electron.*, vol. 56, no. 7, pp. 2366–2373, 2009.
- [123] J. Zhao, P. Ishwar, and J. Konrad, "PRIVACY-PRESERVING INDOOR LOCALIZATION VIA LIGHT TRANSPORT ANALYSIS," in *IEEE*, 2017.
- [124] Q. Wang, X. Zhang, and K. L. Boyer, "Occupancy distribution estimation for smart light delivery with perturbation-modulated light sensing," *J. Solid State Light*, vol. 1, no. 1, p. 17, 2014.
- [125] A. Alarifi, A. Al-Salman, M. Alsaleh, A. Alnafessah, S. Al-Hadhrami, M. Al-Ammar, and H. Al-Khalifa, "Ultra Wideband Indoor Positioning Technologies: Analysis and Recent Advances," *Sensors*, vol. 16, no. 5, p. 707, 2016.
- [126] S. Bartoletti, A. Giorgetti, and A. Conti, "UWB sensor radar networks for indoor passive navigation," *Proc. 2012 Tyrrhenian Work. Adv. Radar Remote Sens. From Earth Obs. to Homel. Secur. TyWRRS 2012*, pp. 140–145, 2012.
- [127] Y. Li, Y. Wang, and D. Wang, "Multiple RGB-D sensor-based 3-D reconstruction and localization of indoor environment for mini MAV," *Computers and Electrical Engineering*, 2017.
- [128] A. E. Kosba, A. Saeed, and M. Youssef, "RASID: A RobustWLAN Device-free Passive Motion Detection System," *Pervasive Comput. ...*, pp. 180–189, 2012.
- [129] X. Chen and L. Zhang, "Poster Abstract : E-Loc : Indoor Localization through Building," pp. 311–312, 2017.
- [130] S. Liu, L. Yin, W. K. Ho, K. V. Ling, and S. Schiavon, "A tracking cooling fan using geofence and camera-based indoor localization," *Build. Environ.*, vol. 114, pp. 36–44, 2017.

- [131] Y. Charlon, N. Fourty, and E. Campo, "A telemetry system embedded in clothes for indoor localization and elderly health monitoring," *Sensors (Switzerland)*, vol. 13, no. 9, pp. 11728–11749, 2013.
- [132] M. Pashaian and M. Mosavi, "Accurate Intelligent Map Matching Algorithms for Vehicle Positioning System," *Int. J. Comput. Sci.*, vol. 9, no. 2, pp. 114–119, 2012.
- [133] S. Gezici, Z. Tian, G. B. Giannakis, H. Kobayashi, A. F. Molisch, H. V. Poor, and Z. Sahinoglu, "Localization via ultra-wideband radios: A look at positioning aspects of future sensor networks," *IEEE Signal Process. Mag.*, vol. 22, no. 4, pp. 70–84, 2005.
- [134] H. Samuel, S. Connell, I. Milligan, D. Austin, T. L. Hayes, and P. Chiang, "Indoor localization using pedestrian dead reckoning updated with RFID-based fiducials," in *Proceedings of the Annual International Conference of the IEEE Engineering in Medicine and Biology Society, EMBS*, 2011, pp. 7598–7601.
- [135] J. Chai, C. Wu, C. Zhao, H. L. Chi, X. Wang, B. W. K. Ling, and K. L. Teo, "Reference tag supported RFID tracking using robust support vector regression and Kalman filter," *Adv. Eng. Informatics*, vol. 32, pp. 1–10, 2017.
- [136] B. Kempke, P. Pannuto, B. Campbell, and P. Dutta, "SurePoint: Exploiting Ultra Wideband Flooding and Diversity to Provide Robust, Scalable, High-Fidelity Indoor Localization," *Proc. 14th ACM Conf. Embed. Netw. Sens. Syst. (SenSys '16)*, pp. 137–149, 2016.
- [137] B. Kempke, P. Pannuto, and P. Dutta, "Harmonium: Asymmetric, Bandstitched UWB for Fast, Accurate, and Robust Indoor Localization," in *2016 15th ACM/IEEE International Conference on Information Processing in Sensor Networks, IPSN 2016 - Proceedings*, 2016.
- [138] J. Hightower, *Learning and Recognizing the PLaces we go*, vol. 7, no. 11, 2015.
- [139] A. Varshavsky, E. de Lara, J. Hightower, A. LaMarca, and V. Otsason, "GSM indoor localization," *Pervasive Mob. Comput.*, vol. 3, no. 6, pp. 698–720, 2007.
- [140] U. Yayan, H. Yucel, and A. Yazıcı, "A Low Cost Ultrasonic Based Positioning System for the Indoor Navigation of Mobile Robots," *J. Intell. Robot. Syst. Theory Appl.*, vol. 78, no. 3–4, pp. 541–552, 2015.
- [141] N. Fujieda, "Attenuation Model for Error Correction of Ultrasonic Positioning System," vol. 7, no. 2, pp. 181–188, 2017.
- [142] S. Yoon, K. Lee, Y. C. Yun, and I. Rhee, "ACMI: FM-based indoor localization via autonomous fingerprinting," *IEEE Trans. Mob. Comput.*, vol. 15, no. 6, pp. 1318–1332, 2016.

- [143] M. M. Rahman, V. Moghtadaiee, and A. G. Dempster, "Design of fingerprinting technique for indoor localization using AM radio signals," in *2017 International Conference on Indoor Positioning and Indoor Navigation, IPIN 2017*, 2017, vol. 2017–Janua.
- [144] A. Popleteev, "Indoor positioning using ambient radio signals: Data acquisition platform for a long-term study," *2016 13th Work. Positioning, Navig. Commun.*, pp. 1–5, 2016.
- [145] H. Hellmers, A. Norrdine, J. Blankenbach, and A. Eichhorn, "An IMU/magnetometer-based Indoor positioning system using Kalman filtering," *2013 Int. Conf. Indoor Position. Indoor Navig.*, no. October, pp. 1–9, 2013.
- [146] J. Chen, "RSSI-based Indoor Mobile Localization in Wireless Sensor Network," *Int. J. Digit. Content Technol. its Appl.*, vol. 5, no. 7, pp. 407–416, 2011.
- [147] N. Point, "Natural Point OptiTrack motion capture system," 2018. [Online]. Available: <https://optitrack.com/>. [Accessed: 22-May-2018].
- [148] Q-Track, "Q-Track – Offering Highly Accurate Real-Time Location Systems to Solve the Most Difficult Indoor Location Problems." .
- [149] J. Barnes, J. Van Cranenbroeck, C. Rizos, A. Pahwa, and N. Politi, "Long term performance analysis of a new ground-transceiver positioning network (LocataNet) for Structural Deformation Monitoring Applications," *FIG Work Week 2007*, no. May, pp. 13–17, 2007.
- [150] Y. Fukuju, M. Minami, H. Morikawa, and T. Aoyama, "DOLPHIN: An autonomous indoor positioning system in ubiquitous computing environment," in *Proceedings - IEEE Workshop on Software Technologies for Future Embedded Systems, WSTFES 2003*, 2003, pp. 53–56.
- [151] J. Park, M. Choi, Y. Zu, and J. Lee, "Indoor localization system in a multi-block workspace," *Robotica*, vol. 28, no. 3, pp. 397–403, 2010.
- [152] C. Goetz, "Air force institute of technology," 2018.
- [153] S. H. Fang and T. N. Lin, "Cooperative multi-radio localization in heterogeneous wireless networks," *IEEE Trans. Wirel. Commun.*, vol. 9, no. 5, pp. 1547–1551, 2010.
- [154] Z. Zhang, Z. Lu, V. Saakian, X. Qin, Q. Chen, and L. R. Zheng, "Item-level indoor localization with passive UHF RFID based on tag interaction analysis," *IEEE Trans. Ind. Electron.*, vol. 61, no. 4, pp. 2122–2135, 2014.
- [155] K. Vadivukkarasi, R. Kumar, and M. joe, "A real time rssi based novel algorithm to improve indoor localization accuracy for target tracking in wireless sensor networks," *ARNPJ. Eng. Appl. Sci.*, vol. 10, no. 16, pp. 7015–

7023, 2015.

- [156] W. Xue, W. Qiu, X. Hua, and K. Yu, "Improved Wi-Fi RSSI Measurement for Indoor Localization," *IEEE Sens. J.*, vol. 17, no. 7, pp. 2224–2230, 2017.
- [157] G. Deak, K. Curran, and J. Condell, "A survey of active and passive indoor localisation systems," *Comput. Commun.*, vol. 35, no. 16, pp. 1939–1954, 2012.
- [158] A. Faralli, N. Giovannini, S. Nardi, and L. Pallottino, "Indoor real-time localisation for multiple autonomous vehicles fusing vision, odometry and IMU data," *Lecture Notes in Computer Science (including subseries Lecture Notes in Artificial Intelligence and Lecture Notes in Bioinformatics)*, vol. 9991 LNCS, pp. 288–297, 2016.
- [159] L.Feng; J.Borenstein; H.R. Everett, "where am i.pdf," 1994.
- [160] V. Renaudin and C. Combettes, "Magnetic, acceleration fields and gyroscope quaternion (MAGYQ)-based attitude estimation with smartphone sensors for indoor pedestrian navigation," *Sensors (Switzerland)*, 2014.
- [161] "analytic geometry - Detecting an Intersection between Simple Shapes - Mathematics Stack Exchange."
- [162] "Locate the centroid of the shaded area."
- [163] S. Executive, "Health and safety in care homes," pp. 1–72, 2014.
- [164] "Stop Falling : Start Saving."
- [165] "Residential care homes & nursing homes."
- [166] A. W. Safety, "Altro Wood Safety used by Norfolk ' s largest care home provider."
- [167] T. O. F. Contents, "Neo electric scooter range owners handbook," vol. 40948, no. Rev C, pp. 1–24.
- [168] D. Béland and J.-P. Viriot Durandal, "Aging in france: population trends, policy issues, and research institutions.," *Gerontologist*, vol. 53, no. 2, pp. 191–7, 2013.
- [169] Unixtimestamp.com, "Unix Time Stamp - Epoch Converter." 2017.
- [170] B. Bischoff, D. Nguyen-Tuong, F. Streichert, M. Ewert, and A. Knoll, "Fusing vision and odometry for accurate indoor robot localization," *2012 12th Int. Conf. Control. Autom. Robot. Vision, ICARCV 2012*, vol. 2012, no. December, pp. 347–352, 2012.
- [171] F. Höflinger, J. Bordoy, N. Simon, J. Wendeberg, L. M. Reindl, and C.

- Schindelhauer, "Indoor-localization system for smart phones," *2015 IEEE Int. Work Meas. Networking, MN 2015 - Proc.*, pp. 59–64, 2015.
- [172] C. Han, K. Wu, Y. Wang, and L. M. Ni, "WiFall: Device-free fall detection by wireless networks," *IEEE INFOCOM 2014 - IEEE Conf. Comput. Commun.*, vol. 16, no. 2, pp. 271–279, 2014.
- [173] R. D. Ainul, P. Kristalina, and A. Sudarsono, "Modified Iterated Extended Kalman Filter for Mobile Cooperative Tracking System," *Int. J. Adv. Sci. Eng. Inf. Technol.*, vol. 7, no. 3, p. 980, 2017.
- [174] Y. Ren, F. D. Salim, M. Tomko, Y. B. Bai, J. Chan, K. K. Qin, and M. Sanderson, "D-Log: A WiFi Log-based differential scheme for enhanced indoor localization with single RSSI source and infrequent sampling rate," *Pervasive and Mobile Computing*, vol. 37, pp. 94–114, 2017.
- [175] V. Malyavej, W. Kumkeaw, and M. Aorpimai, "Indoor robot localization by RSSI/IMU sensor fusion," *2013 10th Int. Conf. Electr. Eng. Comput. Telecommun. Inf. Technol. ECTI-CON 2013*, 2013.
- [176] R. L. H. Don and J. Samarabandu, "Novel velocity model to improve indoor localization using inertial navigation with sensors on a smartphone," 2016.
- [177] N. Ganganath and H. Leung, "MOBILE ROBOT LOCALIZATION USING ODOMETRY AND KINECT SENSOR N . Ganganath and H . Leung Department of Electrical and Computer Engineering Schulich School of Engineering University of Calgary , Calgary , Alberta , Canada Email :{ ngmarasi , leungh }@ ucalga," pp. 91–94, 2012.
- [178] B. Xu, X. Zhou, T. Cheng, Z. Su, and J. Wu, "A new proposal for localization of omni-directional mobile robot by DM tag in indoor environment," *2017 IEEE Int. Conf. Cybern. Intell. Syst. CIS 2017 IEEE Conf. Robot. Autom. Mechatronics, RAM 2017 - Proc.*, vol. 2018–Janua, pp. 140–145, 2018.
- [179] J. Zolghadr and Y. Cai, "Locating a two-wheeled robot using extended Kalman filter," *Teh. Vjesn. - Tech. Gaz.*, vol. 22, no. 6, pp. 1481–1488, 2015.
- [180] D. . García-Sillas, E. . Gorrostieta-Hurtado, J. E. . Vargas Soto, J. . Rodríguez-Reséndiz, and S. . Tovar Arriaga, "Kinematics modeling and simulation of an autonomous omni-directional mobile robot [Modelado y simulación de un robot móvil autónomo omni-direccional]," *Ing. e Investig.*, vol. 35, no. 2, pp. 74–79, 2015.

Appendices

Appendix A: Additional Figures

Chapter 5 – Appendix 1 WTP-HAMS system hardware requirement with its advantages (Appendix A)

Chapter 6 - Appendix 2 WTP-HAMS assessment and experimental strategy flow (Appendix A)

Appendix B – Development Code Snippet

Appendix 3 Online database containing data sets from mobile phone application (Appendix B)

Appendix 4 Novel Odometry model implementation to get improved pose estimates (Appendix B)

Appendix 5 End block of the novel odometry model description (Appendix B)

Appendix 6 Implementing the novel odometry model using real information from wheel encoders and IMU with reference to time (Appendix B)

Appendix 7 Get and process IMU dataset (Appendix B)

Appendix 8 FWHM Model (Appendix B)

Appendix 9 Implementing FWHM on IMU waveform (Appendix B)

Appendix 10 Getting Navigation heading (Appendix B)

Appendix 11 Get location of Wi-Fi routers (Appendix B)

Appendix 12 Consolidate Wi-Fi with closest and further values (Appendix B)

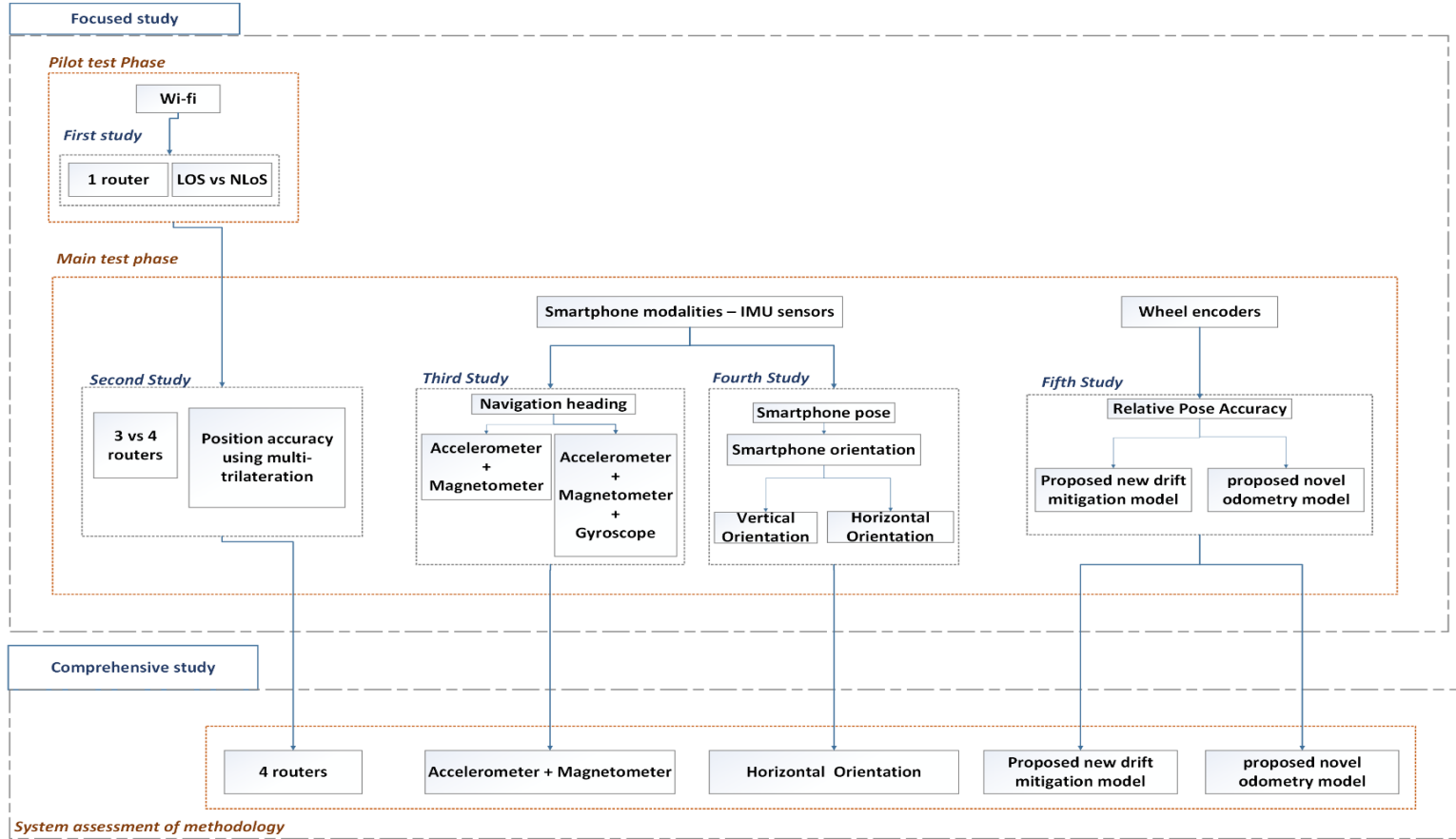
Appendix 13 Defining SDRS log shadowing model parameters to get distance
(Appendix B)

Appendix 14 Trilateration and Multi-trilateration for 3 routers and 4 routers
(Appendix B)

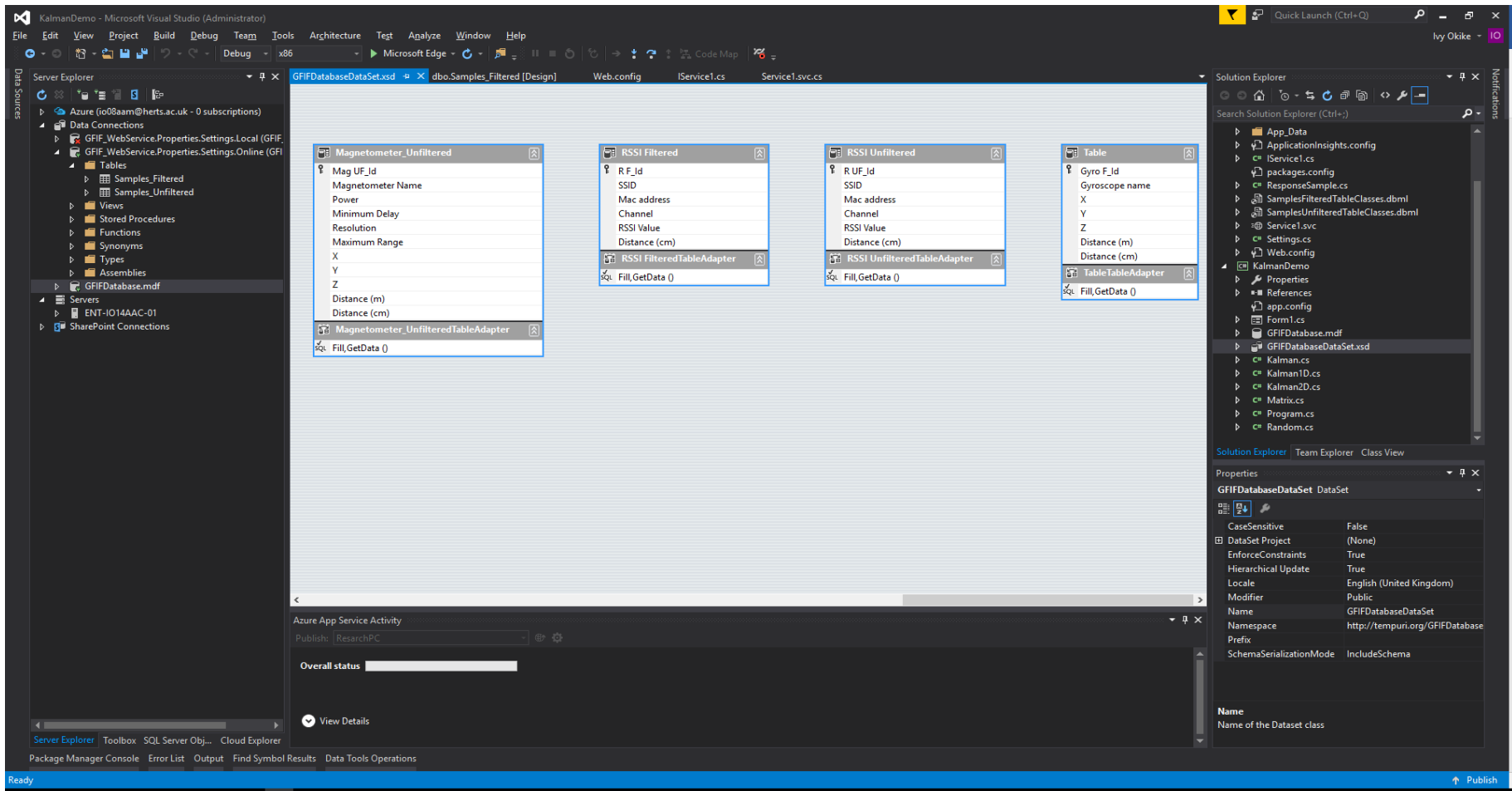
Technology	Category	Amount required	Benefit
Mobility scooter	External	1	Localising mobility impaired users within commercial buildings. Critical in providing complementary data O1 and O2 needed by the wheel encoders to determine travelled distance estimates.
Smart Phone (SP)	External	1	Amalgamate all data extracted from all participating technologies including Wi-Fi, wheel encoders, accelerometer and magnetometer sensors Interface between user and calculation workhouse at the offline phase It is ubiquitous
Wi-Fi sensor modality	Internal	1	This technology is present in all smartphones, therefore it is very inexpensive. Listens and collects Wi-Fi signals parameters emitted from Wi-Fi routers/APs.
Wi-Fi routers/APs	External	Minimum of 4	Provides better relative position estimates with lesser errors when compared to using 3 routers. Mandatory for achieving W1 and W2 Most commercial buildings have at least 7 Wi-Fi routers/APs per floor according to CICSO best practice [10] therefore, making this technology ubiquitous and inexpensive to end users.
Accelerometer sensor modality	Internal	1	This technology is present in all smartphones, therefore it is very inexpensive. It maintenance level is significantly low. Listens and collects measured gravitational impact on rotation acceleration experienced on the SP. Critical in getting AM2 when output is combined with orientation outputs of magnetometer Necessary for providing better pose estimates AMO1 using a novel odometry model which is the combination of O1 and AM2
Magnetometer sensor modality	Internal	1	This technology is present in all SP, therefore it is very inexpensive. It maintenance level is significantly low. Listens and collects measurements of SP orientation relative to the earth's magnetic fields. Critical in getting improved heading estimates AM2 when output is combined with vector rotational outputs of the accelerometer Necessary for providing better pose estimates AMO1 using a novel odometry model which is the combination of O1 and AM2
Wheel encoders	External	2	Two wheel encoders provide better position estimates when distance travelled from both wheels are considered. Important for determining O1, O2, and O3 from mobility scooter after motion. Necessary for deriving improved pose estimates AMO1 from the novel odometry model which is the combination of O1 and AM2

Appendix 1 WTP-HAMS system hardware requirement with its advantages (Appendix A)

Assessment of our proposed WTP-HAMS System



Appendix 2 WTP-HAMS assessment and experimental strategy flow (Appendix A)



Appendix 3 Online database containing data sets from mobile phone application (Appendix B)

```

1  %%
2  % ODOMETRY MOTION MODEL PARAMETERS
3  R = 5 ; %inner wheel radius
4  L = 19.9; %distance between the two rare wheels
5
6  %%
7
8  %%
9
10 % START ODOMETRY CODE BLOCK %
11
12
13 D_L = m_per_tick * (left_ticks-prev_left_ticks); %distance travelled by left wheel
14
15 D_R = m_per_tick * (right_ticks-prev_right_ticks); %distance travelled by right wheel
16
17 D_C = (D_L+D_R)/2; %distance travelled by centre of scooter
18 %Put encoder value here.
19
20 theta_dt = (D_R - D_L)/L;
21 theta_d = theta * (180.0/pi); %heading in degrees
22
23
24 x_dt = D_C * cos(theta); %change in x position
25 y_dt = D_C * sin(theta); %change in y position
26 %copy and paste and execute function to plot from folder
27 %theta_global = vertcat (get_column(filetext, "AMY"),get_column(filetext, "GY"),get_column(filetext, "SFY"));
28
29 theta_global=get_column(filetext2, "AMY");
30 ODO=get_column(filetext2, "ODO");
31 for i=2:length(ODO);
32 [b1,h1]=get_bearing(ODOx(i)-ODOx(i-1),ODOy(i)-ODOy(i-1), theta); %note that this is x_dx and y_dy. See if you can extract from ODO
33 %for straight, y_dx is zero
34 end
35 %sen
36
37 % (x > 0.00001 target_bearing_theta_global = 90.0 - atan(y/x);
38 % (x < -0.00001) target_bearing_theta_global = -90.0 - atan(y/x);
39
40 %%

```

Appendix 4 Novel Odometry model implementation to get improved pose estimates (Appendix B)

```
%%  
%{  
% END ODOMETRY CODE BLOCK %%  
theta_new = theta + theta_dt;  
x_new = x + x_dt;  
y_new = y + y_dt;  
%}  
%%  
%%  
  
%}
```

Appendix 5 End block of the novel odometry model description (Appendix B)

```

97 %%
98 location = 'C:\Users\IO14AAC\Desktop\readings+fab\organised\ALL READINGS_NEW\motion\Horizontal\true\0-1';
99 files = dir(fullfile(location, '*.json')); %get file names in location into an array
100 u=[]; %initialising end point
101 t=[]; %initialising for means
102 ends=[]; %initialise end point
103 means=[]; %initialise %means
104 for i=1:length(files)
105     if i ~=1 %ignore timestamp column
106         u=[]; %reinitialise variable
107         t=[]; %reinitialise variable
108     end
109     fname=strcat(location,'\',files(i).name);
110     filetext=fileread(fname); %read json da file
111     filetext2=jsondecode(filetext); %decode json data
112     names=fieldnames(filetext2.sensors)'; %get field names
113
114     for i =2:length(names)
115         temp_end=[filetext2.sensors(length(filetext2.sensors)).(names{i})]; %get last row
116         temp_mean=mean([filetext2.sensors(2:length(filetext2.sensors)).(names{i})]); %get mean of all rows
117         times=[];
118         u=[u temp_end];
119         t=[t temp_mean];
120     end
121     times=[];
122     for i =1:length(filetext2.sensors)
123         times=[times str2num([filetext2.sensors(i).timestamp])/1000; %get timestamps into an array called timestamp
124         end
125         u=[str2num([filetext2.sensors(i).timestamp]) u]; %add the timestamp
126         t=[mean(times) t]; %get mean of all the time stamps
127         ends=vertcat(ends, u); %add this to the global Endpoint data ends
128         means=vertcat(means, t); %add this to the global mean data ends
129     end
130
131     clear temp_end, clear temp_mean, clear u, clear t, clear filetext %clear filetext2#
132
133
134     location = 'C:\Users\IO14AAC\Desktop\readings+fab\organised\ALL READINGS_NEW\motion\Horizontal\true\0-1';
135     files = dir(fullfile(location, '*.json')); %get file names in location into an array
136
137     for i=1:length(files)

```

Appendix 6 Implementing the novel odometry model using real information from wheel encoders and IMU with reference to time (Appendix B)

```

133
134 - location = 'C:\Users\IO14AAC\Desktop\readings+fab\organised\ALL READINGS_NEW\motion\Horizontal\true\0-1';
135 - files = dir(fullfile(location, '*.json')); %get file names in location into an array
136
137 - for i=1:length(files)
138 -     idx=i;
139 -     fname=strcat(location, '\', files(idx).name);
140
141 -     filetext=fileread(fname);
142 -     %filetext26=jsondecode(filetext);
143 -     eval(['filetext',int2str(idx),'=jsondecode(filetext);'])
144 -     eval(['temp= filetext',int2str(idx),';'])
145 -     times=[];
146 -     for i =1:length(temp.sensors)
147 -         times=[times str2num([temp.sensors(i).timestamp])]; %get timestamps into an array called timestamp
148 -     end
149 -     times=(times-times(1))/1000; %get absolute time
150
151 -     AMY=get_column(temp, "AMY");
152 -     % GY=get_column(temp, "GY");
153 -     % GDY=get_column(temp, "GDY");
154 -     % SFY=get_column(temp, "SFY");
155 -     % AY=get_column(temp, "AY");
156 -     figure(2)
157 -     subplot(floor(length(files)/5)+1,5,idx) %create subplot with 5 plots per row
158 -     plot (times,AMY, 'DisplayName','AMY')
159 -     legend('show')
160 -     hold on
161 -     %plot (times,smooth(AMY), 'DisplayName','AMY')
162 -     %plot (times,GY, 'DisplayName','GY')
163 -     %plot (times,GDY, 'DisplayName','GDY')
164 -     %plot (times,AY, 'DisplayName','AY')
165 -     %plot (times,SFY, 'DisplayName','SFY')
166 -     ylabel('Amplitude (rad)');
167 -     xlim([0 4])
168 -     xlabel('Time (s)');
169 -     hold off
170 - end
171
172
173 - location = 'C:\Users\IO14AAC\Desktop\readings+fab\organised\ALL READINGS_NEW\motion\Horizontal\true\0-1';

```

Appendix 7 Get and process IMU dataset (Appendix B)

```

1 function width = fwhm(x,y)
2
3 % function width = fwhm(x,y)
4 %
5 % Full-Width at Half-Maximum (FWHM) of the waveform y(x)
6 % and its polarity.
7 % The FWHM result in 'width' will be in units of 'x'
8 %
9 %
10 % Rev 1.2, April 2006 (Patrick Egan)
11
12
13 y = y / max(y);
14 N = length(y);
15 lev50 = 0.5;
16 if y(1) < lev50 % find index of center (max or min) of pulse
17     [garbage,centerindex]=max(y);
18     Pol = +1;
19     disp('Pulse Polarity = Positive')
20 else
21     [garbage,centerindex]=min(y);
22     Pol = -1;
23     disp('Pulse Polarity = Negative')
24 end
25 i = 2;
26 while sign(y(i)-lev50) == sign(y(i-1)-lev50)
27     i = i+1;
28 end %first crossing is between v(i-1) & v(i)
29 interp = (lev50-y(i-1)) / (y(i)-y(i-1));
30 tlead = x(i-1) + interp*(x(i)-x(i-1));
31 i = centerindex+1; %start search for next crossing at center
32 while (sign(y(i)-lev50) == sign(y(i-1)-lev50)) && (i <= N-1)
33     i = i+1;
34 end
35 if i ~= N
36     Ptype = 1;
37     disp('Pulse is Impulse or Rectangular with 2 edges')
38     interp = (lev50-y(i-1)) / (y(i)-y(i-1));
39     ttrail = x(i-1) + interp*(x(i)-x(i-1));
40     width = ttrail - tlead;
41 else
42     Ptype = 2;
43     disp('Step-Like Pulse, no second edge')
44     ttrail = NaN;

```

Appendix 8 FWHM Model (Appendix B)

```

211 % plot (times,GX, 'DisplayName','AX')
212 % plot (times,SFX, 'DisplayName','SFX')
213 %plot (times,GY, 'DisplayName','GY')
214 ylabel('Amplitude (rad)');
215 xlabel('Time (s)');
216 hold off
217
218
219 eval(['temp= filetext',int2str(idx),'.']) %create temp variable with the specified idx
220 %temp=smooth(AMY); %put span (default is 5) that you are confident will provide better estimation of odometry start e.g. smooth (AMY, span)
221 temp1=smooth(AMY,50); %get smoothed version of AMY
222 [M,I]=max(temp1-min(temp1)); %get the maximum value in the curve and the index of that maximum value
223 x=1:length(temp1); % get index of dataset
224 fw=fwhm(x, temp1-min(temp1)); %Remove the negative offset
225 startpoint=I-floor(fw/2);
226 endpoint=I+floor(fw/2);
227 %we also want to know what our full width is in terms of time so we can fit
228 %a motion profile to it.
229 fw_t=fwhm(times, temp1-min(temp1));
230
231
232 v_calc= (1.8*1000)/(str2num([temp.sensors(endpoint).timestamp]) - str2num([temp.sensors(startpoint).timestamp])); %give velocity in M/s known
233 initial_pos=0;
234
235 cur_pos=0;
236 t=[];
237
238
239 for i = 2:length(temp.sensors) %ignore first row and start from next increment
240 dt= str2num([temp.sensors(i).timestamp]) - str2num([temp.sensors(i-1).timestamp]);
241 if i<=startpoint+1 %ignore anything before startpoint+1
242 t=[t 0];
243 elseif i> endpoint+1 %ignore anything after endpoint
244 t=[t 0];
245 else
246 t=[t dt];
247 end
248 end
249
250 ODO=[(v_calc*t/1000) 0];
251 ODO=cumsum(ODO); %cumulative sum

```

Appendix 9 Implementing FWHM on IMU waveform (Appendix B)

```
1 function [bearing, heading_error] = get_Bearing(x,y,theta) %get bearing/heading after dt
2 %x is change in x direction
3 %y is change in y direction
4 if x> 0.00001
5     bearing = 90.0 - atand(y/x);
6 elseif x<-0.00001
7     bearing = -90.0 - atand(y/x);
8 else
9     bearing = 0; %something is wrong with this
10 end
11 heading_error=bearing-(theta); %something is wrong with this... sent you a message on the chat box
12
13 if heading_error>180
14     heading_error=heading_error-360;
15 elseif heading_error<180
16     heading_error=heading_error+360;
17 end
```

Appendix 10 Getting Navigation heading (Appendix B)

```

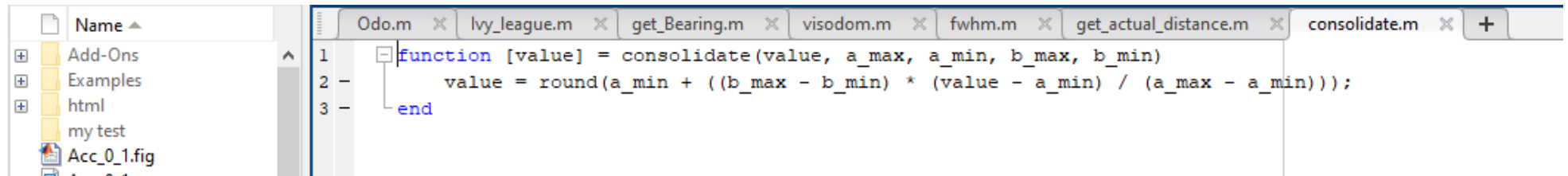
Current folder
Name
Add-Ons
Examples
html
my test
Acc_0_1.fig
Acc_0_1.png
Acc_0_1 ONLY.fig
Acc_0_1 ONLY.png
AMX & AMY_SAMPLE 5...
AMX & AMY_SAMPLE 5...
fwhm.m
fwhm.zip
GDY_AMX_SFX.fig
GDY_AMX_SFX.png
GDY_AMY_SFY.fig
GDY_AMY_SFY.png
get_Bearing.m
get_column.m
GRYO WITHOUT DRIFT.fig
GRYO WITHOUT DRIFT.p...
GYRO ONLY.fig
GYRO ONLY.png
lvy_league.m
Moving mean_sample 5...
Moving mean_sample 5...
normalisation.m
Odo.m
odometry_1.fig
odometry_1.png
Sensor data on Xaxis of ...
SFX.fig
SFX.png
SFY.fig

fwhm.m (Function)
function width = fwhm(x,y)
fwhm(x, y)

Editor - C:\Users\10144AC\Desktop\ITERATION FILE\archive\get_actual_distance.m
Odo.m x lvy_league.m x get_Bearing.m x visodom.m x fwhm.m x get_actual_distance.m x +
1 function [plane] = get_actual_distance()
2 plane = cell(1, 7);
3 [plane_r, plane_c] = size(plane);
4
5 %y x (router locations)
6 ra_loc = [1 1];
7 rb_loc = [1 7];
8 rc_loc = [2 5];
9 rd_loc = [3 1];
10 re_loc = [3 7];
11
12 sh = [198 170 165 168 169 137]; % [293 198 170 165 168 169 137];
13 sv = [480 427];
14
15
16 % x_d = 170; %evenly spaced
17 % y_d = 450;
18 for r = 1 : plane_r
19     for c = 1 : plane_c
20         mob_loc = [r c];
21
22         loc_diff_a = [get_distance_from_matrix(sh, ra_loc(2), mob_loc(2)) get_distance_from_matrix(sv, ra_loc(1), mob_loc(1))];
23         loc_diff_b = [get_distance_from_matrix(sh, rb_loc(2), mob_loc(2)) get_distance_from_matrix(sv, rb_loc(1), mob_loc(1))];
24         loc_diff_c = [get_distance_from_matrix(sh, rc_loc(2), mob_loc(2)) get_distance_from_matrix(sv, rc_loc(1), mob_loc(1))];
25         loc_diff_d = [get_distance_from_matrix(sh, rd_loc(2), mob_loc(2)) get_distance_from_matrix(sv, rd_loc(1), mob_loc(1))];
26         loc_diff_e = [get_distance_from_matrix(sh, re_loc(2), mob_loc(2)) get_distance_from_matrix(sv, re_loc(1), mob_loc(1))];
27
28         loc_diff_a = abs(ra_loc - mob_loc).*[y_d x_d];
29         loc_diff_b = abs(rb_loc - mob_loc).*[y_d x_d];
30         loc_diff_c = abs(rc_loc - mob_loc).*[y_d x_d];
31         loc_diff_d = abs(rd_loc - mob_loc).*[y_d x_d];
32         loc_diff_e = abs(re_loc - mob_loc).*[y_d x_d];
33
34         da = round(sqrt(loc_diff_a(1)^2 + loc_diff_a(2)^2));
35         db = round(sqrt(loc_diff_b(1)^2 + loc_diff_b(2)^2));
36         dc = round(sqrt(loc_diff_c(1)^2 + loc_diff_c(2)^2));
37         dd = round(sqrt(loc_diff_d(1)^2 + loc_diff_d(2)^2));
38         de = round(sqrt(loc_diff_e(1)^2 + loc_diff_e(2)^2));
39
40         plane(r, c) = [da db dc dd de];
41     end
42 end
43

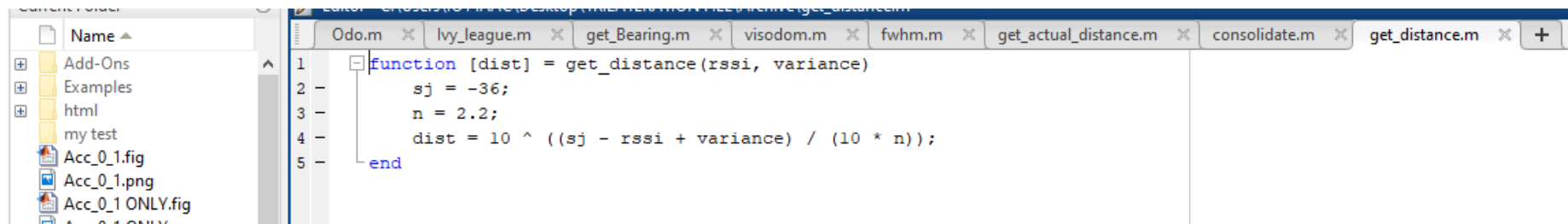
```

Appendix 11 Get location of Wi-Fi routers (Appendix B)



```
1 function [value] = consolidate(value, a_max, a_min, b_max, b_min)
2     value = round(a_min + ((b_max - b_min) * (value - a_min) / (a_max - a_min)));
3 end
```

Appendix 12 Consolidate Wi-Fi with closest and further values (Appendix B)



```
1 function [dist] = get_distance(rssi, variance)
2     sj = -36;
3     n = 2.2;
4     dist = 10 ^ ((sj - rssi + variance) / (10 * n));
5 end
```

Appendix 13 Defining SDRS log shadowing model parameters to get distance (Appendix B)

<ul style="list-style-type: none"> ▢ Add-Ons ▢ Examples ▢ html ▢ my test Acc_0_1.fig Acc_0_1.png Acc_0_1 ONLY.fig Acc_0_1 ONLY.png AMX & AMY_SAMPLE 5... AMX & AMY_SAMPLE 5... fwhm.m ▢ fwhm.zip GDY_AMY_SFV.fig GDY_AMY_SFV.png GDY_AMY_SFV.fig GDY_AMY_SFV.png get_Bearing.m get_column.m GRYO WITHOUT DRIFT.fig GRYO WITHOUT DRIFT.p... GYRO ONLY.fig GYRO ONLY.png lvy_league.m Moving mean_sample 5... Moving mean_sample 5... normalisation.m Odo.m odometry_1.fig odometry_1.png Sensor data on Xaxis of ... Sensor data on Xaxis of ... Sensor data on Yaxis of ... Sensor data on Yaxis of ... SFX.fig SFX.png SFY.fig 	<pre> 1 2 3 4 5 6 7 8 9 10 11 12 13 14 15 16 17 18 19 20 - 21 - 22 - 23 - 24 - 25 - 26 - 27 - 28 - 29 - 30 - 31 - 32 - </pre>	<pre> function [x, y] = trilateration(B, BeaconN) % 2D Trilateration to determine the location of the unknown node % Syntax: % B - Beacon matrix, % B(i,:) represents a beacon, % B(i,1) is the x coordinate of Beacon i, % B(i,2) is the y coordinate of Beacon i, % B(i,3) is the d(istance) from the unknown node to Beacon i. % BeaconN - Number of Beacons % [x, y] - the x, y coordinates of the unknown node % algorithm: % Q = inv(D'*D)*D'*b % where D = 2* [x1- x2, y1-y2; x1-x3, y1-y3; ...; x1-xn, y1-yn] % b = [x1^2-x2^2+y1^2-y2^2+d1^2-d2^2; ...; x1^2-xn^2+y1^2-yn^2+d1^2-dn^2] % Q = [x;y] the coordinates of the unknown node. % Author: % Yuting Zhang <ytzhang@bu.edu> % 10/24/2012 D = zeros(BeaconN -1, 2); b = zeros(BeaconN -1, 1); for i = 1 : BeaconN -1 D(i, :) = [B(1,1) - B(i+1, 1), B(1, 2) - B(i+1, 2)]; b(i) = B(1,1)^2 - B(i+1,1)^2 + B(1,2)^2 - B(i+1,2)^2 - B(1,3)^2 + B(i+1,3)^2; end D = 2 * D; DT = D'; Q = (DT * D) \ DT * b; x = Q(1); y = Q(2); end </pre>
--	---	---

Appendix 14 Trilateration and Multi-trilateration for 3 routers and 4 routers (Appendix B)

